INFORMATION TO USERS

This manuscript has been reproduced from the microfilm master. UMI films the text directly from the original or copy submitted. Thus, some thesis and dissertation copies are in typewriter face, while others may be from any type of computer printer.

The quality of this reproduction is dependent upon the quality of the copy submitted. Broken or indistinct print, colored or poor quality illustrations and photographs, print bleedthrough, substandard margins, and improper alignment can adversely affect reproduction.

In the unlikely event that the author did not send UMI a complete manuscript and there are missing pages, these will be noted. Also, if unauthorized copyright material had to be removed, a note will indicate the deletion.

Oversize materials (e.g., maps, drawings, charts) are reproduced by sectioning the original, beginning at the upper left-hand corner and continuing from left to right in equal sections with small overlaps.

Photographs included in the original manuscript have been reproduced xerographically in this copy. Higher quality 6" x 9" black and white photographic prints are available for any photographs or illustrations appearing in this copy for an additional charge. Contact UMI directly to order.

Bell & Howell Information and Learning
300 North Zeeb Road, Ann Arbor, MI 48106-1346 USA
800-521-0600

FROM ORGANOMETALLIC CATIONS TO CARBENES :

AN NMR, STRUCTURAL AND REACTIVITY STUDY.

By

JAMES A. DUNN, B. Sc.

A Thesis

Submitted to the School of Graduate Studies

In Partial Fulfillment of the Requirements

for the Degree

Doctor of Philosophy

McMaster University

FROM ORGANOMETALLIC CATIONS TO CARBENES :

AN NMR, STRUCTURAL AND REACTIVITY STUDY.

DOCTOR OF PHILOSOPHY (1998) McMaster University

(Chemistry) Hamilton, Ontario

TITLE: From Organometallic Cations to Carbenes : An NMR, Structural and Reactivity Study.

AUTHOR: James A. Dunn, B. Sc. (University of Western Ontario)

SUPERVISOR: Dr. M. J. McGlinchey

NUMBER OF PAGES: xii, 219

Abstract

The electronic requirements of the short-lived 4n π anti-aromatic fluorenyl indenyl and cyclopentadienyl cations have been studied by investigating the dynamic processes exhibited by their dicobalt hexacarbonyl alkynyl clusters in solution. It is suggested that the 12π fluorenyl complex requires the least amount of electronic assistance from a neighboring $Co(CO)_3$ moiety (and consequently the cyclopentadienyl ligand requires the most). That is, the experimental evidence indicates the following cationic stability trend: fluorenyl (12π electrons) > indenyl (8π electrons) > cyclopentadienyl (4π electrons). However, these cationic clusters did not yield single crystals suitable for an X-ray crystallographic study and efforts were focused on synthesizing neutral models for these complexes. Isolobal replacement of a formal $Co(CO)_3^+$ vertex with a $Fe(CO)_3$ moiety, in the fluorenyl and indenyl systems yields neutral iron-cobalt clusters, $(Me_3Si\text{-}C{=}C{=}C_9H_8)FeCo(CO)_6$ and (1-trimethylsilylethynyl-2,3-diphenylindenyl)$FeCo(CO)_6$, the structures of which were determined by X-ray diffraction. This work provided insight into the mechanism for the formation of these iron-cobalt complexes. Conclusions about the electron requirements that these 4n π anti-aromatic cations impose on the neighboring metal center have been drawn.

In contrast to anti-aromatic species, aromatic ligands such as $C_7H_7^+$ do not require electronic assistance from neighboring organometallic moieties. However, if these

species possess bulky substituents, then a compromise between π delocalization and steric strain occurs. The attempt to monitor the electronic requirements of a $C_7Cl_6R^+$ moiety led to an investigation of the chemistry of the polychlorinated cyclic system, C_7Cl_8. Treatment of C_7Cl_8 with various organometallic reagents yielded *syn*-$C_{14}Cl_{12}$, presumably *via* coupling of intermediate C_7Cl_6 carbenes.

The reactions of dimethoxycarbene [$(MeO)_2C$:], generated by the thermal decomposition of 2,2-dimethoxy-5,5-dimethyl-Δ^3-1,3,4-oxadiazoline with polychlorinated olefins and ketones were investigated. Treatment of [$(MeO)_2C$:] with octachlorocycloheptatriene or octachlorobicyclo[3.2.0]hepta-3,6-diene yielded dimethoxy(hexachloro)heptafulvene and dodecachloroheptafulvene. It is proposed that an initial displacement of a chloride ion (S_N2') by dimethoxycarbene occurs resulting in cationic intermediates which can then undergo further reaction to yield the observed products. Reaction of hexachlorotropone and dimethoxycarbene was also investigated and methyl-2-pentachlorophenyl-2-oxo-ethanoate was observed. Mechanisms to account for the observed products were proposed, and the structures of some of these products were determined using X-ray crystallography.

Acknowledgments

I would like to thank my supervisor and mentor, Dr. M. J. McGlinchey for guidance, support and discussions provided during my graduate studies. Words cannot adequately describe the contributions you have made to my scientific career.

I would also like to acknowledge the contributions of my supervisory committee: Dr. Warkentin, I would like to express my gratitude for your patience, support and helpful discussions in my desire to learn a little about reactive intermediates. I thank Dr. G. J. Schrobilgen for his support and inspiring words over the years.

I am very grateful to all of the technical staff of the chemistry department. Special thanks to Dr. J. Britten for obtaining many late night (after hockey) crystal structures and for not hanging up on me when I phoned on weekends with questions; your contributions have been significant. Thanks to Dr. Don Hughes and Mr. Brian Sayer for helping with the various NMR problems, and for always taking the time to answer my questions; also to Dr. Richard Smith and the members of the mass spectrometry facility. To the ladies in the Chemistry Department Office: thanks for all the interesting conversations.

I would also like to mention a few of the many people I have gotten to know throughout the years in the MJM (Luc, Hari, Lisa, Suzie, Ralph, Pippa, Bill, Mark, Stacey and John K.) and JW (John P., Dave, Paul, Nadine) labs. John, thanks for all the good times (some of them I can not quite remember), conversations and words of inspiration.

You are a true friend. Ralph and Mark, my defensive duo, thanks for making me look better than I really am and for the good times. Pippa, you are a friend I could always talk to. Lisa, thanks for all the interesting "non-chemistry" conversations and for putting up with my antics and Luc, thanks for showing me the ropes. Dave and Paul, thanks for the interesting times and the Phoenix Cup memories. We almost did it. Lastly, to the new guy, John K.: it's nice to see a Western influence in the lab again.

Special thanks to all of my "non-chemistry" buddies. Even though you guys will never read this document (and don't want to), you have kept me sane during the last years.

Most importantly, I would like to thank my family for all their support and for putting up with me during the stressful times. And finally to Michelle, I could not have done this without your patience and support. You are my inspiration.

Table of Contents

List of Figures

List of Tables

Chapter One

Introduction

1.1 Carbocations

1.1.1 General Concepts

Carbocations in the simplest form can be thought of as derivatives of the trivalent positively charged species CH_3^+, where the hydrogen atom may be replaced by other organic substituents. Thus, the general concept of carbocations encompasses cations of carbon containing compounds that are singly charged organic species and usually possess an even number of electrons. Typically, carbocations are classified into two categories, 1) classical (trivalent) and 2) non-classical (pentacoordinate or more). Trivalent or classical carbocations are also commonly referred to as carbenium ions and contain six valence electrons at an sp^2-hybridized electron-deficient carbon center. The geometry at this carbon center is usually planar unless affected by steric interference or skeletal rigidity. The structure of the trivalent carbocation can be described in terms of a two-electron, two-center bond. In contrast to trivalent (classical) carbocations, pentacoordinate[a] (or higher) carbocations (or carbonium ions) are termed "non-classical". Although the carbon atom is surrounded by eight valence electrons, (at least) two

[a] It should be noted here that penta-coordinate implies a species with 5 or more ligands within a reasonable bonding distance from the electron-deficient carbon atom.

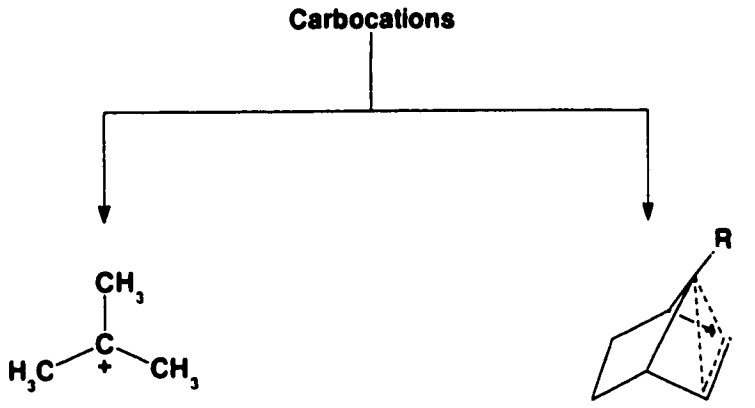

electrons are involved in multi-center bonding (i.e. a 2-electron 3-center bond). This results in an overall electron-deficient species. The three general methods for synthesizing carbocations include,[1] (1) heterolytic fission of a larger molecular entity as in an S_N1 or ionization process (equation 1), (2) addition of cationic species (e.g. a proton) to a neutral molecule (equation 2), and (3) the loss of one electron from a neutral molecule to generate a radical cation.

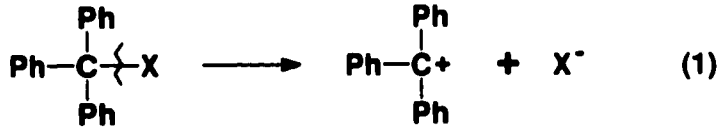

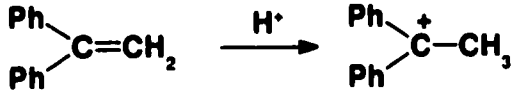

It is also easy to envisage the formation of a carbocationic species *via* addition of an acid and subsequent heterolytic fission. For example, treatment of triphenylmethanol with an appropriate Brönsted acid (addition of a cation) results in the formation of an oxonium ion intermediate. Subsequent cleavage of the carbon oxygen bond then gives the triphenyl methyl cation (equation 3).

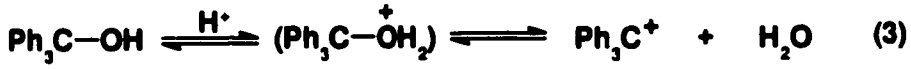

1.1.2 Factors Affecting The Stability of a Carbocation.

The "stability" of a carbocationic species is usually thought of with reference to another species from which it can be derived, or relative to a molecule to which the cation can revert. Thus, the term "stability" as it applies to carbocations is only relative. The factors affecting the stability of a carbocation are (1) intermolecular (external) factors and (2) intramolecular (internal) factors. Intermolecular effects generally include the interactions of the carbocation with a negatively charged counter ion, and with the solvent. In order to stabilize these short-lived intermediates, counter ions of low nucleophilicity are required. Olah and coworkers[2] have extensively studied cationic systems generated by use of superacids. (The universally accepted definition of a superacid[3] is any acid system that is stronger than 100% H_2SO_4, such as HSO_3F:SbF_5). Typically, the employment of superacids results in the formation of very weakly nucleophilic counter ions as the anionic charge is dispersed over many electronegative substituents (such as fluorine). As a result, the counter ion will not interact (or react) with the electron deficient carbon atom. It is important to note that carbocationic centers do not necessarily require such extreme conditions, as there are other factors that inherently influence carbocationic stability. Nevertheless, a weakly nucleophilic counter ion is a common characteristic for "stable" cations.

In contrast, intramolecular or internal effects are based on the structural framework of the carbocation and include contributions from resonance, hyperconjugation and substituent effects. The resonance description of conjugated systems can qualitatively give a simple explanation for the increased stability of certain

cations. For example, the stability of the triphenylmethyl cation (**1**) may be attributed to the various canonical structures, some of which are shown:

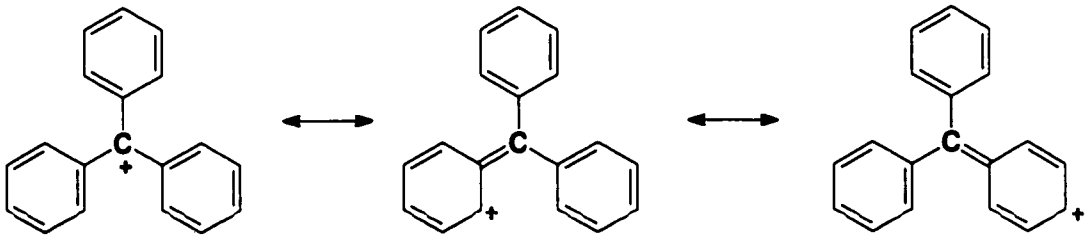

1

Furthermore, electronic contributions from substituents bonded to the carbocationic center can lead to increased stability of an electron-deficient center. The transmission of the effect of an electron-donating (or electron-withdrawing) group through σ bonds is termed the inductive effect.[4] Carbocations bearing substituents that inductively donate electron density to the cationic carbon center will ultimately be more stable than those that do not. However, the stability of a positively charged species such as the *t*-butyl cation can also be rationalized by contributions from hyperconjugation. This concept is described as the overlap interaction of an appropriately oriented σ bond with a *p* orbital to provide electron delocalization involving the σ bond, with little nuclear reorganization.[5] The recent X-ray crystal structure determination of the t-butyl cation has provided experimental evidence in support of this theory.[6] The structure revealed an average C-C bond length of 1.442(5) Å, significantly shorter than a normal C_{sp^2}-CH_3 bond length of 1.503 Å,[6] and consistent with the expectation for charge delocalization *via* hyperconjugation.

1.2 Aromaticity vs. Anti-Aromaticity

1.2.1 General Concepts

The ability of a cationic species to spread its charge over two or more atoms through resonance contributors results in an increased stability. For example, a charged species such as $C_7H_7^+$ (**2**) can form stable salts, and has equally contributing canonical forms whereby the positive charge is distributed over all of the carbon atoms.

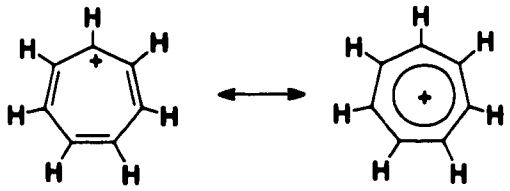

2

The cycloheptatrienyl (or tropylium) cation (**2**) was first prepared by Doering and Knox[7] as its bromide salt and is considered to be aromatic. Although the concept of aromaticity is fundamental in chemistry, there is still no concise definition.[8] Originally, the concept applied to those compounds such as benzene, that had shown an unexpected stability quantified thermodynamically by their enthalpy of hydrogenation. It was calculated that benzene had 150 kJ mol^{-1} (this value is defined as the resonance energy of benzene) less energy available for reaction than expected. Later, Hückel extended the concept of aromaticity by using molecular orbital theory and developed a system (still applicable today) for predicting aromaticity: an aromatic species is a planar, conjugated cyclic polyene and possesses (4n+2) π electrons (n = 0,1,2...). More specifically, in aromatic compounds, electron density is delocalized through π orbitals, resulting in their enhanced stability toward chemical reaction. These species can be neutral (C_6H_6), cationic ($C_7H_7^+$), or anionic ($C_5H_5^-$), so long as they conform to Hückel's rule. The

stabilities of these species are rationalized by the presence of 6π electrons in a closed shell, as shown by the Hückel molecular orbital (HMO) energy level diagrams for $C_5H_5^-$, C_6H_6 and $C_7H_7^+$ (Figure 1.1).

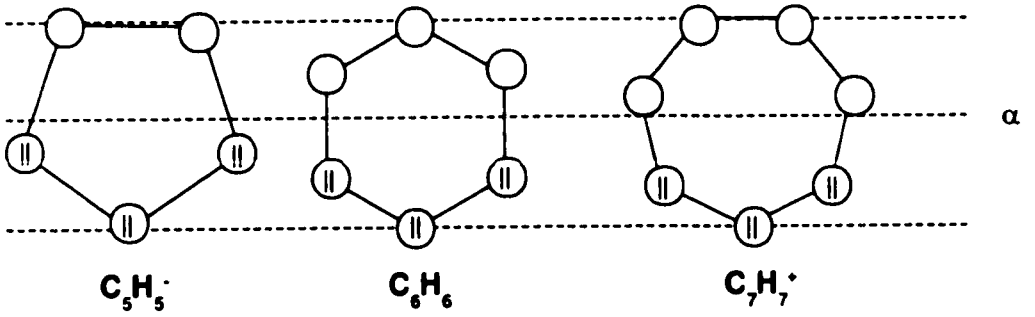

Figure 1.1: Hückel Molecular Orbital Energy Level Diagrams for $C_5H_5^-$, C_6H_6, $C_7H_7^+$.

In contrast to the aromatic (4n+2)π series of polycyclic compounds, there is a corresponding group of cyclic compounds that contain 4n π electrons, classified as anti-aromatic. Breslow has suggested that an anti-aromatic species be categorized as a compound that is cyclic, conjugated, and thermodynamically less stable than its corresponding acyclic analogues.[9] However, the terminology is more useful in describing compounds that are destabilized, not stabilized by delocalization. These species, such as $C_5H_5^+$and $C_7H_7^-$ are predicted to have an open shell triplet ground state configuration as shown by their HMO energy level diagrams (Figure 1.2).

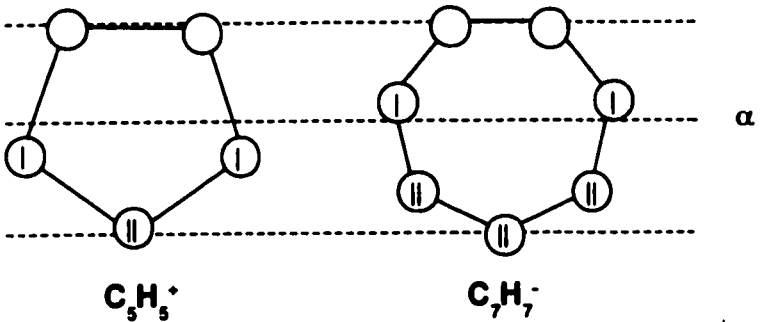

Figure 1.2: Hückel Molecular Orbital Energy Level Diagrams for $C_5H_5^+$ and $C_7H_7^-$.

It should be noted that non-planar species such as C_8H_8 (1,3,5,7-cyclooctatetraene) that do not conform to either definition of aromatic/anti-aromatic are termed non-aromatic.

Although the qualitative definitions of aromatic/anti-aromatic species may be ambiguous, investigations of the physical properties exhibited by these compounds have led to a better understanding and quantification of the concept. To assess the aromatic/anti-aromatic nature of a compound thoroughly, the following criteria should be examined: aromatic stabilization energy, geometry (i.e., equal bond lengths), magnetic anisotropy, magnetic susceptibility exaltation, ring current effects, ^1H nuclear magnetic resonance (NMR) chemical shifts and (the most recently developed criterion), nucleus-independent chemical shift (NICS).

1.2.2 The Criteria

1.2.2.1 Magnetic Criteria

The magnetic criteria for assessing aromaticity involve diamagnetic anisotropy and diamagnetic susceptibility exaltation (Λ). A group that has different currents induced by the B_o field as a result of different orientations in the external field is said to have diamagnetic anisotropy.[10] That is, the magnitudes of the diamagnetic susceptibilities along the three perpendicular axes of the molecule are not equal. For example, it has been determined from single crystals that the naphthalene molecule, an aromatic compound (Figure 1.2) exhibits an enhanced diamagnetic anisotropy. It was shown that the largest diamagnetic susceptibility (K^3) occured perpendicular to the plane of the molecule and that the susceptibilities along the other principal axes (K^1, K^2) were small.

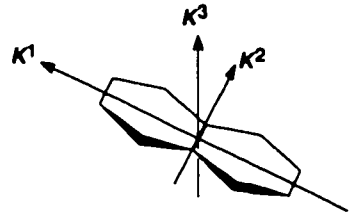

Figure 1.3 :Principal axes in naphthalene.

In contrast to the aromatic compounds, 1,3,5,7-cyclooctatetraene (an 8π non-aromatic compound) did not exhibit an enhanced diamagnetic susceptibility, and the experimental value is in close accord with that expected from four single and four double bonds.

The measurement of the anisotropy of a compound from a single crystal has proven difficult, and consequently Dauben and coworkers[11] introduced a new parameter, diamagnetic anisotropy exaltation (Λ), which could be measured by NMR methods. The exaltation, Λ, of a compound is defined as the difference between the susceptibility exhibited by a compound, χ_M and that predicted for a cyclic polyene of that structure neglecting the contribution from the ring current, $\chi_{M'}$. It was determined that aromatic compounds exhibited large exaltations (i.e benzene : $\Lambda = -13.7\ 10^{-6}$ $cm^3\ mol^{-1}$) whereas non-aromatic species possessed values close to zero (e.g. cyclooctatetraene : $\Lambda = 0.9\ 10^{-6}$ $cm^3\ mol^{-1}$).

1.2.2.2 Ring Current: Chemical Shifts

Ring current effects, and consequently aromaticity, have also been quantified by ^1H NMR spectroscopy.[12] The ring current exhibited by the benzene molecule has been

used to explain the difference of its ^1H chemical shift (δ = 7.24) in comparison to cyclooctatetraene (δ = 5.72). A more striking indication of ring current effects has been shown by comparison of [18]annulene (aromatic) and the [18]annulene dianion (anti-aromatic).[13] It was shown in the former that the protons on the periphery of the ring resonate at δ = 9.28 whereas signals corresponding to the inner protons are at much lower frequency, δ = -3.0. In contrast, the anti-aromatic dianion exhibits resonance signals located at δ = -1.1 (outer protons) and 20.8 and 29.5 (inner protons). In systems that do not possess internal protons (or other nuclei), the chemical shifts of protons in bridging positions can be measured to assess the aromaticity/anti-aromaticity of a compound. Computationally, this idea has been extended to the calculation of Li^+ chemical shifts,[14] the advantage being that the aromatic character of individual rings in polycyclic systems can be assessed.

More recently, Schleyer and coworkers[15] have proposed a new criterion, the nucleus independent chemical shift (NICS). This theoretical criterion is based on the computation of the magnetic shieldings at the ring centers (determined by the nonweighted mean of the heavy atoms) and has been shown to correlate well with the previous criteria. An added advantage provided by the NICS criterion is that the magnetic properties of each ring can be individually assessed in a polycyclic compound.

1.2.2.3 Geometry

A further criterion for the determination of aromaticity is that of structure. As a result of a full delocalization of π electrons, species that are characterized as aromatic should possess equal carbon-carbon bond lengths (e.g., benzene C-C = 1.39 Å). The

determination of such a factor depends on the ability to characterize the desired compound by X-ray crystallographic methods. In contrast, the framework for anti-aromatic compounds should have alternating single and double C-C bond lengths. A disadvantage of this method is that single crystals of a compound are required for X-ray crystallographic determination. As it is not always possible to characterize species using this technique, theoretical calculational packages have proven useful.

Table 1.1 : Summary of Physical Criteria in Assessing Aromaticity/Anti-Aromaticity.

Property	**Aromatic Species**	**Anti-Aromatic Species**
Energy	Aromatic Stabilization	Anti-Aromatic Destabilization
Geometry	Aromatic bond length equalization	Anti-Aromatic bond length Alternation
Ring Current	Diatropic	Paratropic
Magnetic Exaltation (Λ)	Negative Λ, Diamagnetic susceptibility exaltation	Positive Λ, Paramagnetic susceptibility exaltation
Nucleus Independent Chemical Shifts (NICS)	Negative value	Positive value

1.3 Metal Stabilized Carbocations

A third method of stabilizing a transient carbocation involves the use of neighboring groups that can provide electronic assistance to help alleviate developing cationic centers. This idea is nicely exemplified in the hydrolysis of 2,2'-dichlorodiethyl sulfide (**3**), the Mustard Gas of World War I.

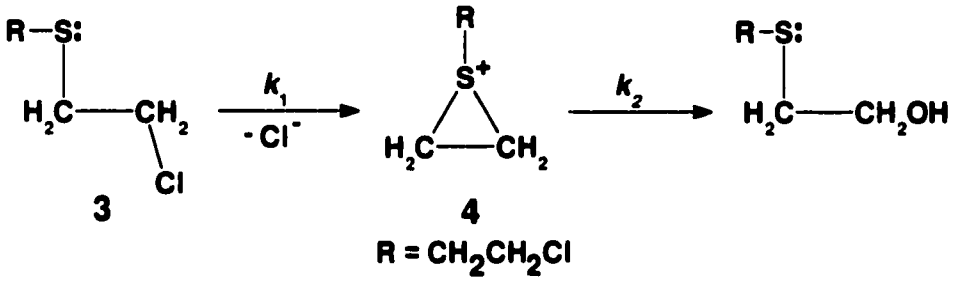

The lone pair of electrons from the sulfur atom can assist in alleviating a developing positive charge on the primary carbon atom. The intermediate **4** (a sulfonium ion) is then hydrolyzed to the corresponding alcohol.[16] The concept of neighboring group electronic assistance by heteroatoms has been thoroughly reviewed previously,[17] and it is not surprising that this idea has been extended to include the electron-rich organometallic moieties,[18] an area in which our group is currently focussed.

There are a wide variety of organometallic moieties that have been shown to provide electronic assistance to neighboring electron deficient carbon centers, and include such metal fragments as $(C_5H_5)Fe(C_5H_4)$,[19] (cyclobutadienyl)$Co(C_5H_5)$,[20] and the $Cr(CO)_3$ tripod.[21] The profound effect that the metal substituent has on the cationic charge of proximally attached atoms is compelling, and evidence from kinetic measurements, theoretical calculations, Nuclear Magnetic Resonance (NMR) data, and X-ray crystallographic studies, supports the hypothesis of a metal-ligand interaction. For

coordination of a $Cr(CO)_3$ moiety, the hydrolysis of benzyl halides has been shown to exhibit a 10^5 solvolysis rate enhancement.[21] This phenomenon is attributed to the stabilization of the cationic intermediate through direct interaction with the electron-rich chromium atom. Further support for a metal-to-ligand interaction was convincingly shown by the X-ray crystallographic structure determination of the ferrocenylmethyl cation, (**5**).[22,23]

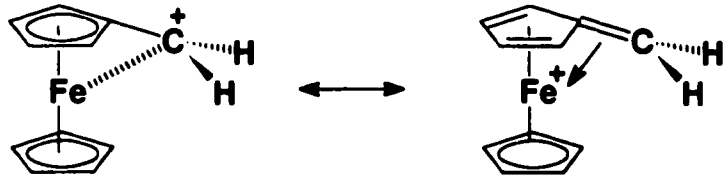

5

The data revealed that the sp^2-hybridized carbocationic carbon exhibited a bend of 22° toward the iron atom, and the structure of the complex was rationalized in terms of a fulvene ligand coordinated to a $(C_5H_5)Fe^+$ moiety.

1.3.1 Trimetallic Clusters and Cations

The ability of trimetallic clusters to assist in alleviating the positive charge of neighboring molecular fragments has also been intensively investigated.[24] The understanding of the bonding in these systems mainly stems from Extended Hückel Molecular Orbital (EHMO) calculations performed by Schilling and Hoffmann[25] who determined the interactions of the frontier orbitals in the triangular M_3L_9 fragments $Fe_3(CO)_9$ and $Co_3(CO)_9^{3+}$ with a capping ligand such as the carbyne moiety, CH^{3-}. Their investigation showed that each of the $M(CO)_3$ units contributed three frontier molecular

orbitals to the triangular unit, namely a d_{xy} hybridized orbital, a d_{z^2} orbital and a hybrid orbital with a combination of s, p_z, and d_{z^2} character. A combination of the in-plane d_{xy} orbitals (one from each $M(CO)_3$ moiety) form a filled low lying doubly degenerate 1*e* set (responsible for metal-metal bonding interactions), as well as a vacant high-lying a_2 orbital which is entirely out-of-phase. Interaction of the d_{z^2} orbital from each $M(CO)_3$ fragment results in a filled π-type orbital and a doubly degenerate π* set. The interaction diagram of the $M(CO)_3$ fragments to form the triangular $M_3(CO)_9$ unit is shown in Figure 1.4.

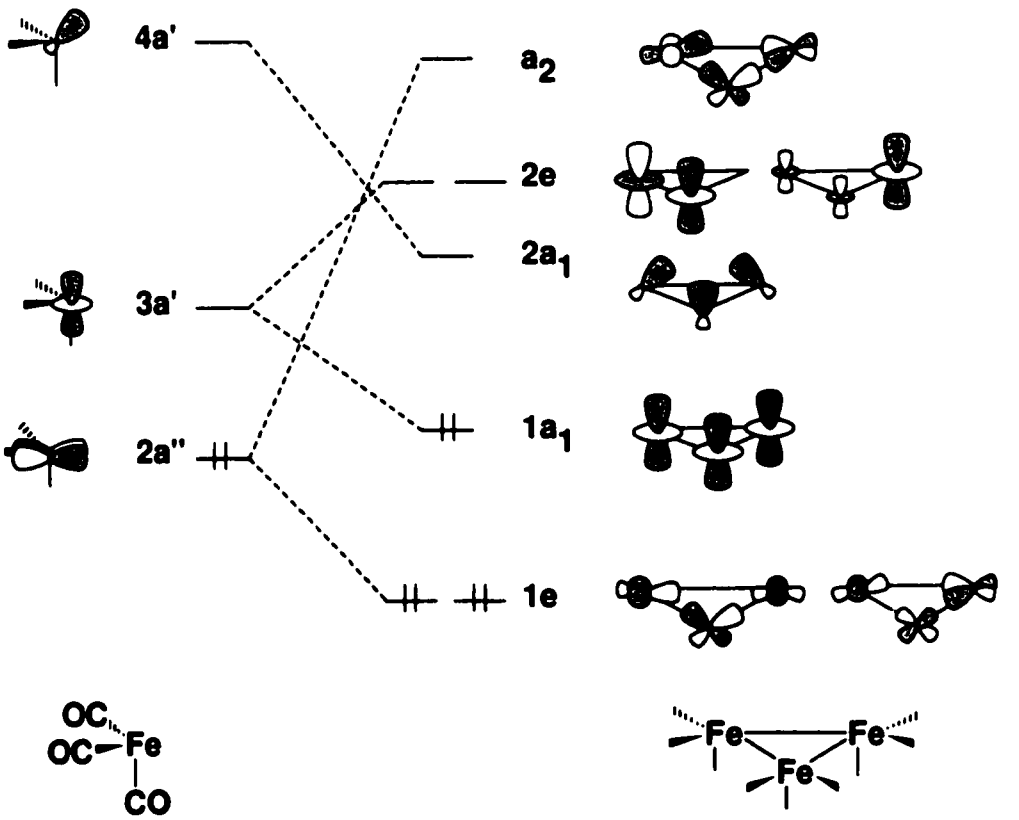

Figure 1.4 : Orbital Interaction Diagram for three $Fe(CO)_3$ Units to Form $Fe_3(CO)_9$.

Fragment EHMO analysis was then used to determine the interaction of the capping carbyne moiety, CH^{3-}. The orbital calculations revealed that the filled sp-hybridized orbital of the capping carbyne (CH^{3-}) interacted with the vacant $2a_1$ combination (a mixture of s, p_z and d_z^2 orbitals) produced from the $M(CO)_3$ units. Furthermore, it was found that the doubly degenerate occupied π orbitals of the capping group had the correct symmetry to overlap with the *2e* acceptor pair. The interaction diagram for the triangular $Co_3(CO)_9^{3+}$ unit with the carbyne is shown in Figure 1.5.

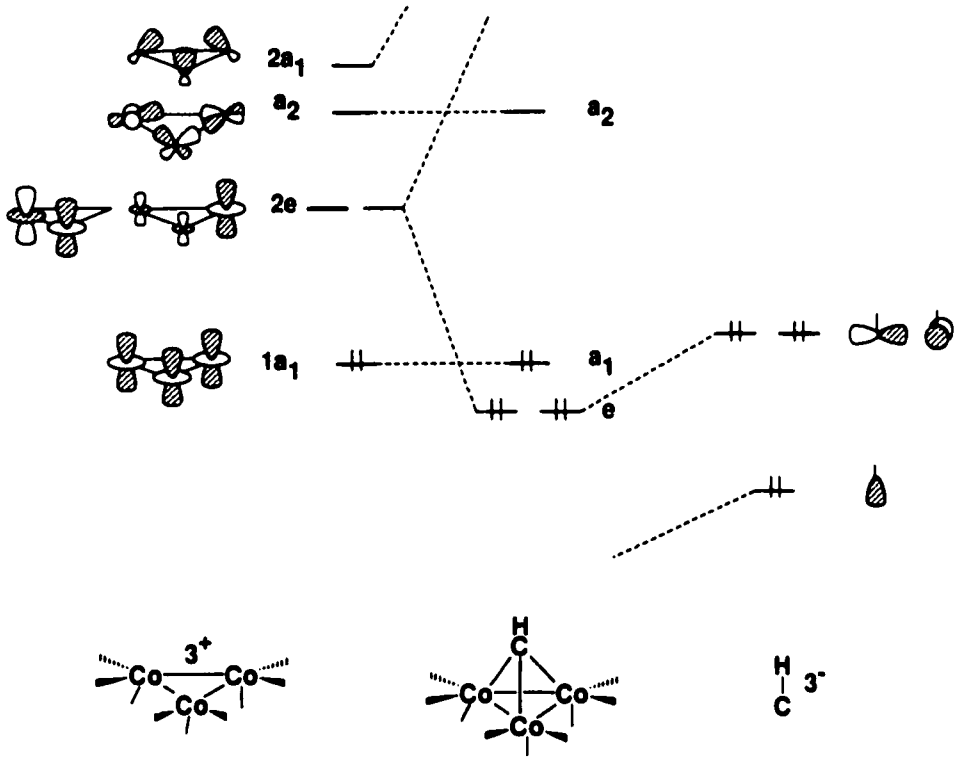

Figure 1.5 : Orbital Interaction Diagram For $Co_3(CO)_9^{3+}$ and CH^{3-}.[25]

Schilling and Hoffmann[25] then extended these calculational studies to cationic clusters such as $[Co_3(CO)_9C{=}CH_2]^+$ (**6**). Examination of the different conformations

possible for **6** revealed that an energy minimum was obtained when the CH_2 moiety was bent towards one of the $Co(CO)_3$ vertices as seen in **6a**. In contrast, an energy maximum was calculated for structure **6b** when positive charge was localized on the methylene carbon atom (i.e., CH_2^+ adopted an upright orientation with respect to the basal plane). The stabilization of the bent structure exhibited by **6** was rationalized in terms of the interaction of the vacant p_z orbital of the CH_2 moiety with the filled d_{z^2} orbital on the metal (Figure 1.6). Furthermore, the EHMO calculations revealed that the energy gap between the highest occupied molecular orbital (HOMO) and the lowest unoccupied molecular orbital (LUMO) increased as the CH_2 fragment leaned towards the metal vertex. Moreover, it was shown that the total energy was at a global minimum when the alkylidene moiety was at its optimum angle.

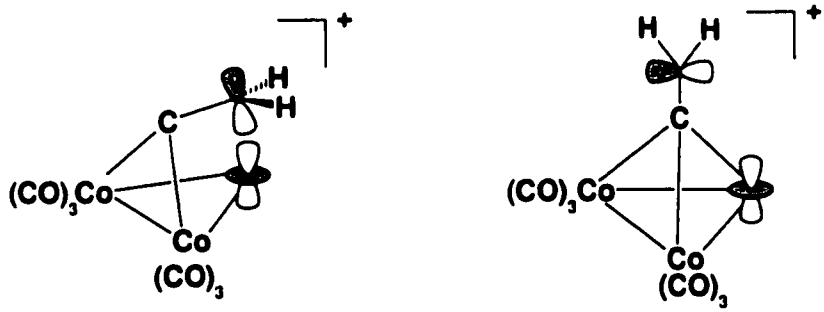

6a — **energy minimum**

6b — **energy maximum**

Figure 1.6: Interaction of a vacant p_z orbital with a filled d_{z^2} of cobalt in **6**.

Although the absolute structure of **6** has not been determined by X-ray crystallography, the "bent" geometry exhibited by these cationic $Co_3(CO)_9$-complexes has been supported by spectroscopic evidence (NMR), as well as by data on closely related organometallic clusters.

1.3.2 Stabilizing Carbocations using Dimetallic Clusters

The theoretical framework provided by trimetallic compounds of the type M_3L_9 (see section 1.3.1) can be applied to organometallic tetrahedral clusters possessing two metal vertices. The isolobal analogy states that chemically different molecular fragments which possess frontier orbitals of similar symmetry, energy, extension in space and electron occupancy can be interchanged.[26] Using this argument, a $Co(CO)_3$ vertex of $[Co_3(CO)_9C{=}CR_2]^+$ (**6**) can be effectively replaced with an isolobal CH unit to yield the propargyl cation, $[Co_2(CO)_6(HC{\equiv}C\text{-}CR_2)]^+$ (**7**).

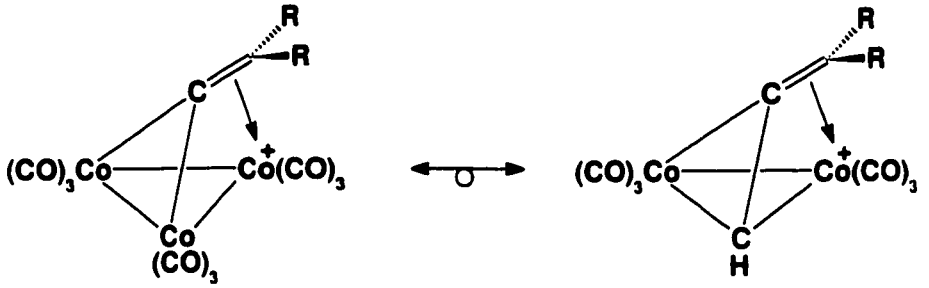

6 **7**

Figure 1.7 : Replacement of a $Co(CO)_3$ moiety with an isolobal CH group.

Synthetically, **7** can be easily generated upon protonation of its alkynol precursor, $Co_2(CO)_6(HC{\equiv}C\text{-}CR_2OH)$.[27]

As was the case with the trimetallic complexes, the structure of the dicobalt cluster cations can be rationalized using two limiting canonical forms; the cation could be localized on the sp^2-hybridized carbon atom or localized on the cobalt atom. In fact, Hoffmann[28] has calculated that the upright structure, where the CH_2 fragment would bear the positive charge, is 17.5 kcal/mol higher in energy when compared with the bent

isomer. The experimental evidence obtained from variable temperature NMR is also consistent with charge localization onto a metal vertex (i.e., a bent structure). For example, Nicholas[29] has shown that $[Co_2(CO)_6(HC{=}C\text{-}CMe_2)]^+$ exhibits two distinct methyl resonances in the ^{13}C NMR at 233 K. Additional evidence was provided by EHMO calculations on a closely related molecule, $[FeCo(CO)_6(HC{\equiv}C\text{-}CH_2)]$, which reveal that the CH_2 unit leans towards the $Fe(CO)_3$ vertex.[24] This cluster is the result of an isolobal replacement of a $Co(CO)_3^+$ by an $Fe(CO)_3$ moiety and these clusters should, in principle, be isostructural (see section 1.5).

The ability of dimetallic alkyne clusters to stabilize cations is not limited to dicobalt hexacarbonyl compounds. Sokolov and coworkers[30] have investigated the chemistry of the Group VI metals, molybdenum and tungsten, in an effort to stabilize β-carbocations. This approach was similar to the method used by Nicholas and involved the treatment of $(C_5H_5)M(CO)_2$ (M = Mo, W) with an alkynol ligand to generate the analogous tetrahedral clusters, $[Cp_2M_2(CO)_4(HC{\equiv}C\text{-}CR_2OH]$ (**8**). Protonation would then yield the corresponding cluster cations **9** as shown in Figure 1.8.

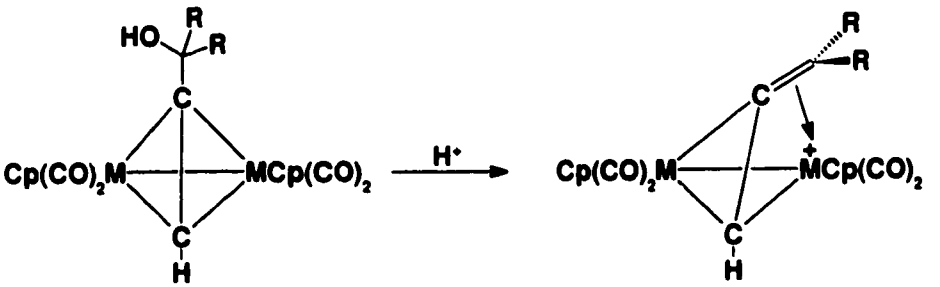

8 **9**

Figure 1.8 : Protonation of an alkynyl alcohol (**8**) to give its corresponding cluster **9**.

The use of the Group VI metals has a significant advantage over their dicobalt hexacarbonyl counterparts in that they yield stable cations that have been characterized by X-ray crystallography, a technique which has been instrumental in determining the migration pathway of the CR_2 fragment from one metal vertex to the other (see section 1.3.3).

1.3.3 Dynamic Processes Exhibited by Di-cluster Cations

Although dicobalt hexacarbonyl cluster cations have until very recently resisted all efforts to yield X-ray quality crystals, variable-temperature NMR spectroscopy has been crucial in understanding the dynamic processes such species can exhibit in solution. Although reports by Mislow[31] and by Nicholas[27] suggested that these dicobalt hexacarbonyl species exhibited fluxionality under various temperature conditions, it was Schreiber and coworkers[32] who were the first to elucidate the mechanisms involved. It was shown from studies of dicobalt hexacarbonyl cationic clusters possessing diastereotopic nuclei, that two migration processes could occur for the alkylidene moiety ($=CR_2$) (Scheme 1.1).

The first process was an antarafacial migration of the CR_2 ligand from one cobalt tricarbonyl vertex to the other, while the second was a simple C_α-C_β bond rotation about the formal double bond so as to interchange the R_a and R_b substituents. The latter was determined to be a higher energy process, and may be attributable to the poorer interaction of the empty p_z orbital of the CR_2^+ moiety with the filled d_z^2 orbital of the cobalt (Scheme 1.1). The barrier for the rotation about the C_α-C_β bond in the dicobalt hexacarbonyl species can be determined readily by monitoring the coalescence behavior

of the R_a and R_b nuclei in the ^{13}C NMR (or ^1H) spectra. In contrast, the measurement of the activation energy for the antarafacial migration process by NMR spectroscopic methods requires an internal probe such as a diastereotopic alkylidene moiety; thus, these barriers are not always obtainable.

Dimetallic clusters of the type $[Cp_2Mo_2(CO)_4(HC{\equiv}C\text{-}CR_2]^+$ have also been shown to exhibit these two fluxional processes. In contrast to the $Co_2(CO)_6$-propargyl cations, the barriers for the C_α-C_β rotation and antarafacial migration processes of the CR_2^+ moiety can both be detected straightforwardly by simultaneously monitoring the relevant nuclei using either ^1H or ^{13}C NMR spectroscopy. The antarafacial migration process equilibrates the cyclopentadienyl rings but not the R_a and R_b groups; interconversion of the latter substituents requires rotation about the C_α-C_β bond.

Scheme 1.1 : Fluxional process exhibited by the dimetallic clusters.

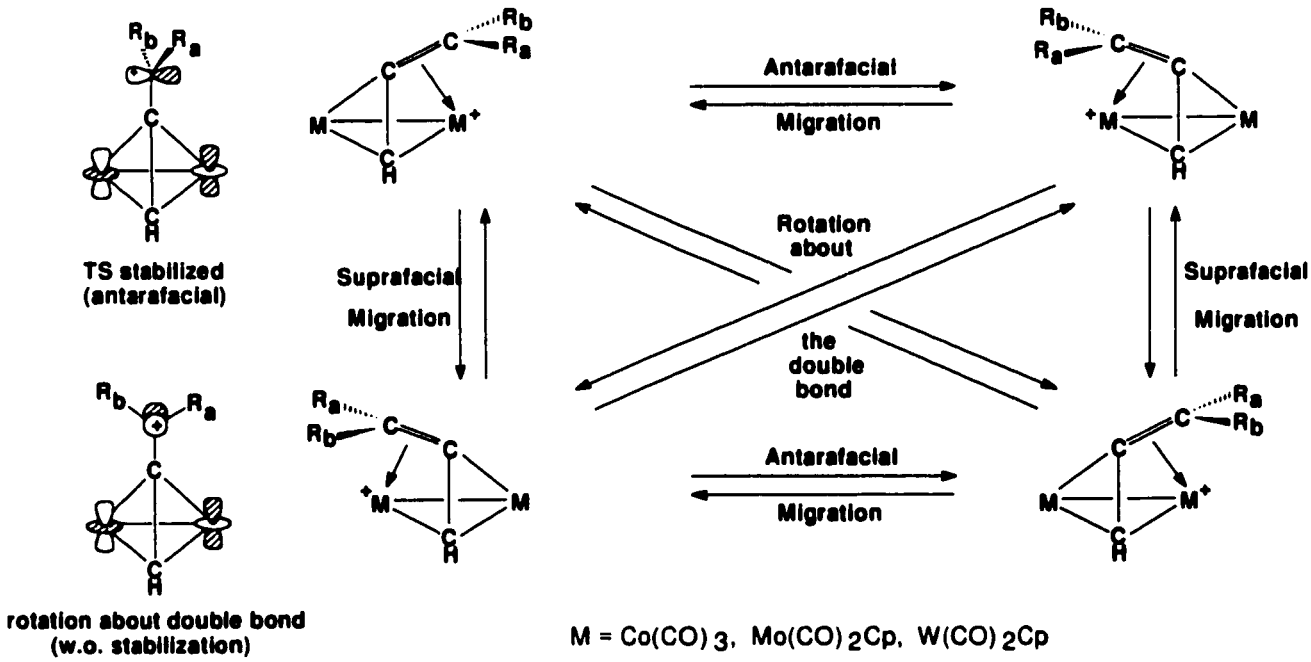

To reiterate, the interconversion of the alkylidene substituents (R_a and R_b in Scheme 1) requires the rotation about the formal double bond (C_α-C_β). However, the antarafacial migration process equilibrates the metal vertices but maintains the difference between the R_a and R_b substituents (Scheme 1.1).

The significance of these fluxional processes should not be underestimated as the calculated activation energy can yield important information about the interaction between the CR_2^+ fragment and the metal atom. It has been shown that the barrier for the antarafacial migration process of the CR_2^+ fragment is dependent on the electronic nature of the carbocationic center. For example, the antarafacial migration process of the CR_2^+ moiety increases from ~10 kcal/mol for tertiary cations to ~18 kcal/mol for primary cations, indicating that the more stable tertiary centers have less need for electronic assistance than do secondary or primary cations.[24,33] Indeed, for some tertiary cations, the barriers for the antarafacial migration process and for the rotation about the carbon-carbon double bond are the same within experimental error.[34,] These data suggest that tertiary cations are less firmly attached to the metal center, and once the cationic carbon leaves the proximity of a cobalt or molybdenum atom rotation about the C-CR_aR_b bond can occur readily. In contrast, the activation energy for the interconversion of the methylene environments of a primary carbocationic species has been shown to be higher than the barrier for the antarafacial migration process. For example, El Amouri[33j] and coworkers have measured the activation energy for each process in the fulvene complex $[\eta^5:\eta^5\text{-}(C_5H_4\text{-}C_5H_4)Mo_2(CO)_4(MeC{\equiv}C\text{-}CH_2)]^+$. The barrier to the antarafacial migration process at 343 K was 17.7 ± 0.4 kcal/mol whereas interconversion of the methylene hydrogens required 19.1 ± 0.4 kcal/mol. To put these values in perspective, 2D EXSY

experiments were performed and the rate constants for each process measured. It was shown that at 343 K a ratio of $k_{int}/k_{rot} = 7$ was observed, statistically implying that for each interconversion (rotation) there would be seven antarafacial migrations.

1.3.4 X-ray Data

The ultimate goal in the study of such species lies in unambiguously determining the structure of these cationic clusters by X-ray crystallography. As has been stated, crystallographic data on cations stabilized by dicobalt hexacarbonyl moieties (or a mono cluster) have hitherto remained elusive. Although the first X-ray structure of a $[Co_2(CO)_6]$-complexed of a propargyl cation (**10**) was reported recently,[35] it should be noted that the cationic carbon was protected by two dicobalt hexacarbonyl clusters (Figure 1.9).

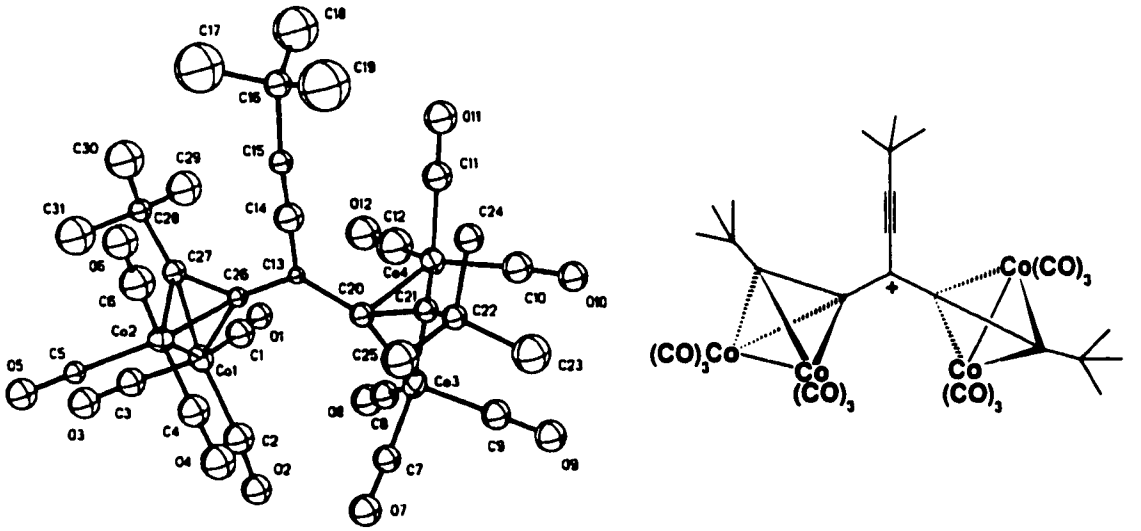

Figure 1.9 : Molecular structure of **10**.[35]

In contrast to cations possessing a simple Co_2C_2 tetrahedral cluster, dimolybdenum cations have been conveniently characterized by X-ray crystallography. A variety of structures for these clusters have been determined and have revealed that the alkylidene moiety always leans towards a molybdenum vertex, the extent of which is determined by the carbocationic character of the CR_2^+ fragment. For example, the Mo-C^+ interatomic distances for primary (2.44-2.46 Å) to secondary (2.61-2.63 Å) to tertiary cations (2.74-2.91 Å) typically increase, presumably because there is less need for electronic assistance from the metal center.[24,33]

1.4 Synthetic Utility and Reactivity of Alkyne Metal Clusters and Cations.

Studies of alkyne metal clusters have not been restricted to the stabilization of transient intermediate cations solely with the goal of determining the activation barriers of fluxional processes. Indeed, dicobalt hexacarbonyl complexes have been found to be very valuable in synthetic organic chemistry. These clusters are easily prepared by direct reaction of $Co_2(CO)_8$ and an alkyne ligand, and typically yield stable compounds.[36] The synthetic utility of these clusters involves (1) use as a protecting group for the alkynyl functionality,[37] (2) a component in the Pauson-Khand reaction to give 2-cyclopenten-1-ones by reactions with olefins, [38] and more recently, (3) the novel rearrangement of 1-(1-alkynyl)cyclopropanols to 2-cyclopenten-1-ones *via* dicobalt hexacarbonyl complexes.[39]

Although the uses of the $Co_2(CO)_6$-alkyne clusters have wide synthetic applicability, it is the utility of their corresponding cations that attracts attention. These metal stabilized "transient" carbocations can be employed as intermediates in synthetic transformations such as (1) the Nicholas reaction,[40] (2) intramolecular cyclizations,[41]

(3) biological transformations and more recently, (4) intramolecular allyl transfer reactions.[42] In the case of the Nicholas reaction (Scheme 1.2), the cationic cluster (**11**) can be treated with a nucleophile to generate a new cluster (**12**).

Scheme 1.2 : The Nicholas Reaction

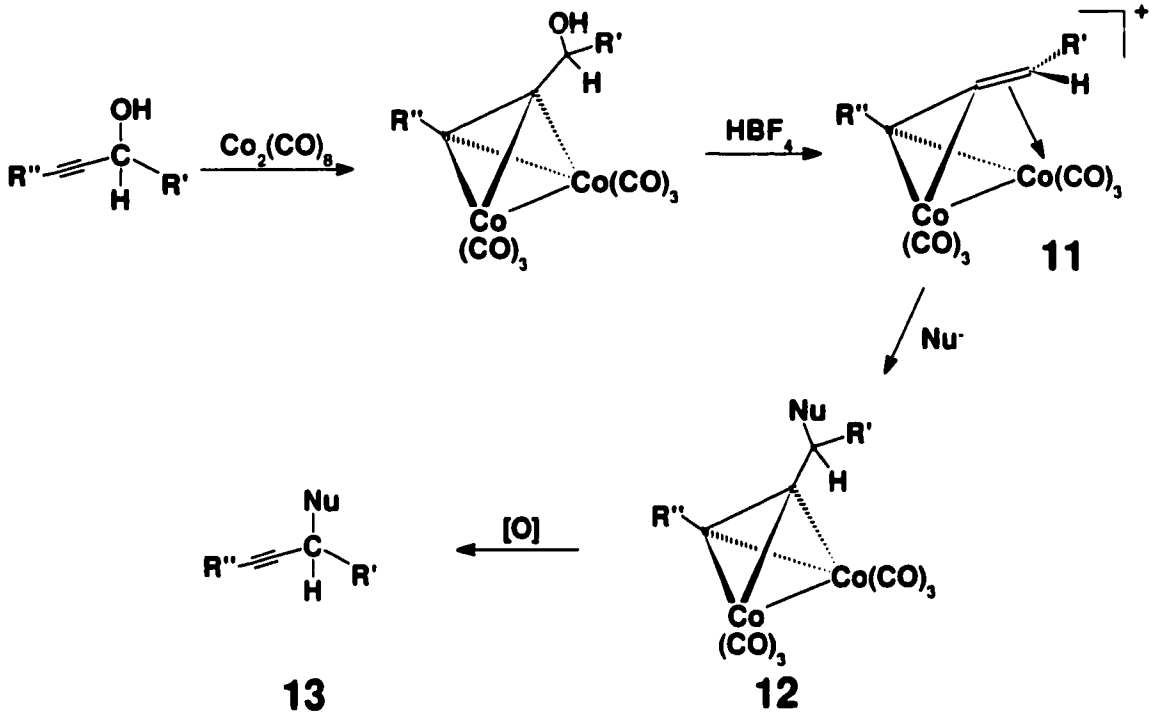

Typically, only weak nucleophiles such as alcohols, phenols (at oxygen) and amines are needed to react with the alkylidene carbon atom.[40] An added advantage of these systems is that the reaction may be performed without isolation of the cationic cluster (**11**). Moreover, the $Co_2(CO)_6$ moiety can be removed (if desired) under oxidizing conditions by using $Fe(NO_3)_3$,[43] $(NH_4)_2Ce(NO_3)_6$ (CAN),[44] or Me_3NO[45] to regenerate the free alkyne functionality, *viz.***13** (Scheme 1.2), a method that has been used in the synthesis of biologically active molecules such as enediynes,[46] (+)-begamide E,[47] blastinomycine,[48] tetrapyrroles,[49] and cyclocolorenone.[50] It is noteworthy that, upon protonation, the

elimination of the OH_2 leaving group in **14** apparently proceeds *via* an antiperiplanar transition state with anchimeric assistance from the metal center. Such a mechanism is consistent with the observed retention of configuration in nucleophilic displacement reactions of chiral clusters (**15**) (Scheme 1.3).[51,52]

Scheme 1.3

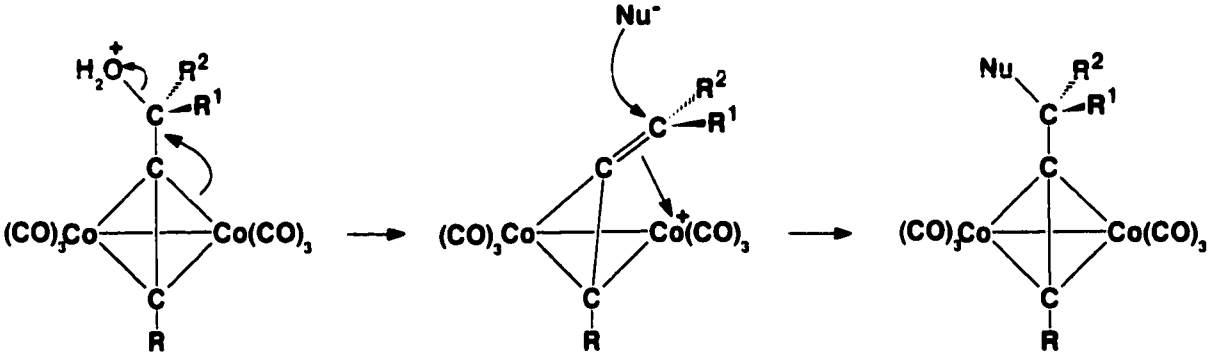

It has also been demonstrated by Grove and coworkers[53] that dicobalt hexacarbonyl stabilized propargyl cations assist in the facile assembly of tricyclic ring systems *via* intramolecular Friedel-Crafts alkylation on relatively electron rich aromatic rings (**16a** and **16b**) as shown below.

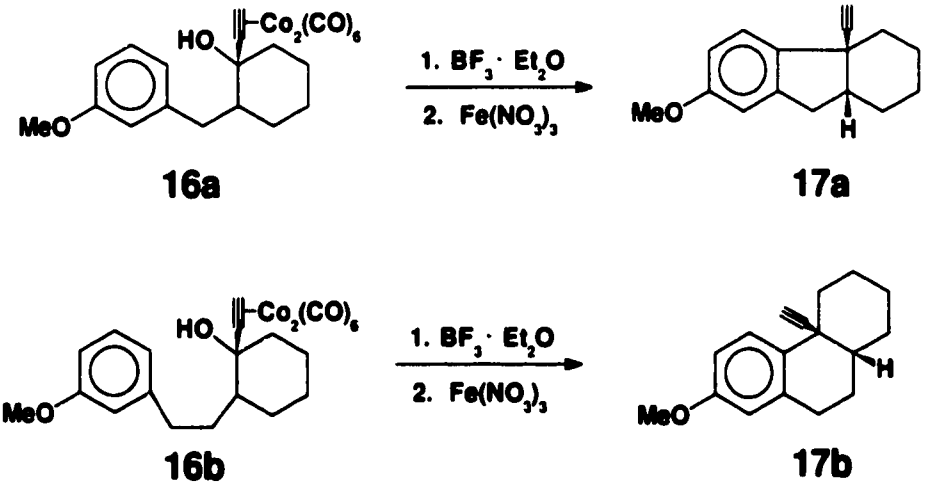

The cluster cation mediated cyclization products (**17a** and **17b**) had predominantly *cis* stereochemistry of the ring junction substituents. The mechanism for this process was was examined by Malisza and coworkers[54] who have recently shown that $Co_2(CO)_6$-alkyne substituents on cyclohexane moieties occupy the equatorial position. One could then envisage an attack of a pseudo axial aromatic ring (implying an equatorial location for the benzyl substituent) at the formally cationic carbon to yield the fused five and six membered rings.

More recently, Ruffolo *et al.*[42] have nicely shown that an intramolecular transfer of substituents promoted by cluster stabilized cations can occur. It was reported that, if the $Co_2(CO)_6$ cluster contained a potential site for protonation (e.g., an alcohol and an allylsilane) at opposite termini of the alkyne, intramolecular nucleophilic attack could occur (Scheme 1.4).

Scheme 1.4

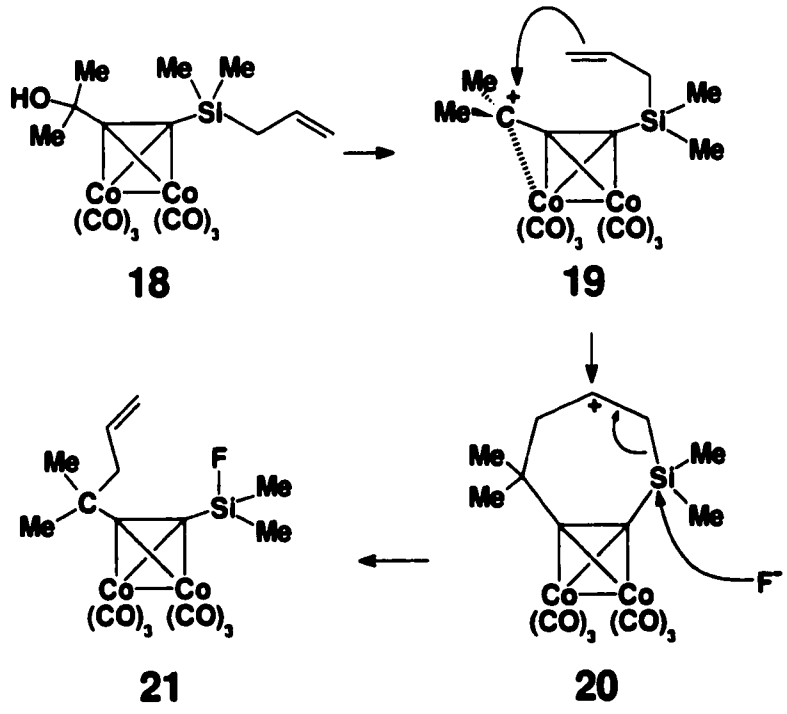

It was postulated that treatment of the cluster (**18**) with an acid would yield the cationic species (**19**), which would then undergo attack by the allyl substituent of the other terminus to generate the intermediate (**20**). Subsequent attack of the fluoride anion at silicon would then yield the isolated product (**21**). In effect, the overall process, is an intramolecular allyl transfer from one terminus to the other.

In comparison to the $CpMo(CO)_2$ moiety, the ability of a $Co(CO)_3$ group to stabilize a proximal CR_2^+ fragment, is much poorer (see preceding sections).[55] The difference in the stability of these cluster cations parallels the marked contrast in reactivity of $[Co_2(CO)_6]$- and $[Cp_2Mo_2(CO)_4]$-propargyl cations with nucleophiles. For example, acetone can be used as a solvent in the molybdenum systems, whereas in the cobalt cations the alkylidene fragment is susceptible to nucleophilic attack by acetone molecules.[56] The greater reactivity of cobalt cations has been rationalized in terms of pK_R^+ acidity values based on the following equilibrium (equation 4).[33c]

$$M_2L_6(HC{\equiv}C{-}CH_2OH) + H_3O^+ \rightleftharpoons M_2L_6(HC{=}C{=}CH_2)^+ + 2H_2O \quad (4)$$

$$M_2L_6 = Co_2(CO)_6 \text{ or } Cp_2Mo_2(CO)_4$$

The difference in the Lewis acidity values (for $Co_2(CO)_6$: pK_R^+ ~ -7; $Cp_2Mo_2(CO)_4$: pK_R^+ ~ 3) corresponds to approximately 10^{10} in terms of the K_R^+ values and is a testament to the relative stabilities of the cations. As a result, cobalt cations require much more acidic conditions (pH < 1) than do their molybdenum counterparts to remain stable in solution. Thus, stronger acids (such as HBF_4) are needed to protonate the neutral alkynol dicobalt clusters. Furthermore, in a kinetic study, Mayr and colleagues[57]

examined the reactivity of a wide-ranging series of nucleophiles with various cobalt cations, and their analysis was found to be in close argument with the literature reports.

1.5 The Isolobal Analogy

1.5.1 Background.

The concept of the isolobal relationship (denoted as ⟷) between the molecular fragments $(CH)^{3-}$ and $Co(CO)_3^{3-}$ has previously been mentioned. Although these moieties are neither isostructural nor isoelectronic, they possess frontier orbitals which appear very similar (not identical). The energy diagrams (deduced from EHMO calculations) for both $Co(CO)_3$ and CR are shown in Figure 1.10.

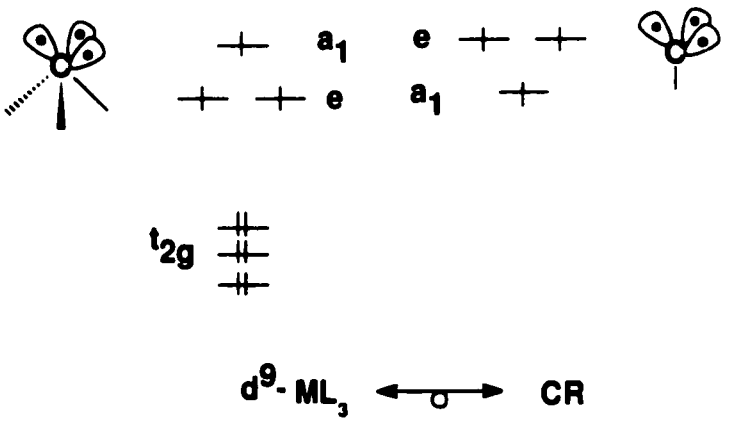

Figure 1.10 : Energy diagram for $Co(CO)_3$ and CH.

Hoffmann rationalized that the differences (i.e., the ordering of the a_1 and e energy levels) were of minor consequence, and that frontier orbital characteristics remained similar. In each case, both fragments can be thought of possessing three frontier orbitals

containing three electrons. Further support for the similarity of these two fragments is provided by the gradual metamorphosis of an organic to an inorganic tetrahedral cluster, as exemplified below:

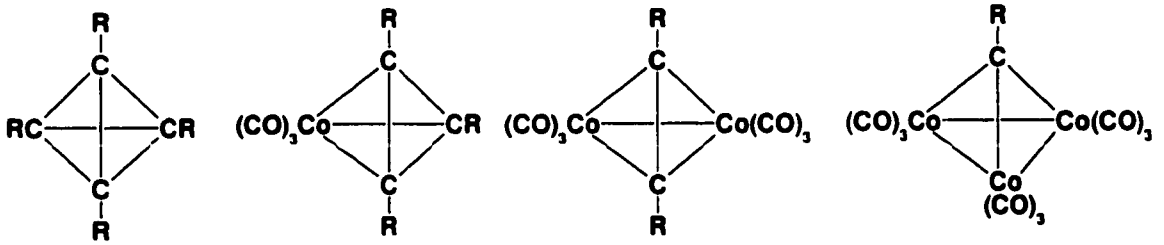

Hoffmann also showed that an isolobal relationship exists between the CR fragment and other transition metal moieties, such as $CpMo(CO)_2$ (a 3 electron donor), and it has already been shown that tetrahedrane clusters incorporating two $CpMo(CO)_2$ moieties exist as stable complexes. The isolobal relationships among some organic fragments with their organo-transition metal analogues are depicted below.

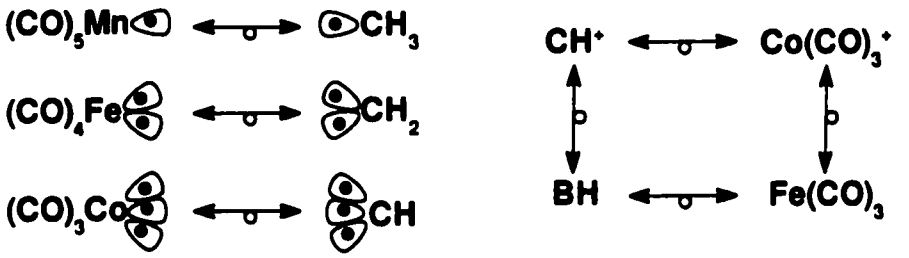

One can envision an even wider array of analogies (than those shown above) between organic and inorganic fragments, or even two distinct sets of organometallic fragments. The isolobal relationship, however, should also be viewed with caution. Although theoretically the concept allows for the interchanging of "similar" moieties, there is no guarantee that the replacement of one fragment by an isolobal partner will lead to the

existence of a stable new compound. For instance, the isolobal relationship between CH_2 and $Fe(CO)_4$ provides one example of the experimental limitations of the analogy. Ethylene, C_2H_4 can be viewed as the coupling product of two CH_2 fragments, and is a gas at room temperature. Replacement of one CH_2 unit by $Fe(CO)_4$ yields the carbenoid species, $(CO)_4Fe{=}CH_2$. However, if the both methylene fragments are replaced by $Fe(CO)_4$ units the analogy would, in principle, yield the unstable species $Fe_2(CO)_8$. species.

$$H_2C{=}CH_2 \longleftrightarrow (CO)_4Fe{=}CH_2 \longleftrightarrow (CO)_4Fe{=}Fe(CO)_4$$

"unstable"

1.5.2 The isolobal relationship between $Fe(CO)_3$ and $Co(CO)_3^+$.

By the same reasoning it should be formally possible to replace a $Co(CO)_3^+$ vertex by an $Fe(CO)_3$ moiety. The fragments are isoelectronic and possess three frontier orbitals containing two electrons for cluster bonding. The neutral $CoFe(CO)_6$ analogues of the $Co_2(CO)_6^+$ stabilized clusters can be prepared from the $Co_2(CO)_6$-alkynol dicobalt precursors, and the isolobal replacement of the $Co(CO)_3^+$ vertex by $Fe(CO)_3$ should in principle yield clusters that exhibit similar geometry, as shown in Figure 1.11.

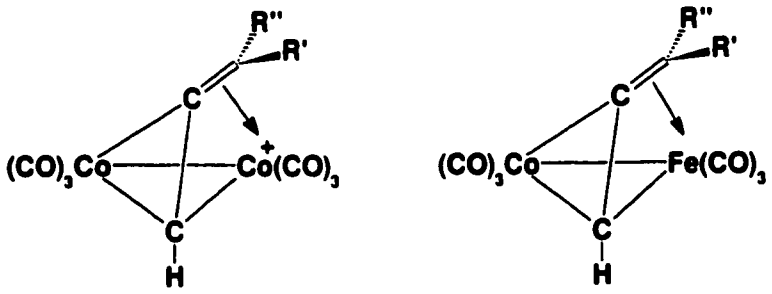

Figure 1.11: Structural comparison of a $Co_2(CO)_6^+$-cluster and an $FeCo(CO)_6$ analogue.

Indeed, the X-ray crystal structure of the neutral $(MeC{\equiv}C\text{-}CH_2)FeCo(CO)_5PPh_3$ species (**24**) has been determined and reveals that the alkylidene fragment leans towards the iron atom as expected (Figure 1.12).[58]

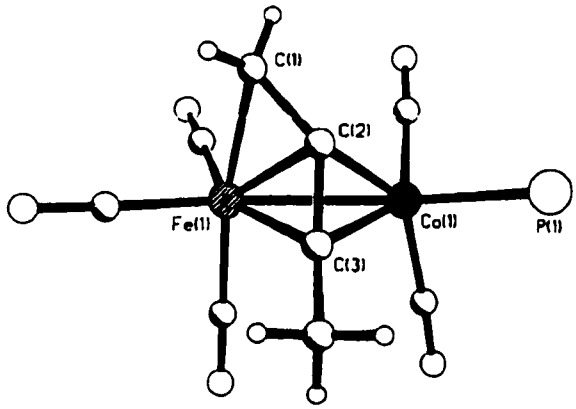

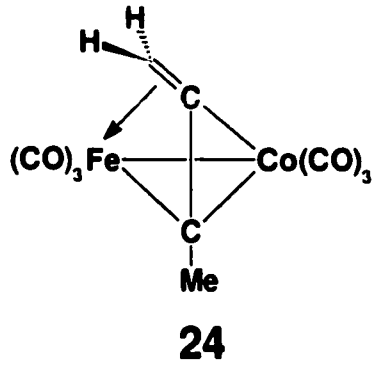

24

Figure 1.12 : X-ray structure of $(MeC{\equiv}C\text{-}CH_2)FeCo(CO)_5PPh_3$ (**24**).

Furthermore, it has been shown that the geometry exhibited by $(MeC{\equiv}C\text{-}CH_2)FeCo(CO)_5PPh_3$ (**24**) is in excellent agreement with EHMO calculations for the energy minimized structure of $[Co_2(CO)_6(HC{\equiv}C\text{-}CH_2)]^+$ for which no X-ray data are currently available.

Although the spectroscopic data of many of these iron-cobalt metal clusters have been reported, these species are typically isolated as oils and so far only one X-ray crystal structure of an iron-cobalt cluster is known.

1.6 *Objectives of the Project*

As has been alluded to previously, our interest lies in the preparation and characterization of metal-stabilized short-lived carbocationic intermediates. The goal of this research was not to stabilize "any cationic intermediate" as such a task would be

trivial and monotonous. More specifically, we have an interest in 4n π anti-aromatic compounds. The anti-aromaticity of the cyclopentadienyl (4π), indenyl (8 π), and fluorenyl (12 π) cations has received considerable attention from organic chemists, and one would logically expect these cations to decrease in stability from the fluorenyl cation (potential stabilization from two benzyl groups) to the cyclopentadienyl cation (no benzyl group stabilization). Our original goal was to investigate the stability of these cations from an organometallic perspective. Could we qualitatively determine (*via* variable-temperature NMR spectroscopy) any differences in electronic assistance these cationic ligands would require from a neighboring metal center (chapter 2)? Ultimately, if structures of these cluster cations were to be unambiguously determined by X-ray crystallography, the effect of "anti-aromaticity" in these compounds could perhaps be compared. In contrast to the study of these "anti-aromatic" compounds, the effect of a neighboring metal center on an aromatic moiety should be markedly different. We are interested in the effect that bulky substituents (e.g., chloro or phenyl groups) would have on Hückel-type aromatics; these might include the perchlorocycloheptatrienyl cation (or perchlorotropylium ion) $C_7Cl_7^+$. Our goal was to probe the effects of the chlorine substituents on the geometry of the seven-membered ring. Would a perchlorotropylium cation require assistance from a neighboring metal center? This thesis deals with aspects discussed above as well as the unanticipated problems encountered in attempting to achieve these goals.

Chapter Two

Anti-Aromatic Cations

2.1 Introduction: Background

The aromatic character and ready availability of cyclopentadienyl, indenyl and fluorenyl anions contrasts with the relative inaccessibility of the corresponding cations (**25-27**) which have been the subject of an extensive series of laser flash photolysis studies,[59] and also numerous mass spectrometric investigations.[60]

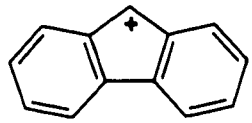

25

fluorenyl
12 π

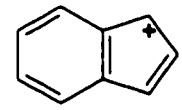

26

indenyl
8 π

27

cyclopentadienyl
4 π

Kinetic measurements have revealed that hydrolyses of 9-fluorenyl esters are retarded by a factor of approximately 10^7 relative to those of closely analogous benzhydryl systems which do not involve destabilizing effects.[61] The proposed anti-aromatic nature of the 9-fluorenyl cation (**25**) is supported by (1) the general 4n π rule, (2) the fact that the reported pK_R value for the 9-phenyl-9-fluorenyl cation (-10.8) is 4 units lower than the triphenyl methyl cation, Ph_3C^+ (-6.6), and (3) solvolysis reactions indicating that these species are much less reactive

than the corresponding benzhydryl derivatives. Nevertheless, the debate concerning the anti/non-aromatic character of the fluorenyl cation continues to attract attention.[14,62]

Despite repeated attempts, the isolation of the parent fluorenyl cation (**25**), $C_{13}H_9^+$ has remained elusive. Olah and coworkers[63] have shown that treatment of 9-fluorenol, 9-chlorofluorene, or 9-bromofluorene with FSO_3H, FSO_3H-SbF_5, or SbF_5 in SO_2ClF at -120 °C immediately yields dark, unidentifiable polymeric materials.

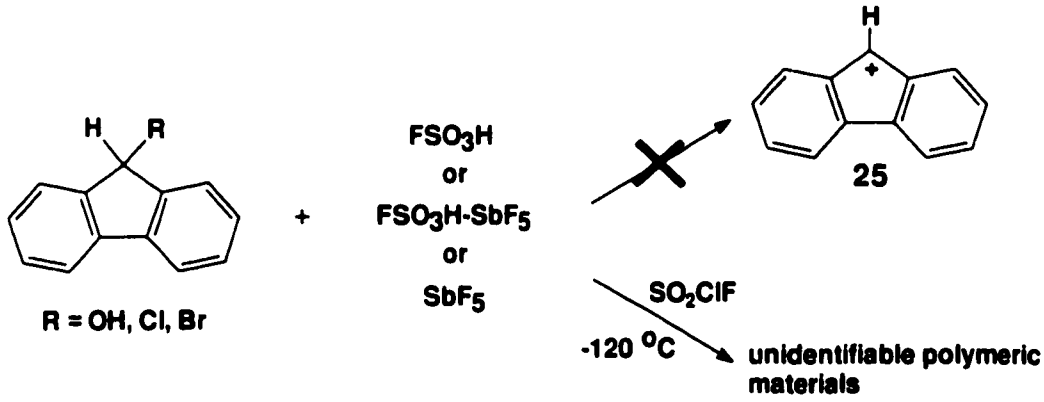

In contrast, under similar acidic conditions, benzhydryl alcohol yielded the stable diphenylmethyl cation characterized by its NMR spectra.

However, fluorenyl cations bearing either an alkyl, phenyl, chloro, ester, or hydroxy substituent at the C(9) position are preparable in a FSO_3H/SbF_5 or SbF_5/SO_2ClF solution at -78°C, and their ^1H and ^{13}C NMR spectra have been reported.[63,64,65] Furthermore, it was suggested that these 9-substituted fluorenyl cations did not involve antiaromatic destabilization effects. Novak and coworkers have investigated the proposed antiaromatic nature of the fluorenyl and 9-methyl-fluorenyl cations.[62a] Their investigation revealed that the fluorenyl system (**25**) was slightly less effective than the two phenyl groups of Ph_2CH^+ in stabilizing a positive charge and the difference in the stabilities of the two cations was

"only" 5.7 kcal/mol. Similarly, the 9-methyl-fluorenyl cation was shown to be of comparable stability (2.4 kcal/mol) to the α-methyl benzhydryl cation.

More recently, the postulated anti-aromatic nature of **25** has been analyzed computationally invoking the criteria for aromaticity. On the basis of magnetic susceptibility exaltation, the fluorenyl cation is considered *non-aromatic*, whereas the NICS criterion calculates the two benzyl rings as being "almost non-aromatic" and the central cyclopentadienyl ring as anti-aromatic.[14] Nevertheless, the question of the anti-aromatic nature of the fluorenyl cation (**25**) continues to attract attention.

In contrast to **25** and its derivatives, the 8π indenyl (**26**) and 4π cyclopentadienyl (**27**) cations are accepted as anti-aromatic on the basis of experimental and theoretical work. Consequently, the stability would be expected to decrease from **25** to **27** owing to the increasing anti-aromatic character. Very recently, Tidwell has provided clear experimental evidence for the transient intermediacy of the 1-methyl-2,4-bis-(*tert*-butyl)cyclopentadienyl cation, and has calculated that the relative rates of solvolysis of fluorenyl, indenyl, and cyclopentadienyl trifluoroacetates are approximately $3x10^4$, $3.5x10^2$, and 1, respectively.[66]

It has been suggested that the corresponding cyclopentadienyl cation, $C_5R_5^+$ (**28**) might rearrange through the square pyramidal (C_{4v}) geometry,[67] that could be categorized as a *nido*-octahedral cluster analogous to B_5H_9.[68] Attempts, however, to detect degenerate rearrangements of fluorenyl cations *via* such pyramidal intermediates were unsuccessful.[63]

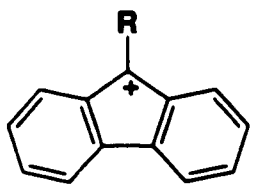

25

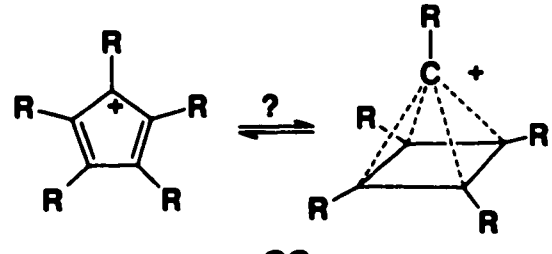

28

2.2 *Anti-Aromatic Cations : An Inorganic Approach*

Although studies involving these 4n π cations (**25-27**) have been widely investigated, the electronic nature of these systems has yet to be studied from an organometallic perspective. A different approach invokes the stabilization of such short-lived species as organometallic complexes,[24,69] and one can then take advantage of a variety of structural and spectroscopic techniques to probe their electronic requirements. More recently, examples of metal-stabilized transient intermediates have included X-ray crystallographic characterizations of the $[(endo\text{-}2\text{-propynylbornyl})Mo_2(CO)_4(C_5H_5)_2]^+$ and $(exo\text{-}2\text{-propynylfenchyl})Co(CO)_3Mo(CO)_2(C_5H_5)_2]^+$ cations, **29** and **30**, respectively.[55b,70] It was shown that the cluster cation in both cases was stable towards Wagner-Meerwein rearrangement (which is established for the free cation).

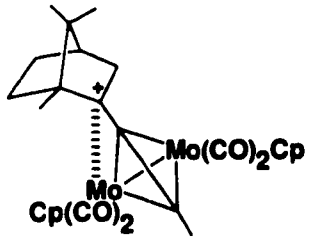

29

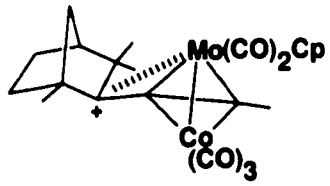

30

In a related study, Olah and de Meijere[71] have presented compelling NMR evidence that, unlike most cyclopropyl cations, the ferrocenyl-substituted system, **31**, does not ring-open to the corresponding allyl cation **32**.

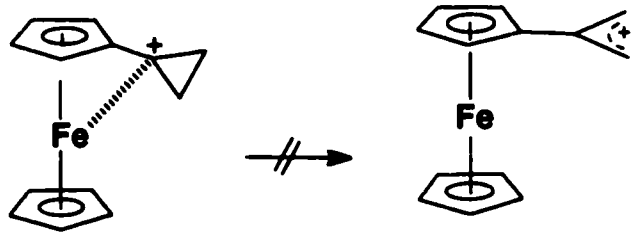

31 **32**

This chapter describes the investigation into the preparation and characterization of a series of fluorenyl, indenyl and cyclopentadienyl cations stabilized as their dicobalt hexacarbonyl cluster complexes. Although it has been shown that these types of systems do not give X-ray quality crystals, one of the primary interests has been in characterizing models for such cationic species, and the isolobal replacement of a $[Co(CO)_3]^+$ vertex by an $Fe(CO)_3$ moiety yields stable, neutral fluorenyl and indenyl complexes. These mixed metal complexes can be considered as models for their respective dicobalt hexacarbonyl clusters, and can be conveniently characterized by X-ray crystallography.

2.3 Results and Discussion

2.3.1 Fluorenyl- and indenyl-$Co_2(CO)_6$ cations.

With the ultimate aim of isolating a metal-stabilized fluorenyl cation, fluorenone was treated with the lithium salt of trimethylsilylethyne; subsequent quenching with water yielded 9-trimethylsilylethynyl-9-fluorenol (**33**). The alcohol (**33**) was then treated with $Co_2(CO)_8$ to give the tetrahedral dicobalt cluster (**34**) which exhibits six aromatic ^{13}C resonances (Figure 2.1). Protonation of **34** with HBF_4 in CD_2Cl_2 at -78°C resulted in the immediate development of a deep red coloration, indicating the formation of the cation (**35**). The ^{13}C NMR spectrum of **35** at -78°C exhibits thirteen resonances for the fluorenyl skeleton and eight of these peaks represent proton-bearing carbons. The spectral data require that these are grouped into two independent sets, each made up of four CH units, and it is evident from these data that the two six-membered rings are non-equivalent at low temperature, as anticipated for the unsymmetrical structure **35**, shown in Scheme 2.1

Scheme 2.1 : Synthetic route to Cluster Cation **35**.

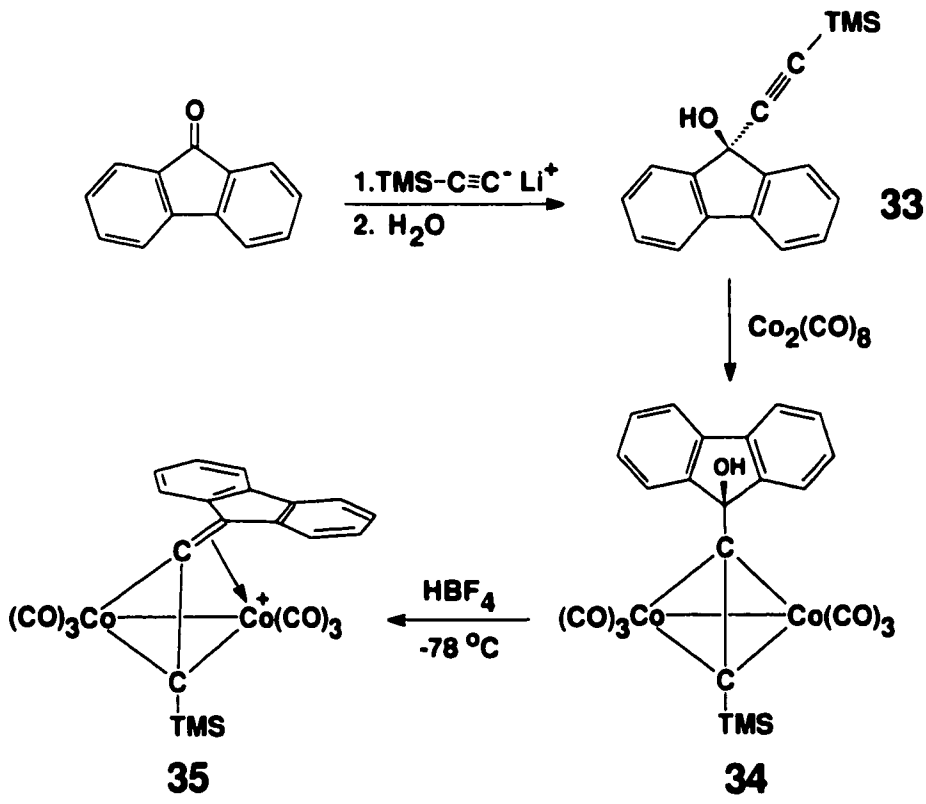

Selected variable-temperature ^{13}C NMR spectra of the cobalt-stabilized fluorenyl cation **35** are shown in Figure 2.1, and they reveal peak coalescences between symmetry-related resonances.

The Gutowsky-Holm approximation[72] yields a $\Delta G^{\ddagger}$ value of 12.2 ± 0.5 kcal mol^{-1} for the fluxional process that equilibrates the *exo* and *endo* six-membered ring environments; this activation energy is in the normal range for cobalt-stabilized tertiary carbocations.[73] Interestingly, the resonance attributable to C(9), the formally cationic carbon, exhibits a noticeable temperature-dependent chemical shift.

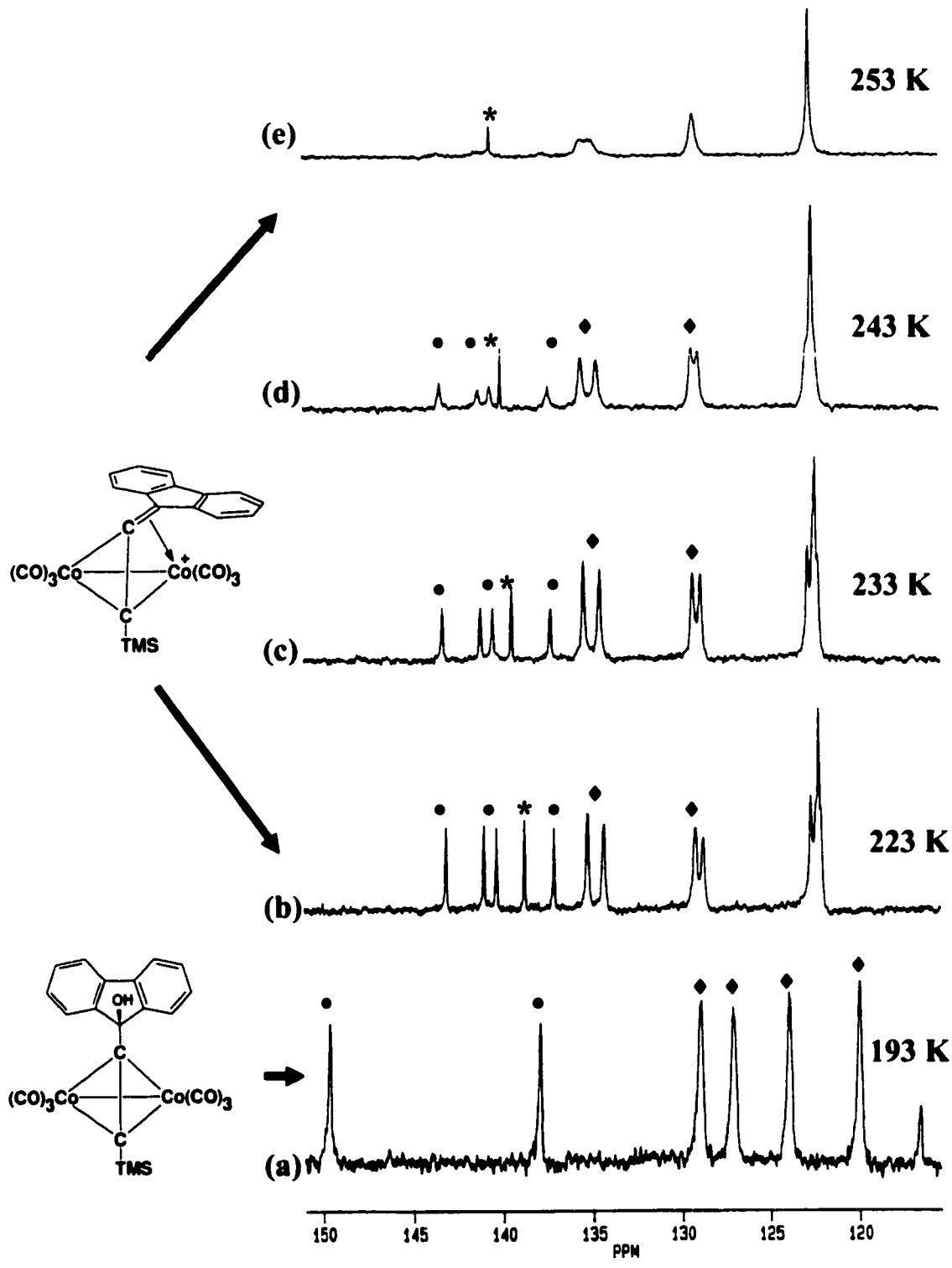

Figure 2.1: Selected Variable-Temperature ^{13}C NMR of **34** (a) and **35** (b-e). [Legend : (*) denotes C(9) resonance of the fluorenyl skeleton, (•) denotes ring junction carbon atoms, (♦) denotes fluorenyl *C*-H resonances].

In this particular system there is no probe, such as diastereotopic isopropyl methyl groups to follow the rate of the antarafacial migration of the fluorenyl ligand between metal centers, and it was necessary to incorporate a chelating bis(diphenylphosphino)methane (dppm) ligand to label the cobalt vertices, as in **36** (Scheme 2.2).

Scheme 2.2

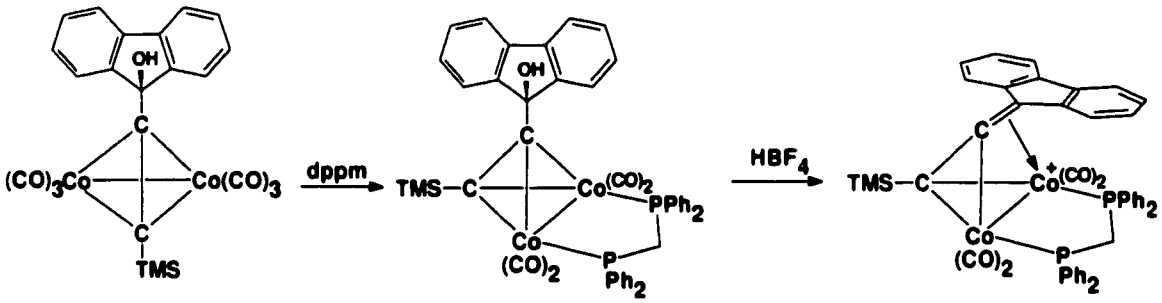

34 **36** **37**

The variable-temperature NMR data on the corresponding cation $[(C_{13}H_8\text{-}C{\equiv}C\text{-}SiMe_3)Co_2(CO)_4(dppm)]^+$, **37**, yield $\Delta G^{\ddagger}$ values of 11.4 ± 0.5 kcal mol^{-1} and 12.0 ± 0.5 kcal mol^{-1} for the antarafacial migration and *exo/endo* interconversion processes, respectively. The former was obtained from the temperature-dependent equilibration of the phosphorus environments (^{31}P NMR at 203 K shows peaks at 24.4 and 21.3 ppm, with $^2J_{P\text{-}P}$ = 69.7 Hz) as shown in Figure 2.2, while the latter was derived from the coalescence behavior of the fluorenyl ring carbon resonances. These two barriers do not differ significantly, as is commonly the case with tertiary cations.

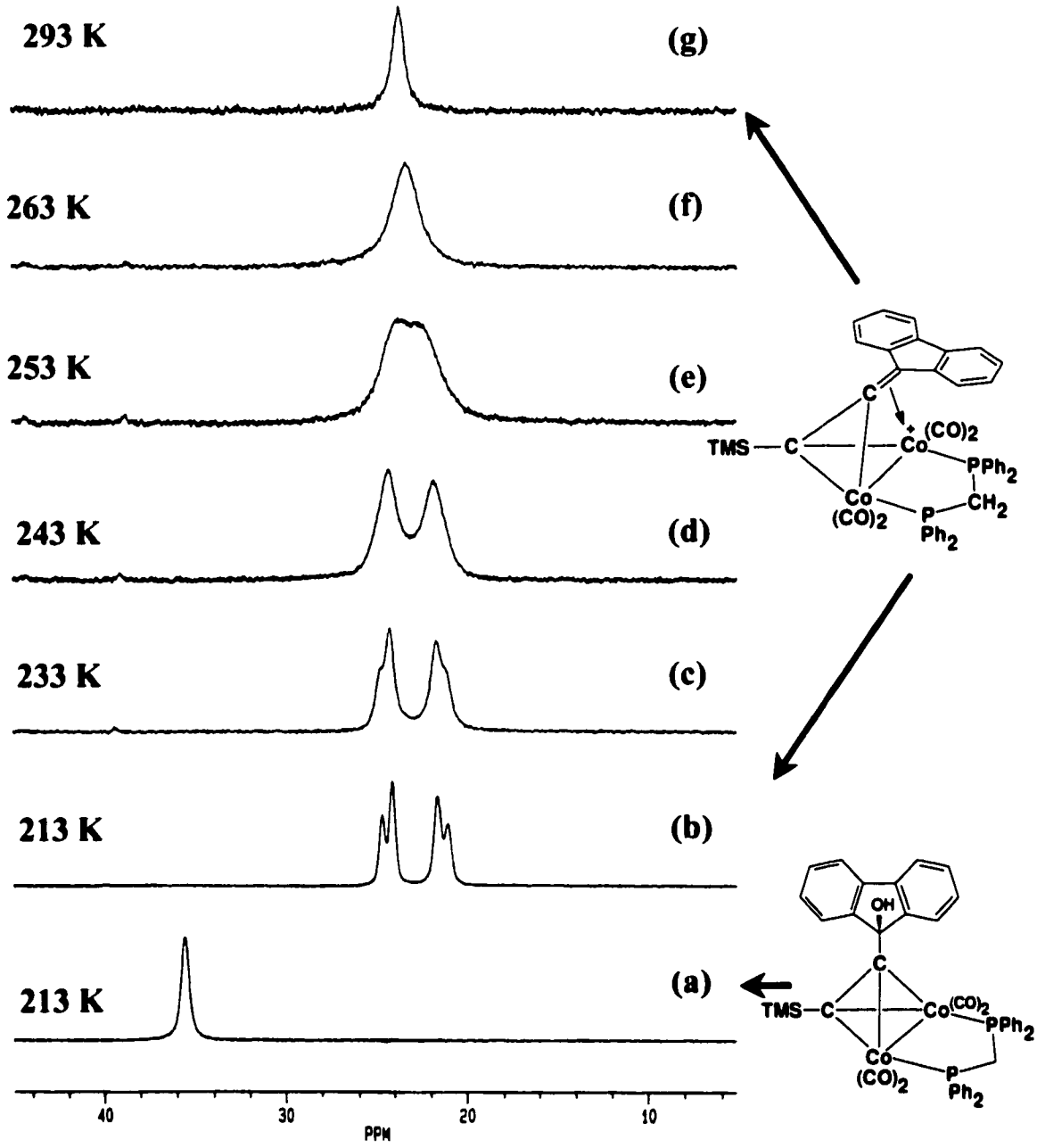

Figure 2.2: Selected Variable-Temperature ^{31}P NMR of Clusters **36** (a) and **37** (b-g).

Although indenone polymerizes readily, except at very low temperatures,[74] derivatives with bulky substitutents at the C(2) and C(3) positions can be prepared, and the 2,3-diphenyl derivative is commercially available. In an analogous fashion to the generation of the cluster-stabilized fluorenyl cation (**35**), the 2,3-diphenylindenol-$Co_2(CO)_6$ complex, (**39**), was prepared from its corresponding alcohol, (**38**), and protonated to yield the indenyl cationic cluster (**40**), as shown in Scheme 2.3 (see following page). The variable-temperature ^{13}C NMR spectra of **40** exhibit only four CH and four olefinic resonances assignable to the indenyl moiety. Furthermore, the spectra do not change with temperature until the onset of decomposition as one approaches 273 K. Thus, the cation appears to exist as a single isomer, but it is not possible to differentiate between isomers **40a** and **40b** in which the 6-membered ring is oriented *endo* or *exo*, respectively, relative to the cobalt-cobalt bond; this point is addressed below.

In an attempt to detect fluxional behavior in an indenyl cluster cation, the bis(diphenylphosphino)methane complex (**41**) was synthesized. The stereogenic center at the C(1) position results in diastereotopic cobalt vertices and, consequently, their attached phosphorus atoms (^{31}P NMR peaks at 34.6 and 30.4 ppm, with $^2J_{P\text{-}P}$ = 114.6 Hz). Subsequent protonation of **41** to form the cation (**42**) gives rise to a ^{31}P NMR spectrum exhibiting only two equally intense doublet resonances (at 38.8 and 15.2 ppm, with $^2J_{P\text{-}P}$ = 57.2 Hz) as shown in Figure 2.4. Once again, there is no change in the spectrum over a temperature range of 213-268 K, implying that a single isomer (with the benzo ring either *exo* or *endo*) is formed. Above this temperature, there is gradual line broadening and loss of the phosphorus-phosphorus coupling constant. From these observations, the barrier for the migration of the indenyl moiety between cobalt vertices can be estimated to be at least 13.5

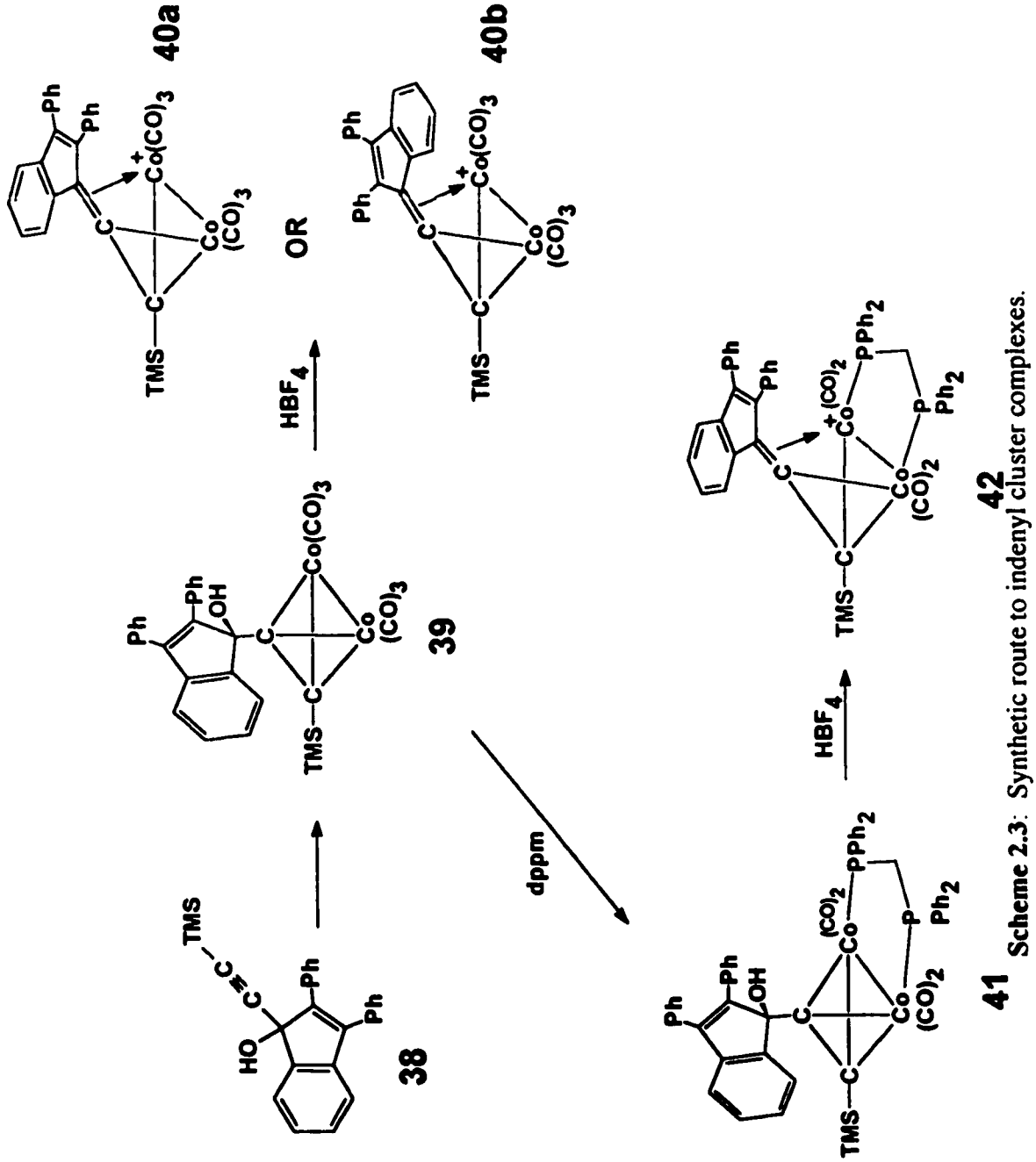

Scheme 2.3: Synthetic route to indenyl cluster complexes.

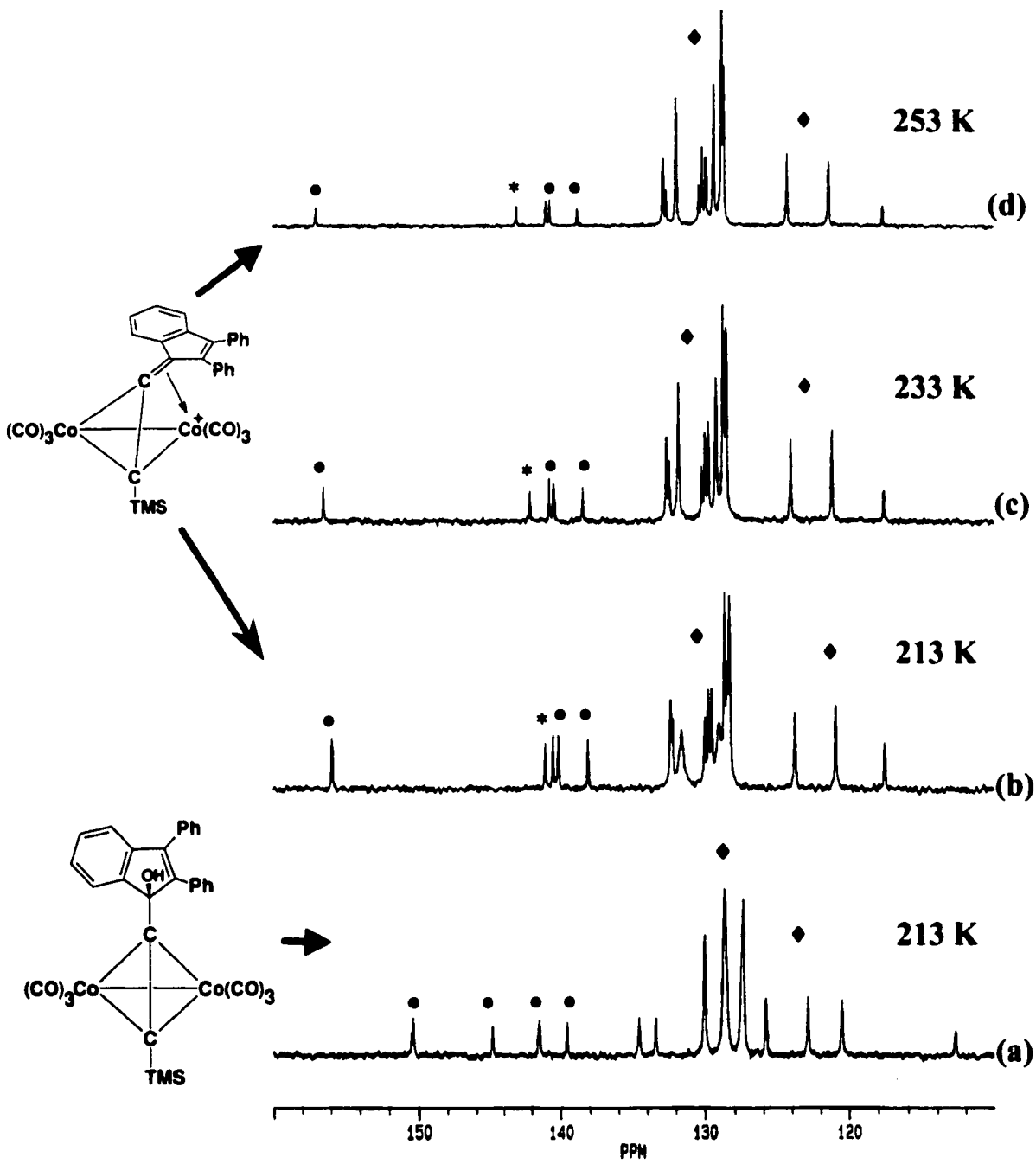

Figure 2.3 : Variable Temperature ^{13}C NMR of **39** (a) and **40** (b-d). [Legend : (*) denotes C(1) resonance of the indenyl skeleton, (•) denotes ring junction carbon atoms, (♦) denotes *C*-H resonances].

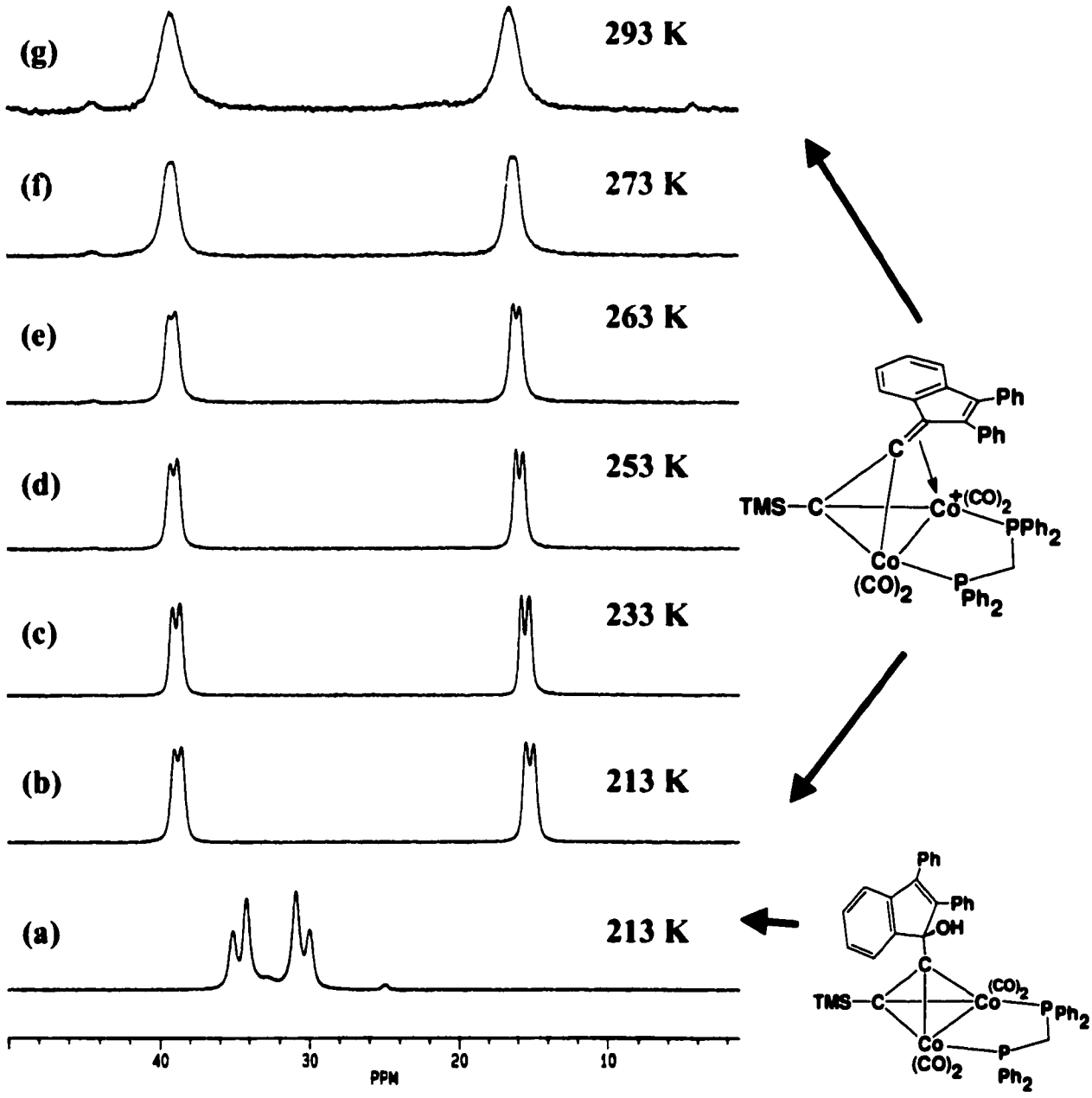

Figure 2.4 : Variable Temperature ^{31}P NMR of **41** (a) and **42** (b-g).

kcal mol^{-1}, but probably much higher.

2.3.2 Cyclopentadienyl-$Co_2(CO)_6$ cations.

In light of the above observations, it was anticipated that a cyclopentadienyl cation would require a greater amount of electronic assistance from the neighboring $Co(CO)_3$ group. However, the preparation of cyclopentadienyl analogues of the fluorenyl cation (**35**) and the indenyl cation (**40**) require the availability of cyclopentadienones, and such molecules only resist Diels-Alder dimerization when bulky substituents are present.[75] Thus, the cyclopentadienyl clusters (**43a,b**) and the corresponding cations (**44a,b**) derived from tetraphenylcyclopentadienone and from 2,5-diethyl-3,4-diphenylcyclopentadienone, respectively were prepared (*via* the synthetic methodology outlined in Scheme 2.3).

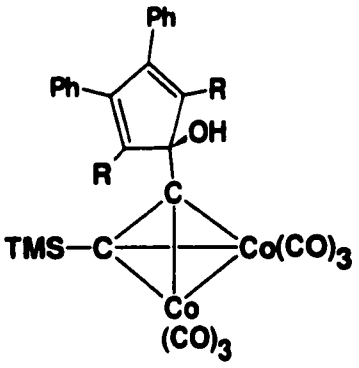

43a : R = Ph
43b : R = Et

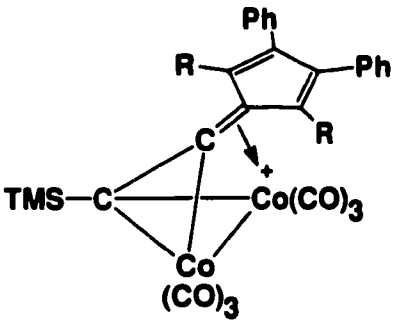

44a : R = Ph
44b : R = Et

The ^{13}C NMR spectra of **44a** are complicated by the presence of many overlapping phenyl resonances, but the diethyl cation (**44b**) provides a more tractable system. In this latter case, the carbon resonances of the two ethyl groups (CH_2's at 18.4 and 18.1 ppm; CH_3's at 16.8 and 14.7 ppm) are distinct over the range 213-263 K, at which temperature decomposition becomes evident. That is, there is no equilibration of the *exo* and *endo* ethyl environments on the ^{13}C NMR time-scale, as shown in Figure 2.5.

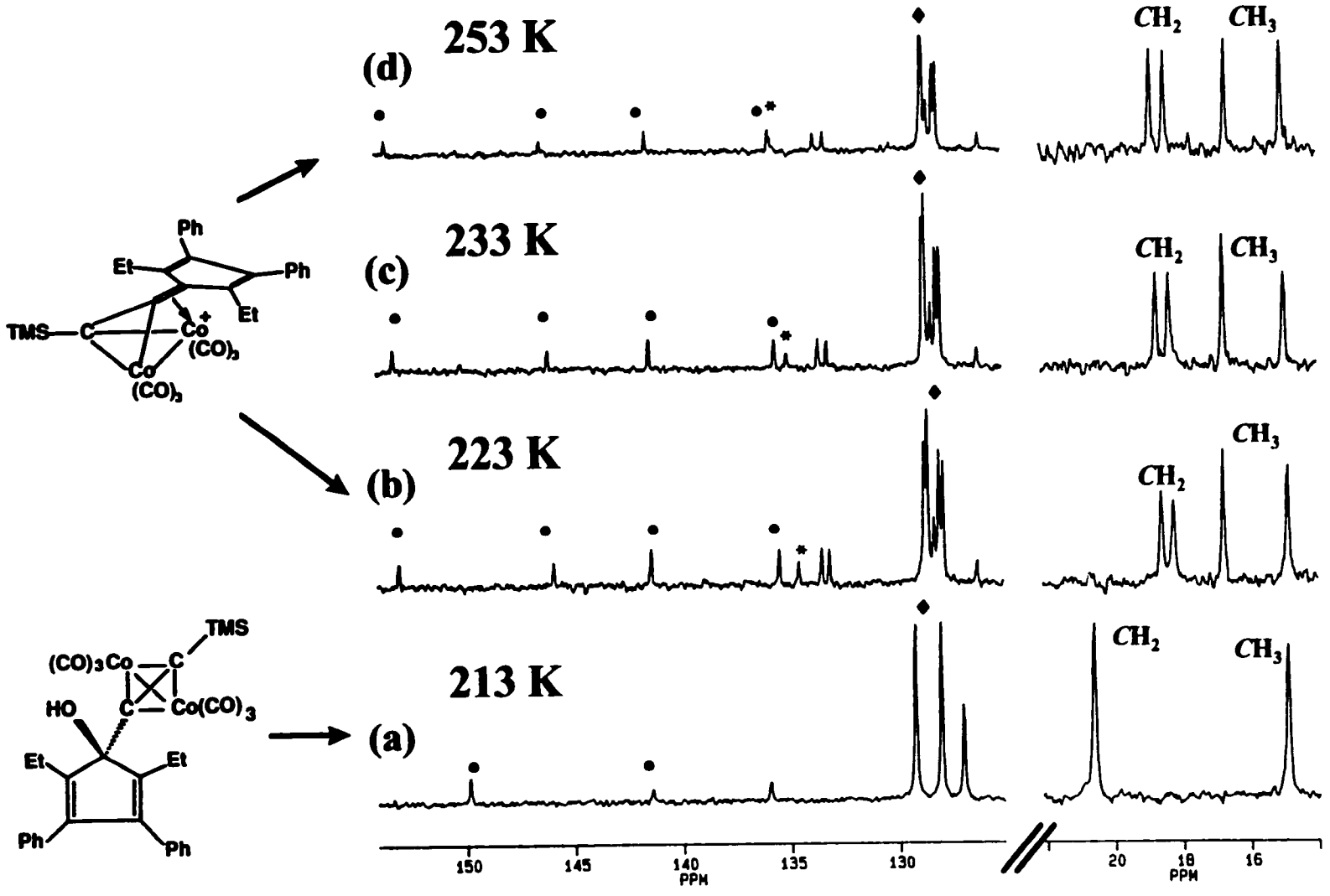

Figure 2.5 : Selected Variable Temperature ^{13}C NMR of **43b** (a) and **44b** (b-d). Legend :(*) = cationic carbon, (•) = *C*-H resonances, (♦) = cp ring carbons.

As was the case with the fluorenyl and indenyl analogues, the cyclopentadienyl clusters (**44a,b**) required the incorporation of a probe to investigate the antarafacial migration process. Thus, the dppm-substituted dicobalt clusters (**45a,b**) were synthesized and their corresponding cations (**46a,b**) examined; the ^{31}P NMR spectra at 193 K showed in each case the expected two doublets with $^{2}J_{P\text{-}P}$ values of 58.9 Hz and 60.5 Hz, respectively (Figure

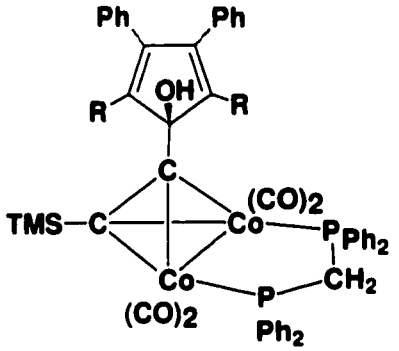

45a : R = Ph
45b : R = Et

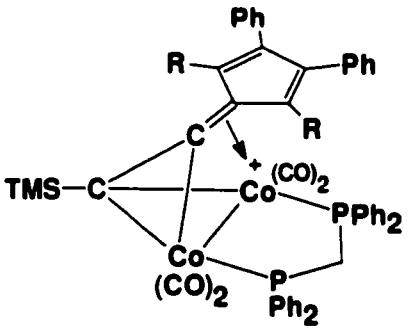

46a : R = Ph
46b : R = Et

2.6). These resonances for cation **46b** remain distinct until 248 K, at which temperature decomposition is evident. This data can only indicate a minimum $\Delta G^{\ddagger}$ value of $\approx$ 12 kcal mol^{-1}, but the true barrier toward migration of the cyclopentadienyl ligand between cobalt vertices is presumably considerably higher. In contrast, the temperature dependence of the spectrum of **46a** is surprisingly different as there is a collapse of the phosphorus coupling constants at 203 K. Furthermore, the coalescence of the phosphorus resonances is observed at 233 K, yielding a $\Delta G^{\ddagger}$ value of $\approx$ 9.6 kcal mol^{-1}. The marked difference in the dynamic properties of **46a,b** is attributed to the steric interactions of the cyclopentadienyl phenyl substituents with the PPh_2 groups of dppm.[76] Thus, because of the steric interactions in **46a**, it is conceivable that the interatomic distance between the metal center and the cyclopentadienyl ligand would be greater than that in **46b**. Moreover, without X-ray

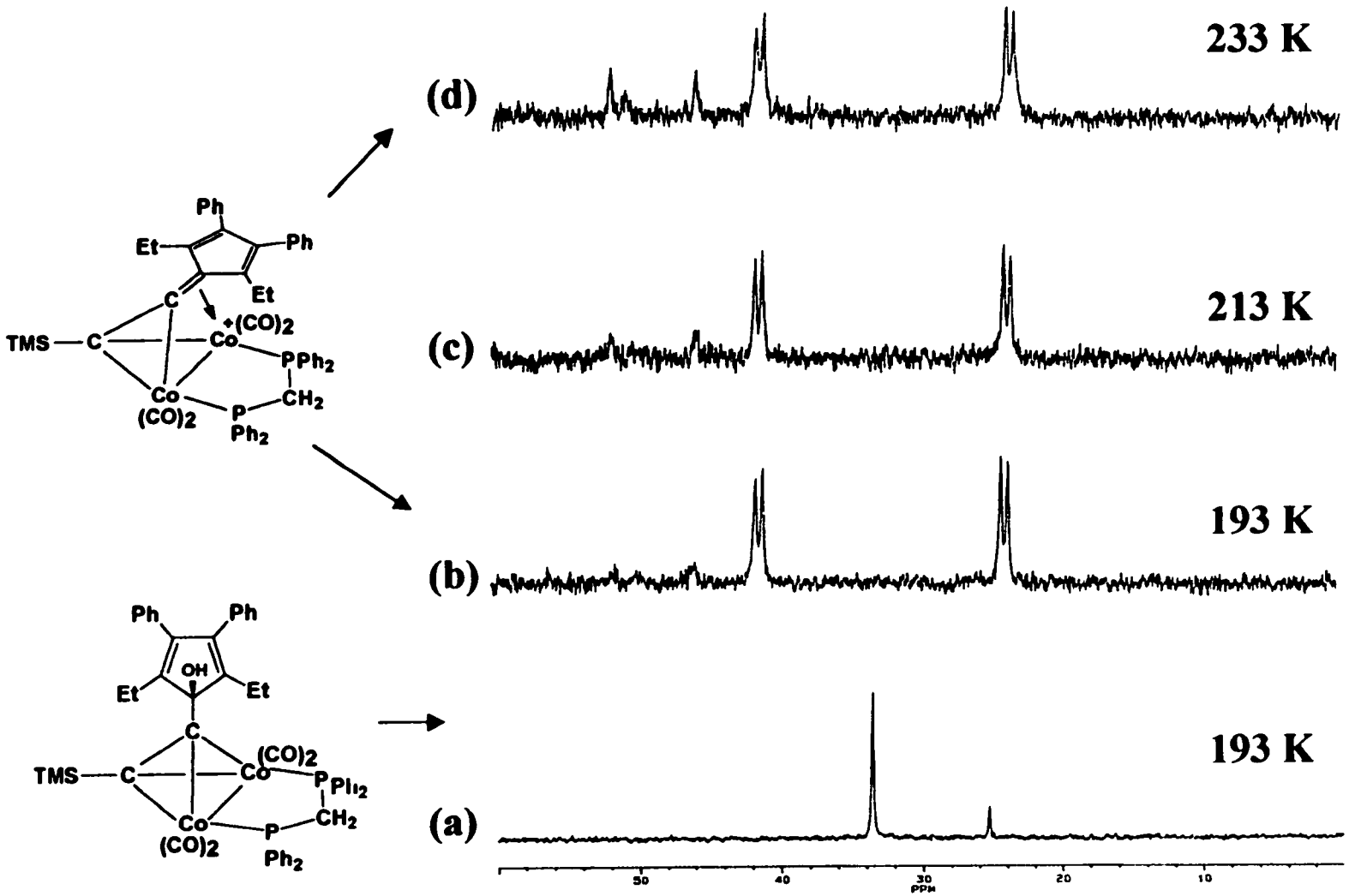

Figure 2.6 : Variable Temperature ^{31}P NMR Spectra for Cluster **45b** (a) and **46b** (b-d)

crystallographic data, one cannot be certain whether the dppm ligand bridges axial or equatorial sites.

2.3.3 Fe-Co Complexes: Models for $Co_2(CO)_6$- cluster cations.

Not surprisingly, our attempts to isolate crystals of the dicobalt cluster cations met with little success. However, it has been shown that isolobal substitution of a $Co(CO)_3^+$ vertex in $[Co_2(CO)_6(HC{\equiv}C\text{-}CR_2)]^+$ by an $Fe(CO)_3$ unit yields $[CoFe(CO)_6(HC{=}C{=}CR_2)]$. These neutral iron-cobalt clusters have been suggested as excellent models for the structure of their corresponding dicobalt cluster cations.[77,78] This view is further supported by molecular orbital calculations which yield almost identical energy-minimized geometries for such pairs of clusters. For this reason, the synthesis and structural characterization of the neutral cluster [($Me_3SiC{=}C{=}$fluorenyl)$FeCo(CO)_6$], **47** was carried out.

The neutral $Fe(CO)_3$ analogues of the $Co(CO)_3^+$ cationic clusters can be prepared directly from cobalt precursors. Thus, treatment of (propargyl alcohol)$Co_2(CO)_6$ with $Fe(CO)_5$ in refluxing acetone yields ($HC{=}C{=}CH_2$)$FeCo(CO)_6$, **48**; this same reaction is also applicable to the diol ($HOCH_2\text{-}C{\equiv}C\text{-}CH_2OH$)$Co_2(CO)_6$ which, upon treatment with $Fe(CO)_5$ in acetone, gives ($CH_2{=}C{=}C{=}CH_2$)$Fe_2(CO)_6$, **49**, as depicted in Scheme 2.4.[79]

Scheme 2.4

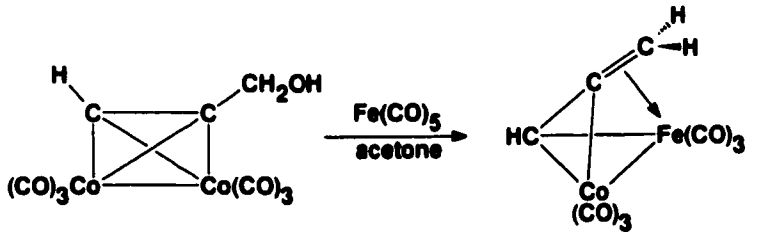

48

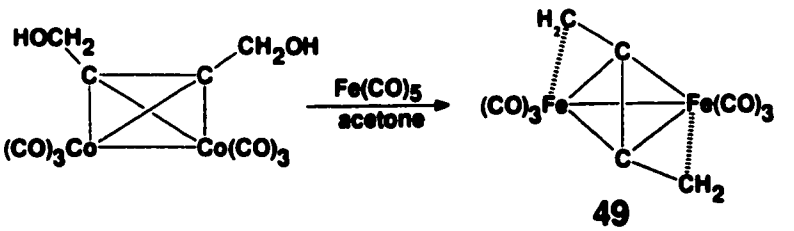

49

One might suggest that these (butatriene)$Fe_2(CO)_6$ complexes[80] may be regarded as models for the corresponding dicationic di-cobalt clusters. In particular, [bis(biphenylene)butatriene]$Fe_2(CO)_6$ (**50**)[81] which has been prepared directly from the cumulene, may be regarded as a model for the dication (**51**).

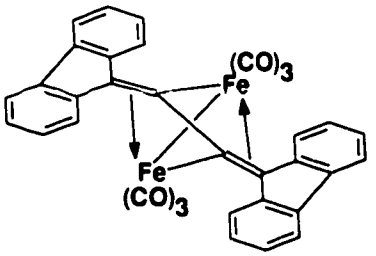

50

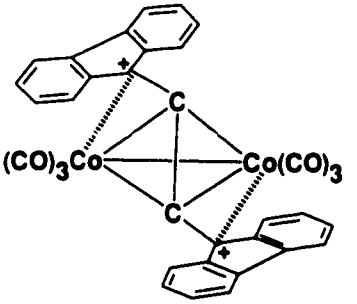

51

The reaction of (9-trimethylsilylethynyl-9-fluorenol)$Co_2(CO)_6$ (**34**) with $Fe(CO)_5$ in refluxing acetone gave, after chromatographic separation, crystals of [$FeCo(CO)_6$(TMS-C=C=fluorenyl)] (**47**) whose structure appears as Figure 2.7. The bending of the fluorenyl unit towards the iron atom is quite evident; the Fe(1)-C(9) interatomic distance is 2.626(11) Å and the Fe(1)-C(10)-C(9) angle is 102.4°.

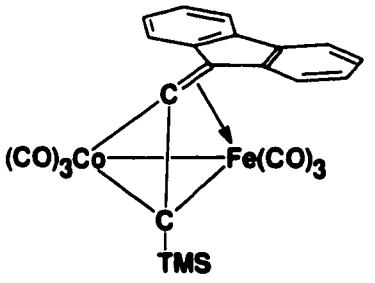

47

These may be compared with the EHMO-calculated values of 2.73 Å and 108° (see below). Furthermore, the C(11)-C(10) and C(10)-C(9) distances are 1.351(8) and 1.348(9) Å, respectively, and these values appear to be more indicative of an allenyl C=C=$C_{13}H_8$ system than of an acetylenic C≡C-$C_{13}H_8$ linkage. It is also noteworthy that the peripheral six-membered rings are each bent away from the central five-membered ring through

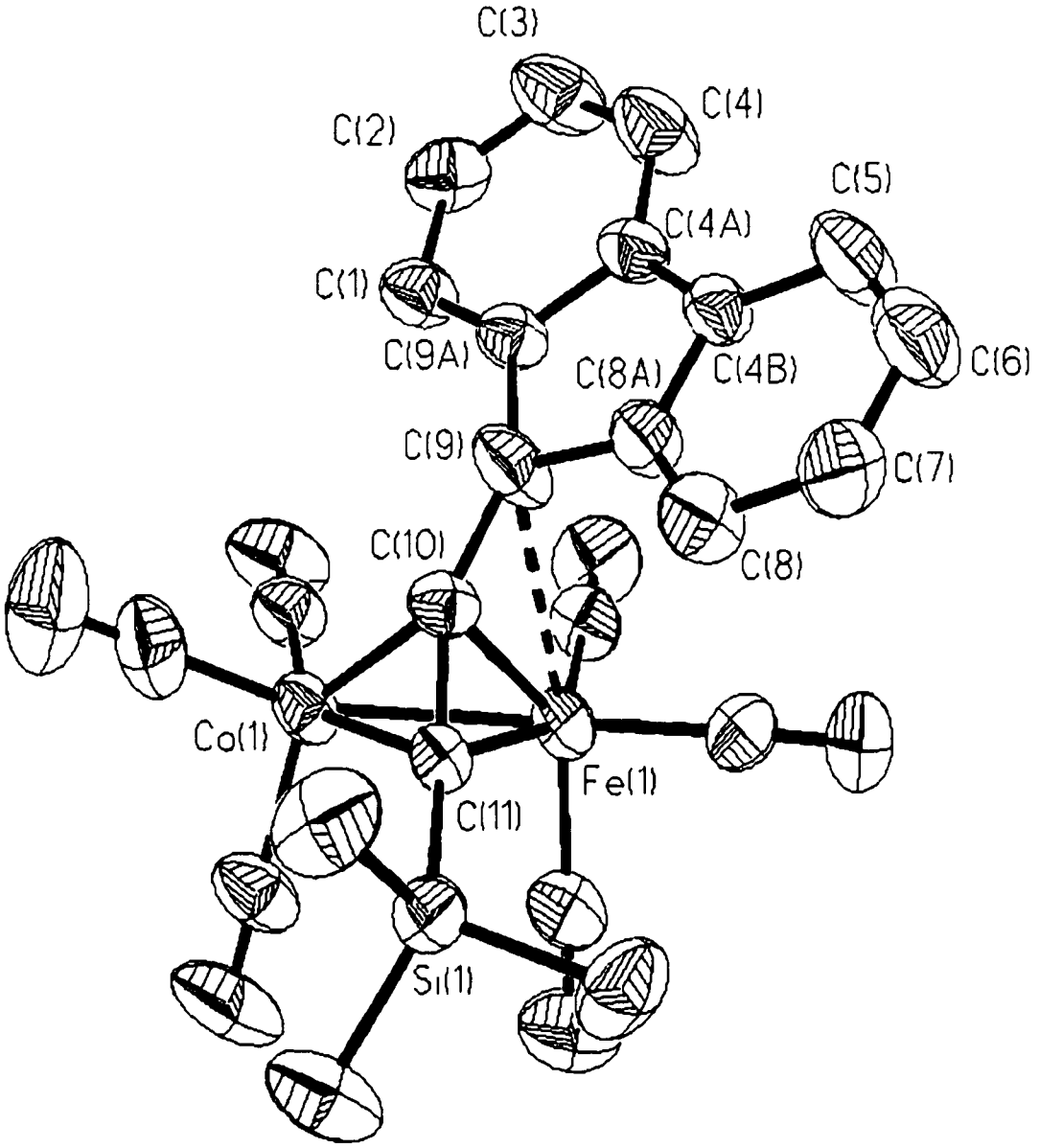

Figure 2.7 : Molecular structure of **47** (30 % probability ellipsoids). Selected bond lengths (Å) and angles (deg). Fe(1)-C(9) 2.626 (11), C(9)-C(10) 1.351 (8), C(10)-C(11) 1.348 (9), Fe(1)-C(10)-C(9) 102.4 (3).

approximately 5°.

Although it is difficult to differentiate crystallographically between the cobalt and the iron atoms in such a molecule, the structure can be rationalized by application of the electron counting rules. For example, if the structure were drawn with the fluorenylidene ligand coordinated to the cobalt atom, the electron counts at Co and Fe would be nineteen and seventeen, respectively, unless the cluster is a zwitterion, as shown in **52**. Furthermore, the location of the cobalt atom in **47** and **53** is supported by an examination of the ^{31}P NMR spectrum of $(MeC{\equiv}C\text{-}CH_2)FeCo(CO)_5PPh_3$ (**24**) which indicated an enhanced broadening of the phosphorus resonance due to its attachment to the quadrupolar ^{59}Co nucleus.[58]

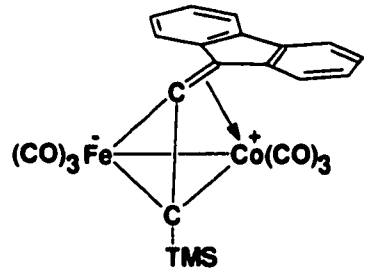

52

Stimulated by this result, the synthesis of the 2,3-diphenylindenyl iron-cobalt cluster was attempted. Indeed, treatment of the 2,3-diphenylindenol-dicobalt cluster (**39**) with $Fe(CO)_5$ in excess acetone yielded X-ray quality crystals of the mixed metal cluster **53**, and the structure appears as Figure 2.8. The orientation of the 6-membered ring in the *endo* position is readily apparent (suggesting that the corresponding dicobalt cationic cluster exists as the *endo* isomer **40a**.

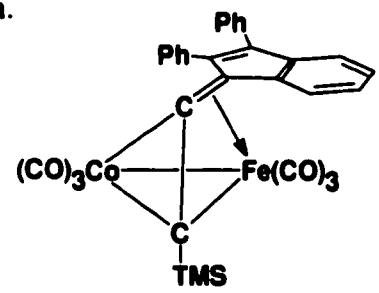

53

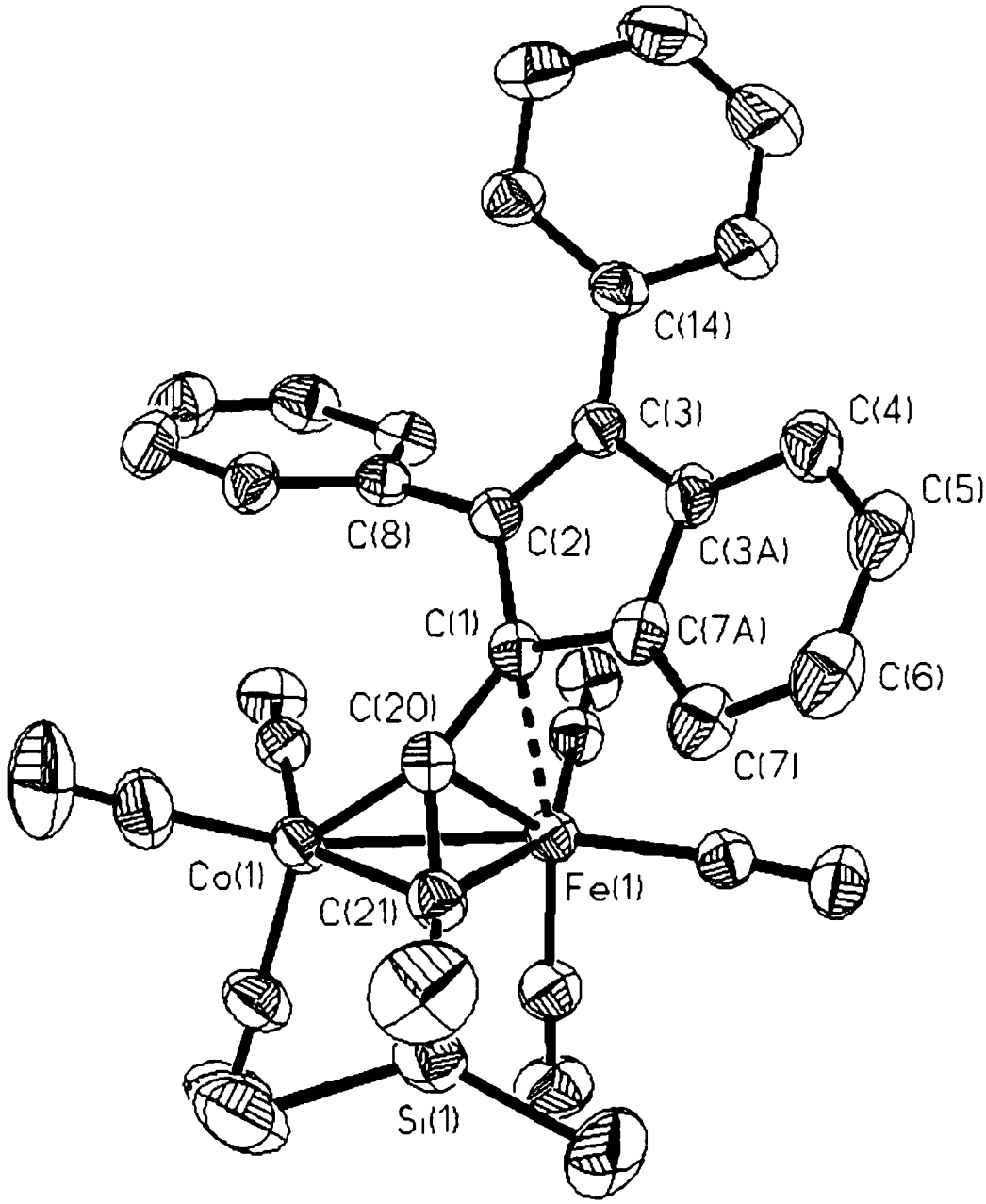

Figure 2.8 : Molecular structure of **53** (30 % probability ellipsoids). Selected bond lengths (Å) and angles (deg). Fe(1)-C(1) 2.346 (2), C(1)-C(20) 1.387 (4), C(20)-C(21) 1.355 (4), Fe(1)-C(20)-C(1) 85.4 (2).

However, the most important observation is the Fe-C(1) distance in **53**, which is now only 2.346(2) Å, markedly shorter than the corresponding Fe-C(9) value in the fluorenyl analogue (**47**) as well as the Fe(1)-C(20)-C(21) bend angle of 85.4(2). As with **47**, the alkyne-derived unit exhibits allene-like character; the C(1)-C(22) and C(22)-C(23) distances are 1.387(4) Å and 1.355(4) Å, respectively. These significant differences in interatomic distances of Fe-C_β suggest that the 8π indenyl ligand requires greater electronic assistance from the iron metal than does its 12π fluorenyl counterpart.

Attempts to extend this series to synthesize the analogous iron-cobalt clusters bearing 4 π cyclopentadienyl moieties, *i.e.* neutral analogues of cations **44a** and **44b**, were unsuccessful and instead, yielded, complexes of the type $(Co_2(CO)_6[TMS\text{-}C{\equiv}C\text{-}C_5R_4]Fe(CO)_2H$ in which the incoming iron carbonyl moiety binds in an η^5 fashion to the cyclopentadienyl ring. The discussion of the X-ray structures of these trimetallic systems and their mechanistic implications is deferred to Chapter Three.

It is clearly relevant to compare the structures of the iron-cobalt fluorenyl cluster (**47**) and the di-iron fluorenylidene complex (**50**). The latter determination dates back 25 years and was obtained from film data; moreover, no absorption correction was applied.[81] Nevertheless, the essential features of the molecular geometry are clear. The triene backbone in **50** is no longer linear, and the fluorenyl moieties lean toward the iron atoms. The quoted Fe•••CR_2 distances are approximately 2.40 Å.

When we compare the structures of the known vinylidene clusters in which the capping group leans towards an $Fe(CO)_3$ vertex, it is clear that the Fe•••CR_2 distance is a sensitive probe of the strength of this interaction. To put this in perspective, we note that a comprehensive survey of the Mo•••C^+ distances in clusters of the type

$[Cp_2Mo_2(CO)_4(RC{\equiv}C\text{-}CR'R'')]^+$ reveals that the molybdenum-to-carbocation distance is in the range 2.44-2.55 Å for primary cations, but increases to 2.61-2.63 Å for secondary cations, and can reach 2.74-2.92 Å for tertiary carbocations.[24,33] Moreover, there is a very clear inverse relationship between Mo•••C^+ distances parameter and the NMR-derived activation energies for antarafacial migration between molybdenum centers, i.e., the longer the Mo•••C^+ bond, the lower the barrier.

There are apparently only three relevant X-ray crystal structures in which $(OC)_3Fe{\bullet\bullet\bullet}CH_2$ distances have been reported.[82] In $Cp_2W_2(CO)_4Fe(CO)_3\text{-}C{=}CH_2$ (**54**),[83] $(MeC{=}C{=}CH_2)Fe(CO)_3Co(CO)_2PPh_3$ (**55**),[58] and $(CH_2{=}C{=}C{=}CH_2)Fe_2(CO)_5PPh_3$ (**56**),[80a] the iron-carbon distances are 2.21 Å, 2.195 Å, and 2.208 Å, respectively. These relatively short bonds can be considered as arising from the interaction of CH_2^+ (*i.e.* primary) cations with $[Fe(CO)_3]^-$ vertices. In contrast, in $(Me_2C{=}C{=}C{=}CMe_2)Fe_2(CO)_6$,[80b] and $(Me_3SiC{=}C{=}$fluorenyl$)FeCo(CO)_6$ (**47**) the Fe•••C interatomic distances of 2.401 Å and 2.633 Å, respectively, are a manifestation of the weaker bonding between a tertiary cation and the formally anionic $Fe(CO)_3$ moiety. The interactions of the ligands in **47** and **53** with the $Fe(CO)_3$ vertex are depicted in Figure 2.9 for comparison.

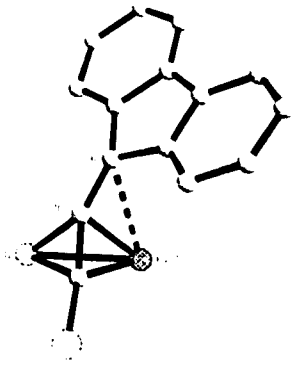

47

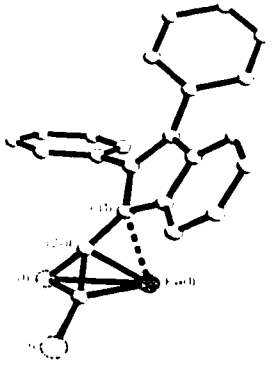

53

Figure 2.9 : Comparison of the Interaction of Fe-C in **47** and **53**. For clarity, only the tetrahedral cluster cores are shown.

The relatively short (2.347 Å) Fe-C(1) bond in the indenyl cluster (**53**) supports the hypothesis that the less stable "indenyl cation" has more need of electronic assistance from the "$Fe(CO)_3$" unit than does a "fluorenyl cation". It would be interesting to synthesize an extended series of such iron-cobalt clusters in order to probe the effect of changing the character of the vinylidene moiety.

2.3.4 Extended Hückel Molecular Orbital (EHMO) calculations.

Molecular orbital calculations at the extended Hückel level have allowed some understanding of the factors controlling the geometry of metal-stabilized cluster cations.[84] It has previously been suggested that when the formally sp^2-hybridized carbocationic center is allowed to lean towards a metal vertex, the enhanced overlap between the virtual *p* orbital on the CR_2^+ moiety and a filled metal *d* orbital of suitable symmetry leads to marked stabilization of the system. Figure 2.10 shows the result of bending a cyclopentadienyl cation towards one of the cobalt vertices in $[(C_5H_4\text{-}C{\equiv}CR)Co_2(CO)_6]^+$; the total electronic energy is minimized at a bend angle, θ, of approximately 35°, after which point unfavorable steric interactions with the carbonyl ligands begin to dominate. Concomitantly, the LUMO, which arises from out-of-phase overlap between the aforementioned carbon *p* orbital and metal *d* orbital rises sharply in energy, thus markedly increasing the HOMO-LUMO gap.

For the fluorenyl cluster cation (**34**) EHMO calculations predict a θ value of 25°, and a $Co{\cdots}C^+$ distance of 2.71 Å for the energy-minimized geometry. Calculations for the analogous indenyl and cyclopentadienyl clusters, **57** and **58**, suggest somewhat larger θ values (**57**: θ = 30°, $Co{\cdots}C^+$ = 2.62 Å; **58**: θ = 35°, $Co{\cdots}C^+$ = 2.53 Å), as anticipated for the enhanced anti-aromatic character of these ring systems.

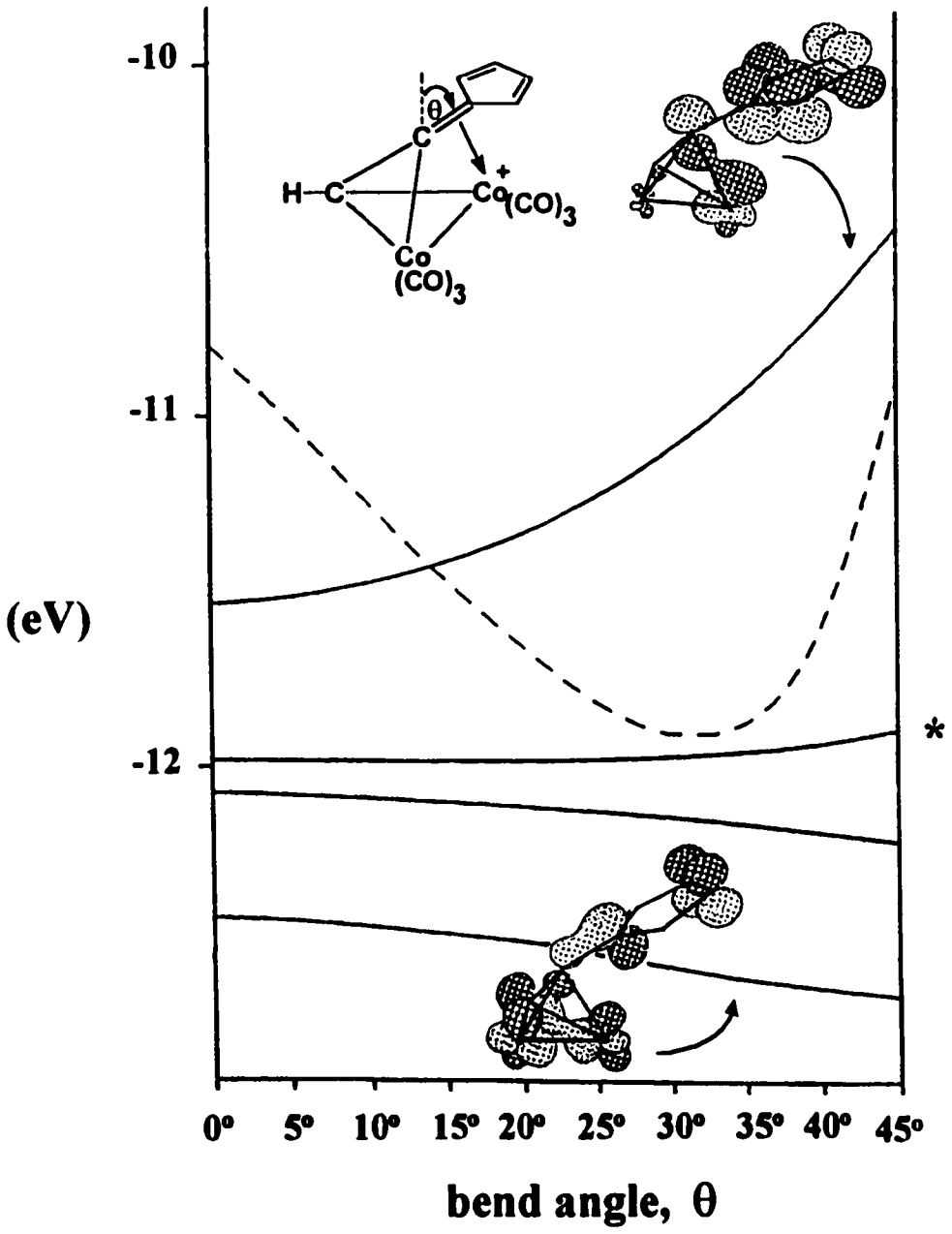

Figure 2.9 : EHMO-derived Walsh diagram showing the effect of bending a cyclopentadienyl cation towards a cobalt vertex. The HOMO is denoted by (*) and the total energy is indicated by the dashed line, which is drawn to a different scale.

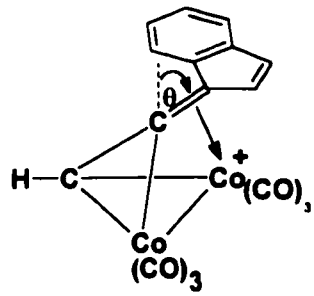

57

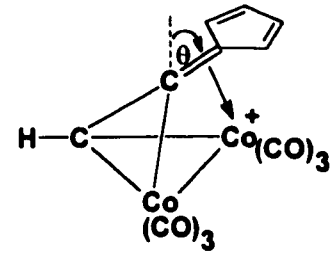

58

Although it is assumed that computations at a higher level of theory would lead to better calculated geometries and more reliable energy values, the difference in electronic requirements of these 4n π cations is evident.

In contrast to species that require varying degrees of a metal•••C^+ interaction to help alleviate a developing positive charge, it is also relevant to note that cationic fragments in which the charge can be readily delocalized may have no need of assistance from neighboring organometallic units. For example, the pyrylium salts (**59**) and (**60**),[85] and also the ferrocenyl-tropylium salt (**61**),[86] have been characterized crystallographically. In these species the cationic units retain their planarity and there is no indication of a metal•••C^+ interaction.

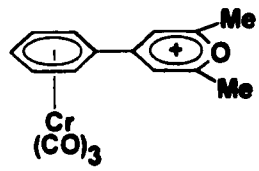

59

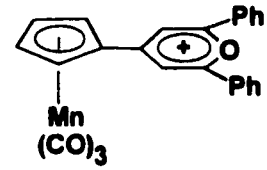

60

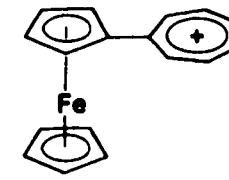

61

2.4 Summary

The syntheses and NMR characterization of alkynyl-fluorenyl, -indenyl, and -cyclopentadienyl cations stabilized by coordination to a $Co_2(CO)_6$ moiety have been performed. The barriers determined for the dynamic processes exhibited in solution are

consistent with the idea that the 4 π cyclopentadienyl cation is less stable than its 8 π indenyl and 12 π fluorenyl counterparts. In the first two instances, isolobal replacement of one tricarbonylcobalt vertex by an $Fe(CO)_3$ moiety yields stable iron-cobalt clusters whose X-ray crystal structures can be considered as models for their corresponding dicobalt cluster cations. Furthermore, the structures of these iron-cobalt complexes are in close accord with the energy-minimized geometries predicted from extended Hückel molecular orbital calculations for their respective dicobalt cluster cations. Although neutral iron-cobalt analogues of the cyclopentadienyl clusters (**44**) could not be prepared, the X-ray crystallographic data from the fluorenyl and indenyl systems **47** and **53** are consistent with the variable-temperature NMR spectroscopic data collected for their dicobalt counterparts, **35** and **46**. The X-ray crystallographic data and the activation energies obtained from variable-temperature NMR for these complexes are summarized in Tables 2.1 and 2.2.

Table 2.1 : Summary of Crystallographic Details for Iron-Cobalt Clusters, **47** and **53**.

Complex	Fe•••CR_2 (Å)	Fe-C_α-C_β (deg)
$(Me_3Si\text{-}C{\equiv}C{=}C_9H_8)FeCo(CO)_6$, **47**.	2.629 (8)	102.4 (2)
{2,3-Diphenyl-1-(trimethylsilylethynyl)-indenyl}$FeCo(CO)_6$, **53**.	2.347 (2)	85.4 (2)

Table 2.2: Sum of Calculated Barriers for Fluxional processes as Determined by ^{13}C and ^{31}P NMR Data

Cationic Cluster Complex	$\Delta G^{\#}$ (kcal mol^{-1}) ^{13}C NMR	^{31}P NMR
$[(Me_3Si\text{-}C{=}C{=}C_9H_8)Co_2(CO)_6]^+$, **35**.	12.2	-
[{2,3-Diphenyl-1-(trimethylsilylethynyl)-indenyl}$Co_2(CO)_6]^+$, **40**.	No change with temp	-
[{5-Trimethylsilylethynyl-1,4-diethyl-2,3-diphenylcyclopentadienyl}$Co_2(CO)_6]^+$, **44b**.	No change with temp	-
$[(Me_3Si\text{-}C{=}C{=}C_9H_8)\text{-}Co_2(CO)_4dppm]^+$, **37**.	12.0	11.5
[{2,3-Diphenyl-1-(trimethylsilylethynyl)-indenyl}$Co_2(CO)_4dppm]^+$, **42**.	No change with temp	12.7[a]
[{5-Trimethylsilylethynyl-1,4-diethyl-2,3-diphenylcyclo-pentadienyl}$Co_2(CO)_4dppm]^+$, **46b**.	-	12.1[b]

[a,b] Coalescence not observed. [a]Calculated value based on collapse of ^{31}P-P coupling constant. [b] Value determined at the decomposition temperature (248 K), no collapse of ^{31}P-P was observed. Actual value is probably much higher.

Chapter Three

The Isolobal Replacement of $Co(CO)_3^+$ with $Fe(CO)_3$: Mechanistic Implications

3.0 Introduction

Our investigation into the molecular dynamics of the 4n π series of anti-aromatic cations stabilized by dicobalt hexacarbonyl clusters has been discussed in the preceding chapter. More specifically, the fluorenyl, indenyl and cyclopentadienyl cations do not conform to the Hückel Rule for planar aromatic systems; [61-63] nevertheless, these species have been prepared as their alkynyl-dicobalt clusters.[87] Although dicobalt-hexacarbonyl cluster cations possessing a single tetrahedral unit have yet to be unambiguously characterized by X-ray crystallography, the most closely analogous system that has been structurally characterized is the neutral iron-cobalt cluster in which a $Co(CO)_3^+$ vertex had been replaced by a $Fe(CO)_3$ moiety.[79] However, prior to the present work on anti-aromatic cations, there have been no reported structures of iron-cobalt mixed metal clusters of the type, $[FeCo(CO)_6(RC{=}C{=}CR_2)]$. Molecular orbital calculations indicate that these mixed metal species are excellent structural models for the cationic dicobalt systems. It has been shown in the preceeding chapter that the structures of the fluorenyl and indenyl iron-cobalt hexacarbonyl clusters, **47** and **53**, can be conveniently characterized by X-ray crystallography. These clusters exhibit $Fe{\cdots}CR_2$ interatomic distances of 2.629 (8) Å and 2.347 (2) Å, respectively. Thus, one might anticipate that

the corresponding cyclopentadienyl cluster complexes, **62** and **63** would possess even shorter Fe•••CR_2 interatomic distances than the fluorenyl and indenyl analogues, as the 4π cyclopentadienyl cluster would be expected to have even greater need for electronic assistance from the neighboring metal center.

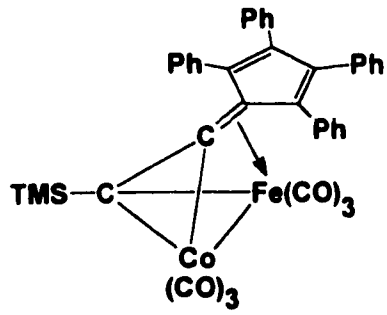

62

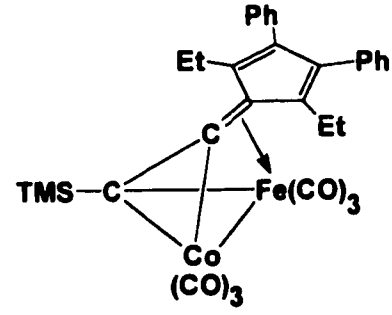

63

The syntheses of the cyclopentadienyl Fe/Co cluster complexes **62** and **63** were attempted. Surprisingly, these experiments did not yield the anticipated products **62** and **63**, but rather the trimetallic clusters (η^5-Fe(CO)$_2${μ-H}[$C_5Ph_2R_2$-C≡C-TMS]$Co_2(CO)_6$), where R = Ph (**64**) or Et (**65**), and may provide insight into an understanding of the mechanism of the $Co(CO)_3$/$Fe(CO)_3$ vertex replacement process.

3.1 Results and Discussion

3.1.1 Synthetic and Structural Aspects.

The precursor (alkynylcyclopentadienol)$Co_2(CO)_6$ complexes were treated with iron pentacarbonyl and heated under reflux in acetone for 1-3 days with the intent of preparing the iron-cobalt clusters (**62**) and (**63**) as structural models of the [(alkynyl-cyclopentadienyl)$Co_2(CO)_6$]$^+$ cations (**44a,b**), respectively. In both cases, after repeated chromatographic separations, a brownish red compound was isolated as the major product. The ^{13}C NMR spectra of these products revealed two distinct resonances

attributable to iron carbonyls (δ ≈ 216-218) and cobalt carbonyls (δ ≈ 214, 202), and the appearance of signals in the region δ 100-110 suggested the possibility of an η^5-bonded iron carbonyl moiety. Furthermore, the spectroscopic data (^{1}H NMR, ^{13}C NMR, IR) collected indicated the loss of the OH functionality. The molecules were unambiguously identified by means of X-ray crystallography; however, the determination of the structure of the tetraphenyl derivative **64** posed severe problems.

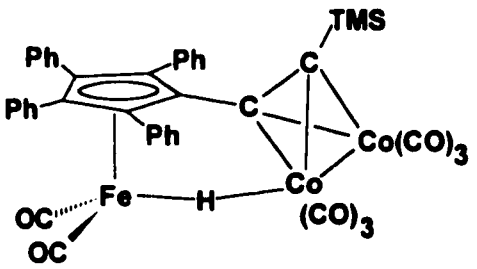

64

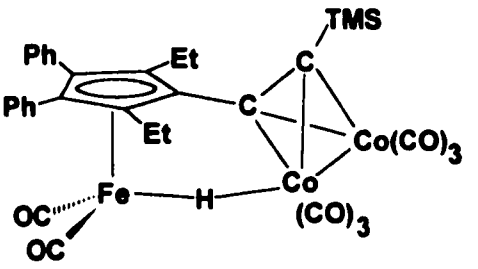

65

The only available crystals of **64** were very small and, even with a rotating anode X-ray source and a CCD area detector, the data collection was extremely challenging, yielding 106,000 reflections. The cell has P $\bar{1}$ symmetry and is large (V = 10710 Å^3), with Z = 10, and contained five pairs of independent molecules. The overall structure of **64** is shown in Figure 3.1 and reveals that both $Co(CO)_3$ vertices are intact, the hydroxyl group present in the starting material **62** is lost, and an $Fe(CO)_2$ moiety is π-complexed to the cyclopentadienyl ring. The iron atom is apparently linked to one of the cobalt atoms, but the observed interatomic distance of 2.890 (8) Å is too long to be considered a bond. The presence of a bridging metal hydride is the most probable explanation. Unfortunately, in an attempt to confirm our hypothesis, the treatment of **64** with CCl_4 (in the expectation of detecting $CHCl_3$) was inconclusive;[88] subsequent heating at reflux in CCl_4 led to decomposition. The crystallographic difficulties arose due to decay of the crystals and

the existence of multiple rotamers in the cell.

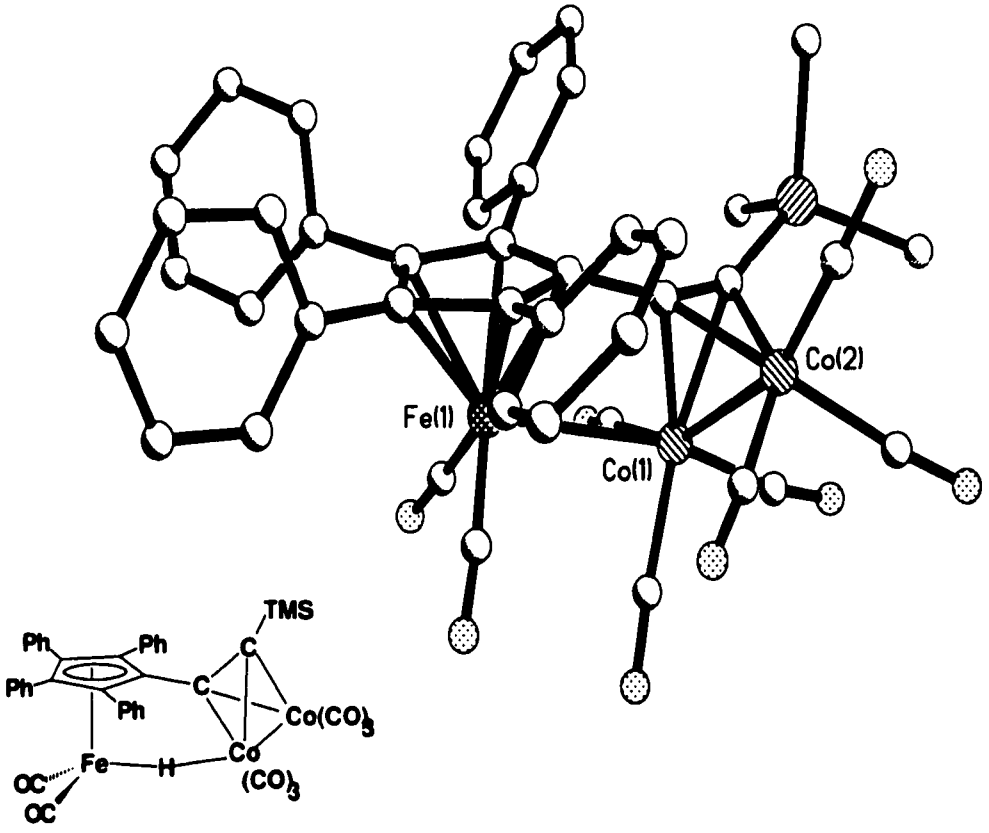

Figure 3.1 : X-ray structure of **64**; only one of the five rotamers is shown. Hydrogen atoms are omitted for clarity.

The orientations of the four peripheral phenyl substituents on the cyclopentadienyl ring were different in each of the five molecules in the asymmetric unit of the cell, and space fill diagrams illustrating these differences are shown in Figure 3.2. In principle, the numerous orientations of the phenyl substituents in **64**, in conjunction with the structural data on a variety of $(C_5Ph_5)ML_n$ complexes[89] could be helpful in a Bürgi-Dunitz analysis of the pathway for propellor inversion in C_nPh_n systems.

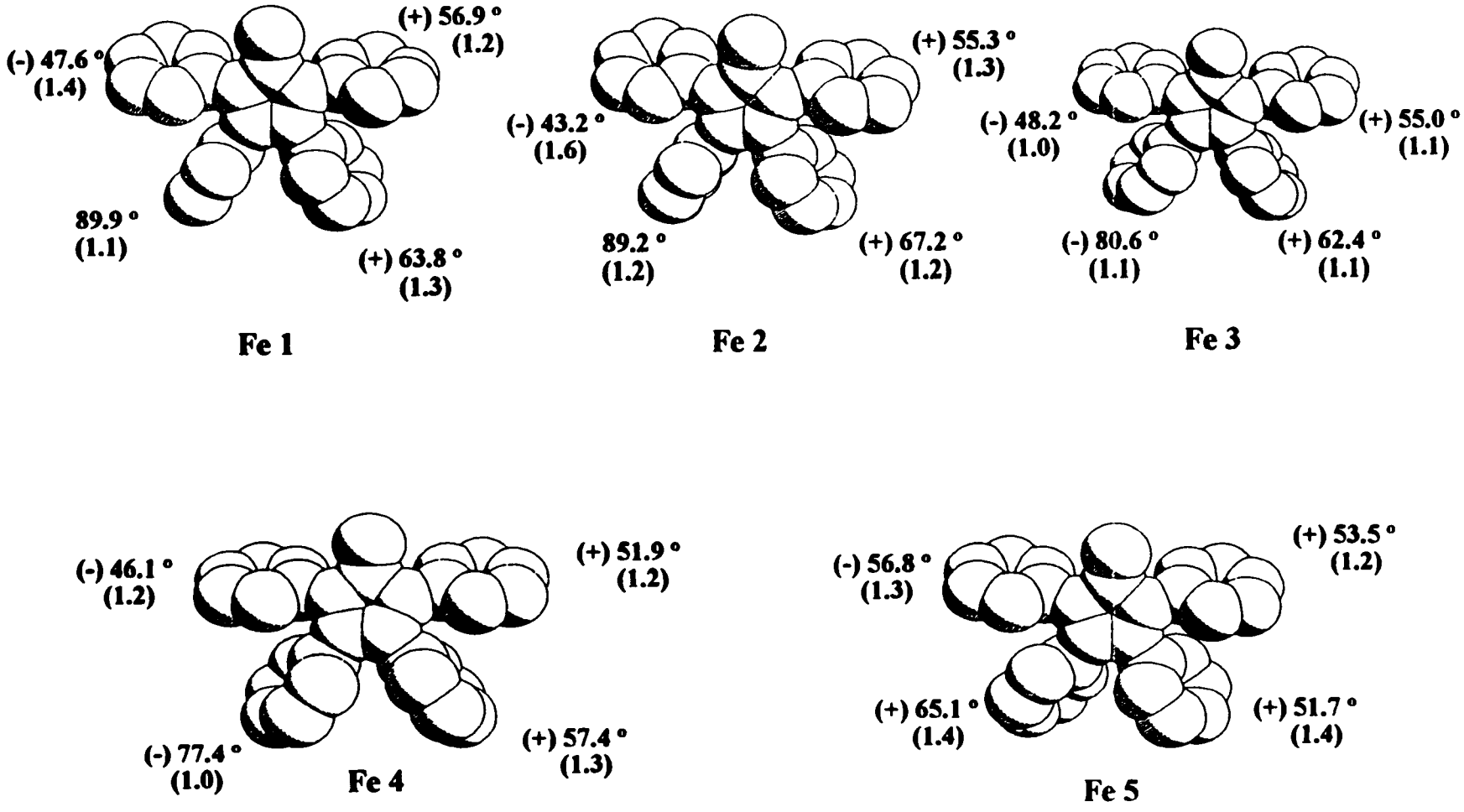

Figure 3.2 : Space fill diagram of the five crystallographically characterized rotamers of **64** showing dihedral angles between the phenyl and cyclopentadienyl rings (errors in parenthesis). For clarity, only the C_5Ph_4R fragment is shown.

The crystal structure determination of the 5-trimethylsilylethynyl-1,4-diethyl-2,3-diphenylcyclopentadienyl cluster (**65**) did not suffer from rotamer complications. The X-ray crystal structure appears as Figure 3.3. The metrical features of **65** are similar to those of **64**; the iron-cobalt interatomic distance is 2.887 (8) Å, once again too long to be considered a bond, and the existence of a bridging hydride is again invoked. The molecule does not possess a mirror plane in the solid state, and this asymmetry is maintained in solution. Spectroscopic data (^{13}C NMR) reveal distinct resonances for each ethyl substituent (δ 18.5, 18.2, 17.2, 16.3), as well as two different pairs of carbonyl signals (δ 218.4, 215.6, 214.1, 201.8), even at room temperature.

Furthermore, treatment of **62** and **63** with $Fe(CO)_5$ yielded a second product, $[\eta^4\text{-}Fe(CO)_3](OH)C_5Ph_2R_2\text{-}C{\equiv}C\text{-}TMS$, where R = Ph (**66**) or R = Et (**67**), identified by NMR spectroscopy and mass spectrometry. The ^{13}C NMR spectrum of **67** was consistent with an $\eta^4\text{-}Fe(CO)_3$ cyclopentadiene complex and revealed only one set of resonances attributable to the ethyl substituents (δ = 19.3, 14.1) as well as two signals (δ = 153.1, 151.3) consistent with a cyclopentadiene backbone and one signal assigned to the iron carbonyls (δ = 215.7). These $Fe(CO)_3$ derivatives of the original 5-trimethylsilylethynylcylopentadienols are thought to arise *via* initial decomposition of **62** and **63** under refluxing conditions to the respective alkynyl cyclopentadienols; subsequent coordination of an iron tricarbonyl moiety would generate the observed products.

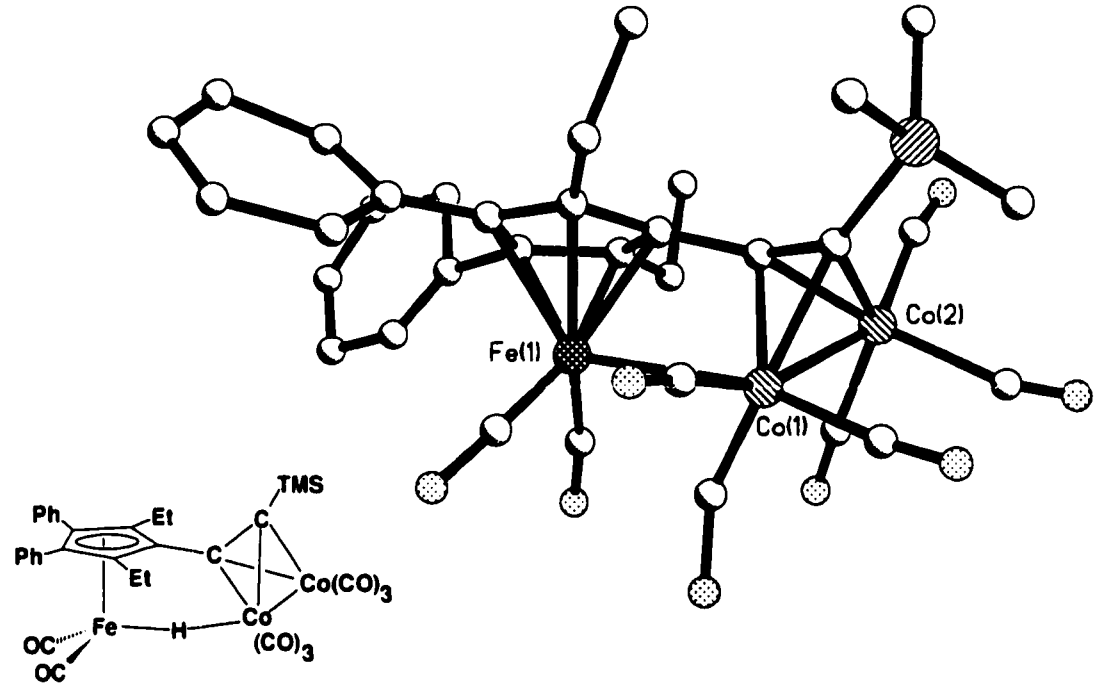

Figure 3.3 : X-ray structure of **65**. Hydrogen atoms are omitted for clarity.

Because of the stereogenic center at the C_5 position, both **66** and **67** could, in principle, exist as diastereomers shown as **66a,b** and **67a,b**. However, the simplicity of the NMR data suggests that only one isomer is formed in each case, and X-ray data are required to establish the structure unequivocally.

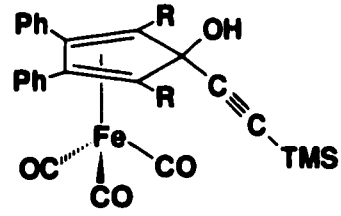

66a : R = Ph
67a : R = Et

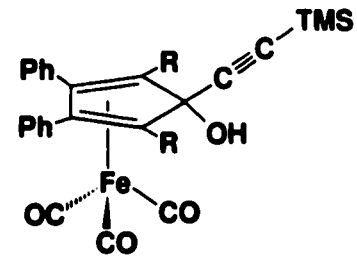

66b : R = Ph
67b : R = Et

It is noteworthy that the alkyne moiety in **66** does not react with excess $Co_2(CO)_8$ to yield the corresponding tetrahedral cluster, **68**, even after prolonged reaction times. If in fact

the $Fe(CO)_3$ π-complex were the *endo* isomer **66a**, this lack of reactivity could arise from steric factors imposed on the alkyne moiety as shown in Scheme 3.1.

Scheme 3.1

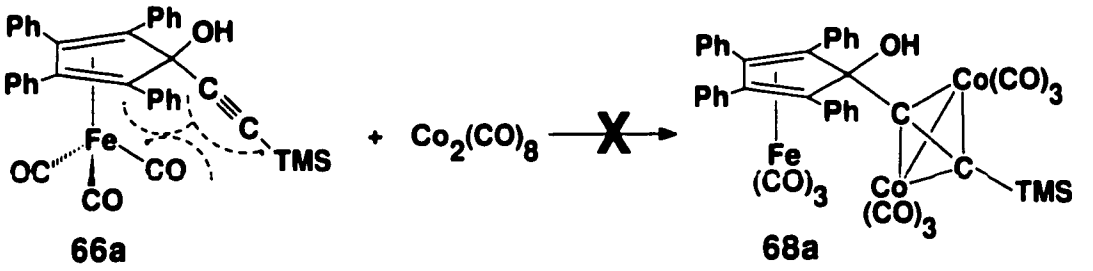

3.1.2 Mechanistic Implications

The reaction of (propargyl alcohol)-$Co_2(CO)_6$ clusters or their corresponding diols $(HOCR_2C{\equiv}CCR_2OH)Co_2(CO)_6$ with iron pentacarbonyl in refluxing acetone was originally reported by Victor.[79] The reaction was described as an apparent "dehydroxylation" process, and several iron-cobalt or di-iron complexes have now been unambiguously determined by X-ray crystallography. Although the isolobal replacement of a $Co(CO)_3^+$ vertex with $Fe(CO)_3$ has ample precedence in the literature, the "dehydroxylation" mechanism for this transformation is unclear and speculation has focussed on the possible role of intermediate metal hydrides. Chini[90] demonstrated that $Co_2(CO)_8$ and $Fe(CO)_5$ react in acetone to form the tetrahedral hydride cluster $HFeCo_3(CO)_{12}$. Moreover, Geoffroy[91] has reported that $MeCCo_3(CO)_9$ and $Fe(CO)_4^{2-}$ yield, upon protonation, the hydride cluster $MeCCo_2FeH(CO)_9$ (**69**).

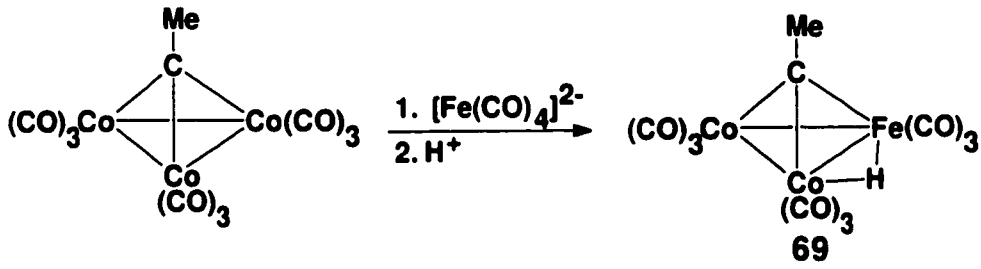

69

Thus, the mechanism for the conversion of $(HC{\equiv}C\text{-}CH_2OH)Co_2(CO)_6$ into $(HC{\equiv}C\text{-}CH_2)FeCo(CO)_6$ may involve the formation of an intermediate metal hydride (**70**), as shown in scheme 3.2. Subsequent elimination of water would yield the neutral iron-cobalt cluster. The overall formation of **23** from the dicobalt hexacarbonyl cluster has the appearance of an apparent "dehydroxylation" of the alcohol by $Fe(CO)_5$.

Scheme 3.2

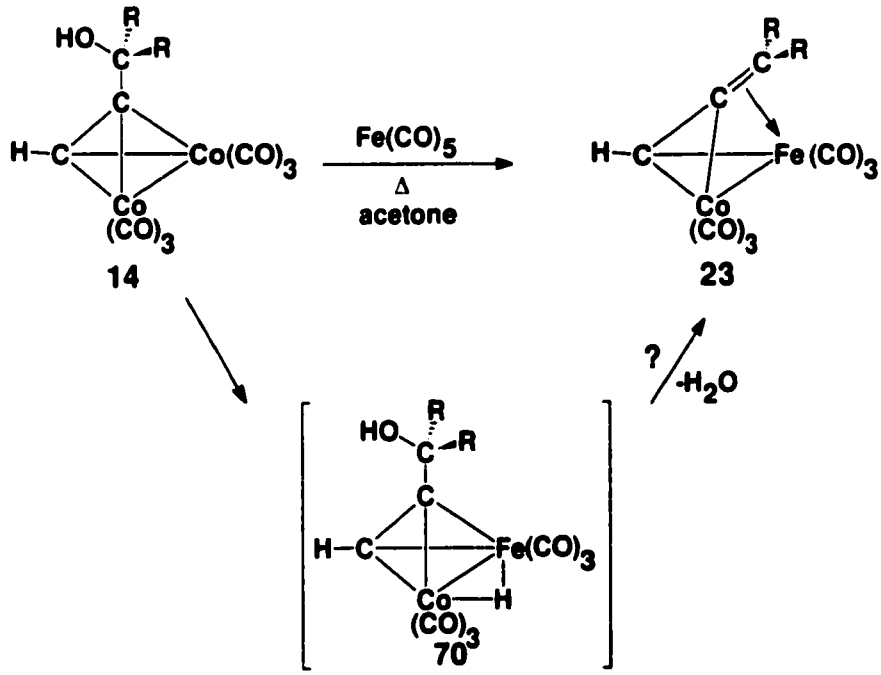

Despite repeated attempts, the dimetallic iron-cobalt complexes **62** and **63** could not be isolated and the formation of the trimetallic species **64** and **65** might suggest an

alternative mechanistic possibility. Initial nucleophilic attack by the hydroxyl group[92] on a carbonyl ligand of $Fe(CO)_5$ could, in principle, yield the hydrido metal carboxylate **71**. One should recall that the formation of $[HFe(CO)_4]^-$ from $Fe(CO)_5$ and KOH is well established to proceed through loss of carbon dioxide (as bicarbonate) from an intermediate carboxylate species.

As shown in Scheme 3.3, one can envision two competing pathways. In the case of the cyclopentadiene ligand, decarbonylation and η^4-coordination to the 5-membered ring could precede decarboxylation to yield **72**, which possesses an $Fe(CO)_2H$ moiety, and accounts for the isolated products **64** and **65**. In contrast, coordination to the cyclopentadiene ring of an indenyl or fluorenyl ligand would be disfavored due to the resulting loss of aromaticity in the six-membered rings. Although bis(η^5-indenyl)iron has been reported,[93] apparently no fluorenyl analogues of ferrocene are presently known. This is in keeping with reported extended Hückel molecular orbital calculations on a series of sandwich compounds (η^5-C_5H_5)Fe(η^5-L) where L = cyclopentadienyl, indenyl, and fluorenyl which revealed a noticeable decrease in the binding energy of the ligand L as the extra six-membered rings were added.[94] To return to Scheme 3.3, it is postulated that the tetrahedral cluster could undergo expansion to adopt a square-based pyramidal structure (**73**).

Scheme 3.3

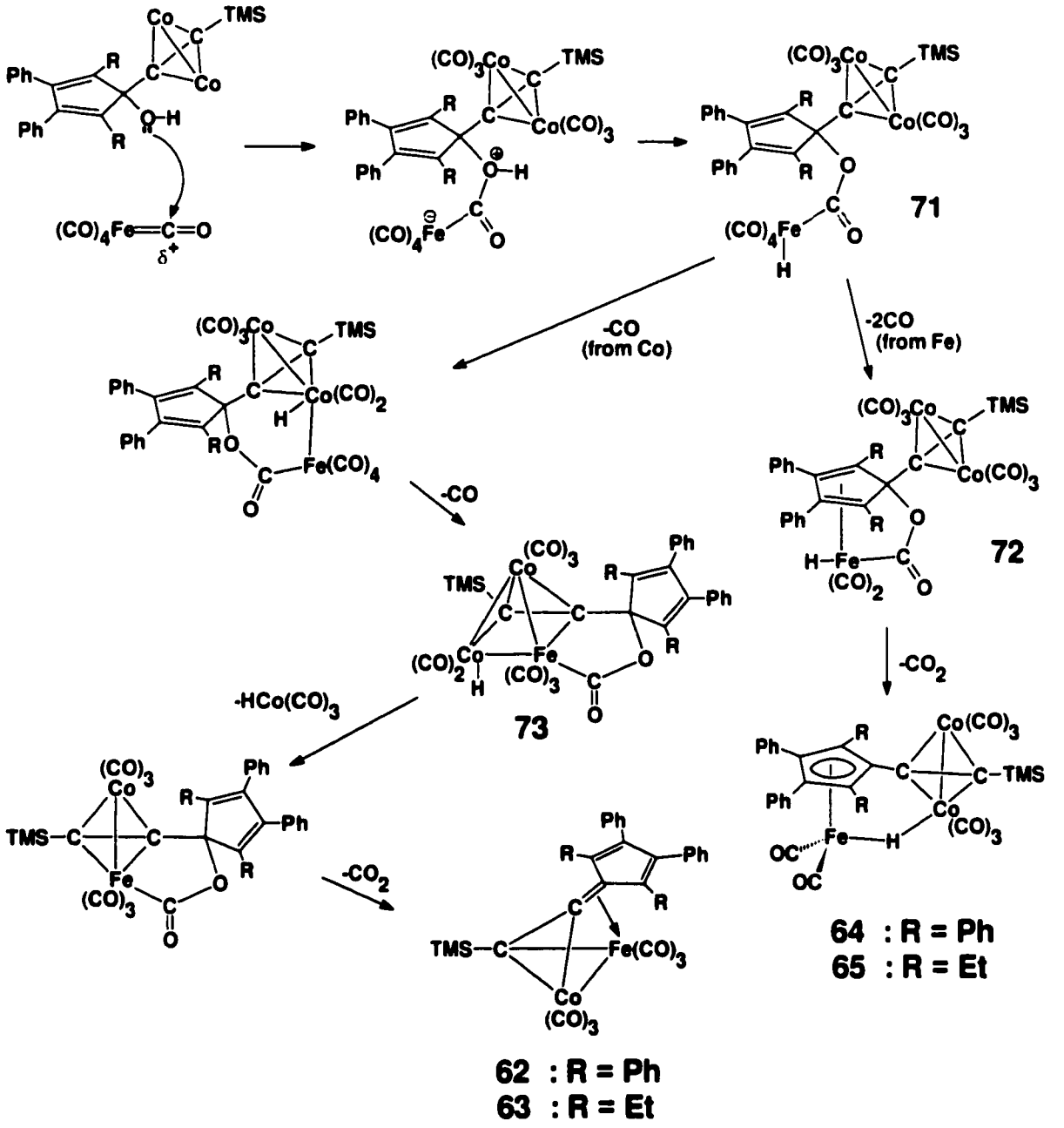
71
-CO
(from Co)
-2CO
(from Fe)
72
-CO
-CO2
-HCo(CO)3
73
-CO2
64 : R = Ph
65 : R = Et
62 : R = Ph
63 : R = Et

Although the apical and the basal plane cobalts in **73** would formally be assigned 19 and 17 electrons, respectively, the overall skeletal electron count is consistent with a *nido* octahedron, and cluster expansion[95] or vertex replacement,[96] reactions are well precedented. Lastly, decarboxylation could yield the observed mixed metal cluster **62**, as typified by **47** and **53**.

3.2 Summary

In contrast with its fluorenyl and indenyl analogues, the reaction of dicobalt hexacarbonyl cyclopentadienol clusters with $Fe(CO)_5$ do not yield isolobal substitution products. However, the isolation of the trimetallic clusters **64** and **65** suggests an alternative mechanistic pathway for the formal replacement of a $Co(CO)_3^+$ vertex with $Fe(CO)_3$ involving a decarboxylation step. While it is recognized that these mechanistic proposals are somewhat speculative, and the role of acetone solvent remains unclear, the advancement of these ideas may, in fact, lead to an elucidation of these processes.

Chapter Four

Perchlorinated Cyclic Olefins : Part 1

4.0 Introduction

The ability of transition metals to alleviate the electron deficiency of a proximal carbon atom is well established. In contrast to that of the anti-aromatic species that have been investigated in this work, it has been shown that aromatic cations such as the tropylium ion, $C_7H_7^+$, do not require electronic assistance from a neighboring transition metal moiety. Consequently, the tropylium ligand in ferrocenyl-tropylium salt (**61**) exhibits a planar geometry as predicted by the $(4n+2)\pi$ Hückel rule.

However, if the hydrogen atoms of the tropylium ligand are replaced by sterically demanding phenyl (**74**) or chlorine (**75**) substituents, a compromise must be struck between π delocalization favored by a planar ring and the steric demands imposed by the bulky substituents.

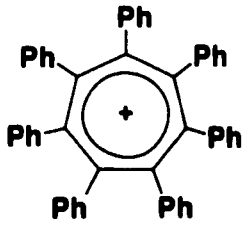

74

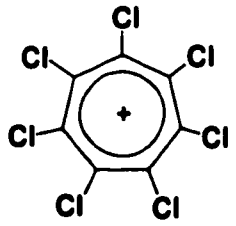

75

More specifically, the heptaphenyltropylium cation, $C_7Ph_7^+$ (**74**) has received considerable attention,[97] and recently it has been shown that the central seven-membered ring does not exhibit a planar geometry, as shown in Figure 4.1.[98]

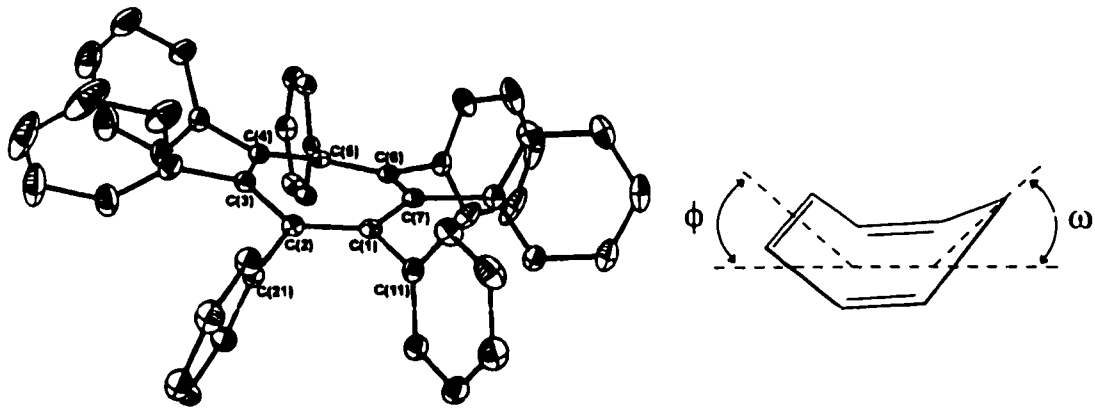

Figure 4.1 : X-ray crystal structure of $C_7Ph_7^+$ (**74**).

The X-ray crystallographic data for **74** reveal that the C(1)-C(7)-C(6) and the C(2)-C(3)-C(4)-C(5) planes deviate from planarity by 11° (ω) and 13° (ϕ), respectively.

Although the $C_7Cl_7^+$ cation can be readily synthesized (see section 4.2),[99] the structure of **75** has not been determined crystallographically. However, one may gain insight into the expected geometry of **75** from the structure determination of the closely analogous hexachlorotropone, C_7Cl_6O, **76**.[100,101] It has been reported that in **76** the bulky chlorine substituents do not permit the ring to maintain the electronically favoured planar geometry, but, rather, it adopts a boat conformation with ω and ϕ values of 29° and 24°, respectively.

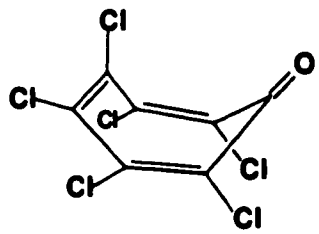

76a

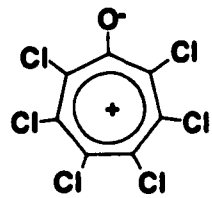

76b

If the canonical contributor **76b**, is considered, then the geometries exhibited by the

seven-membered rings in **75** and **76** may be in close accord. If in fact, the geometry of the polychlorinated tropylium cation **75** is puckered, then it would be of interest to probe the electronic demand that such a species would impose upon a neighboring metal center.

4.1 Attempted Metal Stabilization of the C_7Cl_6R Cation

In an attempt to probe the molecular dynamics of a metal-stabilized sterically encumbered tropylium cation, hexachlorotropone (**76**) was treated with the lithium salt of trimethylsilylethyne. However, the desired product [7-trimethylsilylethynyl-1,2,3,4,5,6-hexachlorocycloheptatrien-7-ol] (**77**) was not observed; the isotopic distribution pattern of $^{35/37}Cl$ (in the mass spectrum) indicated the presence of only five chlorine atoms. The ^{13}C NMR spectrum revealed four resonances of intensity ratio 1:1:2:2 (δ 137.5, 135.7, 132.9 and 128.8) as well as a signal at δ 173.5 (IR υ_{CO} = 1683 cm^{-1}), suggesting the formation of a benzenoid product whereby the ketone functionality had remained intact. These data indicated the product from the reaction of **76** and the trimethylsilylethynyl anion was consistent with a semi-benzilic acid rearrangement product, [2,3,4,5,6-pentachlorophenyl-1-trimethylsilylethynyl ketone] (**78**), as depicted in Scheme 4.1. To ensure that the triple bond functionality was indeed present, **78** was treated with dicobalt octacarbonyl to give **79**, and the structure was unambiguously determined by X-ray crystallography as depicted in Figure 4.2.

Scheme 4.1

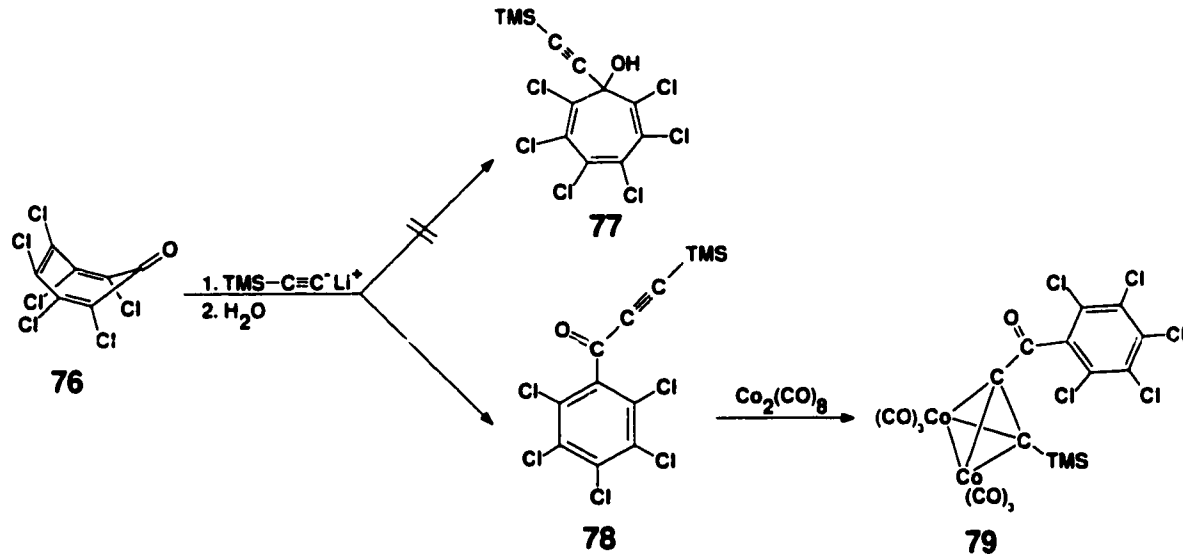

Figure 4.2 : X-ray Crystal Structure of **79**.

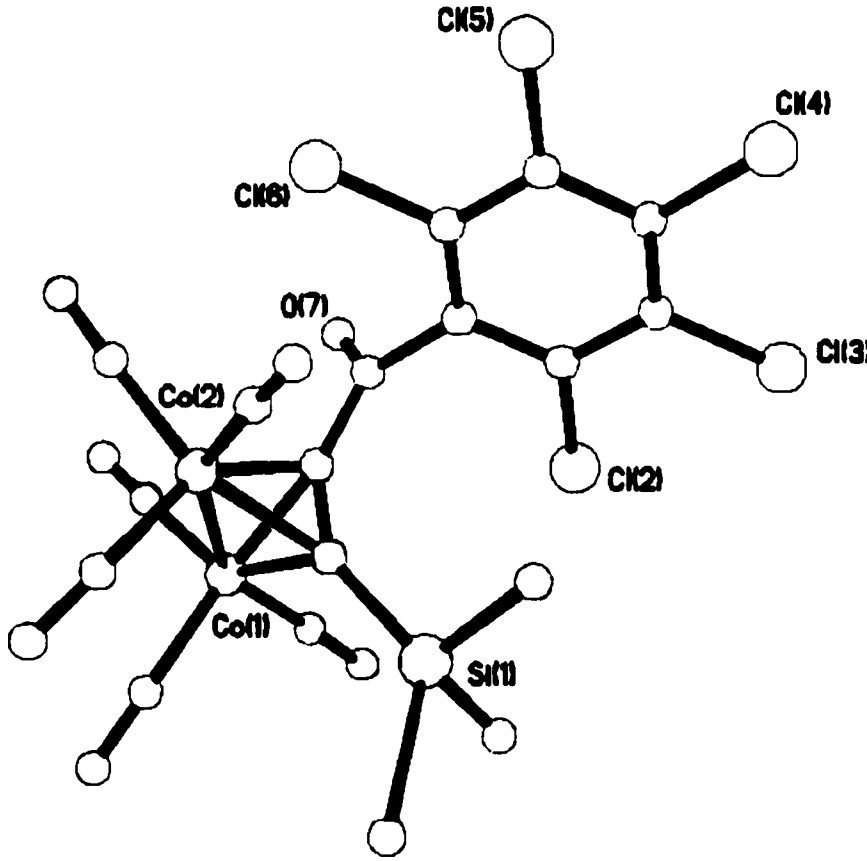

4.1 Sterically Demanding Ligands : C_7Cl_8

The attempted study of the interaction of a $C_7Cl_6R^+$ fragment and a $Co(CO)_3^+$ vertex was unsuccessful. However, the chemistry of C_7Cl_8 was investigated as an example of a sterically hindered molecule, an extension of the work by Chao *et. al.* [102] on the heptaphenylcycloheptatriene ligand. Although perfluorinated ligands, such as C_5F_5, C_6F_6, or C_8F_8, have received considerable attention,[103,104,105] perchlorinated systems appear to have been less thoroughly investigated. A number of perchlorocyclopentadienyl complexes, *e.g.* $(\eta^1\text{-}C_5Cl_5)Mn(CO)_5$, $(\eta^5\text{-}C_5Cl_5)Mn(CO)_3$, and $(\eta^5\text{-}C_5Cl_5)_2Ru$ are known,[106,107] and recently $(\eta^6\text{-}C_6Cl_6)Cr(CO)_3$ has been obtained by repeated lithiation and chlorination procedures.[108] However, so far as we are aware there are no examples of organometallic derivatives possessing a C_7Cl_7 ligand. It has been claimed[109] that $Fe_2(CO)_9$ reacts with perchloro(3,4-dimethylenecyclobutene) and with perchlorofulvene to give organo-iron complexes, but their identity has not been confirmed by X-ray crystallography.

4.2 The structure of C_7Cl_8.

The synthesis of octachlorocycloheptatriene was first described by West in 1968[101] and involves a [2+2] cycloaddition reaction of hexachlorocyclopentadiene, C_5Cl_6, with trichloroethylene to give the bicyclo[3.2.0]heptene, **80**. Dehydrochlorination using a suitable base yields the diene **81**, as in Scheme 4.2 and subsequent thermolysis in the presence of aluminum chloride gives octachlorocycloheptatriene, **82**, presumably by the symmetry-forbidden disrotatory ring opening of the intermediate cation to the heptachlorotropylium ion, **75**, which can recapture a chloride from the chloroaluminate anion.

Scheme 4.2

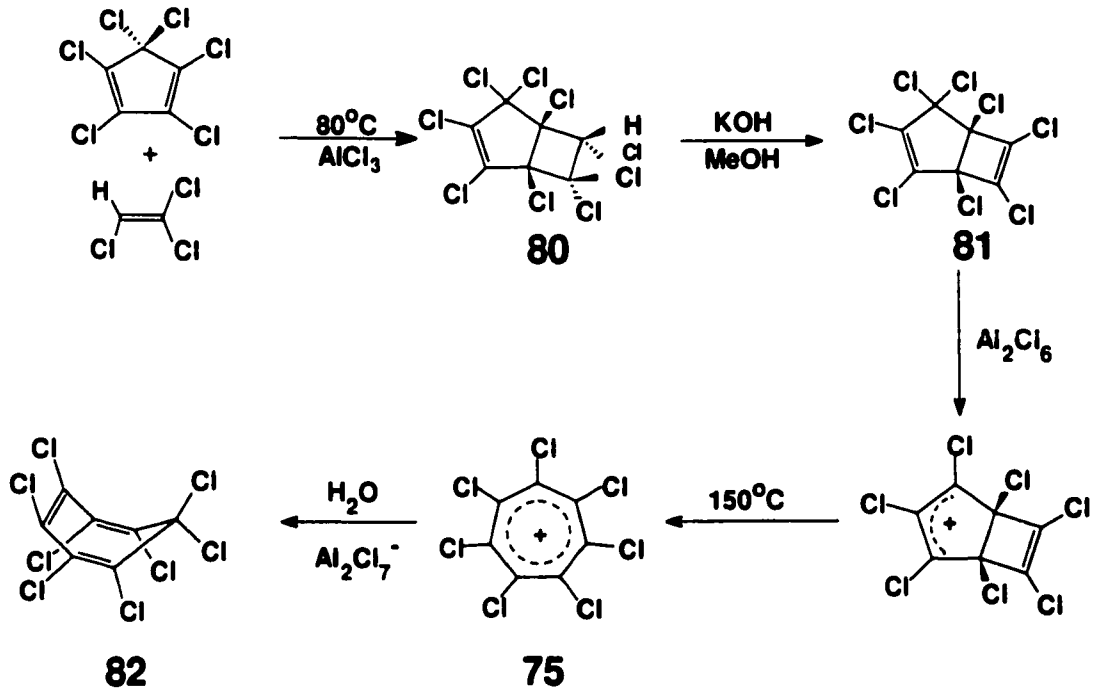

Although the position of the unique hydrogen in C_7Cl_9H (**80**) is not known with certainty, the structure of the related molecule $C_7Cl_8H_2$ (**83**) has been established by an X-ray diffraction study,[110] and the structure is shown below.

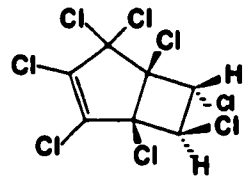

83

It is noteworthy that the two isomers of C_7Cl_8, namely **81** and **82**, give readily interpretable mass spectra since their chlorine isotope patterns are immediately evident.

The boat-shaped geometry of cycloheptatriene (**84**) was originally established from electron diffraction measurements. The dihedral angles between C(6)-C(7)-C(1) [plane 1], (C(1)-C(2)-C(5)-C(6) [plane 2], and (C(2)-C(3)-C(4)-C(5) [plane 3] are 144° (ω = 36°) for [plane 1]/[plane 2], and 140° (ϕ = 40°) for [plane 2]/[plane 3], respectively.[111]

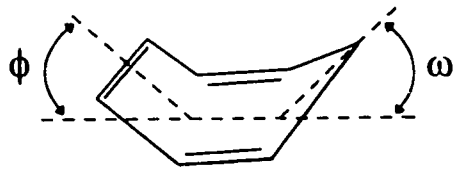

84

In the severely hindered heptaphenyl analogue, C_7Ph_7H (**84**), the corresponding values of ω and ϕ are 55° and 35°, respectively. That molecule is initially generated (see Scheme 4.3) as conformation **85a** whereby the unique phenyl substituent occupies an equatorial site; however, the ring flips irreversibly to the axial conformer **85b**, which has been structurally characterized by X-ray diffraction.[102]

Scheme 4.3

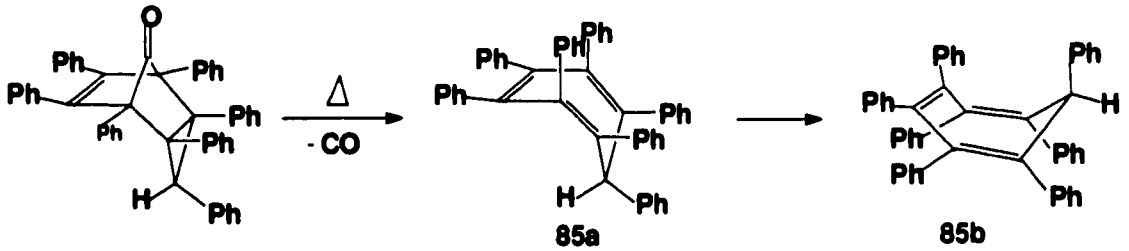

Furthermore, the recently reported X-ray crystallographic data of perchloroheptafulvene (**86**) reveal that the geometry exhibited by the ring deviates considerably from planarity. Analogously, the seven-membered ring in dodecachloro[1.6.7]quinarene (**87**) is also markedly non-planar.[112]

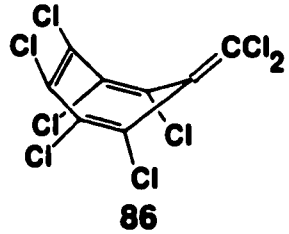

86

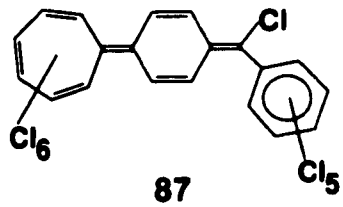

87

Since we had in hand X-ray quality crystals of C_7Cl_8 (**82**) we obtained diffraction data, and the resulting structure appears as Figure 4.3. Octachlorocycloheptatriene adopts a boat

conformation in which the CCl_2 unit and the C(2)-C(3)-C(4)-C(5) plane are bent with values of $\omega = 51.8°$ and $\phi = 32.4°$, respectively. There is clear bond alternation whereby the single bonds average 1.479 Å, and the mean double bond length is 1.336 Å; there is no indication of a norcaradiene-type structure (**88**) as is known for 7,7-dicyanocycloheptatriene.[113]

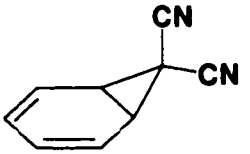

88

Overall, these data suggest that the steric hindrance within polychlorinated seven-membered rings is substantial, and that the system should exhibit a high barrier towards boat-to-boat conformational flipping.

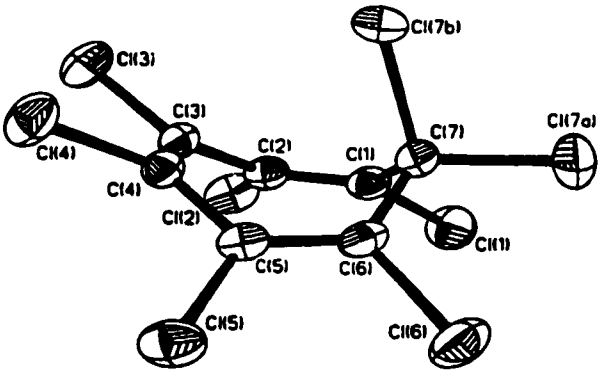

Figure 4.3 : X-ray structure of C_7Cl_8 (**82**)

4.3 Reactions of C_7Cl_8 with organometallics.

The chemistry of octachlorocycloheptatriene (**82**) with organometallic moieties appears to be limited. Apparently, only a single reaction of **82** with a transition metal complex.[114] Treatment of octachlorocycloheptatriene with nickelocene results in the coupling of a C_5H_5 fragment with a C_7Cl_7 unit (see Scheme 4.4); subsequent intramolecular

Diels-Alder addition yielded the cage compound **89**. The perchloro analogue of **89**, *viz.* **90**, has been characterized crystallographically as the product resulting from the reaction of **82** with tetrachlorodiazocyclopentadiene.[115]

Scheme 4.4

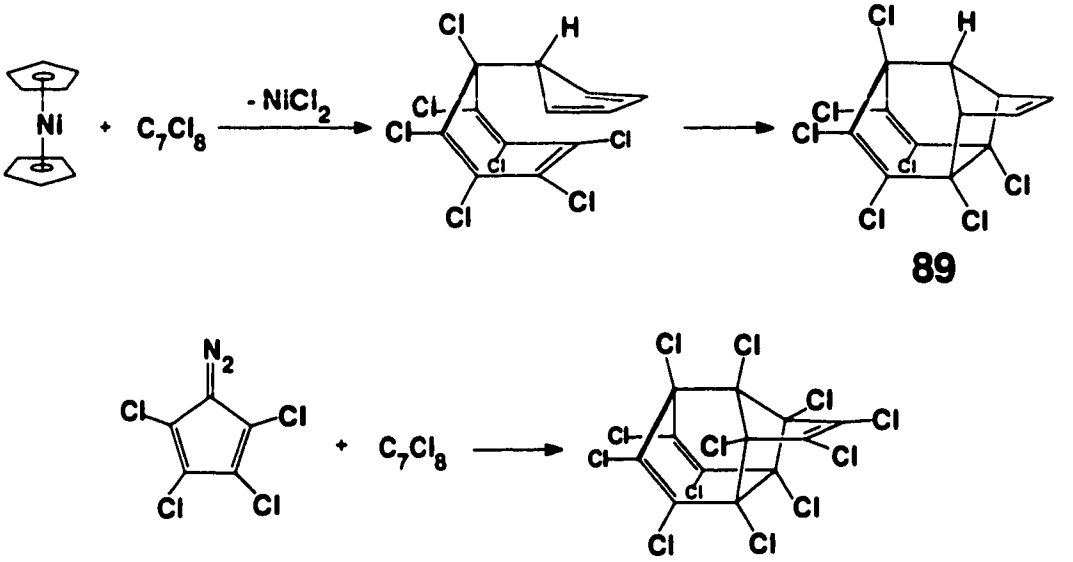

In an attempt to prepare metal carbonyl complexes possessing a C_7Cl_7 fragment, **82** has been treated with a number of organometallic precursors, *viz.* $[(C_5H_5)Fe(CO)_2]^-$, $Fe_2(CO)_9$, $Co_2(CO)_8$, $(acac)Rh(C_2H_4)_2$, and $(Ph_3P)_2Rh(CO)Cl$. In all cases, the sole organic product isolated was *syn*-perchloroheptafulvene (**91**). This molecule, previously synthesized *via* reaction of C_7Cl_8 with methyllithium, had been structurally characterized by X-ray diffraction, despite a crystallographic disorder problem.[116] The published data had an unsatisfactory modelling of this disorder, and since crystals of **91** were obtained by a different route, a data set was collected in the hope of resolving the disorder, but the same difficulty was encountered. The clam-shaped geometry allows the molecules to pack randomly with the central double bond "up" or "down", as indicated in Figure 4.4. The structure was modelled by assigning half occupancies to all atoms except C(3), C(6), C(10),

C(13), and their corresponding chlorines. The crystallographic disorder, showing only the carbon framework for clarity, is illustrated in Figure 4.4, while Figure 4.5 depicts the geometry of a single molecule of **91**.

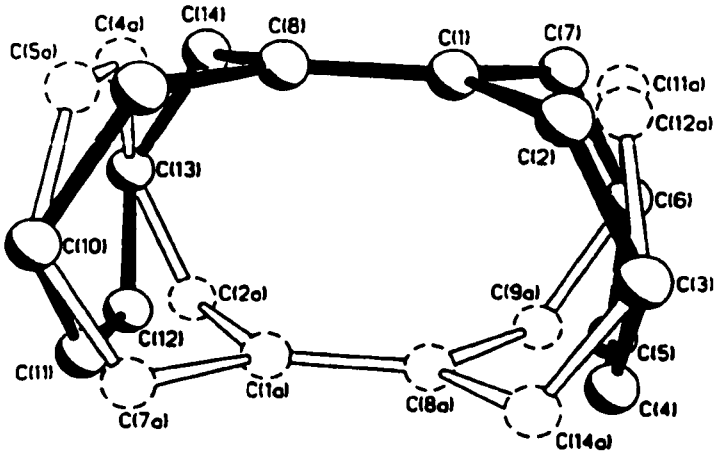

Figure 4.4 : Disorder of *syn*-$C_{14}Cl_{12}$ (**91**) omitting the chlorine atoms for clarity

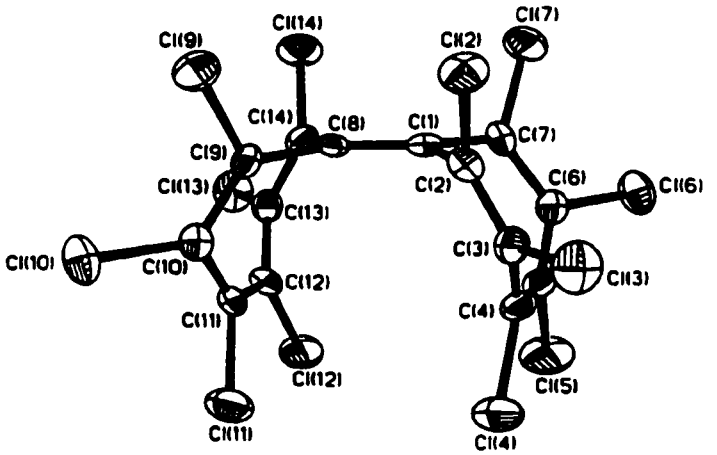

Figure 4.5 : X-ray structure of *syn*-$C_{14}Cl_{12}$, **91**.

The seven-membered rings are severely bent with interplanar angles of 124.7° (ω = 55.3°) and 147.5° (ϕ = 32.5°), in good agreement with the values determined for the C_7Cl_8 ligand. Furthermore, the central carbon-carbon double bond is markedly pyramidal in that the atoms C(1) and C(8) lie 0.09 Å out of the plane containing C(2), C(7), C(9), and C(14).

Alternatively, this facet of the structure can be described by defining an angle of 173.5° (θ = 6.5°) between the plane containing C(1), C(2), and C(7), and the C(1)=C(8) vector. Each Cl-C=C-Cl moiety is essentially planar and appears to be isolated from its neighboring double-bonded fragment.

It has previously been suggested[116] that *syn*-$C_{14}Cl_{12}$, might arise by lithiation at one of the dichloro positions of C_7Cl_8 to yield C_7Cl_7Li which, in turn, could attack a second molecule of **82** to produce perchloroditropyl (**92**) as in Scheme 4.5. A second lithiation, followed by *cis* elimination of LiCl, could yield **91**. Furthermore, when subjected to prolonged heating, the isomerization of **91** to the known *anti*-$C_{14}Cl_{12}$ (**93**) occurs as originally described by West, Dahl, and their colleagues.[117] Continued heating of **93** to 340° brings about loss of chlorine and rearrangement to decachlorophenanthrene (**94**).

Scheme 4.5

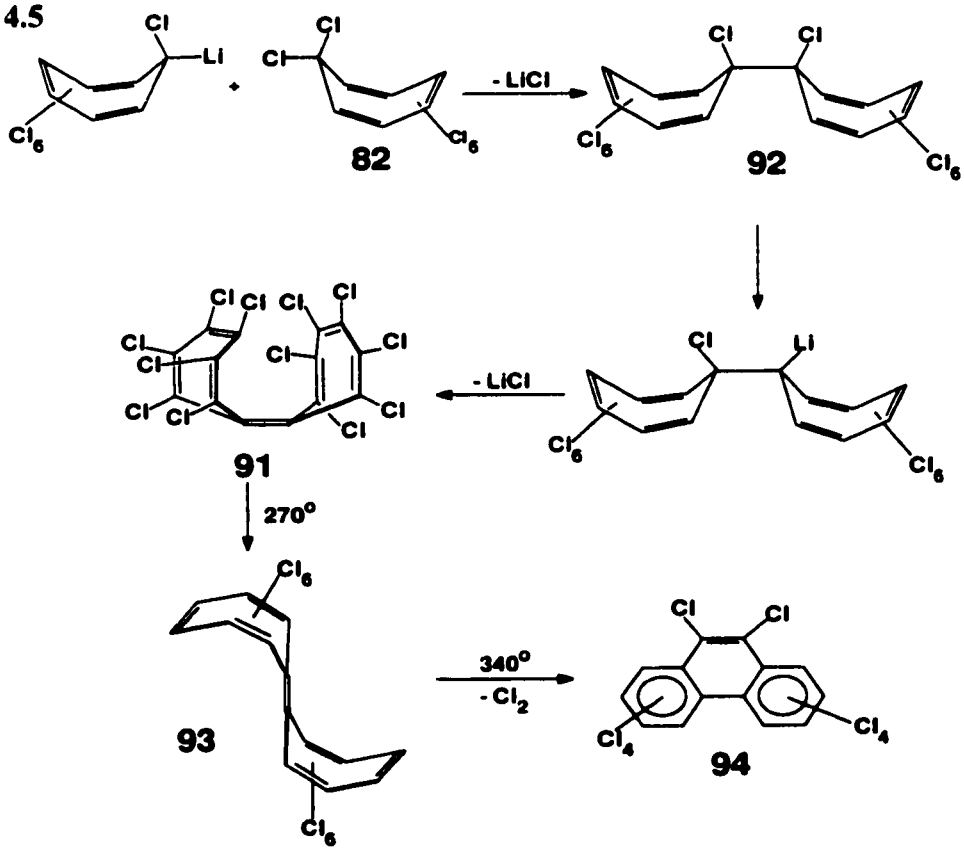

However, it has been well established that the treatment of *gem*-dichloro species with n-BuLi results in the formation of a carbene intermediate as shown in Scheme 4.6.[118]

Scheme 4.6 : Classical Method of Generating Carbenes

Consequently, we have focussed on the possible intermediacy of a hexachlorotropylidene-metal complex. Analogous C_7H_6 carbene complexes of iron (**95**, Scheme 4.7), tungsten and ruthenium and other transition metals have been synthesized.[119] However, despite repeated efforts, we have been unable to obtain any evidence for such perchlorocarbene complexes; the metal-containing products are merely well-known materials such as $CoCl_2$ or $FeCl_2$. Moreover, if *syn*-$C_{14}Cl_{12}$ arises as the result of a metal-template induced coupling, one must still account for the observed *syn* stereochemistry. On the other hand, if, as we suspect, the metal merely dechlorinates C_7Cl_8 to give hexachlorotropylidene, C_7Cl_6, then one must consider the possible fate of this carbene intermediate.

Scheme 4.7 : Synthetic route to a Fe carbene complex, **95**.

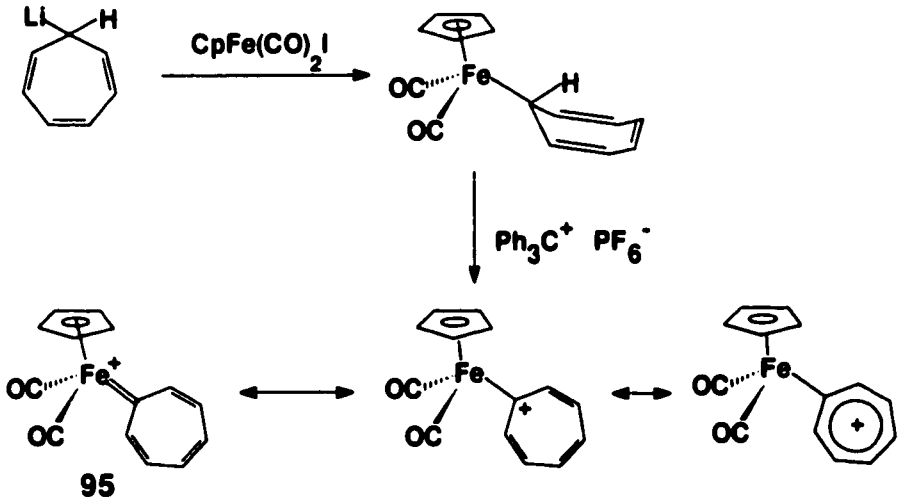

95

Furthermore, it is relevant to note that the reaction of decachloro(4-allylidenecyclopentene)

(**96**) with $Fe_2(CO)_9$ leads to the cyclization product octachlorobicyclo[3.3.0]octa-1,3,7-triene (**98**).[120] One could envisage metal-promoted dechlorination, as in Scheme 4.8, to produce an intermediate carbene **97** which inserts into a C-Cl bond and, after a chlorine [1,5] sigmatropic shift, yields the bicyclo species (**98**).

Scheme 4.8

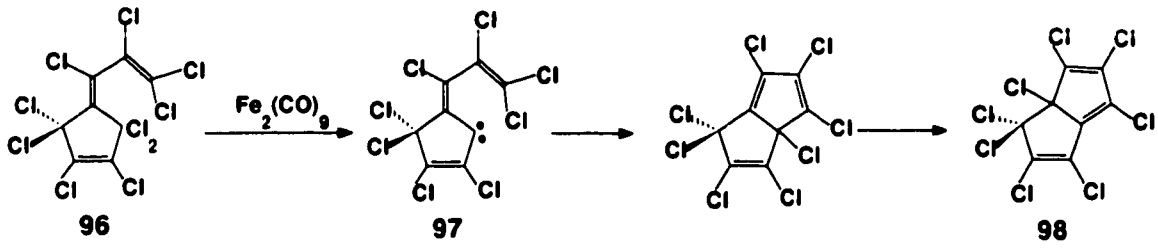

96 **97** **98**

In recent years, the chemistry of the "nucleophilic carbenes" has received much attention.[121] These species, typified by $[(MeO)_2C:]$, have singlet character whereby the electron-deficiency at the carbene center is considerably alleviated by π-donation from the adjacent oxygen (or an electron donor atom) atoms to the formally vacant p_z orbital on carbon. These carbenes are sufficiently long-lived that, in the absence of a suitable trap, they can give good yields of dimer. Similarily, the C_7Cl_6 carbene could dimerize to form product **91**. To investigate this possibility, the EHMO-derived frontier orbital patterns for C_7H_6 and for C_7Cl_6 were determined. They are depicted in Figure 4.6 (following page).

The structure of C_7H_6 has been intensively studied with respect to the relative stabilities of the planar tropylidene carbene and the allene-like cyclohepta-1,2,4,6-tetraene.[122] Indeed, it has even been claimed that the carbene form does not represent an energy minimum, but rather is merely the transition state for the interconversion of enantiomeric allenes.[123]

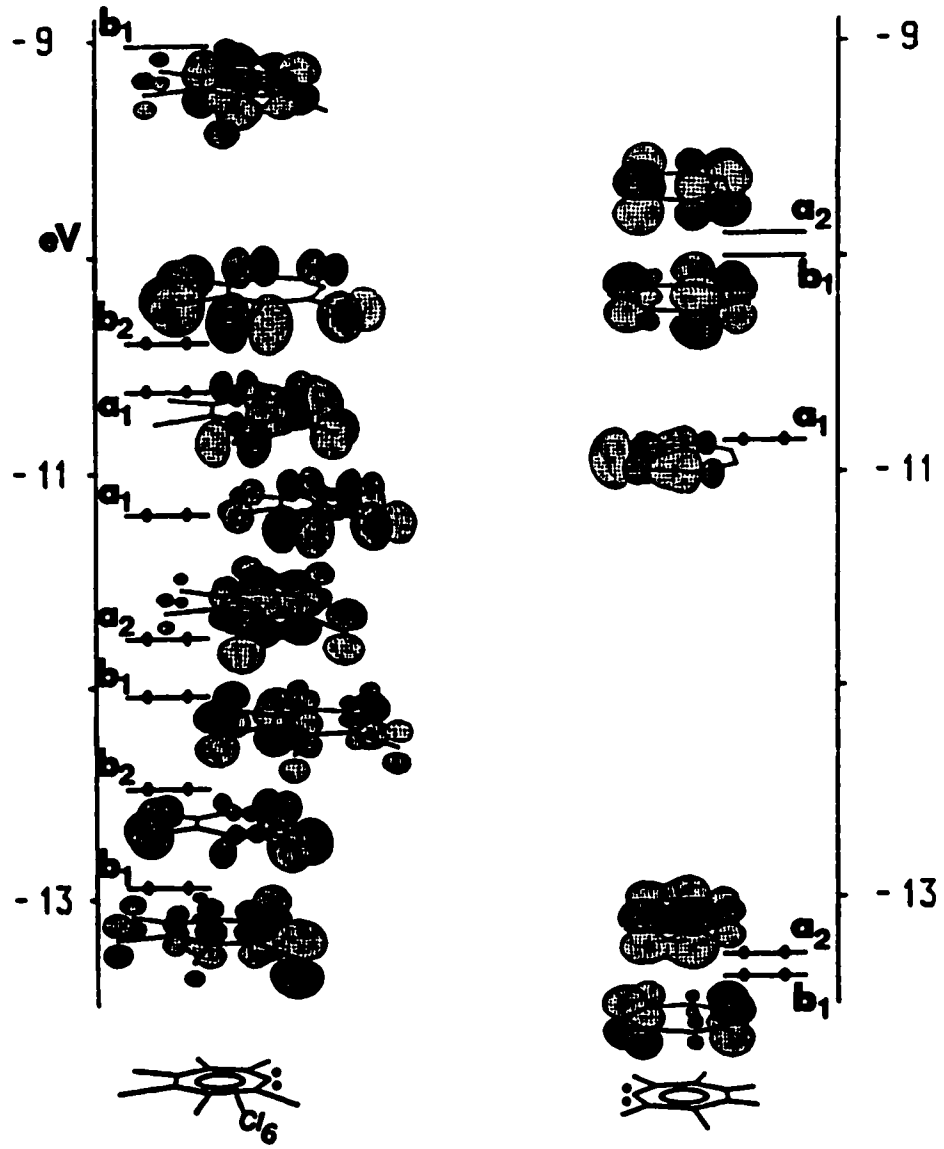

Figure 4.6 : Comparison of EHMO-derived frontier orbitals for C_7H_6 and C_7Cl_6

As mentioned previously, numerous metal-tropylidene systems have been described,[119] but there is also an X-ray structure of the cyclohepta-1,2,4,6-tetraene form which has been

trapped as a stable $(Ph_3P)_2Pt(C_7H_6)$ complex (**99**), as depicted in Figure 4.7.[124]

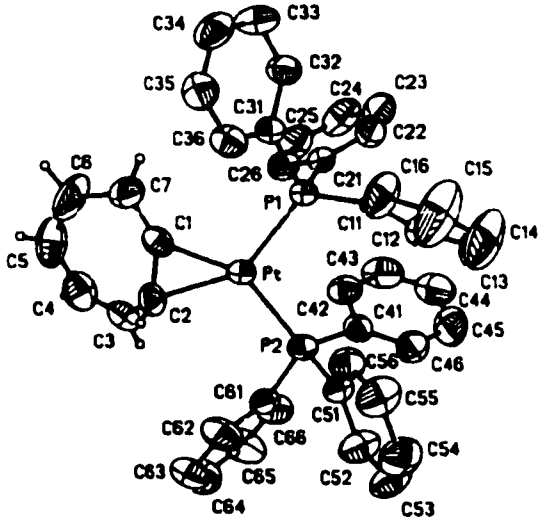

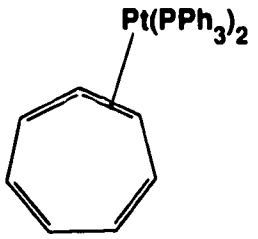

99

Figure 4.7: X-ray crystal structure of $(Ph_3P)_2Pt(C_7H_6)$, **99**.

For the present purposes, only the carbenes are compared since, even if C_7Cl_6 preferentially adopts the cyclic allene structure, its behavior is apparently carbene-like. In C_7H_6, the HOMO has a large in-plane component on the carbene carbon, while the LUMO has predominant π^* character.[122] By way of contrast, in C_7Cl_6 the HOMO is localized entirely on the peripheral chlorines, and lies just above the "σ lone pair" on the carbene carbon, as anticipated for a singlet species. It can be seen from Figure 4.6 that there is a markedly enhanced HOMO-LUMO gap in the chlorinated system which can be traced to participation of the chlorine p_z orbitals with the π manifold of the ring. One may conclude that C_7Cl_6 could be a relatively long-lived carbene with a high propensity to dimerize. Such an interaction between two carbenes would involve donation of the in-plane lone pair of electrons on the carbene carbon of one C_7Cl_6 fragment into the LUMO of its reaction partner. Moreover, the *syn* stereochemistry may well arise as the result of secondary orbital

interactions, a phenomenon commonly invoked to account for the formation of *endo* adducts in the Diels-Alder reaction.[125] However, it has been proposed by Untch that the base-induced dehydrohalogenation of chlorocycloheptatriene yields 1,2,4,6 cycloheptatetraene. Analogous to this rationale, an alternate dimerization pathway for the formation of **91** *via* the intermediate 2,3,4,5,6-hexachloro-1,2,4,6-cycloheptatetraene species (**100**) could occur as shown in Scheme 4.9. Calculations at the semi-empirical level (PM3) shed little light on a favoured dimerization pathway, however, an intermediate allene species (**100**) can not be ruled out. In particular, the orthogonal character of the allene double bonds should be favored by the presence of two bulky chloro substituents.

Scheme 4.9

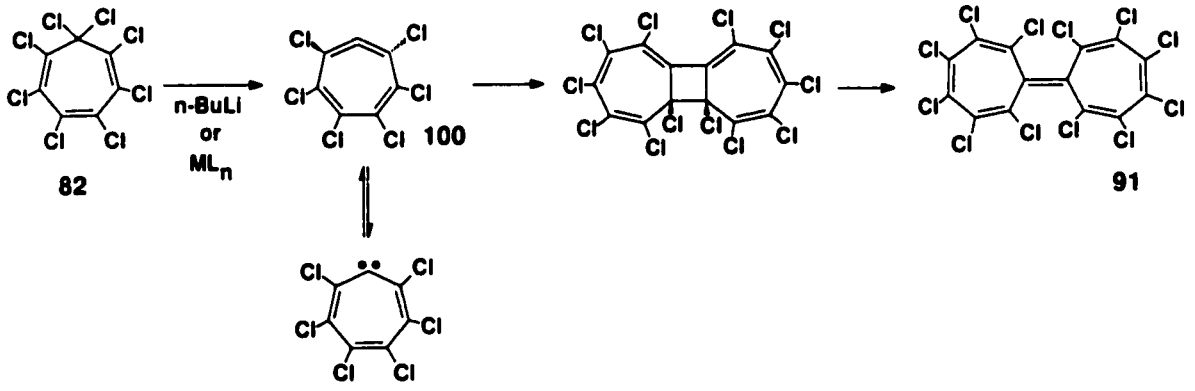

It is noteworthy that the conversion of *syn*-$C_{14}Cl_{12}$ (**91**) to *anti*-$C_{14}Cl_{12}$ (**93**) requires prolonged heating at 270 °C;[117] clearly, this process has a very large activation energy. The steric problems encountered by a planar C_7Cl_6 moiety as it manoeuvers its way past the neighboring chlorines in the other half of the molecule impose an extremely large barrier. However, even in the absence of large chlorine substituents, heptafulvalenes are not planar species. Early calculations by Dewar suggested that planar $C_{14}H_{12}$ would exhibit bond fixation rather than a delocalized structure in which all bond lengths were rather similar.[126]

A subsequent X-ray crystal structure confirmed this prediction of alternating single and double bonds, but also showed the molecule to be non-planar.[127] As shown in Figure 4.8, $C_{14}H_{12}$ adopts the *anti* conformation with interplanar angles of 173° ($\theta = 7^{o}$), 155° ($\omega = 25^{o}$) and 164° ($\phi = 16^{o}$), respectively.

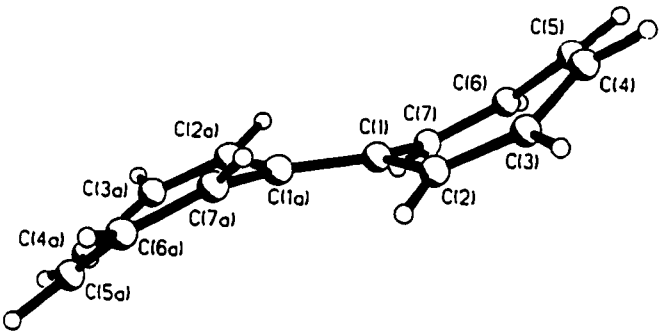

Figure 4.8 : X-ray structure of $C_{14}H_{12}$.

This result may be rationalized with the aid of molecular orbital calculations at the extended Hückel level. Figure 4.9 presents a Walsh diagram depicting the gradual flattening of $C_{14}H_{12}$. The energy minimum is found for θ, ω, and ϕ values each within one degree of those found in the X-ray crystal structure. We see that bending the molecule symmetrically into an *S* shape (*i.e.* after breaking the D_{2h} symmetry of the planar molecule we preserve C_{2h} symmetry throughout the process) stabilizes the HOMO and raises the LUMO. In the planar molecule, the HOMO reveals a substantial π^* overlap between the central C=C moiety and the two outer fragments; this destabilizing interaction is decreased as the molecule bends. Concomitantly, the LUMO loses some degree of in-phase π-type overlap, and the net result is to augment the HOMO-LUMO gap. The bent structure is calculated to be approximately 8.5 kcal mol^{-1} more stable than the planar form.

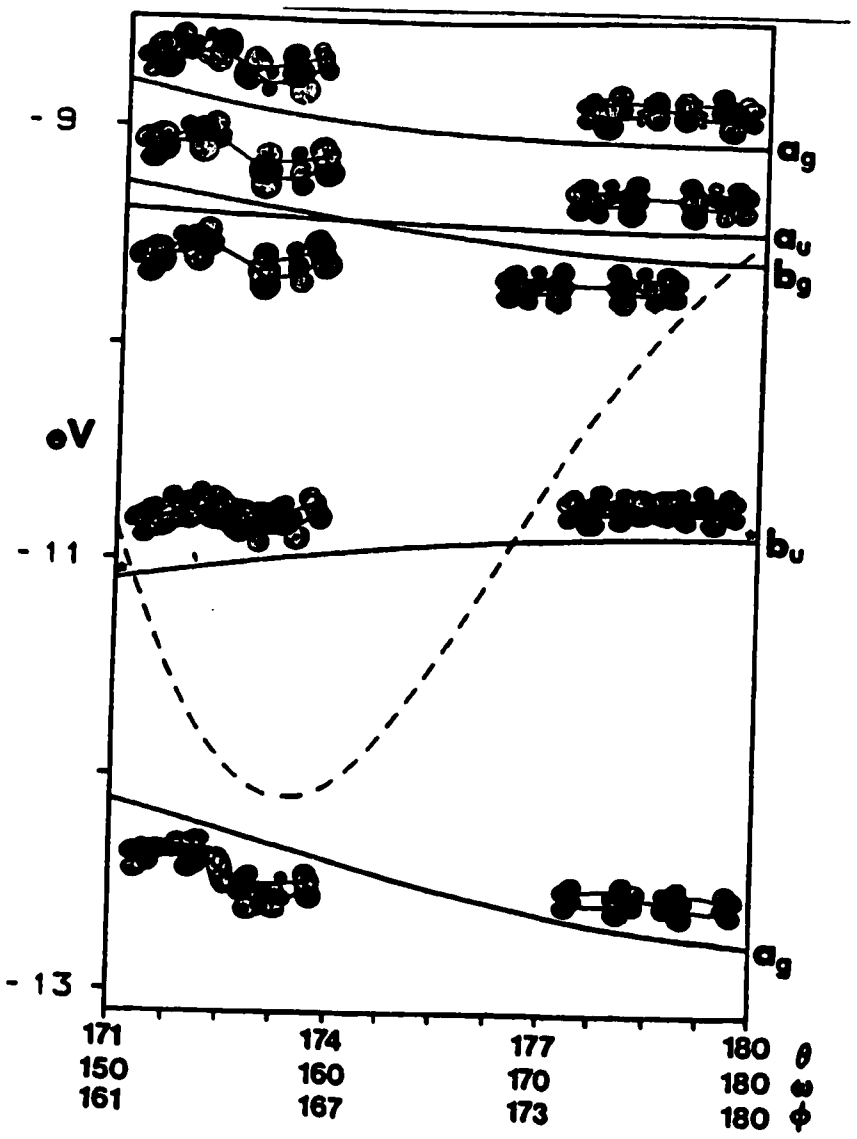

Figure 4.9 : EHMO-derived Walsh diagram depicting the symmetrical flattening of *anti*-$C_{14}H_{12}$ from a C_{2h} geometry to D_{2h}. The HOMO is marked with an asterisk. (The dashed line represents the total electronic energy and is drawn to a different scale.).

These effects are not just the result of crystal packing forces; heptafulvalene is known to undergo symmetry-allowed $[_{\pi}14_a+_{\pi}2_s]$ cycloaddition with tetracyanoethylene as the twisted shape of the $C_{14}H_{12}$ is ideally suited for *antara* addition to the 14π system to give

the adduct **101**.[128]

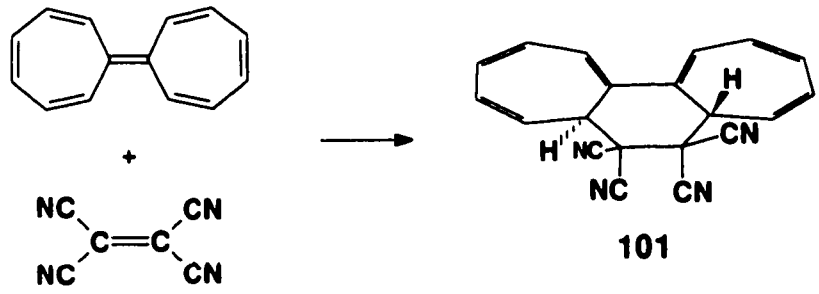

101

4.4 Summary

Octachlorocycloheptatriene (**82**) adopts a severely bent boat conformation, closely analogous to that found for C_7Ph_7H. Treatment of **82** with metal carbonyls does not yield isolable organometallic complexes but rather the dimerization product *syn*-perchloroheptafulvalene (**91**), presumably *via* a dechlorination mechanism. The high barrier to conformational change from **91** to its *anti*-isomer (**93**) may be attributable principally to unfavorable steric interactions between the chlorine substituents.

Chapter Five

Perchlorinated Cyclic Olefins : Part II - Reactivity towards Dimethoxycarbene

5.0 Introduction: Carbenes -General Properties

Reactions of octachlorocycloheptatriene (**82**) with organolithium reagents resulted in the exclusive formation of the dimerization product *syn*-$C_{14}Cl_{12}$ (**91**) and our hypothesis suggested that the coupling was a result of a carbene/allene intermediate species, C_7Cl_6.[129]

Carbenes are neutral, divalent, electron-deficient species that possess a non-bonding pair of electrons. The two electrons are either paired, occupying an sp^2-hybridized orbital (singlet state) or in a parallel arrangement occupying an sp^x and a p orbital (triplet state).

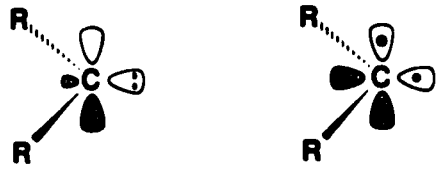

sp^2 singlet **sp^2 triplet**

Typically, carbenes are highly reactive intermediates; however, recent literature reports also suggest the existence of stable carbenes that have been characterized by X-ray diffraction.[130] The electronic properties and consequently the reactivity of carbene species are ultimately affected by the nature of the R substituents. A singlet/triplet ground state is determined by the π donor ability of the R substituent. Substituent effects

can best be put in perspective by comparison of the singlet-triplet energy gaps of halocarbenes and alkoxycarbenes to the simple methylene molecule, CH_2 (no π donation). After years of conflicting data, only recently has the singlet-triplet separation for methylene been established to be approximately 9 kcal mol^{-1} favoring the triplet ground state. In contrast, if the hydrogen atoms are replaced by halogens or alkoxy substituents conjugative stabilization through donation by the lone pairs into the vacant *p* orbital of the carbene carbon results in dipolar character (Figure 5.1) and stabilizes the singlet state (ΔE_{ST} ($:CF_2$) $\approx$ 56 kcal mol^{-1}, ΔE_{ST} ($:C(OMe)_2$) $\approx$ 76 kcal mol^{-1}).[131]

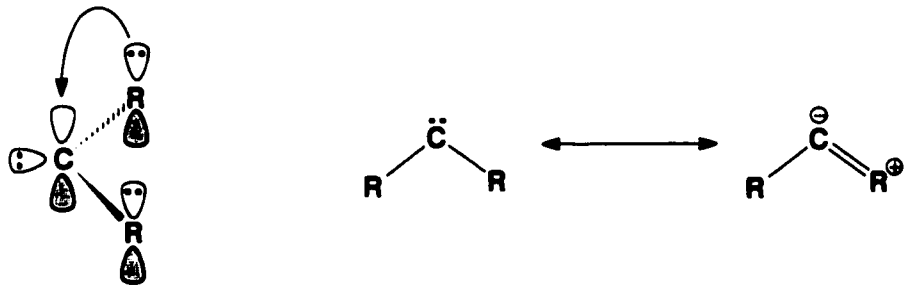

Figure 5.1: Resonance diagram depicting the dipolar character of $:CR_2$

Since carbenes are electron-deficient, they typically tend to be electrophilic in terms of chemical reactivity. For example, the strong electron-withdrawing effect of the fluorine atoms in difluorocarbene causes a strong σ polarisation of opposite direction (to π donation) resulting in a strongly *electrophilic* carbene and this property is best exemplified by the preference of dihalocarbenes to yield cyclopropanation products with electron-rich olefins such as tetramethylethylene. In contrast, carbenes that possess directly bonded substituents (such as amino groups) that are very strong π donors tend to exhibit nucleophilic character.

5.1 Dimethoxycarbene : Background

Dimethoxycarbene (**103**) is considered to be a *nucleophilic* carbene.[132] Donation by the lone pairs of the oxygen atom of the methoxy substituents into the formally vacant p-orbital of the carbene results in dipolar character (see Figure 5.1) and also strongly stabilizes the singlet state[131,133] This resonance interaction not only influences its ground state stability, but it also provides stabilization of positive charge in the transition states and intermediates of reactions involving nucleophilic attack by the carbene carbon's lone pair of electrons.[134]

Dimethoxycarbene (**103**) has been generated from 7,7-dimethoxynorbornadienes,[135] dimethoxydiazirine,[136] hexamethoxycyclopropane,[137] and 2,2-dimethoxy-5,5-dimethyl-Δ^3-1,3,4-oxadiazoline (**102**, equation. 5).[138] Δ^3-1,3,4-Oxadiazolines, such as **102**, are established thermal precursors of dialkoxy-, alkoxyamino-, and alkoxy(thioalkoxy)carbene intermediates.[138,139]

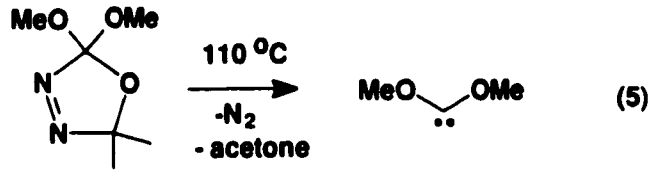

102 **103** (5)

The nucleophilic character of **103** is exemplified by its preference for reaction with electron-deficient olefins, such as dimethylfumarate, dimethylmaleate,[140] and styrene,[141] as well as strained olefins[138d] over more electron-rich olefins such as tetramethylethylene.[134,142] Dimethoxycarbene has also been shown to undergo [1+4] cycloaddition reactions with tetraphenylcyclopentadienone,[143] with tropone,[143] and with tetrazines.[144] Although a concerted mechanism may be responsible for the formation of [1+4] cycloaddition products, such conjugate additions may also be the result of stepwise addition of **103**.

The addition of **103** to electron-deficient alkynes such as dimethyl acetylenedicarboxylate (DMAD)[140] can yield cyclopropenone ketal intermediates which can ring open thermally to give dioxyvinylcarbenes.

Dimethoxycarbene (**103**) has also been shown to attack 2,4-dinitro-fluorobenzene and hexafluorobenzene (Scheme 5.1), by nucleophilic aromatic substitution, to afford acetals of aroyl fluorides.[145]

Scheme 5.1

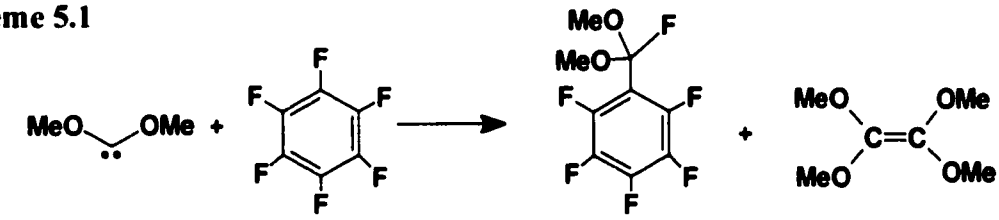

103 **104** **105**

The formal insertions of a carbene intermediate into carbon-halogen bonds can occur by different mechanisms depending on the nature of the carbene intermediate. Carbenes may insert into C-X bonds from the singlet spin state by: (1) initial formation of a halonium ylide intermediate followed by fragmentation to an ion pair, (2) a concerted mechanism, (3) halogen abstraction to give a radical pair, or (4) nucleophilic substitution which results in an ion pair which collapses to form products as illustrated in Scheme 5.2.

Scheme 5.2

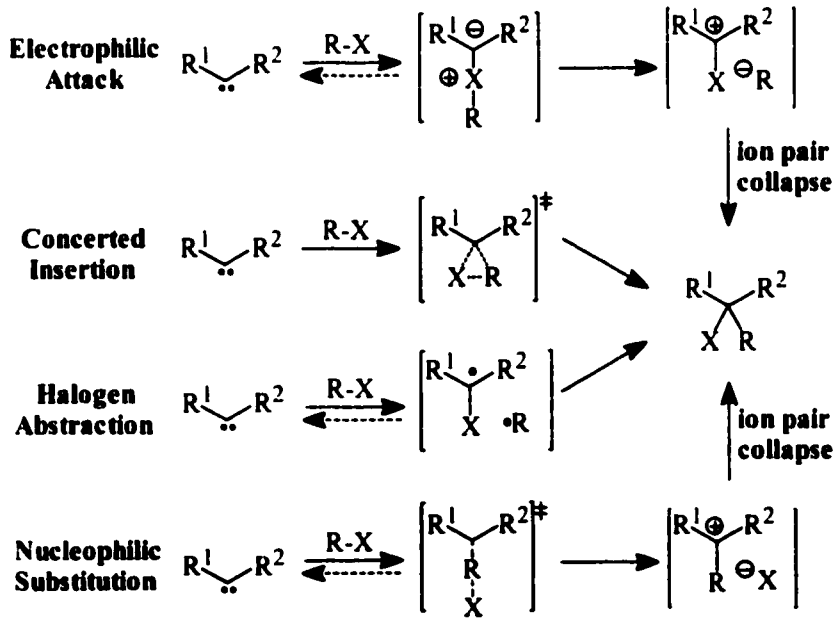

Very little information about the reactivity of **103** towards halogenated traps is known. Stimulated by the previous study (Chapter Four), the reactions of dimethoxycarbene (**103**) with polychlorinated cyclic olefins and ketones were investigated.

5.2 Results and Discussion.

5.2.1 Reaction of Dimethoxycarbene (103) with octachlorocycloheptatriene (82).

After thermolysis of oxadiazoline **102** at 110 °C in benzene containing octachlorocycloheptatriene (**82**) at an initial concentration of 0.1 M (1.1 equivalents relative to **102**) for 24 hours, radial chromatography yielded two major products (Scheme 5.3). These products were identified as dimethoxy(hexachloro)heptafulvene (**111**, 12% yield) and dodecachloroheptafulvalene (**91**, 56% yield). The GC-MS analysis of the crude reaction mixture, prior to chromatography, revealed the presence of octachlorotoluene, a known thermal decomposition product of **82**.[99] Thermolysis of **82** under identical conditions resulted in only 10% conversion of **82** to octachlorotoluene, with the remainder being starting material. A prolonged thermolysis experiment (2 weeks) converted octachlorocycloheptatriene fully to octachlorotoluene. Dimethoxy-(hexachloro)heptafulvene (**111**), a ketene acetal, was stable enough to permit identification by conventional spectroscopic techniques. However, this product was found to be very sensitive to atmospheric moisture. Prolonged exposure to air led to the decomposition of **111** to a single product **112** which was identified by standard methods as well as by X-ray crystallography (Figure 5.2).

Scheme 5.3

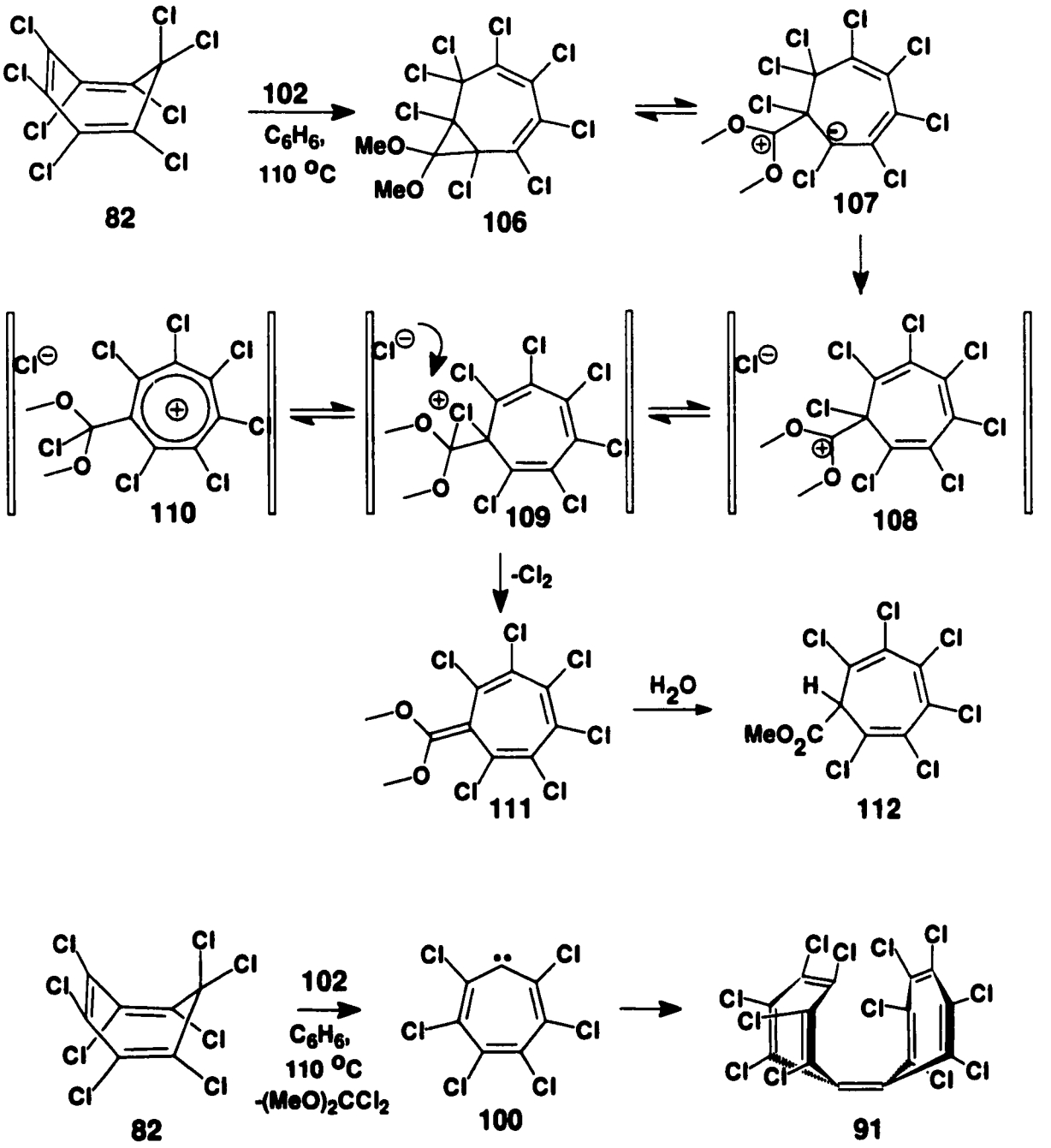

The fact that the cycloheptatriene moiety remained intact is in contrast to the reaction of **82** with methanol which yields the ring contraction product methyl perchlorobenzoate.[99] The mechanism for the formation of **112** from **111** presumably involves initial protonation at the ketene acetal double bond, followed by attack of water and subsequent

hemi-orthoester hydrolysis.

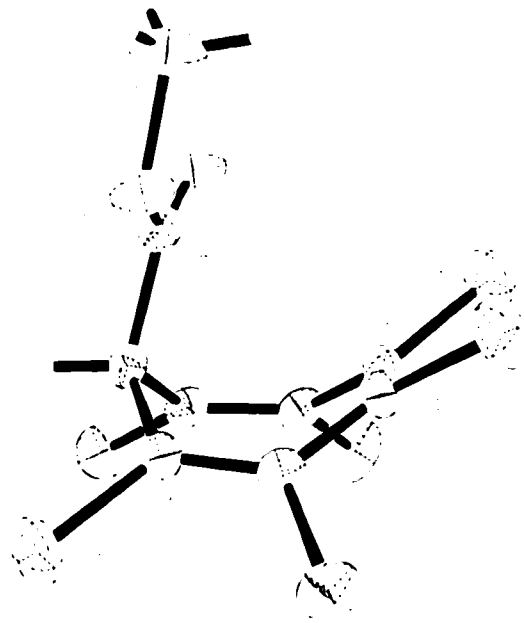

Figure 5.2 : X-ray structure of $C_7Cl_6(H)CO_2Me$, **112**.

The most straightforward mechanism for the formation of **111** appears to involve attack by dimethoxycarbene (**103**) at one of the double bonds of **82** (S_N2', or S_N2'', or S_N2''') to yield a dipolar intermediate such as **107** which may be thermally equilibrated with a cyclopropane intermediate (**106**). Subsequent loss of a chloride anion would then yield ion pair **108** which may exist as a chloronium ion (**109**) or as a cycloheptatrienyl cation/chloride anion pair (**110**). Heptachlorocycloheptatrienyl cation has been shown to exist as a stable salt[99] and, although the geometry has not been determined, it is unlikely to be planar.[98] The relative stabilities of the structures **108**, **109**, and **110** are not known but the chloronium ion intermediate (**109**) is expected to be more stable than the analogous structures in the reaction of **103** with hexachlorocyclopentadiene. Pezacki *et al.*[146] have shown the reaction of **103** with hexachlorocyclopentadiene yields three major

products, 5-carbomethoxy-1,2,3,4,5-pentachlorocyclopentadiene (**113**), 4,5-dicarbomethoxy-1,2,3,5-tetrachlorocyclopenta-diene (**114**), and 4,5,5-tricarbomethoxy-1,2,3-trichlorocyclopentadiene (**115**).

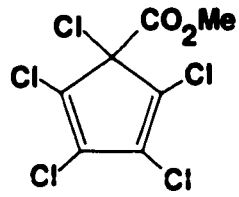

113

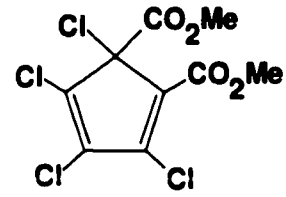

114

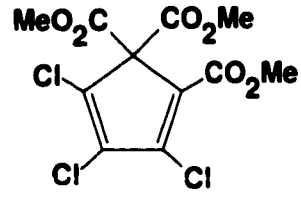

115

In this particular system, the formation of a chloronium ion intermediate was ruled out owing to the anti-aromatic nature of the cyclopentadienyl cation and product formation was rationalized in terms an intermediate zwitterion wherein positive charge was localized on the carbene carbon (**116**). Returning to Scheme 5.3, one of the ion pairs **108**, **109**, or **110** must then undergo dechlorination (in effect, the reverse of Cl_2 addition to ketene acetal **111**) rather than dechloromethylation. Dechlorination is in keeping with a chloronium ion structure which has the majority of the positive charge on chlorine rather than on the former carbene carbon. Within the chloronium ion **109**, the bridged chlorine must be more electrophilic than the methyls of the methoxy groups. If positive charge were localized on the former carbene carbon then demethylation (*viz.* **113**, **114** and **115**), instead of dechlorination, would be expected.

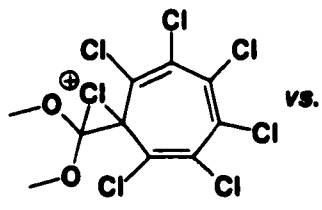

109

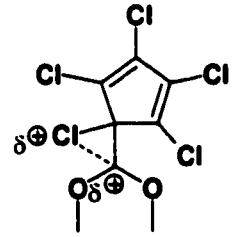

116

The formation of *syn*-dodecachloroheptafulvalene (**91**) was surprising. The selective

formation of *syn*-**91** in the reactions of *n*-BuLi,[116,117] and of various organometallic reagents[129] with **82** has been observed previously, and hexachlorocycloheptatrienylidene (**100**) has been implicated in the selective formation of this kinetic product.[129] *Syn*-**91** can be interconverted to *anti*-**93** but only at temperatures of 270 °C or higher.[117] It is postulated that **100** is formed in the thermal reaction of **103** with **82** and that it arises from either (a) electrophilic attack by **103** at an sp^3 hybridized carbon atom followed by elimination or (b) *via* an α-elimination in **117**, both giving the dimethoxyacetal of phosgene as a co-product,[147] although we cannot discount other possible mechanisms can not be discounted for the formation of **91**. Dimethoxycarbene (**103**) could also react like organolithium reagents, leading to *gem*-dechlorination (**82**→**100**).[118] The formation of carbene **100** in the reaction of **103** with **82** implicates a "carbene-to-carbene transfer" (a carbene reaction with a trap to generate a stable product and a new carbene) and such transfer reactions have been observed previously in reactions involving carbonyl groups.[148] Carbene **100** does not arise from the thermolysis of ketene acetal **111** which was found to be thermally stable in benzene at 110 °C for several days.

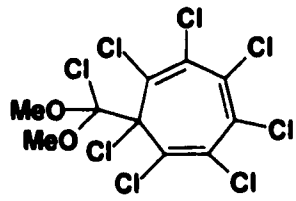

117

Cycloheptatrienylidene is known to exist in equilibrium with cycloheptatetraene and phenylcarbene, as are benzannulated analogues of cycloheptatrienylidene.[124,149] One expects that the perchlorocycloheptatrienylidene would also exist in equilibrium with the analogous perchlorinated isomers (Equation 6) and that the non-planar perchlorocycloheptatetraene would be favored to alleviate steric interactions between the

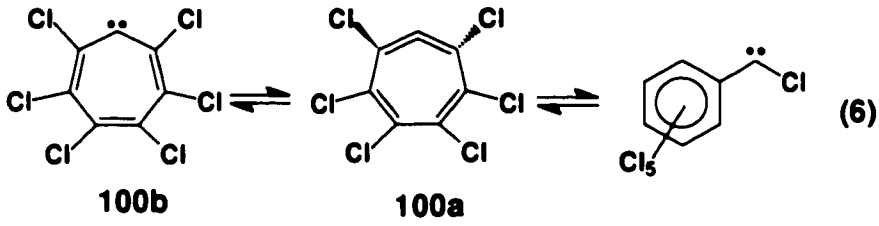

100b **100a** (6)

bulky chlorines. Trapping of cycloheptatrienylidene/cycloheptatetraene and benzannulated analogues by way of [4+2]cycloadditions with diphenylisobenzofuran (**DPIBF**) have been achieved previously.[150] The trapping of the proposed perchloro **100a** with **DPIBF** in the thermolysis of oxadiazoline **103** with octachlorocycloheptatriene (**82**) was attempted. Thermolysis of **102** in benzene at 110 °C in the presence of 0.1 M (1.1 equiv. with respect to **102**) of **82** and 0.2 M **DPIBF** yielded, after radial chromatography, products **111** and **91** as well as olefin **121** and an isomer of **121** which could not be purified despite repeated attempts. The basic structural features of compound **121** were identified by standard spectroscopic techniques, however, the *Z* configuration was determined by X-ray crystallography (Figure 5.3). It is suggested that olefin **121** originates from the trapping of **100a** by diphenylisobenzofuran *via* a [4+2]cycloaddition to give the Diels-Alder adduct **118** which, at 110 °C, then undergoes a Cope rearrangement to yield norcaradiene **119** (Scheme 5.4). Subsequent fragmentation to either a zwitterion (**120**) or a diradical, and rearrangement would be expected to give both *E* and *Z* forms of **121**. Fragmentation of zwitterion from the conformer where the anion and the alkoxy leaving group are anti-periplanar would give (*Z*)-**120** exclusively and may account for the selective formation of the *Z* isomer. Although it cannot be proven that **121** arises from carbene **100b**,[151] Cope rearrangements of this type (Scheme 5.4) are known to occur readily at elevated temperatures in cycloheptatrienes.

Scheme 5.4

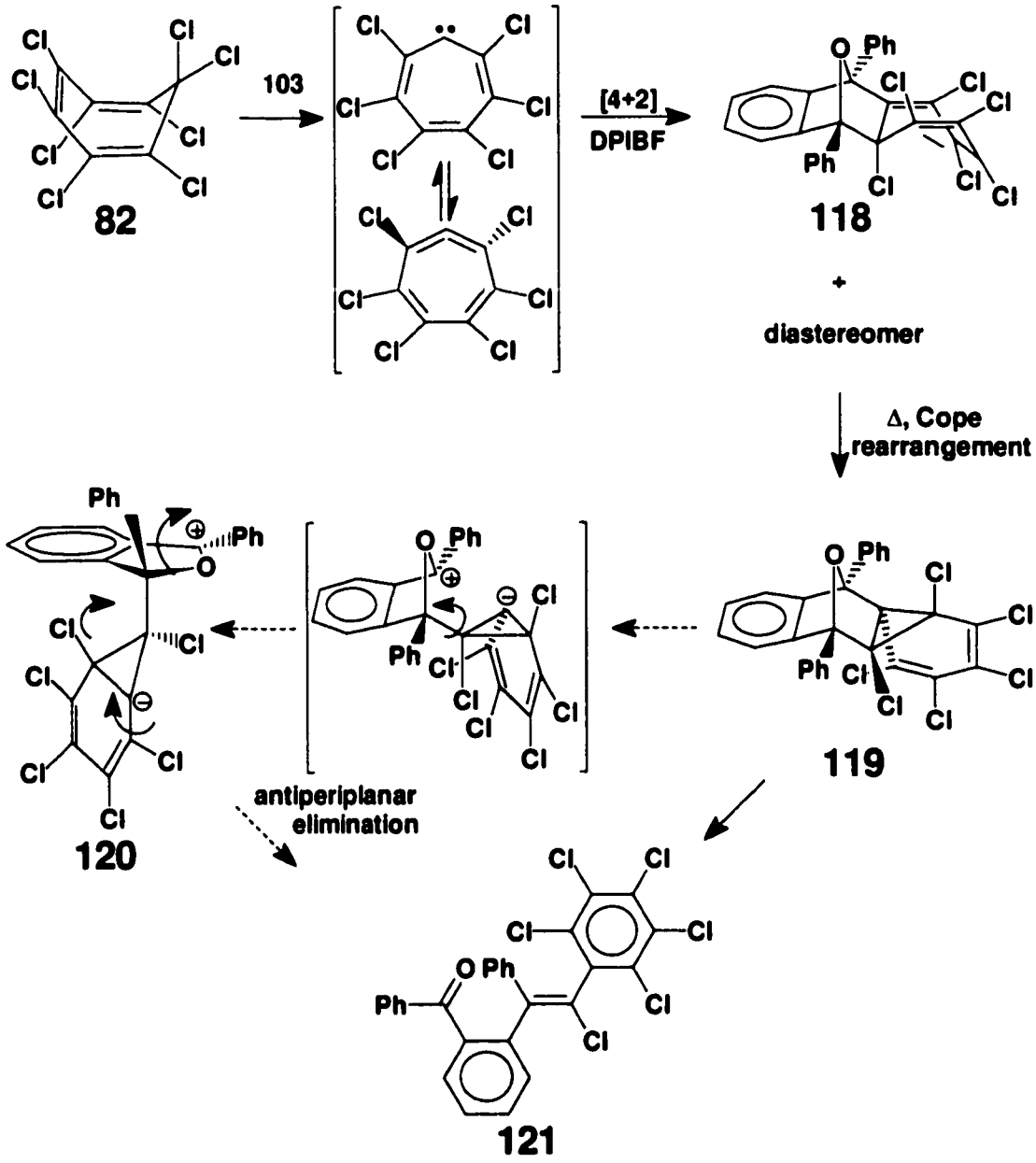
82
103
[4+2]
DPIBF
118
diastereomer
Δ, Cope
rearrangement
119
antiperiplanar
elimination
120
121

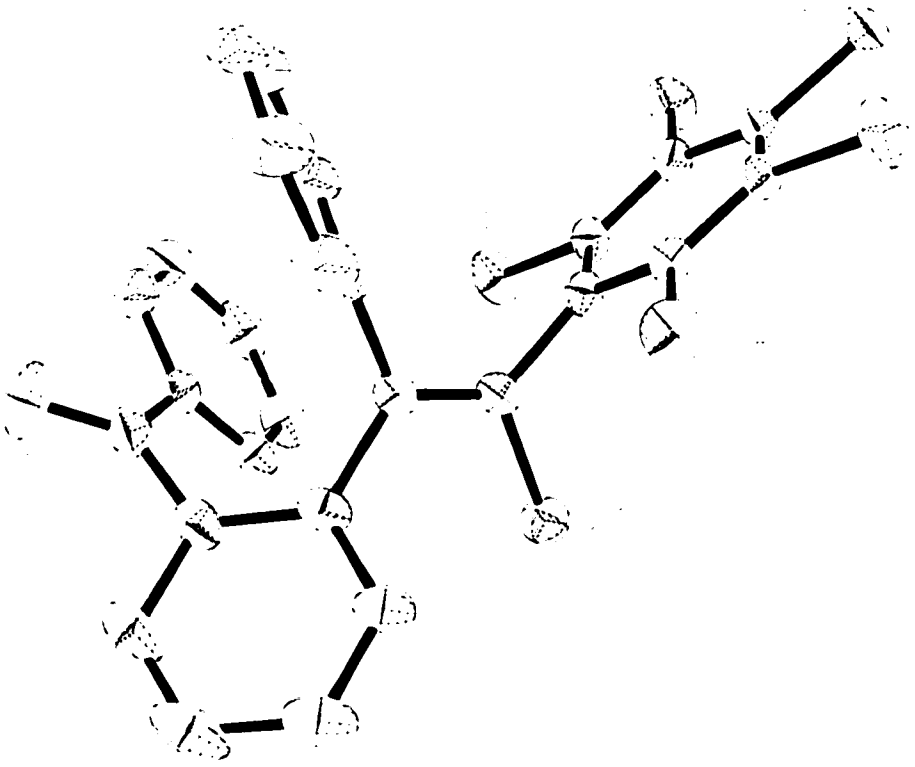

Figure 5.3: X-ray structure of (*Z*)-2-(2-Benzoylphenyl)-1-chloro-1-pentachlorophenyl-2-phenylethene,**121**. Hydrogen atoms are omitted for clarity.

5.2.2 Reaction of dimethoxycarbene (103) with octachlorobicyclo[3.2.0]hepta-3,6-diene (81).

Surprised by the reactivity of dimethoxycarbene (**103**) towards octachlorocycloheptatriene (**82**), the chemistry of **103** with the isomer of C_7Cl_8, octachlorobicyclo[3.2.0]hepta-3,6-diene (**81**) was investigated. Thermolysis of oxadiazoline **102** at 110 °C in benzene containing **81** at an initial concentration of 0.1 M (1.1 equivalents relative to **102**) for 24 hours yielded, after radial chromatography, dimethoxy(hexachloro)heptafulvene (**111**, 3% yield) and dodecachloroheptafulvalene (**91**, 11% yield). The remaining material was found to be unreacted **81** and carbene

dimer (tetramethoxyethylene) Reaction of **103** with octachlorocycloheptatriene (**82**) and with **81** gave the same products in roughly the same ratio suggesting that they were formed through a common intermediate. In keeping with our previous interpretations, we suggest that **103** attacks **81** to give a dipolar structure which then loses a chloride anion to give ion pair **122** (Scheme 5.5). Migration of a chlorine atom to the former carbene carbon by way of chloronium ion **123** would then give the allylic cation **124** which is analogous to the cation intermediate postulated for the aluminum chloride catalyzed conversion of **81** to octachlorocycloheptatriene (**82**).[99] Allylic cation **124** could then undergo a disrotatory ring opening[99] to yield the cycloheptatrienyl cation in ion pair **110**, an intermediate common to the reactions of **103** with both **82** and **81**. The lower yields from the latter presumably implies that **81** is less reactive than **82** towards **103**.

Scheme 5.5

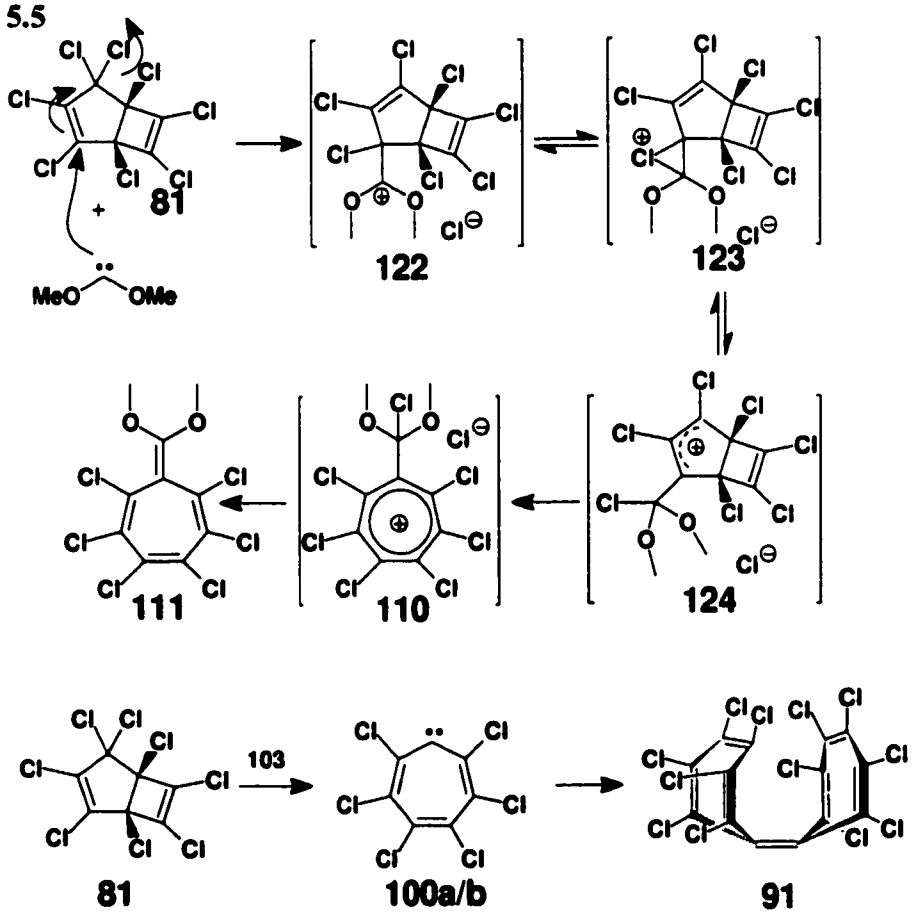

5.2.3 ***Reaction of Dimethoxycarbene (2) with hexachlorotropone (76).***

The facile rearrangements of 2-substituted tropones or tropolones to benzenoid derivatives in reactions with nucleophiles have been vigorously explored.[152] Although the chemistries of **82** and **76** have been scarcely investigated, independent reports by Scherer[153] and West *et al.*[99] have shown that both of these compounds afford methyl pentachlorobenzoate upon dissolution in methanol. The thermolysis of **76** and oxadiazoline **102** in benzene at 110 °C at an initial concentration of 0.1 M afforded, after radial chromatography, methyl 2-pentachlorophenyl-2-oxo-ethanoate (**129**) as the major product (44%). The isotopic abundance pattern from the mass spectrum was consistent with five chlorine substituents (see Figure 5.5) and the infra-red data suggested the presence of two C=O (IR = 1763 and 1738 cm^{-1}) functional groups. Furthermore, ^{13}C NMR spectroscopic data revealed four peaks in the aromatic region with an intensity ratio of 1:1:2:2 (^{13}C NMR δ 136.2, 135.4, 132.8, 129.4 ppm) and indicated the formation of a six-membered ring. This is in keeping with the reported rearrangements of troponoids to benzenoid derivatives.[152] The GC-MS analysis of the crude product mixture, prior to chromatography, confirmed that **129** was the major fraction (*ca.* 69%). In addition, unreacted hexachlorotropone (**76**, *ca.* 20%) was detected as well as three minor products which were identified as methyl pentachlorobenzoate (*ca.* 7 %), pentachlorobenzoyl chloride (*ca.* 2 %), and hexachlorobenzene (*ca.* 2 %). The latter two products are known thermal decomposition products of hexachlorotropone which presumably arise *via* a norcaradienone intermediate.[99b,154] It is suggested that **129** arises through nucleophilic attack by dimethoxycarbene at the carbonyl carbon generating a zwitterion intermediate **125**, presumably in equilibrium with the unobserved oxirane **126**

(Scheme 5.6). There is precedence for the formation of such intermediates in reactions of **103** with other carbonyl compounds.[155] Subsequent ring contraction *via* a stepwise semi-benzilic acid rearrangement is analogous to the formation of methyl pentachlorobenzoate from the reaction of C_7Cl_8 (**82**) with methanol.[99]

Scheme 5.6

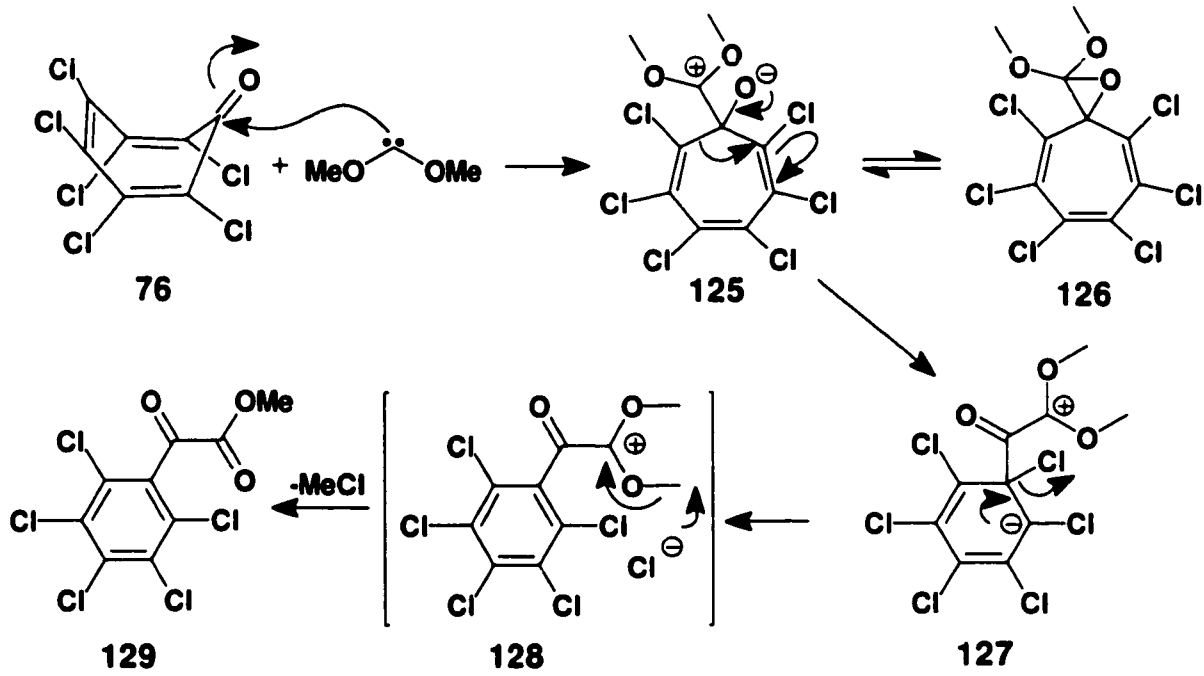

Figure 5.4 : Electron Impact mass spectrum of **129**

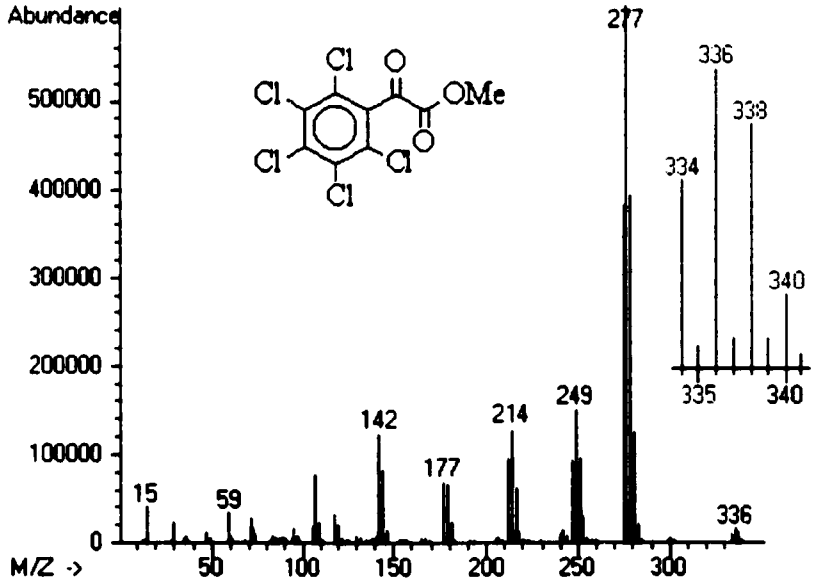

Reactions of hexachlorotropone with nucleophiles, including thiols, amines,[153] and organolithium reagents,[156] have been shown to give exclusively benzenoid products rather than nucleophilic addition without ring contraction. Ring contraction to intermediate **127** and subsequent elimination of a chloride anion would yield a new ion-pair intermediate, **128**. Dechloromethylation in **128** would then account for the observed product **129**. Another possible route to **129** could involve the reaction of **103** with pentachlorobenzoyl chloride; an analogue to the reaction of **103** with benzoyl chloride.[157] To assess the extent to which the reaction of **103** with pentachlorobenzoyl chloride contributes to the formation of **129**, we carried out the thermolysis of hexachlorotropone **76** in benzene (0.1 M) at 110 °C. The GC-MS of the product mixture revealed low yields of pentachlorobenzoyl chloride (*ca.* 5 %) and hexachlorobenzene (*ca.* 2 %) as well as starting material (*ca.* 93 %). Therefore, the pathway involving the reaction of pentachlorobenzoyl chloride with **103** can only be a minor contributor to the formation of **129**.

To account for the formation of methyl pentachlorobenzoate, an insertion of **103** into a C-Cl bond of hexachlorobenzene, followed by hydrolysis on exposure to air was considered. Dimethoxycarbene has been shown to be capable of nucleophilic aromatic substitution leading to formal carbon-halogen insertion products.[145] However, under similar thermolysis conditions, **103** did not react with hexachlorobenzene. The origin of methyl pentachlorobenzoate is therefore uncertain. Loss of CO from keto ester **129** may be a possibility.

Although other mechanisms involving nucleophilic attack at the ring carbons have been suggested for analogous systems and cannot be discounted,[152a,b] they are less likely

to occur in the formation of **129**. The reason is that the geometry of hexachlorotropone (**76**) has been shown to deviate considerably from planarity.[100,101] Arguments based on geometric constraints have been put forth previously to explain the selectivity in reaction pathways.[153] The boat-like geometry of **76** would result in an increased susceptibility for attack at the carbonyl carbon while simultaneously inhibiting the double bond shift associated with attack at the C-2 carbon.[153] In contrast, the C-7 position in **82** would be more sterically encumbered and as a result the double bonds in **82** would be the most likely site for attack by **103**. The possible pathways which could result in the same end products have been reviewed for 2-chlorotropones and tropolones and similar arguments pertaining to hexachlorotropone apply.[152]

5.3 Summary

Dimethoxycarbene reacts with octachlorobicyclo[3.2.0]hepta-3,6-diene (**81**) and octachlorocycloheptatriene (**82**) containing leaving groups in the alpha position by nucleophilic substitution (S_N2' or S_N2'') leading to ion pair intermediates. The latter undergo dechlorination to afford dimethoxy(hexachloro)heptafulvene (**111**) and Cl_2 owing to a chloronium ion intermediate. The unsaturated perchloroketone hexachlorotropone (**76**) is attacked at the carbonyl carbon atom to afford a dipolar intermediate that can initially rearrange without loss of a Cl^- moiety. These results are in keeping with the *nucleophilic* nature of dimethoxycarbene (**103**).

Chapter Six

Current and Future Work

6.0 Introduction: 7-Norbornenyl and 7-Norbornadienyl cations

The chemistry that has been investigated in Chapters Two and Three has led to the development and initial study of related projects. To reiterate, carbocations are termed either "classical" (trivalent) or "non-classical" (pentacoordinate or higher) and examples of the latter include the extensively investigated 7-norbornenyl (**130**) and 7-norbornadienyl (**131**) cations, whereby the overlap between the vacant *p* orbital at the C(7) position and the filled π orbital of the alkene alleviates the electron deficieny at C(7) and leads to charge delocalization.

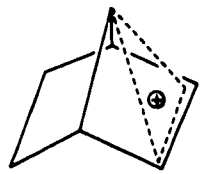

130

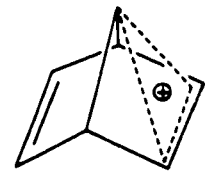

131

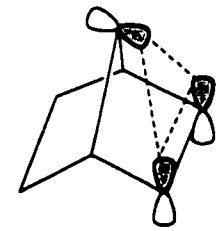

Speculation concerning the nature of the bonding in these cations arose from the initial discovery of the high solvolytic reactivity in the 7-norbornene[158] and 7-norbornadiene[159] systems. It was shown that the solvolyses of **132** and **133** (X = OTs) occurred 10^4 and 10^{11} times faster than that of the related 7-norbornyl system (**134**),[b] respectively, and this discrepency was rationalized by the formation of a nonclassical cationic intermediate

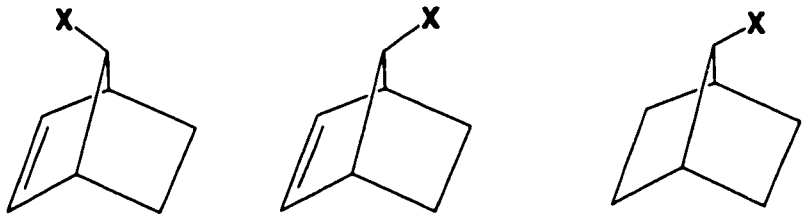

132 **133** **134**

(**130**). Moreover, the observed retention of the *anti*-configuration in the solvolysis of **133** further supported a nonclassical carbocation intermediate. However, the existence of the rapidly equilibrating pair of isomers (**135a,b**) has also been proposed as an alternative for

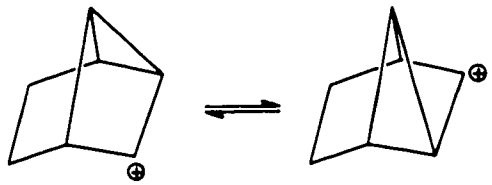

135a **135b**

130.[160] Extensive ^{13}C NMR spectroscopic studies have been carried out to investigate this possibility and on the basis of chemical shifts and one-bond ^{13}C-H coupling constants, as well as theoretical[161] and solvolytic data (see above), the possibility of intermediate **135a,b** was ruled out.

Despite the extensive interest in the bonding nature exhibited in these systems, only recently has the absolute structure of a 7-norbornenyl cation been determined, thus providing concrete data about structure and bonding in these systems. Treatment of 2,3-dimethyl-7-chloro-7-phenyl-2-norbornene (**136**) with silver hexafluoroantimonate yielded the corresponding salt (**137**) *via* elimination of silver chloride as shown in Scheme 6.1.[162]

---

[b] Solvolysis rates of 7-norbornadienyl systems to **131** are much larger.

Scheme 6.1

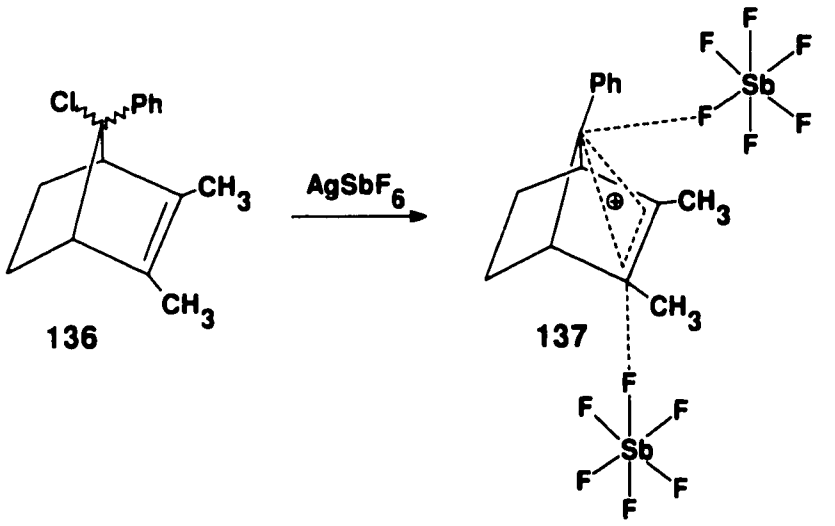

The structure of **137** was unambiguously determined by X-ray diffraction and revealed C(7)-C(2) and C(7)-C(3) interatomic distances of 1.86 (1) Å, as well as a lengthening of the C(2)-C(3) double bond (1.38 (1) Å, standard value for a tetraalkyl substituted double bond is 1.33(1) Å[163]). These structural features indicated a strong interaction of the empty *p* orbital and the π electrons of the C(2)-C(3) double bond and the existence of a five fold (nonclassical) coordination exhibited by the C(7) atom (depicted in Figure 6.1).

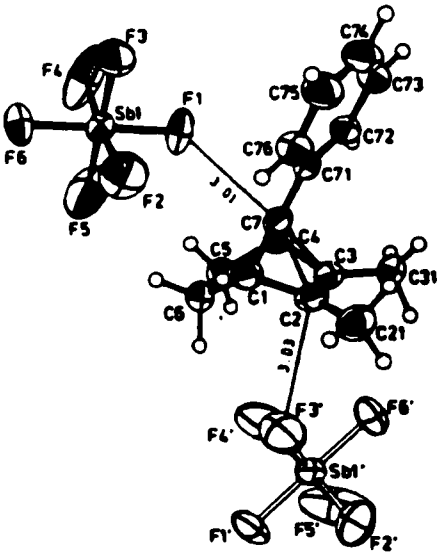

Figure 6.1 : X-ray Structure of **137**.

More recently, Evans *et al.*[164] have reported the isolation of a samarium complex incorportating a norbornadienyl moiety (**138**), *via* reaction of $(C_5Me_5)_3Sm$ and CO. The complex was unequivocally determined by X-ray diffraction (Figure 6.2) and an in depth analysis of the geometrical parameters revealed that the C(7)-C(2) and C(7)-C(3) distances were 1.867(4) Å. Furthermore, a significant lengthening of the C(2)-C(3) double bond was observed (C(2)-C(3) = 1.426(4) Å compared to C(5)-C(6) = 1.328(5) Å) and these structural features of **138** indicated that the structure could be formally viewed as the zwitterion **138a**, containing a 7-norbornadienyl cation.

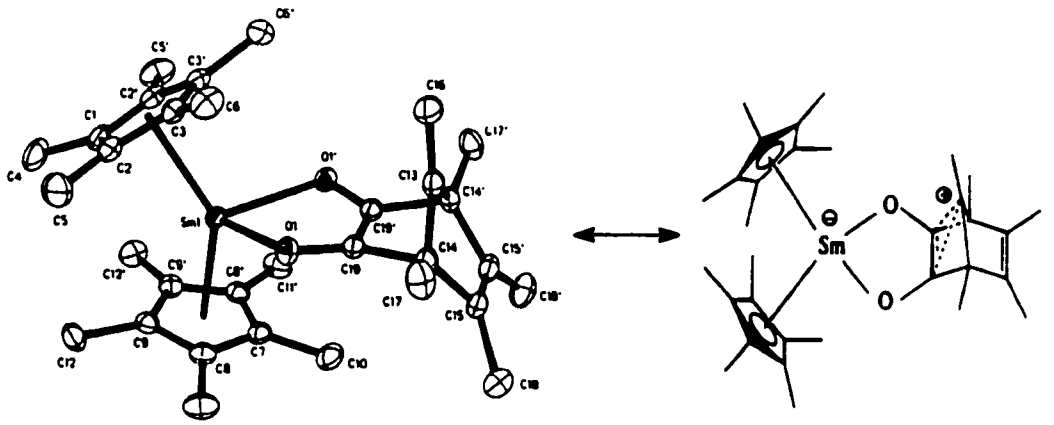

138 **138a**

Figure 6.2 : X-ray structure of **138**.

6.2 Norbornenyl and Norbornadienyl Cations: An Organometallic Approach.

Extensive studies of 7-norbornenyl and 7-norbornadienyl cations and derivatives have been conducted to investigate the nature of the bonding exhibited in these species. However, so far as we are aware there has only been one report (see above) of these species incorporating a transition metal moiety. Our underlying goal has been to investigate the chemistry of metal-stabilized 7-norbornenyl and 7-norbornadienyl cations.

As we had 5-trimethylsilyl-substituted cyclopentadienols (**139**) in hand, we attempted the synthesis of 7-norbornenols *via* Diels-Alder reactions of alkenes and alkynes with **139**.

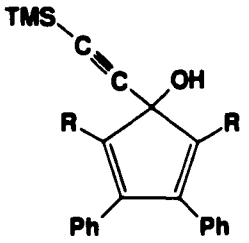

139a R = Et
139b R = Ph

Initial investigations suggested that electron-poor dienophiles were required for the [4+2] cycloaddition reactions to proceed (i.e. no addition reaction of **139** and diphenyl acetylene was observed even under refluxing conditions in toluene for one week). The 2,5-diethyl-3,4-diphenylcyclopentadienol (**139a**) had proven to be a more tractable system in the study of metal-stabilized anti-aromatic cations,[87] and consequently, with the intent of isolating a 7-norbornenol species, the reaction of **139a** and tetracyanoethylene (TCNE) at room temperature was attempted. Surprisingly, only a single product was observed. Although the spectral data (^{1}H, ^{13}C NMR, MS) indicated a [4+2] cycloaddition had occurred, the data were not consistent with the Diels-Alder adducts (**140**, **141**, Scheme 6.2).

Scheme 6.2

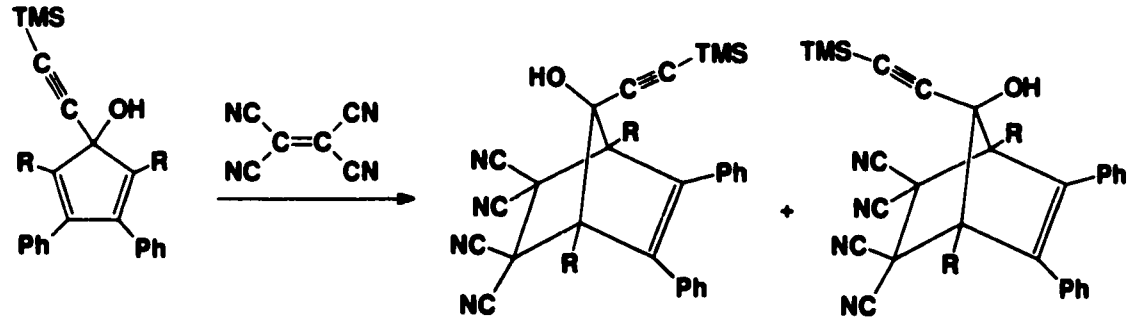

139a : R = Et
139b : R = Ph

140a : R = Et
140b : R = Ph

141a : R = Et
141b : R = Ph

Moreover, the data suggested an asymmetric product. The ^{1}H NMR data revealed four proton resonances ($\delta \approx$ 2.49-1.98, multiplets arising from diastereotopic methylene H's) of equal intensity and a pair of signals of triplet multiplicity ($\delta \approx$ 0.88 and 0.79 ppm), attributable to the ethyl substituents, as well as a broad peak at δ = 8.01 ppm (which exchanged upon addition of D_2O). In addition, the ^{13}C NMR exhibited distinct ethyl resonances (δ =20.5, 20.4 ppm (CH_2) and 8.5, 8.3 ppm (CH_3)), and indicated presence of only three cyano substituents (δ = 112.4, 112.2, 111.4 ppm). Since the NMR data were not structurally definitive, an X-ray diffraction study was attempted. The product was identified as the tricyclic species, **142a** and is depicted as Figure 6.3. More importantly, the structure of **142a** reveals an imine functionality (the hydrogen atom was located from the Fourier difference map) whereby the hydrogen atom occupies a *syn* orientation to the oxygen atom. The formation of **142a** presumably occurs *via* initial [4+2] cycloaddition, subsequent intramolecular cyclization and proton transfer.

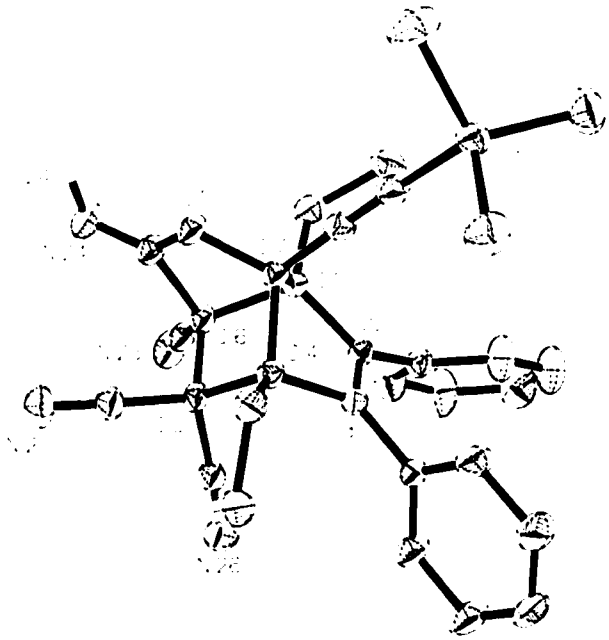

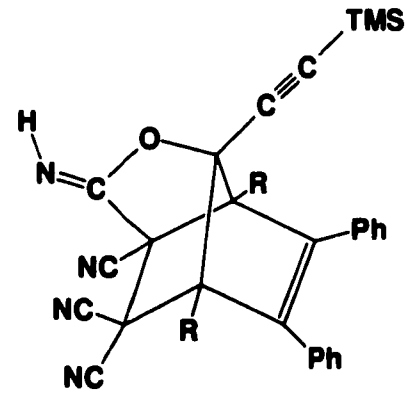

142a R = Et
142b R = Ph

Figure 6.3 : X-ray structure of **142a**.

It is noteworthy the formation of diastereomer **141a** was not observed in the reaction and may be attributable to steric effects from the trimethylsilylethynyl substituent.

In principle, intramolecular cyclization could be avoided by utilizing an alkyne ligand such as dimethylacetylenedicarboxylate (DMAD) in the Diels-Alder reaction with **139**. The resulting [4+2] cycloaddition product, 2,3-dicarbomethoxy-1,4-diethyl-5,6-diphenyl-7-trimethysilyl-2,5-norbornadien-7-ol (**143** and **144**) could then be protonated with a suitable acid to give **145** or treated with dicobalt octacarbonyl to yield the tetrahedral cluster, **17**. Subsequent protonation of **146** should yield the cluster-stabilized 7-norbornadienyl cation (**147**, Scheme 6.3). The effect of the metal complex on the formation of a nonclassical cation (i.e., is the cation delocalized?) could be investigated by direct comparison with the data from analogous studies of the free cation.

Scheme 6.3

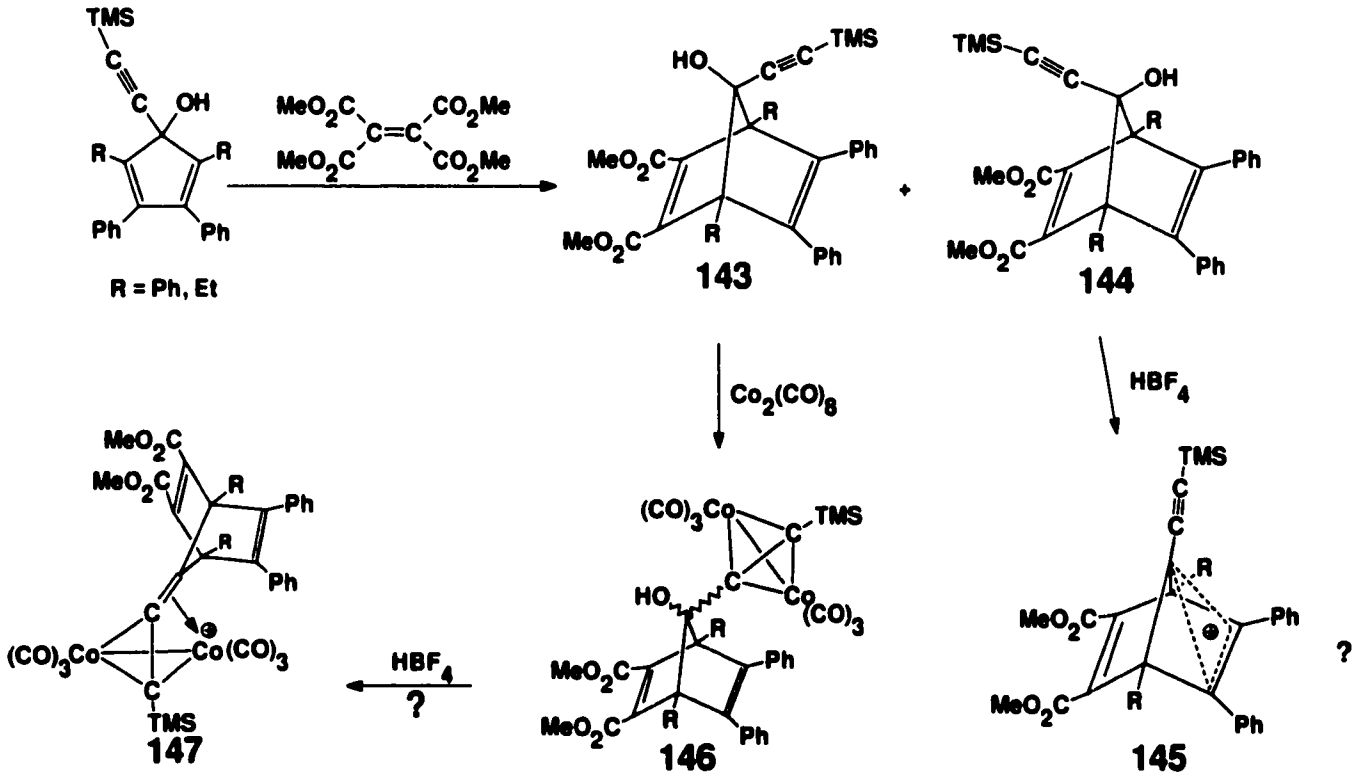

Furthermore, should the synthesis of the 7-trimethylsilylethynyl norbornadienes be successful, analogous studies using 4-ferrocenyl-1-trimethylsilylethynyl-2,3,5-triphenylcyclopentadien-1-ol (**149**) could be investigated.

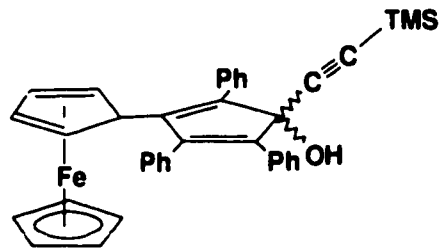

149

In this particular system, it would be of interest to determine the effect of the ferrocenyl moiety on the formation of a nonclassical cation. Incorporation of a dicobalt hexacarbonyl cluster would provide an intramolecular competition between the cluster substituent and the ferrocenyl moiety in terms of neighboring group stabilization.

6.3 Anti-Aromatic Cations Revisited.

The original goal of stabilizing an anti-aromatic 4π electron cyclopentadienyl cation incorporating a dicobalt hexacarbonyl metal cluster was successful, the synthesis of a structural model has remained elusive. In keeping with cluster-stabilized cations, the synthesis of the ferrocenyl-substituted cyclopentadienone, namely 4-ferrocenyl-2,3,5-triphenylcyclopentadien-1-one provides an attractive alternative. The structure of the ferrocenylmethyl cation (**5**) has been determined by X-ray crystallography[22] and one could envisage treatment of **148** with the lithium salt of trimethylsilylethyne to generate 4-ferrocenyl-1-trimethylsilylethynyl-2,3,5-triphenylcyclopentadien-1-ol (**149**). Subsequent protonation of **149** with $HBF_4 \cdot Et_2O$ at low temperature would, in principle, yield the ferrocenyl-stabilized cyclopentadienyl cation, **150**. (Scheme 6.4). With the goal of investigating the effect that the 4π anti-aromatic

cyclopentadienyl cation imposes on the ferrocenyl moiety, an X-ray crystallographic study of **150** could be carried out and the structure directly compared to the geometrical features exhibited by **5**. Thus, the synthesis of **150** would provide an alternative route to a metal-stabilized cyclopentadienyl cation. Furthermore, treatment of **149** with $Co_2(CO)_8$ would yield the dicobalt hexacarbonyl cluster (**151**); again subsequent protonation of **151** would provide a direct intramolecular competition between the dicobalt cluster and the ferrocenyl substituent.

Scheme 6.4

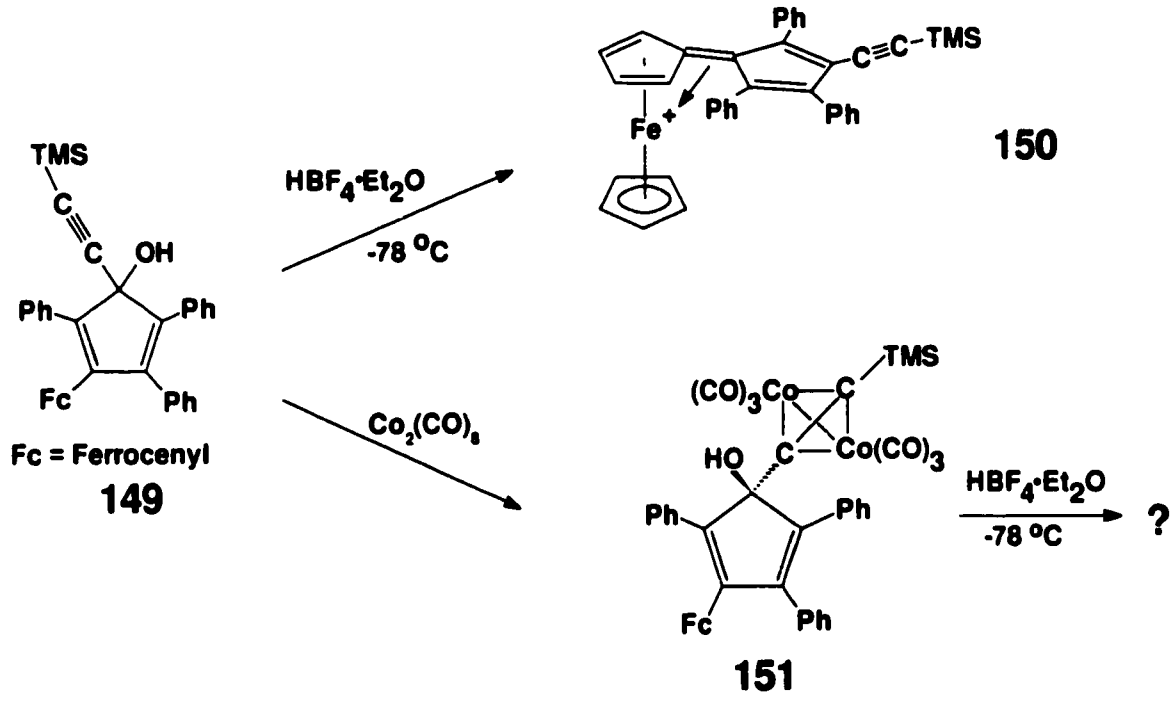

In summary, cations incorporating dicobalt hexacarbonyl moieties have been vigorously examined but the analogous studies of the 7-norbornenyl and 7-norbornadienyl cations have not. The generation of trimethylsilylethynyl cyclopentadienols (**139**) potentially provides a viable synthetic route to norbornen-7-ols and norbornadien-7-ols *via* Diels-Alder reaction. This work presented herein is preliminary and there remains much to do.

Chapter Seven

Experimental

7.1 General Information

All reactions were carried out under an atmosphere of dry nitrogen employing conventional benchtop and glovebag techniques. All solvents were dried according to standard procedures before use.[165] Silica gel (particle size: 20-45 microns) was employed for flash column chromatography. Melting points (uncorrected) were determined on a Thomas-Hoover melting point apparatus.

7.2 NMR Spectra

^{1}H and ^{13}C solution NMR spectra were acquired on a Bruker DRX 500, AM 300 or AM 200 spectrometer. ^{31}P solution NMR spectra were acquired on a Bruker AM-300 spectrometer and referenced to an external 85 % H_3PO_4 sample. All other NMR spectra were referenced to the residual proton signal, or the ^{13}C solvent signal. Two dimensional spectroscopy (^{1}H-^{1}H COSY, ^{1}H-^{13}C shift correlated and long range ^{1}H-^{13}C shift-correlated) were employed if possible for characterization of the compounds.

Spectra for all organometallic cluster cation complexes were acquired on a Bruker AC-300 spectrometer. The sample temperature was maintained by a Bruker Eurotherm B-

VT 2000 variable temperature unit and each temperature was measured by placing a copper-constantan thermocouple contained in an NMR tube, into the probe. Spectra were recorded on spinning samples.

Proton spectra were acquired at 500.130 MHz using a 5 mm broadband inverse probe with triple axis gradient capability. Usually, the spectra were obtained with 16 scans in 32K data points over a 3.931 KHz spectral width (4.168 s acquisition time). The free induction decay (FID) was processed using exponential multiplication (line broadening: 0.15 Hz) and was zero-filled to 64 K before Fourier transformation. Carbon 13-NMR spectra were recorded at 125.758 MHz using a 5 mm broadband inverse probe with triple axis gradient capability. The spectra were acquired over a 28.986 KHz spectral width in 32K data points (0.557 s acquistion time). The ^{13}C 90° pulse width was 4.4 μs. Relaxation delays of 1.0 s were employed and the FIDs were processed using exponential multiplication (line broadening: 4.0 Hz) and zero-filled to 64K before Fourier transformation.

Proton COSY 2-D NMR spectra were recorded in the absolute value mode using the pulse sequence: 90° - t_1 - 45° - ACQ and included pulsed field gradients for coherence selection. Spectra were acquired in 2 scans for each of the 256 FIDs that contained 2K data points in F2 over a spectral width of 3930.82 Hz. The 90° ^1H pulse width was 6.6 ms. A 1.0 s relaxation delay was employed between acquisition. Zero-filling in F1 produced a 1K x 1K data matrix with digital resolution of 3.84 Hz/point in both dimensions. During 2-D Fourier transformation a sine-bell squared window function was applied to both dimensions.

Proton spectra were recorded at 300.135 MHz using a 5 mm QNP probe. Carbon-13 and ^{31}P spectra were aquired at 75.469 MHz and 121.496 MHz, respectively, using the same

probe.

7.3 Mass Spectra

Mass spectra were determined using a VG analytical ZAB-E spectrometer by direct electron impact, chemical ionization or positive electrospray methods. The GC-MS analyses were carried out with a Hewlett Packard 5890 gas chromatograph equipped with a HP-5971A mass selective detector and a DB-1 capillary column (12m x 0.2 mm; Chromatographic Specialities, Inc.).

All masses quoted for polychlorinated compounds are the lowest value of *m/z* in the envelope and correspond to ^{35}Cl; the observed signal intensities correctly matched the pattern required for the number of chlorine atoms in the fragment ion.

7.4 Infra-Red Spectra

Infrared spectra were obtained on a Bio Rad FTS-40 FT-IR spectrometer and a SPC 3200 work station using NaCl (or KBr) solution cells.

7.5 *Elemental Analyses*

Elemental analyses were performed by Guelph Chemical Laboratories Ltd.

7.6 X-ray Crystallographic Data

A summary of the crystal data and structure refinement parameters are listed in the appropriate tables in the appendix. All crystals were grown by slow evaporation of the solvent and were mounted on fine glass fibers with epoxy cement.

X-ray crystallographic data for **47** were collected on a Siemens P4 diffractometer fitted with a FST scintillation counter using a rotating anode with graphite-monochromated Mo-Kα radiation (λ = 0.71073). X-ray crystallographic data for **82** and **91** were collected on a Siemens R3m/V diffractometer with Ag Kα radiation (λ = 0.56086 Å). Three standard reflections were measured after every 97 reflections and showed neither instrument instability nor crystal decay. Data were corrected for absorption using an empirical Ψ scan method. The structures were solved using the Direct Methods routine contained in the SHELXTL-PLUS program library.[166] The molecular parameters for **16** were in agreement with those previously published;[116] however, in that report, the molecular disorder was not clearly illustrated, and we show this phenomenon in Figure 4.9.

X-ray crystallographic data for compounds, **53**, **64**, **65**, **79**, **112**, **121** and **142a** were collected using a P4 Siemens diffractometer, equipped with a Siemens SMART 1K charge-coupled device (CCD) area detector (employing the program SMART[167]) and a rotating anode utilizing graphite-monochromated Mo-Kα radiation (λ = 0.71703 Å). The crystal-to-detector distance was 3.991 cm, and the data collection was carried out in 512 x 512 pixel mode, employing 2 x 2 pixel binning. In all cases, the initial unit cell parameters were determined by a least-squares fit of the angular settings of the strong reflections, and collected using three 4.5° scans (15 frames each) over three different parts of reciprocal space and one complete hemisphere of data was collected, to better than 0.8 Å resolution. Processing of the data was carried out using the program SAINT,[168] which applied Lorentz and polarization corrections to three dimensionally integrated diffraction spots. The program SADABS[169] was employed for the scaling of diffraction data, the application of a decay correction, and an empirical absorption

correction based on redundant reflections. All structures were solved using the direct methods routine outlined in the Siemens SHELXTL program library[170] followed by full-matrix least squares refinement on F^2 with anisotropic thermal parameters for all non-hydrogen atoms. For products, **112** and **142a** hydrogen atom positions were located from a Fourier difference map and then the coordinates refined with isotropic thermal parameters. In all other cases hydrogen atoms were added as fixed contributors at calculated positions riding on the relevant carbon atoms.

For **47** and **65**, the final refined structure revealed that the unit cell contained two independent molecules whose structures differ only slightly. For **53**, the final refined structure was based on a rotational disorder in which the carbon atoms of the $Si(CH_3)_3$ substituent could exist in a minimum of five different conformations. These five different conformations were refined assuming an equal occupancy ratio of 0.2. Refinement of the data, revealed electron density in the second coordination sphere of the molecule and the exact molecular formula could not be determined. This solvent molecule was assumed to be CH_2Cl_2 and allowed to refine as a free variable yielding a final occupancy of 0.64.

The final refinement of **64** revealed five independent molecules in the unit cell. The geometries of the phenyl and cyclopentadienyl rings were idealized. The iron, cobalt and silicon atoms were refined with anisotropic parameters. All remaining atoms were refined isotropically to limit the number of parameters.

7.7 Molecular Orbital Calculations

Molecular orbital calculations were performed via the extended Hückel method using weighted H_{ij}'s;[171] orbital drawings were obtained by use of the program CACAO.[172]

7.8 Syntheses and Spectral Data

(9-Trimethylsilylethynyl)fluoren-9-ol (33).

^{n}BuLi (11.67 mL of a 1.44 M hexane solution, 16.80 mmol) was added dropwise to a solution of trimethylsilylacetylene (1.65g , 16.80 mmol) in ether at -78 °C *via* cannula over a 60 min period, and the solution was allowed to warm to room temperature. After stirring for 1.5 h, the solution was cooled to -78 °C and fluorenone (3.024g, 16.80 mmol) in ether (40 mL) was added dropwise. The solution was allowed to warm to room temperature, stirred for 24 h, washed with distilled water, and the organic layer collected. Removal of ether yielded 9-trimethylsilylethynylfluorenol, **33**, (4.077 g, 14.67 mmol, 87 %) as a light yellow powder, mp 120-121 °C. ^{1}H NMR (500 MHz, CD_2Cl_2): δ 7.69 (d, 2H, $H_{1,8}$, ^3J =7.4), 7.65 (d, 2H, $H_{4,5}$, ^3J=7.4), 7.43 (t, 2H, $H_{3,6}$ ^3J=7.2), 7.38 (t, 2H, $H_{2,7}$, ^3J=7.2), 2.74 (s, OH), 0.19 (s, 9H, Me_3Si); ^{13}C NMR (125 MHz, CD_2Cl_2): δ 147.5 ($C_{8a, 9a}$), 139.5 ($C_{4a, 4b}$), 130.1 ($C_{3,6}$), 129.0 ($C_{2,7}$), 124.6 ($C_{1,8}$), 120.6 ($C_{4,5}$), 105.6 (*C*≡C-TMS), 88.5 (C≡*C*-TMS), 75.3 (C_9), -0.13 (Me_3Si); IR (CH_2Cl_2): $\upsilon_{C\equiv C}$ at 2304 cm^{-1}; MS (e.i.) *m/z* (%): 278 $[M]^+$ (30), 263 $[M\text{-}CH_3]^+$ (100), 202 (25), 165 $[C_{13}H_9]^+$ (15), 73 $[Me_3Si]^+$ (20); HRMS (e.i.) calcd for $C_{18}H_{18}OSi$: 278.1127, found: 278.1132.

$(Me_3Si\text{-}C\equiv C\text{-}C_9H_8OH)Co_2(CO)_6$ (34).

9-(Trimethylsilylethynyl)fluoren-9-ol (0.969 g, 3.49 mmol) dissolved in THF (50 mL) was added dropwise over a 45 min period to dicobalt octacarbonyl (1.26 g, 3.68 mmol) dissolved in THF (30 mL). The solution was then allowed to stir for 24 h at room temperature. After removal of solvent, the product was recrystallized from a hexane/ CH_2Cl_2 (9:1) mixture to give dark brown-red crystals of **34** in quantitative yield, mp 118 °C.

^{1}H NMR (200 MHz, CD_2Cl_2): δ 7.66 (d, 2H, $H_{1,8}$, ^3J = 7.4), 7.60 (d, 2H, $H_{4,5}$, ^3J = 7.5), 7.39 (td, 2H, $H_{3,6}$, ^3J = 7.4, ^4J = 1.3), 7.29 (td, $H_{2,7}$, ^3J = 7.4, ^4J = 1.3), 2.74 (s, OH), 0.43 (s, 9H, Me_3Si); ^{13}C NMR (50 MHz, CD_2Cl_2) δ 200.6 (Co-CO's); 150.9 ($C_{8a, 9a}$), 139.3 ($C_{4a, 4b}$), 129.9 ($C_{3,6}$), 128.0 ($C_{2,7}$), 124.7 ($C_{1,8}$), 120.6 ($C_{4,5}$), 118.2 (*C*≡C-TMS), 83.7 (C_9), 80.4 (C≡*C*-TMS), 0.60 (Me_3Si); IR (CH_2Cl_2): υ_{CO} at 2089, 2053, 2027 cm^{-1}; MS (e.i.) *m/z* (%): 536 $[M\text{-}CO]^+$ (10), 480 $[M\text{-}3CO]^+$ (40), 452 $[M\text{-}4CO]^+$ (10), 424 $[M\text{-}5CO]^+$ (25), 396 $[M\text{-}6CO]^+$ (40), 278 $[M\text{-}Co_2(CO)_6]^+$, 263 $[M\text{-}Co_2(CO)_6\text{-}CH_3]^+$ (100), 180 $[C_{13}H_8OH]^+$ (60), 73 $[Me_3Si]^+$ (70); Anal: Calcd. for $C_{24}H_{18}Co_2SiO_7$ C, 51.08 ; H, 3.21. Found: C, 51.28; H, 3.40.

$[(Me_3Si\text{-}C{\equiv}C{=}C_9H_8)Co_2(CO)_6]BF_4$ (35).

Two drops of HBF_4 were added to **34** in CD_2Cl_2 at -78°C in an NMR tube and the sample immediately turned deep red in colour, indicating the formation of **35**. ^{13}C NMR (75 MHz, CD_2Cl_2, 223 K): δ 192.7 (br., Co-CO's), 142.8, 140.7, 140.0, 138.5 (C_9), 136.8, 135.0, 134.1, 129.0, 128.5, 122.4, 122.0 (br), 121.9, 111.8 (*C*≡C-TMS), 88.7 (C≡*C*-TMS), 1.2 (Me_3Si).

$(Me_3Si\text{-}C{\equiv}C\text{-}C_9H_8OH)Co_2(CO)_4$dppm (36).

$(Me_3Si\text{-}C{\equiv}C\text{-}C_9H_8OH)Co_2(CO)_6$, **34**, (0.356 g, 0.631 mmol) and bis(diphenylphosphino)methane (0.376 g, 0.979 mmol) were dissolved in hexanes (60 mL) and the mixture was heated under reflux for 2 h. After removal of the solvent, the residue was subjected to flash chromatography. Elution with 2:1 hexanes/CH_2Cl_2 solvent mixture yielded **36** (0.365 g, 0.409 mmol, 65 %) as a brownish red powder, mp 208-9 °C. ^{1}H NMR (500 MHz, CD_2Cl_2): δ 7.80-6.65 (m, 28H), 3.52 (br, 2H, CH_2), 2.45 (s, 1H, OH), -0.37 (s,

9H, Me_3Si); ^{13}C NMR (125 MHz, CD_2Cl_2): δ 208.2, 204.4 (CO's), 152.3 ($C_{8a, 9b}$), 139.2 ($C_{4a, 4b}$), 140.1 (*ipso*, br,), 136.7 (*ipso*, br,), 132.7, 131.3 (*meta*), 129.8, 129.4 (*para*), 128.9, 128.8 (*ortho*), 128.3, 127.5, 126.0, 119.9 (C-H's), 114.5 (*C*≡C-TMS), 89.7 (C≡*C*-TMS), 86.9 (C_9), 36.8 (CH_2, t, $^1J(^{31}P-^{13}C)$ = 19.9 Hz), 0.1(Me_3Si); ^{31}P NMR (CD_2Cl_2): δ 35.54 (s); IR (CH_2Cl_2) ν_{CO} at 2018, 1990, 1963 cm^{-1}; MS (pes) *m/z* (%): 892 $[M]^+$ (25), 875 $[M-OH]^+$ (100).

[(Me$_3$Si-C≡C≡C$_9$H$_8$)Co$_2$(CO)$_4$dppm]BF$_4$ (37).

Protonation of **36** with HBF_4 Et_2O at 195K resulted in an immediate deep brown-red solution indicating the formation of the cation **37**. ^{13}C NMR (75 MHz, CD_2Cl_2, 213 K): δ 203.6, 201.8, 197.3, 193.2 (Co-CO's), 149.5, 143.1, 140.1, 139.0, 137.3 ($C_{4a, 4b, 8a, 9, 9a}$), 134.1, 132.7, 131.6-128.2 (broad), 122.9, 122.0, 121.9, 114.3 (*C*≡C-TMS), 86.6 (C≡*C*-TMS), 31.8 (br., CH_2), 1.6 (Me_3Si); ^{31}P NMR (CD_2Cl_2, 213 K): δ 24.37 (d, 1P), 21.31 (d, 1P), $^2J(^{31}P-^{31}P)$ = 69.7 Hz.

1-Trimethylsilylethynyl-2,3-diphenylinden-1-ol (38).

By analogy to the procedure described for **33**, 2,3-diphenylindenone (2.00g, 7.10 mmol) in THF (20 mL) was added to a 3-fold excess of the lithium salt of trimethylsilylethyne. The solution was quenched with water, extracted with ether and, removal of the solvent yielded **38** (2.102g, 5.53 mmol, 78 %), as a light yellow powder, mp 102.5-104 °C. ^1H NMR (500 MHz, CD_2Cl_2): δ 7.70-7.69 (m, 1H), 7.61-7.59 (m, 2H), 7.42-7.39 (br, 4H), 7.36-7.34 (m, 3H), 7.30-7.29 (m, 3H), 7.24-7.23 (m, 1H), 2.69 (s, OH), 0.21 (s, 9H, Me_3Si); ^{13}C NMR (125 MHz, $CDCl_3$): δ 146.3, 144.0, 142.7, 140.2 ($C_{2, 3, 4, 9}$), 134.1,

133.6 (*ipso*), 129.8, 129.2 (*meta, ortho*), 129.1 (*para*), 128.5, 127.91 (*meta, ortho*), 127.86 (*para*), 127.6, 127.2, 123.1, 121.1 ($C_{5, 6, 7, 8}$), 104.9 (*C*≡C-TMS), 89.7 (C≡*C*-TMS), 78.3 (C_1), -0.3 (Me_3Si); IR (CH_2Cl_2) $\upsilon_{C\equiv C}$ at 2309 cm^{-1}; MS (e.i.) *m/z* (%): 380 $[M]^+$ (80), 365$[M-CH_3]^+$ (22), 303 $[M-C_6H_5]^+$ (35), 291 (51), 252 (10), 73 $[Me_3Si]^+$ (100); HRMS (e.i.) calcd $C_{26}H_{24}OSi$: 380.1596, found: 380.1547.

(1-Trimethylsilylethynyl-2,3-diphenylinden-1-ol)$Co_2(CO)_6$, (39).

1-Trimethylsilylethynyl-2,3-diphenylinden-1-ol (0.511g, 1.34 mmol) dissolved in THF (20 mL) was added to a solution of $Co_2(CO)_8$ (0.803g, 2.34 mmol) in THF (20 mL). The solution was stirred for 24 h, the solvent removed by a rotary evaporator, and the residue purified by flash chromatography using a solvent mixture of 1:1 hexanes/CH_2Cl_2 yielding **39** (0.761g, 1.14 mmol, 85 %), as a brown-red powder, mp 153-54 °C. ^1H NMR (500 MHz, CD_2Cl_2): δ 7.67-7.60 (br., 3H), 7.39-7.08 (br., 11H), 2.86 (s, 1H, OH), 0.17 (s, 9H, Me_3Si); ^{13}C NMR (125 MHz, CD_2Cl_2): δ 200.6, 200.2 (Co-CO's), 151.4, 146.4, 142.9, 141.1 ($C_{2, 3, 4, 9}$), 135.5, 134.6 (*ipso*) 130.9, 129.5 (2C), 129.2, 128.3, 128.2 (*o, m, p*), 128.1, 126.7, 123.3,121.4 ($C_{5, 6, 7, 8}$), 114.3 (*C*≡C-TMS), 88.2 (C_1), 80.8 (C≡*C*-TMS), 1.1 (Me_3Si); IR (CH_2Cl_2) ν_{CO} at 2087, 2051, 2022 cm^{-1}; MS (e.i.) *m/z* (%): 582 $[M-3CO]^+$ (45), 498 $[M-6CO]^+$ (70), 422 $[M-Co(CO)_6-OH]^+$ (50), 380 $[M-Co_2(CO)_6]^+$ (65), 365 (40), 291 (35), 282 (70), 252 (20), 73 $[Me_3Si]^+$ (100); Anal: Calcd. for $C_{32}H_{24}Co_2SiO_7$ C, 57.66 ; H, 3.63. Found: C, 57.34; H, 3.42.

[{1-Trimethylsilylethynyl-2,3-diphenylindenyl}$Co_2(CO)_6$]BF_4 (40).

Protonation of **39** in CD_2Cl_2 with two drops of HBF_4 Et_2O resulted in an

immediate deep brown-red solution indicating the formation of the cation **40**. ^{1}H NMR (300 MHz, CD_2Cl_2, 233 K): 7.41-7.29 (m, 10H), 7.20-7.13 (m, 4H), 0.69 (s, 9H, Me_3Si); ^{13}C NMR (75 MHz, CD_2Cl_2, 233 K): δ 192.7 (br., Co-CO's), 156.5, 142.1, 140.7, 140.4, 138.5, 132.6, 132.4, 131.8, 130.2, 130.0, 129.7, 129.2, 128.7 (2C's), 128.5, 124.1, 121.2, 117.6 (*C*≡C-TMS), 89.2 (C≡*C*-TMS), 1.8 (Me_3Si).

{1-Trimethylsilylethynyl-2,3-diphenylinden-1-ol}$Co_2(CO)_4$dppm (41).

39 (0.491 g, 0.737 mmol) and bis(diphenylphosphino)methane (0.432 g, 1.13 mmol) were heated under reflux in hexanes (60 mL) for 2 h. Removal of the solvent, and flash chromatography of the residue using 3:1 hexanes/CH_2Cl_2 eluent, yielded **41** (0.412 g, 0.414 mmol, 56 %), as a brown-red powder, mp 215-16 °C. ^{1}H NMR (300 MHz, CD_2Cl_2): δ 7.67-7.00 (m, 30H), 4.97 (br., 1H, methylene-H), 3.55 (br., 1H, methylene-H), 2.78 (s, OH), 0.03 (s, 9H, Me_3Si); ^{13}C NMR (75 MHz, CD_2Cl_2): δ 208.2, 206.1, 205.6, 201.6 (Co-CO's), 152.4, 148.3, 143.1, 139.6 ($C_{2,3,4,9}$), 139.0, 137.3, 136.1, 134.9 (*ipso C*'s), 132.6, 132.5, 132.0, 131.9, 131.6, 130.6, 129.8, 129.5, 128.8, 128.3, 128.2, 127.5, 127.3, 125.9, 125.1, 120.5, 114.3 (*C*≡C-TMS), 91.0 (C_1), 84.7 (C≡*C*-TMS), 36.8 (t, CH_2, $^{1}J(^{13}C\text{-}^{31}P) = 20.9$ Hz), 1.3 (Me_3Si); ^{31}P NMR (CD_2Cl_2) 34.56 (d), 30.41 (d), $^{2}J(^{31}P\text{-}^{31}P) = 114.6$ Hz); IR (CH_2Cl_2) ν_{CO} at 2018, 1991, 1963 cm^{-1}; MS (pes) *m/z* (%): 994 $[M]^+$ (30), 977 $[M\text{-}OH]^+$; Anal: Calcd. for $C_{55}H_{46}Co_2P_2SiO_5$ C, 66.39 ; H, 4.66. Found: C, 66.33; H, 4.62.

(1-Trimethylsilylethynyl-2,3-diphenylindenyl)$Co_2(CO)_4$dppm]BF_4 (42).

Protonation of **41** in CD_2Cl_2 at 195 K with HBF_4 Et_2O resulted in an immediate deep brown-red solution indicating the formation of the cation **42**. ^{13}C NMR (75 MHz,

CD_2Cl_2, 213 K): δ 202.3, 200.7, 197.3, 193.7 (Co-CO's), 90.5 (C≡*C*-TMS), 35.7 (br.,CH_2), 2.5 (Me_3Si). ^{31}P NMR (CD_2Cl_2, 213 K) δ 38.78 (d), 15.16 (d), $^2J(^{31}P\text{-}^{31}P)$ = 57.2 Hz. A marked increase in complexity of the aromatic region in the ^{13}C NMR spectrum with respect to **41** was observed.

5-Trimethylsilylethynyl-1,2,3,4-tetraphenylcyclopentadien-5-ol (139b).

Following the procedure described for **33**, 2,3,4,5-tetraphenylcyclopentadienone (6.630 g, 17.3 mmol) dissolved in THF (30 mL) was added to (trimethylsilylethynyl)lithium (2-eq.) to yield 5-trimethylsilylethynyl-1,2,3,4-tetraphenylcyclopentadien-5-ol (7.594 g, 15.8 mmol, 91 %) as a yellow powder, mp 179-181 °C. ^1H NMR (500 MHz, $CDCl_3$): δ 7.55 (dd, *ortho*, 4H, $^3J(^1H_o\text{-}^1H_m)$ = 7.9 Hz, $^4J(^1H_o\text{-}^1H_p)$ = 1.7 Hz), 7.23- 7.19 (m, *meta, para*, 6H), 7.13-7.07 (m, *meta, para*, 6H), 6.97 (dd, *ortho*, 4H, $^3J(^1H_o\text{-}^1H_m)$= 7.6 Hz, $^4J(^1H_o\text{-}^1H_p)$= 1.5 Hz), 2.56 (s, OH), 0.12 (9H, Me_3Si); ^{13}C NMR (125 MHz, $CDCl_3$): δ 143.0, 142.6 ($C_{1,2}$), 134.7, 133.8 (*ipso*), 129.82, 129.79 (*meta*), 127.81, 127.76 (*ortho*), 127.2, 127.1 (*para*), 104.9 (*C*≡C-TMS), 91.3 (C≡*C*-TMS), 81.4 (C_5), -0.4(Me_3Si); IR (CH_2Cl_2) $\nu_{c\equiv c}$ at 2306 cm^{-1}; MS (e.i.) *m/z* (%): 482 $[M]^+$ (100), 467 $[M\text{-}CH_3]^+$ (10), 405 $[M\text{-}Ph]^+$ (50), 381 (30), 315 (15), 289 (10), 178 $[C_2Ph_2]^+$ (20), 73 $[Me_3Si]^+$ (40); HRMS (e.i.) calcd for $C_{34}H_{30}OSi$: 482.2065, found: 482.2027.

(5-Trimethylsilylethynyl-1,2,3,4-tetraphenylcyclopentadien-5-ol)$Co_2(CO)_6$ (43a).

5-Trimethylsilylethynyl-1,2,3,4-tetraphenylcyclopentadien-5-ol (1.207 g, 2.50 mmol) dissolved in THF (20 mL) was added dropwise over a 30 min period to dicobalt octacarbonyl (1.084 g, 3.17 mmol) dissolved in THF (15 mL). The solution was stirred for

24 h at room temperature. The product was recrystallized from hexane/CH_2Cl_2 (1:1) to give dark red crystals of **43a** in quantitative yield, mp 169-171 °C. ^{1}H NMR (300. MHz, CD_2Cl_2): δ 7.66 (br., 4H), 7.12 (br., 12H), 7.04 (br., 4H), 2.95 (s, 1H, OH), 0.11 (s, 9H, Me_3Si); ^{13}C NMR (75 MHz, CD_2Cl_2): δ 200.3 (Co-CO'S), 147.0, 144.9 ($C_{1,2}$), 136.7, 134.8 (*ipso*), 130.7, 130.2 (*meta*), 128.2 (br., *ortho*), 128.0, 127.2 (*para*), 110.8 (*C*≡C-TMS), 92.9 (C_5), 81.5 (C≡*C*-TMS), 1.3 (Me_3Si); IR (CH_2Cl_2) υ_{CO} at 2086, 2050, 2020 cm^{-1}; MS (e.i.) *m/z* (%): 580 [M-Co(CO)$_4$-OH]$^+$ (5), 524 [M-Co(CO)$_6$-OH]$^+$ (15), 178 [C_2Ph_2]$^+$ (20), 73 [Me_3Si]$^+$ (100).

[(5-Trimethylsilylethynyl-1,2,3,4-tetraphenylcyclopentadienyl)Co$_2$(CO)$_6$]BF$_4$ (44a).

Protonation of **43a** in CD_2Cl_2 with HBF_4 Et_2O at 195 K resulted in an immediate deepening in colour indicating formation of the cation **44a**. ^{13}C NMR (75 MHz, CD_2Cl_2, 233 K): δ 198.4 (br., Co-CO's), 151.9, 147.8, 141.6, 137.4 ($C_{1,2,3,4}$), 94.1 (*C*≡C-TMS), 83.6 (C≡*C*-TMS), 0.2 (Me_3Si). The ^{13}C NMR spectrum of **44a** exhibited a marked increase of complexity in the aromatic region with respect to that of **43a**.

{5-Trimethylsilylethynyl-1,2,3,4-tetraphenylcyclopentadien-5-ol}Co$_2$(CO)$_4$dppm (45a).

43a (0.250 g, 0.326 mmol) and dppm (0.188 g, 0.490 mmol) were dissolved in THF (50 mL) and stirred at room temperature for 40 h. Removal of the solvent, and flash chromatography of the residue with 2:1 hexanes/CH_2Cl_2 eluent yielded {5-trimethylsilylethynyl-1,2,3,4-tetraphenylcyclopentadien-5-ol}Co$_2$(CO)$_4$dppm (0.126 g, 0.115 mmol, 35 %) as a brown-red powder, mp 193-94 °C. ^{1}H NMR (500 MHz, CD_2Cl_2): δ

7.70-6.98 (m, 40H), 3.57 (q, 1H, methylene-H), 3.43 (q, 1H, methylene-H), 3.30 (s, OH), 0.38 (s, 9H, Me_3Si); ^{13}C NMR (125 MHz, CD_2Cl_2): δ 208.7, 202.4 (Co-CO's), 148.3, 144.4 ($C_{1,2}$), 138.5 (t, *ipso*, $^1J(^{31}P\text{-}^{13}C) \cong {}^3J(^{31}P\text{-}^{13}C)$ = 24.0 Hz), 137.2, 135.9 (*ipso* C's), 134.4 (t, *ipso*, $^1J(^{31}P\text{-}^{13}C) \cong {}^3J(^{31}P\text{-}^{13}C)$ = 17.6 Hz), 132.9, 131.3, 131.2, 130.6, 130.0, 129.5, 128.6, 128.2, 127.8, 127.6, 127.2, 126.8 (*o, m, p, C*-H's), 120.1 (*C*≡C-TMS), 94.8 (C_5), 73.1 (C≡*C*-TMS), 40.1 (t, CH_2, $^1J(^{31}P\text{-}^{13}C)$ = 18.1 Hz), 3.1 (Me_3Si); ^{31}P NMR (CD_2Cl_2): δ 31.78 (s); IR (CH_2Cl_2) ν_{CO} at 2019, 1994, 1964 cm^{-1}; .MS (pes) *m/z* (%): 1096 $[M]^+$ (100).

[{5-Trimethylsilylethynyl-1,2,3,4-tetraphenylcyclopentadienyl}$Co_2(CO)_4$dppm]BF_4 (46a).

Protonation of **45a** in CD_2Cl_2 with HBF_4 Et_2O at 195 K in an NMR tube resulted in an immediate deepening in colour of the solution indicating formation of the cation **46a**. Upon protonation, the ^{13}C NMR spectrum exhibited a marked increase in complexity in the aromatic region with respect to that of **45a**. ^{31}P NMR (CD_2Cl_2, 193 K): δ 39.00 (d), 18.14 (d), $^2J(^{31}P\text{-}^{31}P)$ = 60.5 Hz.

2,5-Diethyl-3,4-diphenylcyclopentadienone

2,5-Diethyl-3,4-diphenylcyclopentadienone was synthesized according to literature procedures.[75] Benzil (15.708g, 74.80 mmol) was added to a solution of alcoholic KOH (1.882g) in absolute ethanol (350 mL). 4-heptanone (20.91 mL, 149.6 mmol) was then added over a period of 30 min. The resulting solution was allowed to stir at room temperature for 48 h. Addition of distilled water to the solution resulted in an immediate formation of a yellow precipitate. The precipitate was dissolved in acetic anhydride and

then a few drops of conc. H_2SO_4 were added. Upon addition of the acid the yellow solution turned deep red in color. The solution was allowed to stir for 1h and upon careful addition to distilled water (250 mL) a deep red solid precipitated from solution. ^1H NMR ($CDCl_3$, 200 MHz) δ 7.50-7.45 (m, 6H), 7.22-7.17 (m, 4H), 2.53 (q, 4H, CH_2), 1.34 (t, 6H, CH_3). ^{13}C NMR ($CDCl_3$, 50 MHz) δ 203.6 (C_1), 153.0 (C_2), 133.5 (C_3), 129.0, 128.5, 128.3, 127.9, 16.7 (CH_2), 14.4 (CH_3). Mass Spectrum (DEI) *m/z* (%) 288 $[M]^+$ (100); 273 $[M\text{-}CH_3]^+$ (15); 245 $[M\text{-}CO\text{-}CH_3]^+$ (15); 231 $[M\text{-}CO\text{-}CH_2CH_3]^+$ (15); 202 $[M\text{-}CO\text{-}2\ CH_2CH_3]^+$ (10); 168$[C_2Ph_2]^+$ (10).

1,4-Diethyl-5-trimethylsilylethynyl-2,3-diphenylcyclopentadien-5-ol (139a)

By analogy to the procedure described for **33**, diethyldiphenylcyclopentadienone[75] (4.987 g, 17.31 mmol) in THF (50 mL) was added to a 2-fold excess of the lithium salt of trimethylsilylethyne. The solution was quenched with water, extracted with ether and, the solvent removed to yield 1,4-diethyl-5-trimethylsilylethynyl-2,3-diphenylcyclopentadien-5-ol (5.709 g, 14.79 mmol, 85 %) as a yellow oil. ^1H NMR (500 MHz, CD_2Cl_2): δ 7.25-7.22 (m, 6H, *m* and *p* H's), 7.06 (d, 4H, *ortho*, $^3J(^1H_o\text{-}^1H_m)$ = 7.7 Hz), 2.58-2.46 (m, 4H, CH_2), 2.37 (s, OH), 1.31 (t, 6H, CH_3, $^3J(^1H\text{-}^1H)$ = 7.6 Hz), 0.28 (s, 9H, Me_3Si); ^{13}C NMR (125 MHz, CD_2Cl_2): δ 145.8 ($C_{1,4}$), 141.4 ($C_{2,3}$), 135.8 (*ipso*), 129.5 (*ortho*), 128.2 (*meta*), 127.3 (*para*), 105.5 (*C*≡C-TMS), 89.5 (C≡*C*-TMS), 81.9 (C_5), 19.6 (CH_2), 14.8 (CH_3), 0.2 (Me_3Si); IR (CH_2Cl_2) $\nu_{c\equiv c}$ at 2305 cm^{-1}; MS (e.i.) *m/z* (%): 386 $[M]^+$ (10), 371 $[M\text{-}CH_3]^+$ (12), 357 $[M\text{-}CH_2CH_3]^+$ (8), 343 (5), 327 (5), 73 $[Me_3Si]^+$ (100).

{1,4-Diethyl-5-trimethylsilylethynyl-2,3-diphenylcyclopentadien-5-ol}$Co_2(CO)_6$ (43b). 1,4-Diethyl-5-trimethylsilylethynyl-2,3-diphenylcyclopentadien-5-ol (0.900 g, 2.33 mmol) dissolved in THF (15 mL) was added dropwise over a 15 min period to dicobalt octacarbonyl (1.114 g, 3.34 mmol) dissolved in THF (40 mL). The solution was stirred for 24 h at room temperature. The residue was purified by flash chromatography using 3:1 petroleum ether/CH_2Cl_2 eluent and recrystallized from a hexane/CH_2Cl_2 (9:1) mixture to give dark red crystals of **43b** (1.311 g, 1.95 mmol, 84 %), mp 123-25 °C. ^{1}H NMR (200 MHz, CD_2Cl_2): δ 7.20-716 (m, 6H), 7.03-6.99 (m, 4H), 2.61-2.39 (m, 4H, CH_2), 2.00 (s, 1H, OH), 1.13 (t, 6H, CH_3, $^3J(^1H-^1H)$ = 7.4 Hz), 0.41 (s, 9H, Me_3Si); ^{13}C NMR (50 MHz, CD_2Cl_2) δ 200.6 (Co-CO's) 149.9 ($C_{1,4}$), 141.5 ($C_{2,3}$), 136.0 (*ipso*), 129.3, 128.1 (*ortho, meta* C's), 127.1 (*para*), 112.0 (*C*≡C-TMS), 91.6 (C_5), 83.1 (C≡*C*-TMS), 20.7 (CH_2), 14.9 (CH_3), 2.0 (Me_3Si); IR (CH_2Cl_2) υ_{CO} at 2087, 2050, 2020 cm^{-1}; MS (e.i.) *m/z* (%): 588 [M-3CO]$^+$ (5), 532 [M-5CO]$^+$ (30), 504 [M-6CO]$^+$ (55), 428 [M-$Co(CO)_6$-OH]$^+$ (12), 386 [M-$Co_2(CO)_6$]$^+$ (10), 371 [M-$Co_2(CO)_6$-CH_3]$^+$ (15), 348 (25), 73 [Me_3Si]$^+$ (100).

[{1,4-Diethyl-5-trimethylsilylethynyl-2,3-diphenylcyclopentadienyl}$Co_2(CO)_6$]BF_4 (44b). Protonation of **43b** in CD_2Cl_2 with HBF_4 Et_2O at 195 K in an NMR tube resulted in an immediate deepening in colour indicating formation of the cation **44b**. ^{13}C NMR (75 MHz, CD_2Cl_2, 223 K): δ 192.4 (br., Co-CO's), 152.8, 145.7, 141.3, 135.3 (C_{1-4}), 134.1 (C_5), 133.4, 133.1 (*ipso*), 128.8 (2C's), 128.6, 128.2, 128.0, 127.8 (*o, m, p*), 93.3 (*C*≡C-TMS), 83.5 (C≡*C*-TMS), 18.5 (CH_2), 18.2 (CH_2), 16.8 (CH_3), 14.8 (CH_3), 1.6 (Me_3Si).

{1,4-Diethyl-5-trimethylsilylethynyl-2,3-diphenylcyclopentadien-5-ol}$Co_2(CO)_4$ dppm (45b). Cluster **43b** (0.495 g, 0.737 mmol) and bis(diphenylphosphino)methane (0.385 g, 1.00 mmol) were dissolved in THF (45 mL) and stirred for 18 h. The residue that remained after evaporation was purified by flash chromatography using a 2:1 hexanes/CH_2Cl_2 solvent mixture to yield {1,4-diethyl-5-trimethylsilylethynyl-2,3-diphenylcyclopentadien-5-ol}$Co_2(CO)_4$ dppm (73 mg, 0.073 mmol, 10 %) as a brownish red powder, mp 197-98 °C. ^{1}H NMR (300 MHz, CD_2Cl_2): δ 7.72 (br., 4H), 7.41-7.30 (m, 10H), 7.11-6.88 (m, 16H), 4.55 (q, 1H, methylene-H), 3.71 (q, 1H, methylene-H, {$^1J(^1H\text{-}^1H) \cong {}^2J(^{31}P\text{-}^1H)$ =11.2 Hz}), 2.06 (q, 4H, CH_2), 1.64 (s, OH), 0.57 (t, 6H, CH_3, $^3J(^1H\text{-}^1H)$ = 7.3 Hz), 0.23 (s, 9H, Me_3Si); ^{13}C NMR (CD_2Cl_2, 75 MHz): δ 208.2, 204.9 (Co-CO's), 151.9, 139.5 ($C_{1,2}$), 139.6 (t, *ipso*, $^1J(^{31}P\text{-}^{13}C) \cong {}^3J(^{31}P\text{-}^{13}C)$ = 23.9 Hz), 136.7 (t, *ipso*, $^1J(^{31}P\text{-}^{13}C) \cong {}^3J(^{31}P\text{-}^{13}C)$ = 16.7 Hz), 136.4 (*ipso*), 132.4, 131.2, 129.7, 129.5 (2C's), 128.9, 128.3, 127.9, 126.6 (*o, m, p*), 110.4 (*C*≡C-TMS), 93.4 (C_1), 86.3 (C≡*C*-TMS), 35.8 (t, CH_2, $^1J(^{31}P\text{-}^{13}C)$ = 21.4 Hz), 21.2 (CH_2), 14.6 (CH_3), 1.3 (Me_3Si); ^{31}P NMR (CD_2Cl_2): δ 32.65 (s); IR (CH_2Cl_2) ν_{CO} at 2015, 1985, 1959 cm^{-1}; .MS (pes) *m/z* (%): 1000 $[M]^+$ (40), 983 $[M\text{-}OH]^+$; Anal: Calcd. for $C_{55}H_{52}Co_2P_2SiO_5$ C, 65.99 ; H, 5.24. Found: C, 66.02; H, 5.40.

[{1,4-Diethyl-5-trimethylsilylethynyl-2,3-diphenylcyclopentadienyl}$Co_2(CO)_4$dppm] BF_4 (46b). The addition of HBF_4 Et_2O to **45b** in CD_2Cl_2 at 195 K in an NMR tube resulted in an immediate darkening of the solution indicating the formation of the cation, **46b**. ^{31}P NMR (CD_2Cl_2, 193 K): δ 41.07 (d), 23.74 (d), $^2J(^{31}P\text{-}^{31}P)$ = 58.9 Hz.

(Me_3Si-C=C=C_9H_8)$FeCo(CO)_6$ (47).

By analogy to the procedure previously described for (Me-C=C=CH_2)$FeCo(CO)_6$,[26] freshly distilled $Fe(CO)_5$ (2.19 g, 11.18 mmol) was added to a solution of **34** (0.784g, 1.39 mmol) dissolved in acetone (35 mL), and the mixture was heated under reflux for 24 h. After removal solvent *in vacuo*, the residue was subjected to flash chromatography on silica gel. Elution with hexanes gave light red crystals of **47** (96 mg, 0.018 mmol, 13 %), mp 300 °C (dec). ^{1}H NMR (500 MHz, CD_2Cl_2): δ 7.98(H_5)§, 7.81 (H_8)§, 7.75 (H_4)$^{\bullet}$, 7.69 (H_1)$^{\bullet}$, 7.48 (H_7)§, 7.37 (H_2)$^{\bullet}$, 7.32 (H_6)§, 7.24 (H_3)$^{\bullet}$; ^{13}C NMR (125.72 MHz, CD_2Cl_2): δ 209.7 (CO's), 145.3 (C_{4a})$^{\bullet}$, 141.4 (C_{4b})§, 141.1 (C_{9a})$^{\bullet}$, 140.6 (C_{8a})§, 129.6 (C_7)§, 129.0 (C_2)$^{\bullet}$, 127.4 (C_6)§, 127.1 (C_3)$^{\bullet}$, 121.3 (C_1)$^{\bullet}$, 120.9 (C_8)§, 120.6 (C_5)§, 120.5 (C_4)$^{\bullet}$, 106.7 (*C*≡C-TMS), 70.0 (C≡*C*-TMS), 2.8 (Me_3Si). [♦ and § denote environments shown by 2D NMR to be in the same ring; assignment of the *exo* and *endo* rings is arbitrary]. IR (CH_2Cl_2): υ_{CO} at 2078, 2039, 2019 cm^{-1}; MS (e.i.) *m/z* (%): 460 [M-3CO]$^+$ (5), 432 [M-4CO]$^+$ (5), 404 [M-5CO]$^+$ (10), 376 [M-6CO]$^+$ (10), 261 [Me_3Si-C≡C-C_9H_8]$^+$ (100), 73 [Me_3Si]$^+$ (66). X-ray quality crystals of **47** were grown from a 5:1 hexanes/CH_2Cl_2 solvent mixture.

{(1-Trimethylsilylethynyl-2,3-diphenyl)indenyl}$FeCo(CO)_6$ (53).

39 (0.484 g, 0.73 mmol) dissolved in acetone (20 mL) was added to a freshly distilled $Fe(CO)_5$ (1.480 g, 6.61 mmol) in acetone (20 mL). The solution was heated under reflux for 12 h while being monitored by TLC (1:1 hexanes/CH_2Cl_2). After removal of the solvent the residue was purified by flash chromatography using 1:1 hexanes/CH_2Cl_2 as the eluent. A dark red band was collected and the solvent removed in *vacuo*. The resulting residue was further purified by chromatography using hexanes

solvent. X-ray quality crystals of the dark red band, **53**, were grown from a 9:1 CH_2Cl_2/hexanes solution (26 mg, 0.04 mmol, 6 %). mp 123-24 °C. ^1H NMR (500 MHz, CD_2Cl_2): δ 7.14-6.82 (m, 14H), 0.59 (s, 9H, Me_3Si); ^{13}C NMR (125 MHz, CD_2Cl_2): δ 210.1 (Fe-CO's), 200.6 (Co-CO's), 144.7, 141.3, 140.5, 133.8, 130.7, 129.8, 129.6, 129.1, 128.6, 128.4, 128.0, 127.8, 125.8, 125.6, 125.0, 121.2, 120.8, 110.2, 70.4, 2.9(Me_3Si); IR (CH_2Cl_2) ν_{CO} at 2079, 2036, 2020 cm^{-1}; MS (e.i.) *m/z* (%): 419 [M-$Co(CO)_6$]$^+$ (40), 364 [M-$FeCo(CO)_6$]$^+$ (18), 289 (20), 207 (25), 73 [Me_3Si]$^+$ (100).

Reaction of {1,4-diethyl-5-trimethylsilylethynyl-2,3-diphenylcyclopentadien-5-ol}$Co_2(CO)_6$ with $Fe(CO)_5$. $Fe(CO)_5$ (9.90 mL, 75.3 mmol) was added over a 25 min period to 1,4-diethyl-5-trimethylsilylethynyl-2,3-diphenylcyclopentadien-5-ol (4.997 g, 7.44 mmol) dissolved in 125 mL of acetone. The solution was refluxed and monitored by TLC approximately every 5 h. After 60 h the solution was cooled, removal of solvent yielded a brown oil. The residue was subjected to flash chromatography using silica gel and 100 % CH_2Cl_2 to filter off decomposed $Co_2(CO)_8$. A second purification (flash chromatography) using 100% hexanes yielded **43b** (730 mg, 15 %), **65**, **67**, and decomposition products. Compound **65** was also purified a third time by flash chromatography using 100% hexanes eluent to yield a brown solid (338 mg, 6.8%). Crude **67** was further purified by flash chromatography a third time using dibasic aluminum oxide and 100% hexanes eluent to yield an red orange oil (26 mg, 1.0 %). **Data for 65.** mp 110-113°C. ^1H NMR (CD_2Cl_2) δ 7.40, 7.31, 7.21 (b, 10 H, 2 phenyl), 2.47 (s, 1H, $CH_{2b'}$), 2.04 (s, 1H, CH_{2b}), 1.57 (s, 1H, $CH_{2a'}$), 1.26 (s, 4H, CH_3, CH_{2a}), 0.88 (s, 3H, CH_3), 0.51 (s, 9 H, Me_3Si). A ^1H resonance attributable to a bridging hydrogen

was not observed. ^{13}C NMR (CD_2Cl_2) δ 218.4, 215.6 (Fe-CO's), 214.2, 202.2 (Co-CO's), 131.9, 131.3, 130.8, 128.8, 128.6, 128.5, 109.8, 109.7, 106.2, 100.1, 95.9, 81.4, 56.3, 18.6, 18.2, 17.2, 16.4, 2.4. IR (CH_2Cl_2) 3691, 3602, 2306, 2067, 2025, 1991, 1965, 1603, 1428, 1283, 1266 cm^{-1}; MS (e.i.) *m/z*: 624 $[M\text{-}Co(CO)_3]^+$, 540 $[M\text{-}Co(CO)_6]^+$, 481 $[M\text{-}Co_2(CO)_6]^+$, 426 $[M\text{-}Co(CO)_8]^+$, 73 $[Me_3Si]^+$. **Data for 67.** ^1H NMR (CD_2Cl_2) δ 7.31, 7.26 (b, 10 H, 2 Ph), 6.56 (s, 1H, OH), 2.31, 2.26 (4H, CH_2), 0.85 (s, 6H, CH_3), 0.13 (s, 9H, Me_3Si). ^{13}C NMR (CD_2Cl_2) δ 215.7 (CO's), 153.1, 151.3 ($C_{2,3}$), 132.4, 131.5, 128.4, 108.2 (*C*≡C-TMS), 96.5 (C_1), 86.7 (C≡*C*-TMS), 19.3 (CH_2), 14.1 (CH_3), 0.1 (Me_3Si); IR (CH_2Cl_2) 3067, 2303, 2074, 2062, 1997, 1921, 1595; 1288, 1263 cm^{-1}; MS (e.i.) *m/z*: 426, 370, 154, 73.

Reaction of 5-trimethylsilylethynyl-1,2,3,4-tetraphenylcyclopentadien-5-ol with $Fe(CO)_5$. $Fe(CO)_5$ (17.00 mL, 129.3 mmol) was added over a 25 min period to 5-trimethylsilylethynyl-1,2,3,4-tetraphenylcyclopentadien-5-ol (7.000 g, 9.11 mmol) dissolved in 125 mL of acetone. The solution was refluxed and monitored by TLC every 5 h. After 48 h the solution was cooled, removal of solvent yielded a brown oil. The residue was subjected to flash chromatography using 100 % hexanes to filter off any unreacted $Co_2(CO)_8$. Further purification under similar conditions yielded compounds **44a** (1.566g, 22 %), **64**, **66**, and unidentified decomposition products. **64** was purified by repeated flash chromatography using 1:1 CH_2Cl_2/Hexanes eluent to yield a brown solid (847mg, 10.8%). **66** was also further purified by repeated flash chromatography using 100% hexanes and an orange solid was obtained (287 mg, 5.0 %). **Data for 64.** mp 107-108 °C. ^1H NMR (CD_2Cl_2) δ 7.32-6.89 (m, 20 H, 4 Phenyl), 0.11 (s, 9 H, Me_3Si). A

signal corresponding to the bridging hydrogen atom was not observed. ^{13}C NMR (CD_2Cl_2) δ 218.4, 217.7, 135.7, 132.6-127.9 (17 peaks + overlapping), 109.9, 109.2, 106.3, 101.5, 82.4, 59.7, 2.2 (Me_3Si). IR (CH_2Cl_2) 3690, 3603, 2066, 2018, 1987, 1965, 1604, 1495, 1417, 1277, 1256 cm^{-1}; MS (e.i.) *m/z*: 636 $[M\text{-}5CO's]^+$, 577 $[M\text{-}Co_2(CO)_6]^+$, 521 $[M\text{-}Co_2(CO)_8]^+$, 466 $[M\text{-}FeCo(CO)_8]^+$, 267 $[C_3Ph_3]^+$, 73 $[Me_3Si]^+$. **Data for 66.** mp. 162-164 °C, ^1H NMR (CD_2Cl_2) δ 7.49-7.17 (br, 20 H, 4 Ph), 2.50 (s, 1H, OH), 0.58 (s, 9H, Me_3Si). ^{13}C NMR (CD_2Cl_2) δ 211.1 (Fe-CO's), 155.0, 154.3 ($C_{2,3}$), 132.6-126.8 (phenyl's), 109.5 (*C*≡C-TMS), 90.2 (C_1), 83.7 (C≡*C*-TMS), -0.3 (Me_3Si); IR (CH_2Cl_2) 3060, 2307, 2078, 2017, 1997, 1965, 1925, 1595, 1498, 1286 cm^{-1}; MS (e.i.) *m/z*: 606, 550, 522, 466, 450, 436, 380, 315, 289, 73.

Reaction of 64 and CCl_4

64 (50 mg, 0.058 mmol) was dissolved in CCl_4 (5 mL) and stirred for 24 h at room temperature. The ^1H and ^{13}C NMR spectra were consistent with those observed for **64** and did not reveal resonances attributable to $HCCl_3$, indicating that reaction had not occurred. Heating of **64** under refluxing conditions led to decomposition of the sample.

Reaction of 65 and CCl_4

Analogous to the treatment of **64** with CCl_4, **65** (50 mg, 0. 065 mmol) was dissolved in CCl_4 (5 mL) and stirred for 24 h at room temperature. Again, the spectral data (^1H, ^{13}C NMR) were consistent with those observed for **65**, indicating that reaction had not occurred.

Reaction of C_7Cl_8 with $Fe_2(CO)_9$

Octachlorocycloheptatriene (**82**, 0.184 g, 0.50 mmol), prepared by West's method[99] and $Fe_2(CO)_9$ (0.182 g, 0.50 mmol) were heated under reflux in tetrahydrofuran (THF) (10 mL) for 24 h. The mixture was cooled, filtered to remove the inorganic salts and the volume reduced under vacuum. Addition of hexane eventually led to the precipitation of light yellow crystals of $C_{14}Cl_{12}$, **91**, (0.080 g, 0.134 mmol, 54%). ^{13}C NMR (CD_2Cl_2) δ 137.0, 132.8, 128.6, 124.0. MS (e.i.) *m/z*: 588 $[M]^+$, 553 $[M-Cl]^+$, 518 $[M-2Cl]^+$, 483 $[M-3Cl]^+$, 448 $[M-4Cl]^+$, 378 $[M-6Cl]^+$, 294 $[C_7Cl_6]^+$, 259 $[C_7Cl_5]^+$, 224 $[C_7Cl_4]^+$, 189 $[C_7Cl_3]^+$.

Reaction of C_7Cl_8 with $Co_2(CO)_8$

$Co_2(CO)_8$ (0.372 g, 1.09 mmol) dissolved in THF (30 mL) was added to a solution of C_7Cl_8 (0.400 g, 1.09 mmol) in THF (10 mL) and allowed to stir at room temperature for 24 h. Filtration, concentration to half volume and treatment with hexane gave a crude solid that was purified by flash chromatography (hexanes) to yield as the sole product $C_{14}Cl_{12}$, **91**, (0.177 g, 0.30 mmol, 55%), identified by its mass spectrum.

Reaction of C_7Cl_8 with $(Ph_3P)_2Rh(CO)Cl$

A mixture of $(Ph_3P)_2Rh(CO)Cl$ (0.345 g, 0.50 mmol) and C_7Cl_8 (0.184 g, 0.50 mmol) in THF (20 mL) was heated under reflux for 24 h. Filtration, concentration to half volume and treatment with hexane gave a crude solid that was recrystallized from $CHCl_3$ to yield as the sole product $C_{14}Cl_{12}$, **91**, (0.095 g, 0.16 mmol, 64%), identified by its mass spectrum.

Reaction of C_7Cl_8 with $Na[Fe(CO)_2(C_5H_5)]$

To a solution of $[(C_5H_5)Fe(CO)_2]_2$ (0.145 g, 0.40 mmol) in THF (10 mL) was added excess Na/Hg. The resulting red solution was filtered, treated with C_7Cl_8 (0.270 g, 0.80 mmol), and allowed to stir at room temperature for 3.5 h, after which time the solution had become brown. Filtration, concentration to half volume and treatment with hexane gave a crude solid that was purified by flash chromatography (hexanes) to yield as the sole product $C_{14}Cl_{12}$, **91**, (0.133 g, 0.224 mmol, 56%), identified by its mass spectrum.

Reaction of C_7Cl_8 with $(acac)Rh(C_2H_4)_2$

A mixture of $(acac)Rh(C_2H_4)_2$ (0.129 g, 0.50 mmol) and C_7Cl_8 (0.184 g, 0.50 mmol) in THF (10 mL) was heated under reflux for 24 h. Filtration, concentration to half volume and treatment with hexane gave a crude solid that was recrystallized from $CHCl_3$ to give X-ray quality crystals of $C_{14}Cl_{12}$, **91**, (0.125 g, 0.34 mmol, 68%), identified by its mass spectrum.

Nonachloro[3.2.0]-3-heptene, C_7HCl_9 (80).

One fifth of 77.58 mmol of trichloroethylene was added over a period of 30 min to a mixture of hexachlorocyclopentadiene (19.99g, 73.27 mmol) and aluminum chloride (1.582g, 11.86 mmol) as the temperature was raised to 80 °C. The remainder of the trichloroethylene was added over 45 min at 80 °C. The reaction was allowed to continue for an additional 1.5 hours and the resulting purple mixture was cooled, poured on to ice and extracted with CH_2Cl_2. Recrystallization from methanol yielded a tan solid (24.26g, 82%), mp 79 °C (lit.[99] 80-81 °C). ^1H NMR ($CDCl_3$, 200 MHz) δ 5.01 (s, 1H). ^{13}C NMR ($CDCl_3$,

50 MHz) δ 137.8, 133.3 ($C_{2,3}$), 91.6 (C_4), 87.1(C_7), 80.9 (C_5), 79.4 (C_1), 70.0 (C_6). MS (e.i.) *m/z*: 400 $[M]^+$, 330$[M-2Cl]^+$, 295 $[M-3Cl]^+$, 271, 236, 166.

Octachlorobicyclo[3.2.0]hepta-3,6-diene (81).

81 was synthesized according to literature procedures[153] and identified by conventional spectroscopic techniques. White solid, mp 53-54 °C (lit.[153] 53 °C); ^{13}C NMR (50.3 MHz, $CDCl_3$) δ 137.4, 134.2, 133.4, 132.2, 89.0, 81.8, 78.7; MS (e.i.) *m/z*: 364 $[M]^+$, 329 (100%) $[C_7Cl_7]^+$, 294 $[C_7Cl_6]^+$, 259 $[C_7Cl_5]^+$, 189 $[C_7Cl_3]^+$, 154 $[C_7Cl_2]^+$, 119 $[C_7Cl]^+$; MS (c.i., NH_3) *m/z*: 382 $[M + NH_4]^+$.

Octachlorocycloheptatriene (82).

82 was synthesized according to literature procedures[99] and identified by conventional spectroscopic techniques. Pale yellow solid, mp 85 °C (lit.[99] 86 °C); ^{13}C NMR (50.3 MHz, CD_2Cl_2) δ 134.5, 134.1, 129.2, 84.3; MS (e.i.) *m/z*: 364 $[M]^+$, 329 (100%) $[C_7Cl_7]^+$, 294 $[C_7Cl_6]^+$, 259 $[C_7Cl_5]^+$, 189 $[C_7Cl_3]^+$, 154 $[C_7Cl_2]^+$, 119 $[C_7Cl]^+$, 84 $[C_7]^+$; MS (c.i., NH_3) *m/z*: 382 $[M+NH_4]^+$.

Hexachlorotropone (76).

76 was synthesized according to literature procedures[99b] and identified by conventional spectroscopic techniques. Yellow solid, mp 82-83 °C (lit.[99b] 82.5); ^{13}C NMR (50.3 MHz, $CDCl_3$) δ 177.5, 136.6, 134.5, 132.4; MS (e.i.) *m/z*: 310 $[M]^+$, 284 (100%) $[M-CO]^+$, 247 $[C_7Cl_5]^+$, 212 $[C_7Cl_4]^+$, 177 $[C_7Cl_3]^+$, 142 $[C_7Cl_2]^+$, 107 $[C_7Cl]^+$; MS (c.i., NH_3) *m/z*: 328 $[M+NH_4]^+$.

[(TMS-C=CCO(C_6Cl_5)] (78).

n-Butyllithium (0.75 mL of a 1.44 M hexane solution, 1.08 mmol) was added dropwise over a 15 min period to a solution of trimethylsilylacetylene (0.14 mL, 0.99 mmol) in ether at -78 ^{o} C *via* cannula and the solution was allowed to warm to 0 ^{o}C. After stirring for 1.5 h, the solution was then cooled to -78^{o}C and C_7Cl_6O (201 mg, 0.48 mmol) dissolved in ether (40 mL) was added dropwise. The solution was slowly warmed to room temperature, stirred for a further 24 h, quenched with distilled water and extracted with ether to yield a white powder (123 mg, 0.33 mmol, 51%), mp 128-130 ^{o}C. ^{1}H NMR (500 MHz, $CDCl_3$) δ 0.24 (9H, Me_3Si); ^{13}C NMR (125 MHz, $CDCl_3$) δ 173.5, 137.5, 135.7, 132.9, 128.8, 105.0, 100.5, -1.0; IR (CH_2Cl_2) 2303, 2090, 1683, 1599, 1439, 1418, 1285, 1273, 1260; MS (e.i.) *m/z*: 275, 247, 212, 177, 142, 107; MS (c.i., NH_3) *m/z*: 390 $(M + NH_4)^+$.

[(TMS-C≡C-C≡O(C_6Cl_5) $Co_2(CO)_6$] (79).

78 (70 mg, .19 mmol) was dissolved in THF (20 mL) and added dropwise over a 45 min period to dicobalt octacarbonyl (64 mg, 0.19 mmol) dissolved in THF (20 mL). The solution was then allowed to stir for 24 h at room temperature. The mixture was subjected to flash chromatography using hexanes, and the cobalt complex was recrystallized from a hexane/CH_2Cl_2 (9:1) mixture to give dark red crystals of **79** in quantative yield. ^{1}H NMR (200 MHz, CD_2Cl_2) δ 0.27; ^{13}C NMR (125 MHz, CD_2Cl_2) δ 199.0, 191.4, 140.2, 135.0, 132.8, 128.5, 106.0, 98.2, 1.2; MS (e.i.) *m/z* (%): 658 $[M]^+$, 275 $[C_7Cl_5O]$.

Reaction of dimethoxycarbene (103) with octachlorocycloheptatriene (82).

A solution of **102** (0.118 g, 0.74 mmol) in benzene (8.1 mL) containing 0.1 M C_7Cl_8 (**82**, 0.300 g, 1.1 mmol) was heated as described above for 24 h at 110 °C. Two major products, **111** and **91**, were isolated using radial chromatography with a gradient of solvents ranging from hexanes to 1:1 hexanes/CH_2Cl_2 as the eluent. Octachlorotoluene was also isolated as a minor product. In an independent experiment, **82** was heated under identical conditions and ≈ 10% was converted to octachlorotoluene. Prolonged heating (2 weeks) resulted in the complete conversion of **82** to octachlorotoluene.

Dimethoxy(hexachloro)heptafulvene (111).

Yield 12 %, white solid, mp 91-91.5 °C; ^{1}H NMR (500 MHz, CD_2Cl_2) δ 3.89 (s, 6 H); ^{13}C NMR (125.7 MHz, $CDCl_3$) δ 162.1, 132.0, 130.4, 126.0, 86.8, 57.9; IR (neat, KBr) 3007, 2956, 2856, 1618, 1555, 1467, 1430, 1320, 1266, 1223, 1192, 1165, 1120, 992, 921, 792, 725, 693, 674, 633 cm^{-1}; MS (e.i.) *m/z*: 368 $[M]^+$, 353 $[C_9H_3O_2Cl_6]^+$, 333 $[C_{10}H_6O_2Cl_5]^+$, 303, 275, 259 $[C_7Cl_5]^+$, 225, 189, 133 $[C_5H_6O_2Cl]^+$, 59 (100 %) $[CO_2Me]^+$; MS (c.i., NH_3) *m/z*: 369 $[M+H]^+$; HRMS calcd for $C_{10}H_6O_2Cl_6$ 367.8499, found 367.8492.

Dodecachloroheptafulvalene (91).

91 was identified on the basis of MS (e.i.) and ^{13}C NMR which were consistent with the reported literature data.[116,129] Yield 56 %.

Octachlorotoluene.

Yield 5 %, white solid, mp 69-71 °C (lit.[99b] 71-72 °C); ^{13}C NMR (50.3 MHz, CD_2Cl_2) δ 138.0, 136.1, 134.7, 132.9, 93.5; MS (e.i.) *m/z*: 364 $[M]^+$, 329 (100 %)

$[C_7Cl_7]^+$, 294 $[C_7Cl_6]^+$, 259 $[C_7Cl_5]^+$, 247 $[C_6Cl_5]^+$, 212 $[C_6Cl_4]^+$, 177 $[C_6Cl_3]^+$, 142 $[C_6Cl_2]^+$, 107 $[C_6Cl]^+$, 71, 47; MS (c.i., NH_3) *m/z*: 382 $[M+NH_4]^+$.

Attempted thermolysis of dimethoxy(hexachloro)heptafulvene (111).

A 0.05 M solution of dimethoxy(hexachloro)heptafulvene (**111**) (0.020 g, 0.054 mmol) in 1 mL of benzene-d_6 was placed into a NMR tube, degassed by means of three successive freeze-pump-thaw cycles, and the tube was then flame sealed. The solution was heated at 110 °C for 24 h and then analyzed by ^{1}H NMR (500 MHz) spectroscopy. No thermal decomposition products of **111** were observed.

Reaction of dimethoxycarbene (103) with octachlorobicyclo[3.2.0]hepta-3,6-diene (81). A solution of **102** (0.118 g, 0.74 mmol) in benzene (8.1 mL) containing 0.1 M octachlorobicyclo[3.2.0]hepta-3,6-diene (0.300 g, 0.82 mmol). The solution was heated as described above for 24 hours at 110 °C. Products **111** and **91** were isolated using radial chromatography in 11 % and 3 % yield, respectively.

7-Carbomethoxy-1,2,3,4,5,6-hexachlorocycloheptatriene (112).

Dimethoxy(hexachloro)heptafulvene (**111**) was found to decompose on prolonged exposure to air. The decomposition product was identified as 7-carbomethoxy-1,2,3,4,5,6-hexachlorocycloheptatriene (**112**). A 0.05 M solution of dimethoxy(hexachloro)heptafulvene (0.100 g, 0.27 mmol) in dichloromethane (5.5 mL) with 2 mL of distilled water was stirred at room temperature for 2 days. The reaction mixture was purified by radial chromatography (hexanes) to yield **112** as a white solid

(85 mg, 89%), mp 86-87 °C; ^{1}H NMR (200 MHz, CD_2Cl_2) δ 4.65 (s, 1H), 3.71 (s, 3H); ^{13}C NMR (50.3 MHz, CD_2Cl_2) δ 165.4, 133.2, 130.6, 127.9, 60.4, 54.2; IR (neat, KBr) 3007, 2954, 2844, 1751, 1641, 1616, 1597, 1575, 1449, 1436, 1291, 1274, 1230, 1152, 1090, 1003, 981, 957, 887, 862, 836, 799, 781, 727, 674, 647 cm^{-1}; MS (e.i.) *m/z*: 354 $[M]^+$, 319 $[C_9H_4O_2Cl_5]^+$, 295 (100 %) $[C_7HCl_6]^+$, 260 $[C_7HCl_5]^+$, 225 $[C_7HCl_4]^+$, 201 $[C_5HCl_4]^+$, 189 $[C_7Cl_3]^+$, 141 , 120, 107, 59 $[CO_2Me]^+$; MS (c.i., NH_3) *m/z*: 372 $[M+NH_4]^+$; HRMS calcd for $C_9H_4O_2Cl_6$ 353.8342, found 353.8339.

Reaction of dimethoxycarbene (103) with octachlorocycloheptatriene (82) containing diphenylisobenzofuran.

A 0.1 M solution of **102** (0.087 g, 0.54 mmol) in benzene (5.4 mL) containing 0.1 M octachlorocycloheptatriene (**82**, 0.200 g, 0.54 mmol) and 0.2 M diphenylisobenzofuran (0.294 g, 1.09 mmol) was heated as described above for 24 h at 110 °C. Radial chromatography using a solvent gradient ranging from hexanes to 1:1 hexanes/ethyl acetate as the eluent, yielded products **111**, **91**, and **121** as well as the hydrolysis product of diphenylisobenzofuran. Another isomer of **121** was also isolated but it could not be attained in either a high enough purity or yield to be fully characterized. This isomer had a mass spectrum identical to that of **121**.

(*Z*)-2-(2-Benzoylphenyl)-1-chloro-1-pentachlorophenyl-2-phenylethene (121).

Yield 16 %, white solid, mp. 158-9 °C; ^{1}H NMR (500 MHz, CD_2Cl_2) δ 7.05-7.80 (m, 14 H) ; ^{13}C NMR (125 MHz, CD_2Cl_2) δ 126.9, 128.1, 128.2, 128.4, 128.5, 128.7, 128.8, 129.5, 130.1, 130.4, 130.6, 130.8, 131.1, 131.3, 132.3, 132.9, 133.3, 134.8, 137.7,

140.4,196.7; IR (neat, KBr) 2924, 2852, 1771, 1736, 1661, 1597, 1579, 1492, 1447, 1315, 1276, 1199, 1179, 1154, 1103, 1074, 1061, 1025, 1001, 937, 848, 803, 768, 738, 704, 643 cm^{-1}; MS (e.i.) *m/z*: 564 $[M]^+$, 529$[C_{27}H_{14}OCl_5]^+$, 494 $[C_{27}H_{14}OCl_4]^+$, 459 $[C_{27}H_{14}OCl_3]^+$, 430, 417, 390, 361, 341, 325, 301, 247, 209 (100 %), 165, 134, 105, 77, 51; MS (c.i., NH_3) *m/z*: 582 $[M + NH_4]^+$; HRMS calcd for $C_{27}H_{14}OCl_6$ 563.9176, found 563.9179.

Reaction of dimethoxycarbene (103) with hexachlorotropone (76).

A solution of **102** (0.093 g, 0.58 mmol) in benzene (6.4 mL) was prepared containing 0.1 M hexachlorotropone (**76**, 0.200 g, 0.64 mmol) was heated as described above for 24 h at 110 °C. GC-MS analysis of the crude reaction mixture revealed four products identified as methyl 2-pentachlorophenyl-2-oxo-ethanoate (**129**) (69 %), pentachlorobenzoyl chloride (2 %), methyl pentachlorobenzoate (7 %), hexachlorobenzene (1 %), as well as unreacted hexachlorotropone (**76**, 20 %). Product **129** was isolated using radial chromatography with a gradient of solvent ranging from hexanes to 1:1 hexanes/CH_2Cl_2 as the eluent. Hexachlorotropone (**76**) was heated under identical conditions and GC-MS analyses of the reaction mixture detected pentachlorobenzoyl chloride (5 %) and hexachlorobenzene (2 %) in ≈ 2:1 ratio, with the remainder being starting material (93 %). Prolonged thermolysis times (2.5 weeks) converted hexachlorotropone fully to hexachlorobenzene and pentachlorobenzoyl chloride. A solution of **102** (0.102 g, 0.64 mmol) in freshly distilled benzene (7.0 mL) containing 0.1 M hexachlorobenzene (0.200 g, 0.70 mmol) was heated for 24 h at 110 °C as described previously. The only product detected (GC-MS) from this reaction was

tetramethoxyethylene.

Methyl 2-pentachlorophenyl-2-oxo-ethanoate (129).

Yield 44 %, white solid, mp 127-28 °C; ^{1}H NMR (300 MHz, CD_2Cl_2) δ 3.95; ^{13}C NMR (75 MHz, CD_2Cl_2) δ 181.3, 159.0, 136.2, 135.4, 132.8, 129.4, 54.1; IR (neat, KBr) 3046, 2967, 2850, 1763, 1738, 1646, 1545, 1439, 1352, 1322, 1273, 1230, 1138, 1031, 955, 867, 823, 789, 737, 683, 666, 634, 609 cm^{-1}; MS (e.i.) *m/z*: 334 $[M]^+$, 275 (100%) $[C_7OCl_5]^+$, 247 $[C_6Cl_5]^+$, 212 $[C_6Cl_4]^+$, 177 $[C_6Cl_3]^+$, 142 $[C_6Cl_2]^+$, 107 $[C_6Cl]^+$, 84, 72, 59 $[CO_2Me]^+$; MS (c.i., NH_3) *m/z*: 352 $[M+NH_4]^+$; HRMS (e.i.) calcd for $C_9H_3O_3Cl_5$ 333.8525, found 333.8536.

Pentachlorobenzoyl chloride.

Identified from the mass spectral (GC-MS) fragmentation pattern. MS (e.i.) *m/z*: 310 $[M]^+$, 275 (100%) $[C_7OCl_5]^+$, 247 $[C_6Cl_5]^+$, 212 $[C_6Cl_4]^+$, 177 $[C_6Cl_3]^+$, 142 $[C_6Cl_2]^+$, 107 $[C_6Cl]^+$, 87, 72, 60.

Methyl pentachlorobenzoate.

Identified from the mass spectral (GC-MS) fragmentation pattern. MS (e.i.) *m/z*: 306 $[M]^+$, 275 (100%) $[C_7OCl_5]^+$, 247 $[C_6Cl_5]^+$, 212 $[C_6Cl_4]^+$, 177 $[C_6Cl_3]^+$, 142 $[C_6Cl_2]^+$, 107 $[C_6Cl]^+$, 83, 71, 59 $[CO_2Me]^+$.

Hexachlorobenzene.

Yield 1 %, white solid, mp 225-227 °C (lit. 227-29 °C); ^{13}C NMR (50.3 MHz,

CD_2Cl_2) δ 132.3; MS (e.i.) *m/z*: 282 (100%) $[M]^+$, 247 $[C_6Cl_5]^+$, 212 $[C_6Cl_4]^+$, 177 $[C_6Cl_3]^+$, 142 $[C_6Cl_2]^+$, 107 $[C_6Cl]^+$, 72; MS (c.i., NH_3) *m/z*: 300 $[M+NH_4]^+$.

Reaction of {1,4-diethyl-5-trimethylsilylethynyl-2,3-diphenylcyclopentadien-5-ol} with tetracyanoethylene. {1,4-Diethyl-5-trimethylsilylethynyl-2,3-diphenylcyclopentadien-5-ol} (160 mg, 0.41 mmol) was dissolved in THF (10 mL) and added to tetracyanoethylene (97 mg, 0.758 mmol) in THF (10 mL). The solution was stirred for 24 h and after removal of the solvent the mixture was subjected to flash chromatography using CH_2Cl_2. Recrystallization using hexanes yielded clear colourless crystals of **142a** (165 mg, 0.32 mmol, 78%), mp 68-70 °C .^{1}H NMR (CD_2Cl_2, 500 MHz) δ 7.99 (s, N*H*), 7.33-7.27 (m, 8H, H_o, H_m), 7.02 (bs, 2H, H_p), 2.49-2.44 (m, 1H, CH_2), 2.14-2.09 (m, 2H, CH_2), 2.01-1.98 (m, 1H, CH_2), 0.88 (t, 3H, CH_3, ^3J (^{1}H-^{1}H) = 7.4 Hz), 0.79 (t, 3H, CH_3, ^3J (^{1}H-^{1}H) = 7.4 Hz), 0.29 (s, 9H, Me_3Si); ^{13}C NMR (CD_2Cl_2, 125 MHz) δ 159.9 (*C*=NH), 146.0, 141.5 ($C_{2,3}$), 132.7 (*ipso*), 132.5 (*ipso*), 129.0, 128.95, 128.93, 128.8, 128.7, 128.6 (*ortho, meta, para*), 112.4 (*C*N), 112.2 (*C*N), 111.4 (*C*N), 100.1 (C≡*C*-TMS), 96.1 (C_7), 93.7 (*C*≡C-TMS), 72.8, 72.5 ($C_{1,4}$), 58.4, 49.6 ($C_{5,6}$), 20.5 (CH_2), 20.4 (CH_2), 8.5 (CH_3), 8.3 (CH_3), 1.2 (Me_3Si); IR (neat, KBr) 3687, 3480, 3317, 2306, 1748, 1627, 1582, 1423, 1280, 1274, 1259, 1225, 1132; MS (e.i.) *m/z* (%): 514 (55) $[M]^+$, 368 (100), 178 (12) $[C_2Ph_2]^+$, 73 (40) $[Me_3Si]^+$; MS (ci, NH_3): 515 $(M+1)^+$.

Reaction of {5-trimethylsilylethynyl-1,2,3,4-tetraphenylcyclopentadien-5-ol} with tetracyanoethylene. {5-Trimethylsilylethynyl-1,2,3,4-tetraphenylcyclopentadien-5-ol} (358 mg, 0.74 mmol) was and tetracyanoethylene (95 mg, 0.74 mmol) were combined and

dissolved in THF (30 mL). The solution was stirred for 6 h and after removal of the solvent the mixture was subjected to flash chromatography using CH_2Cl_2. Recrystallization using hexanes yielded clear colourless crystals of **142b** (383 mg, 0.63 mmol, 85%), mp 187-189 °C (dec.). ^{1}H NMR (CD_2Cl_2, 500 MHz) δ 8.06 (s, N*H*), 7.60 (d, H_o, ^3J (^1H_o-^1H_m) = 7.4 Hz), 7.43-7.06 (m), 6.84 (d, H_o, ^3J (^1H_o-^1H_m) = 7.5 Hz), 0.21 (s, 9H, Me_3Si). ^{13}C NMR (CD_2Cl_2, 125 MHz) δ 159.4 (*C*=NH), 147.2, 141.0 ($C_{2,3}$), 132.7 (*ipso*), 131.7 (*ipso*), 130.5, 130.3, 130.1, 130.0, 129.74, 129.67, 129.4, 129.2, 129.0, 128.6, 128.5 (2C), 128.4 (2C), 113.0 (*C*N), 112.1 (*C*N), 110.5 (*C*N), 103.0 (C≡*C*-TMS), 97.9 (C_7), 94.4 (***C***≡C-TMS), 76.8, 74.9 ($C_{1,4}$), 56.6, 55.3 ($C_{5,6}$), -0.8 (Me_3Si); IR (neat, KBr) 3300, 2306, 1731, 1590, 1446, 1280, 1252, 1232, 1179; MS (e.i.) *m/z* : 610 $[M]^+$; 467 178 [C2P2]$^+$, 73 $[Me_3Si]^+$; MS(ci, NH_3) 611 $(M+1)^+$. HRMS Calcd for $C_{40}H_{30}N_4OSi$ 610.2123 Obs 610.2183.

7. *References and Notes*

1. Bethell, D.; Gold, V. *Carbonium Ions : An Introduction*, Academic Press, New York, **1967**.

2. (a) Olah, G. A. *Angew. Chem., Int. Ed. Engl.* **1995**, *34*, 1393. (b) Olah, G. A.; Prakash, G. K. S.; Sommer, J. *Superacids*, John Wiley and Sons, New York, **1985**.

3. Gillespie, R.J.; Peel, T.E. *J. Am. Chem. Soc.* **1973**, *95*, 5173.

4. Ege, S. *Organic Chemistry*, 2nd ed., D. C. Heath and Co., Lexington,. **1989**. p. 98.

5. Olah, G. A.; Liang, G. *J. Am. Chem. Soc.* **1975**, *97*, 6803.

6. Hollenstein, S.; Laube, T. *J. Am. Chem. Soc.* **1993**, *115*, 7240 and references therein.

7. (a) Doering, W. v. E.; Knox, L. H. *J. Am. Chem. Soc.* **1954**, *73*, 3203. (b) Harmon, K. in *Carbonium Ions*, G.A. Olah and P. v. R. Schleyer, (eds.), Wiley Interscience, New York, **1973**, Ch 2.

8. (a) Garratt, P. *Aromaticity*, John Wiley and Sons, New York, **1986**. (b) Garratt, P. *Aromaticity*, McGraw Hill, New York, **1971**.

9. Breslow, R.; *Acc. Chem. Res.* **1973**, *6*, 393.

10. Lambert, J. B.; Shurvell, H. F.; Lightner, D. A., Cooks, R. G. *Introduction to Organic Spectroscopy*, Macmillan, New York, **1987**. p 44.

11. Dauben Jr.; H. J.; Wilson, J. D.; Laity, J. L. *J. Am. Chem. Soc.* **1969**, *91*, 1991; **1968**, *90*, 811.

12. Elvidge, J. A.; Jackman, L. M. *J. Chem. Soc.* **1961**, 859.

13. Sondheimer, F. *Acc. Chem. Res.* **1972**, *5*, 81.

14. Jao, H.; Schleyer, P. v. R.; Mo, Y.; McAllister, M.; Tidwell, T. T. *J. Am. Chem. Soc.* **1997**, *119*, 7075.

15. Schleyer, P. v. R.; Maerker, C.; Dransfeld, A.; Jiao, H.; Hommes, N. J. v. E. *J. Am. Chem. Soc.* **1996**, *118*, 6317.

16. Morrison, R.T.; Boyd, R. N. *Organic Chemistry*, 4th ed., Allyn and Bacon, Boston, **1983**, p. 495-496.

17. Haynes, L. W.; Pettit, R.; Olah, G. A.; Schleyer, P. v. R. In *Carbonium Ions*, vol 5, Wiley, New York, 1976, p. 2049-2133.

18. Cais, M. *Organomet. Chem. Rev.* **1966**, 1, 435.

19. Gleiter, R.; Seeger, R.; Binder, H.; Fluck, E.; Cais, M. *Angew. Chem., Int. Ed. Engl.* **1972**, *11*, 1028.

20. Seyferth, D.; Merola, J. S. *J. Organomet. Chem.* **1978**, *160*, 275.

21. Holmes, J. D.; Jones, D. A. K.; Pettit, R. *J. Organomet. Chem.* **1965**, *4*, 324.

22. (a) Lupon, S.; Kapon, M.; Cais, M. *Angew. Chem., Int. Ed. Engl.*, **1972**, *11*, 1025. (b) Behrens, U. *J. Organomet. Chem.* **1979**, *182*, 89.

23. Albright, T. A.; Hoffmann, R.; Hoffmann, P. *Chem. Ber.* **1978**, *111*, 1591.

24. McGlinchey, M. J.; Girard, L.; Ruffolo, R. *Coord. Chem. Rev.* **1995**, *143*, 331 and references therein.

25. Schilling, B. E. R.; Hoffmann, R. *J. Am. Chem. Soc.* **1979**, *101*, 3456.

26. (a) Hoffmann, R. *Science* **1981**, *211*, 995. (b) Hoffmann, R. *Angew. Chem., Int. Ed. Engl.* **1982**, *21*, 711.

27. (a) Nicholas, K. M.; Pettit, R. *J. Organomet. Chem.* **1972**, *44*, C21. (b) Connor, R. E.; Nicholas, K. M. *J. Organomet. Chem.* **1977**, *125*, C45.

28. Schilling, B. E. R.; Hoffmann, R. *J. Am. Chem. Soc.* **1978**, *100*, 6274.

29. Padmanabhan, S.; Nicholas, K. M. *J. Organomet. Chem.* **1983**, *268*, 23.

30. Sokolov, V. I.; Barinov, I. V.; Reutov, O. A. *Izv. Akad. Nauk SSR, Ser. Khim.* **1982**, 1922.

31. Edidin, R. T.; Norton, J.; Mislow, K. *Organometallics* **1982**, *1*, 561.

32. Schreiber, S. L.; Klimas, M. T.; Sammakia, T. *J. Am. Chem. Soc.* **1987**, *109*, 5749.

33. (a) Meyer, A.; McCabe, D. J,; Curtis, M. D. *Organometallics* **1987**, *6*, 1491. (b) Sokolov, V. I.; Barinov, I. V.; Reutov, O. A. *Isv. Akad. Nauk SSR, Ser. Khim.* **1982**, 1922. (c) Galakhov, M. V.; Bakhmutov, V. I.; Barinov, I. V.; Reutov, O. A. *J. Organomet. Chem.* **1991**, *421*, 65. (d) Galakhov, M. V.; Bakhmutov, V. I.; Barinov, I. V. *Magn. Res. Chem.* **1991**, *29*, 506. (e) Gruselle, M.; Cordier, C.;

Salmain, M.; El Amouri, H.; Guérin, C.; Vaissermann, J.; Jaouen, G. *Organometallics* **1990**, *9*, 2993. (f) Cordier, C.; Gruselle, M.; Jaouen, G.; Bakhmutov, V. I.; Galakhov, M. V.; Troitskaya, L. L.; Sokolov, V. I. *Organometallics* **1991**, *10*, 2303. (g) Barinov, I. V.; Reutov, O. A.; Polyakov, A. V.; Yanovsky, A. L.; Struchkov, Yu. T.; Sokolov, V. I. *J. Organomet. Chem.*, **1991**, *418* C24. (h) Leberre-Cosquer, N.; Kergoat, R.; L'Haridon, P. *Organometallics* **1992**, *11*, 721. (i) Cordier, C.; Gruselle, M.; Vaissermann, J.; Troitskaya, L. L.; Bakhmutov, V. I.; Sokolov, V. I.; Jaouen, G. *Organometallics* **1992**, *11*, 3825. (j) El Amouri, H.; Vaissermann, J.; Besace, Y.; Vollhardt, K. P. C.; Ball, G. E. *Organometallics* **1993**, *12*, 605. (k) El Amouri, H.; Vaissermann, J.; Besace, Y.; Jaouen, G.; McGlinchey, M. J. *Organometallics* **1994**, *13*, 4426. (l) McClain, M. D.; Hay, M. S.; Curtis, M. D.; Kampf, J. W. *Organometallics* **1994**, *13*, 4377.

34. Downton, P. A.; Sayer, B. G.; McGlinchey, M. J. *Organometallics* **1992**, *11*, 3281.

35. Melikyan, G. G.; Bright, S.; Monroe, T.; Hardcastle, K. I.; Ciurash, J. *Angew. Chem. Int. Ed.* **1998**, *37*, 161.

36. (a) Sternberg, H. W.; Greenfield, H.; Friedel, R.; Wotiz, J.; Markby, R.; Wender, I. *J. Am. Chem. Soc.* **1954**, *76*, 1457. (b) Kemmitt, R. D. W.; Russell, D. R. In *Comprehensive Organometallic Chemistry*; Wilkinson, G.; Ed.; Permagon Press: Oxford, **1982**, *5*, 1.

37. Melikyan, G. G.; Vostrowsky, O.; Bauer, W.; Bestmann, H. J.; Khan, M.; Nicholas, K. M. *J. Org. Chem.* **1994**, *59*, 222.

38. Pauson, P. L. *Tetrahedron* **1985**, *41*, 5855.

39. Iwasawa, N.; Matsuo, T.; Iwamoto, M.; Ikeno, T. *J. Am. Chem. Soc.* **1998**, *120*, 3903.

40. Nicholas, K. M. *Acc. Chem. Res.* **1987**, *20*, 207 and references therein.

41. Schreiber, T.; Sammakia, T.; Crowe, W. E. *J. Am. Chem. Soc.* **1986**, *108*, 3128.

42. Ruffolo, R. Ph. D. Thesis, McMaster University, Hamilton, Ontario, **1997**.

43. Nicholas, K. M.; Pettit, R. *Tetrahedron Lett.* **1971**, *12*, 3475.

44. Seyferth, D.; Wehman, A. T. *J. Am. Chem. Soc.* **1970**, *92*, 5521.

45. (a) Magnus, P.; Becker, D. P. *J. Chem. Soc. Commun.* **1985**, 640. (b) Shvo, Y.; Hazum, E. *J. Chem. Soc. Commun.* **1974**, 336.

46. Magnus, P.; Lewis, R. T.; Huffman, J. C. *J. Am. Chem. Soc.* **1988**, *110*, 6921.

47. Mukai, C.; Moharram, S. M.; Kataoka, O.; Hanaoka, M. *J. Chem. Soc. Perkin Trans. 1* **1995**, 2849.

48. Mukai, C.; Katuoka, O.; Hanaoka, M. *J. Org. Chem.* **1993**, *58*, 2946.

49. Jacobi, P. A.; Rajeswari, S.*Tetrahedron Lett.* **1989**, *30*, 6231.

50. Saha, M.; Bagby, B.; Nicholas, K. M. *Tetrahedron Lett.* **1986**, *27*, 915.

51. Top, S.; Jaouen, G.; McGlinchey, M. J. *J. Chem. Soc. Chem. Commun.* **1980**, 1110.

52. Loim, N. M.; Mamedyarova, I. A.; Nefedova, M. N.; Natzke, G. S.; Sokolov, V. I. *Tetrahedron Lett.* **1992**, 3611.

53. (a) Grove, D. D.; Corte, J. R.; Spencer, R. P.; Pauly, M. E.; Rath, N. P. *J. Chem. Soc. Commun.* **1994**, 49. (b) Grove, D. D.; Miskevich, F.; Smith, C. C.; Corte, J.R. *Tetrahedron Lett.*, **1990**, 6277.

54. Malisza, K. L.; Girard, L.; Hughes, D. W.; Britten, J. F.; McGlinchey, M. J. *Organometallics* **1995**, *14*, 4676.

55. It has been shown that the alkylidene fragment prefers to bend towards a molybdenum vertex in mixed $(CO)_3Co\text{-}CpMo_2(CO)_4$ clusters. For examples see (a) Gruselle, M.; El Hafa, H.; Nikolski, M.; Jaouen, G.; Vaissermann, J.; Li, L.; McGlinchey, M. J. *Organometallics* **1993, *12,*** 4917. (b) Kondratenko, M.; El Hafa, H.; Gruselle, M.; Vaissermann, J.; Jaouen, G.; McGlinchey, M. J. *J. Am. Chem. Soc.* **1995, *117,*** 6907.

56. Nicholas, K. M.; Mulvaney, M.; Bayer, M. *J. Am. Chem. Soc.* **1980**, *102*, 2508.

57. Kuhn, O.; Rau, D.; Mayr, H. *J. Am. Chem. Soc.* **1998**, *120*, 900.

58. Osella, D.; Dutto, G.; Jaouen, G.; Vessières, A.; Raithby, P. R.; De Benedetto, L.; McGlinchey, M. J. *Organometallics* **1993**, *12*, 4545.

59. (a) Lew, C. S. Q.; McClelland, R. A.; Johnston, L. J.; Schepp, N. P. *J. Chem. Soc., Perkin Trans. 2* **1994**, 395. (b) Blazek, A.; Pungente, M.; Krogh, E.; Wan, P. *J. Photochem. Photobiol., A* **1992**, *64*, 315. (c) Cozens, F.; Li, J.; McClelland, R. A.; Steenken, S. *Angew. Chem., Int. Ed. Engl.* **1992**, *31*, 743. (d) Kirmse, W.; Kilian, J.; Steenken, S. *J. Am. Chem. Soc.* **1990**, *112*, 6399. (e) McClelland, R. A.; Mathivanan, N.; Steenken, S. *J. Am. Chem. Soc.* **1990**, *112*, 4857. (f) Mecklenburg, S. L.; Hilinski, E. F. *J. Am. Chem. Soc.* **1989**, *111*, 5471.

60. (a) Tu, Y-P.; Liu, Y-Q.; Liu, S. Y. *Rapid Commun. Mass Spectrom.* **1995**, *9*, 300. (b) Madhusudanan, K. P.; Durani, S.; Reddy, D. M.; Kapil, R. S.; Itagaki, Y.; Nojima, K. *Org. Mass Spectrom.* **1991**, *26*, 298. (c) Srzic, D.; Shevchenko, S. M.; Klasinc, L. *Croat. Chem. Acta* **1988**, *61*, 791. (d) Liehr, J. G.; Brenton, A. G.; Beynon, J. H.; Richter, W. J. *Org. Mass Spectrom.* **1981**, *16*, 139. (e) Tangerman, A.; Thijs, L.; Anker, A. P.; Zwanenburg, B. *J. Chem. Soc., Perkin Trans. 2* **1973**, 458. (f) Gara, A. P.; Massy-Westropp, R. A.; Bowie, J. H. *Aust. J. Chem.* **1970**, 23, 307

61. (a) Bethell, D.; Clare, P. N.; Hare, G. J. *J. Chem. Soc., Perkin Trans. 2* **1983**, 1889. (b) Bethell, D.; Hare, G. J.; Kearney, P. A. *J. Chem. Soc., Perkin Trans. 2* **1981**, 684. (c) Friedrich, E. C.; Taggart, D. B. *J. Org. Chem.* **1978**, *43*, 805.

62. (a) Amyes, T. L.; Richard, J. P.; Novak, M. *J. Am. Chem. Soc.* **1992**, *114*, 8032. (b) Allen, A. D.; Colomvakos, J. D.; Tee, O. S.; Tidwell, T. T. *J. Org. Chem.* **1994**, *59*, 7185. (c) Allen, A. D.; Fujio, M.; Mohammed, N.; Tidwell, T. T.; Tsuji, Y. *J. Org. Chem.* **1997**, *62*, 246.

63. Olah, G. A.; Prakash, G. K. S.; Liang, G.; Westerman, P. W.; Kunde, K.; Chandrasekhar, J.; Schleyer, P. v. R. *J. Am. Chem. Soc.* **1980**, *102*, 4485

64. Korchagina, D. V.; Derendyaev, B. G.; Shubin, V. G.; Koptyug, V. A. *Zh. Org. Khim.* **1971**, *7*, 2582.

65. Johnston, L. J.; Kwong, P.; Shelemay, A.; Lee-Ruff, E. *J. Am. Chem. Soc.* **1993**, *115*, 1664.

66. Allen, A. D.; Sumonja, M.; Tidwell, T. T. *J. Am. Chem. Soc.* **1997**, *119*, 2371.

67. (a) Masamune, S.; Sakai, M.; Ona, H. *J. Am. Chem. Soc.* **1972**, *94*, 8955. (b) Stohrer, W. D.; Hoffmann, R. *J. Am. Chem. Soc.* **1972**, *94*, 1661.

68. Wade, K. Adv. Inorg. Chem. Radiochem. **1976**, 18, 1.

69. Caffyn, A. J. M.; Nicholas, K. M. in *Comprehensive Organometallic Chemistry II*; Wilkinson, G.; Stone, F. G. A.; Abel, E. W., Eds.; Pergamon Press: Oxford, U.K., 1995; Vol. 12.

70. Gruselle, M.; El Hafa, H.; Nikolski, M.; Jaouen, G.; Vaissermann, J.; Li, L.; McGlinchey, M. J. *Organometallics* **1993**, *12*, 4917.

71. Prakash, G. K. S.; Buchholz, H.; Reddy, V. P.; de Meijere, A.; Olah, G. A. *J. Am. Chem. Soc.* **1992**, *114*, 1097.

72. (a) Sanders, J. K. M.; Hunter, B. K.; in *Modern NMR Spectroscopy* Oxford University Press: Oxford, **1987**.

73. (a) Schreiber, S. L.; Klimas, M. T.; Sammakia, S. *J. Am. Chem. Soc.* **1987**, *109*, 5749. (b) Padmanabhan, S.; Nicholas, K. M. *J. Organomet. Chem.* **1983**, *268*, C23.

74. Marvel, C. S.; Hinman, C. W. *J. Am. Chem. Soc.* **1954**, *76*, 5435.

75. Allen, C. H. F. *Chem. Rev.* **1962**, *62*, 653

76. Sutin, K. A.; Kolis, J. N.; Mlekuz, M.; Bougeard, P. Sayer, B. G.; Quillian, M. A.; Faggiani, R.; Lock, C. J. L.; McGlinchey, M. J.; Jaouen, G. *Organometalllics* **1987**, *6*, 439.

77. Osella, D.; Dutto, G.; Jaouen, G.; Vessières, A.; Raithby, P. R.; De Benedetto, L.; McGlinchey, M. J. *Organometallics* **1993**, *12*, 4545.

78. One cannot claim a similar correspondence in susceptibility to nucleophilic attack since the di-cobalt cluster bears a positive charge whereas the iron-cobalt complex is neutral.

79. Victor, R. *J. Organomet. Chem.* **1977**, *127*, C25.

80. (a) Gerlach, J, N.; Wing, R. M.; Ellgen, P. C. *Inorg. Chem.* **1976**, *15*, 2959. (b) Eigemann, S-E.; Förtsch, W.; Hampel, F.; Schobert, R. *Organometallics*, **1996**, *15*, 1511.

81. Bright, D.; Mills, O. S. *J. Chem. Soc., Dalton Trans.* **1972**, 2465.

82. Another closely related molecule is $Co_2Ru(CO)_9C{=}CH^tBu$: Bernhardt, W.; Vahrenkamp, H. *Angew. Chem., Int. Ed. Engl.* **1994**, *23*, 141.

83. Delgado, E.; Jeffery, J. C.; Stone, F. G. A. *J. Chem. Soc., Dalton Trans.* **1986**, 2105.

84. (a) Schilling, B. E. R.; Hoffmann, R. *J. Am. Chem. Soc.* **1979**, *101*, 3456. (b) D'Agostino, M. F.; Mlekuz, M.; Kolis, J. W.; Sayer, B. G.; Rodger, C.A.; Halet, J. F.; Saillard, J.-Y.; McGlinchey, M. J. *Organometallics* **1986**, *5*, 2345. (c) D'Agostino, M. F.; Frampton, C. S.; McGlinchey, M. J. *J. Organomet. Chem.*, **1990**, *394*, 145.

85. Malisza, K. L.; Top, S.; Vaissermann, J.; Caro, B.; Sénéchal-Tocquer, M-C.; Sénéchal, D.; Saillard, J-Y.; Triki, S.; Kahlal, S.; Britten, J. F.; McGlinchey, M. J.; Jaouen, G. *Organometallics*, **1995**, *14*, 5273

86. Brownstein, S. K.; Gabe, E. J.; Hynes, R. C. *Can. J. Chem.* **1992**, *70*, 1011.

87. Dunn, J. A.; Hunks, W., Ruffolo, R.; Rigby, S. S., McGlinchey, M. J. submitted for publication.

88. Schunn, R. A. In *Transition Metal Hydrides* E. L. Muetterties (Ed.), Wiley Inter-Science, New York, **1971**, p. 246.

89. Li., L.; Decken, A.; Sayer, B. G.; McGlinchey, M. J.; Brégaint, P.; Thépot, J-Y.; Toupet, L.; Hamon, J-R.; Lapointe, C.; *Organometallics* **1994**, *13*, 682.

90. Chini, P.; Colli, L.; Peraldo, M. *Gazz. Chim.* Ital. **1960**, *90*, 1005.

91. Epstein, R. A.; Withers, H. W.; Geoffroy, G. L. *Inorg. Chem.* **1979**, *18*, 942.

92. This is analogous to intramolecular nucleophilic attack by an oxygen atom at a δ^+ cyano carbon. Dunn, J. A., McGlinchey, M. J. unpublished result

93. Murphy, V. J.; O'Hare, D. *Inorg. Chem.* **1994**, *33*, 1833.

94. Decken, A.; Rigby, S. S.; Girard, L.; Bain, A. D.; McGlinchey, M. J. *Organometallics* **1997**, *16*, 1308.

95. (a) Haller, K. J.; Andersen, E. L.; Fehlner, T. P. *Inorg. Chem.* **1981**, *20*, 309. (b) Housecroft, C. E.; Fehlner, T. P. *Inorg. Chem.* **1982**, *21*, 1739.

96. (a) Beurich, H.; Vahrenkemp, H. *Angew. Chem. Int. Ed. Engl.* **1981**, *20*, 98. (b) Vahrenkemp, H.; Wucherer, E. J. *Angew. Chem. Int. Ed. Engl.* **1981**, *20*, 680. (c) Richter, F.; Vahrenkemp, H. *Organometallics* **1982**, *1*, 756.

97. Battiste, M. A. *J. Am. Chem. Soc.* **1961**, *83*, 4101.

98. Brydges, S.; Britten, J. F.; Chao, L. C. F.; Gupta, H. K.; McGlinchey, M. J.; Pole, D. L. *Chem. Eur. J.* **1998**, *4*, 1199.

99. (a) West, R.; Kusuda, K. *J. Am. Chem. Soc.* **1968**, *90*, 7354. (b) Kusuda, K.; West, R.; Rao, V.N.M. *J. Am. Chem. Soc.* **1971**, *93*, 3627.

100. Dodge, R.P.; Sime, R.J.; Templeton, D.H. personal communication cited in: Scherer Jr., K.V. *J. Am. Chem. Soc.* **1968**, *90*, 7352.

101. Sünkel, R. *J. Organomet. Chem.* **1990**, *391*, 247.

102. Chao, L.C.F.; Gupta, H.K.; Hughes, D.W.; Britten, J.F.; Rigby, S.S.; Bain, A.D.; McGlinchey, M.J. *Organometallics*, **1995**, *14*, 1139.

103. Hughes, R.P.; Zheng, X.; Ostrander, R.L.; Rheingold, A.L. *Organometallics*, **1994**, *13*, 1567.

104. (a) McGlinchey, M.J.; Tan, T. S. *J. Am. Chem. Soc.* **1976**, *98*, 2271. (b)Middleton, R.; Hull, J.R.; Simpson, S.R.; Tomlinson, C.H.; Timms, P.L. *J. Chem.Soc.Dalton Trans.* **1973**, 120. (c) Barker, J.J.; Orpen, A.G.; Seeley, A.J.; Timms, .L. *J.Chem. Soc. Dalton Trans.* **1993**, 3097.

105. Carl, R.T.; Corcoran, E.W.; Hughes, R.P.; Samkoff, D.E. *Organometallics*, **1990**, *9*, 838 and references therein.

106. Reimer, K.J.; Shaver, A. *Inorg. Chem.* **1975**, *14*, 2707.

107. Hedberg, F.L.; Rosenberg, H. *J. Am. Chem. Soc.* **1973**, *95*, 870.

108. Gassman, P.G.; Deck, P.A. *Organometallics*, **1994**, *13*, 1934.

109. Matsukura, T.; Mano, K.; Fujino, A. *Bull. Chem. Soc. Jpn.* **1975**, *48*, 2464.

110. Buddrus, J.; Preut, H. *Chem. Ber.* **1991**, *124*, 2373.

111. Traetteberg, M. *J. Am. Chem. Soc.* **1964**, *86*, 4265.

112. Drüecke, S.; Imming, P.; Kämpchem, T.; Seitz, G. *Chem. Ber.* **1988**, *121*, 1595.

113. Ciganek, E. *J. Am. Chem. Soc.* **1967**, *89*, 1454.

114. Moberg, C.; Nilsson, M. *Tetrahedron Lett.* **1974**, 4521.

115. Rao, V.N.M.; Hurt, C.J.; Kusuda, K.; Calabrese, J.C.; West, R. *J. Am. Chem. Soc.* **1975**, *97*, 6785.

116. Hügel, H.M.; Horn, E.; Snow, M.R. *Aust. J. Chem.* **1985**, *38*, 383.

117. Ishimori, M.; West, R.; Teo, B.K.; Dahl, L.F. *J. Am. Chem. Soc.* **1971**, *93*, 7101.

118. The treatment of *gem*-dihalides with organometallic reagents such as organolithium reagents is a classic method for generating carbenes. See: Kirmse, W. *Carbene Chemistry*, 2nd ed.; Academic Press: New York, 1971.

119. (a) Allison, N.T.; Kawada, Y.; Jones, W.M. *J. Am. Chem. Soc.* **1978**, *100*, 5224. (b) Riley, P.E.; Davis, R.E.; Allison, N.T.; Jones, W.M. *Inorg. Chem.* **1982**, *21*,1321. (c) Lisko, J.R.; Jones, W.M. *Organometallics*, **1986**, *5*, 1890.

120. Kusuda, K. *Bull. Chem. Soc. Jpn.* **1983**, *56*, 481.

121. (a) Moss, R.A. *Acc. Chem. Res.* **1980**, *13*, 58. (b) Kassam, K.; Warkentin, J. *J. Org. Chem.* **1994**, *59*, 5071, and references therein.

122. (a) Gleiter, R.; Hoffmann, R. *J. Am. Chem. Soc.* **1968**, *90*, 5457. (b) McGregor,S.D.;Jones, W.M. *J. Am. Chem. Soc.* **1968**, *90*, 123. (c) Radom, L.; Schaefer III, H.F.; Vincent, M.A. *Nouv. J. Chim.* **1980**, *4*, 411. (d) Dewar, M.J.S.; Landman, D. *J. Am. Chem. Soc.* **1977**, *99*, 6179. (e) Tyner, R.L.; Jones, W.M.; Ohrn, Y.; Sabin; Jr., J.R. *J. Am. Chem. Soc.* **1974**, *96*, 3765. (f) Kirmse, W.; Loosen, K.; Sluma, H.D. *J. Am. Chem. Soc.* **1981**, *103*, 5935. (g) West, P.R.; Chapman, O.L.; LeRoux. J.P. *J. Am. Chem. Soc.* **1982**, *104*, 1779. (h) Harris, J.W.; Jones, W.M. *J. Am. Chem. Soc.* **1982**, *104*, 7329.

123. (a) Waali, E.E. *J. Am. Chem. Soc.* **1981**, *103*, 3604. (b) For a very recent summary of the current status of the C_7H_6 problem, see: Matzinger, S.; Bally, T.; Patterson,E.V.; McMahon, R.J. *J. Am. Chem. Soc.* **1996**. *118*, 1535.

124. (a)Winchester, W.R.; Jones, W.M. *Organometallics*, **1985**, *4*, 2228. (b) Abboud, K.A.; Lu, Z.; Jones, W. M.. *Acta Crystallogr. Sect. C: Cryst. Struct. Commun.* **1992**, *C48*, 909.

125. Gilchrist, T.L.; Storr, R.C. in *Organic reactions and orbital symmetry, second edition*. Cambridge University Press, Cambridge, U.K. **1979**. pp 118-120.

126. Dewar, M.J.S.; Gleicher, G.J. *J. Am. Chem. Soc.* **1965**, *87*, 685.

127. Thomas, R.; Coppens, P. *Acta Cryst.* **1972**, *B28*, 1800.

128. Doering, W. von E. personal communication cited in: Woodward, R.B.; Hoffmann, R. *The conservation of orbital symmetry*. Verlag Chemie, Weinheim, Germany. **1970**. p 88.

129. Dunn, J. A.; Gupta, H. K.; Bain, A. D.; McGlinchey, M. J. *Can. J. Chem.* **1996**, *74*, 2258

130. (a) Arduengo, A. J.; Harlow, R. L.; Kline, M. *J. Am. Chem. Soc.* **1991**, *113*, 361. (b) Enders, D.; Breuer, K.; Raabe, G.; Runsink, J.; Teles, J. H.; Melder, J-P.; Ebel, K.; Brode, S. *Angew. Chem. Int. Ed.* **1995**, *34*, 1021.

131. Moss, R. A.; Wlostowski, M.; Shen, S.; Krogh-Jespersen, K.; Matro, A. *J. Am. Chem. Soc.* **1988**, *110*, 4443.

132. (a) Moss, R. A. *Acc. Chem. Res.* **1989**, *22*, 15. (b) Moss, R. A. *Acc. Chem. Res.* **1980**, *13*, 58.

133. Rondan, N. G.; Houk, K. N.; Moss, R. A. *J. Am. Chem. Soc.* **1980**, *102*, 1770.

134. Warkentin, J. In "*Advances in Carbene Chemistry*"; Vol. 2, Brinker, U. Ed.; JAI Press Inc.: Greenwich, 1998, pp 245-295.

135. (a) Hoffmann, R. W. *Acc. Chem. Res.* **1985**, *18*, 248. (b) Hoffmann, R. W.; Hagenbruch, B.; Smith, D. M. *Chem. Ber.* **1977**, *110*, 23. (c) Moss, R. A.; Huselton, J. K. *J. Chem. Soc. ,Chem. Commun.* **1976**, 950. (d) Hoffmann, R. W.; Steinbach, K.; Lilienblum, W. *Chem. Ber.* **1976**, *109*, 1759. (e) Hoffmann, R. W.; Steinbach, K.; Dittrich, B. *Chem. Ber.* **1973**, *106*, 2174. (f) Hoffmann, R. W. *Angew. Chem. Int. Ed. Engl.* **1971**, *10*, 529. (g) Hoffmann, R. W.; Wunsche, C. *Chem. Ber.* **1967**, *100*, 943. (h) Lemal, D. M.; Gosselink, E. P.; McGregor, S. D. *J. Am. Chem. Soc.* **1966**, *88*, 582. (i) Lemal, D. M.; Lovald, R. W.; Harrington, R. W. *Tetrahedron Lett.* **1965**, 2779. (j) Hoffmann, R. W.; Hauser, H. *Tetrahedron.* **1965**, *21*, 891. (k) Hoffmann, R. W.; Hauser, H. *Tetrahedron Lett.* **1964**, 197. (l) Lemal, D. M.; Gosselink, E. P.; Ault, A. *Tetrahedron Lett.* **1964**, 579.

136. (a) Ge, C.-S.; Jefferson, E. A.; Moss, R. A. *Tetrahedron Lett.* **1993**, *34*, 7549. (b) Moss, R. A.; Włostowski, M.; Terpinski, J.; Kmiecik-Lawrynowicz, G.; Krogh-Jespersen, K. *J. Am. Chem. Soc.* **1987**, *109*, 3811. (c) Du, X.-M.; Fan, H.; Goodman, J. L.; Kesselmayer, M. A.; Krogh-Jespersen, K.; LaVilla, J. A.; Moss, R. A.; Shen, S.; Sheridan, R. S. *J. Am. Chem. Soc.* **1990**, *112*, 1920. (d) Moss, R. A.; Włostowski, M.; Shen, S.; Krogh-Jespersen, K.; Matro, A. *J. Am. Chem. Soc.* **1988**, *110*, 4443. (e) Moss, R. A.; Shen, S.; Włostowski, M. *Tetrahedron Lett.* **1988**, *29*, 6417.

137. Moss, R. A.; Cox, D. P. *Tetrahedron Lett.* **1985**, *26*, 1931.

138. (a) El-Saidi, M.; Kassam, K.; Pole, D. L.; Tadey, T.; Warkentin, J. *J. Am. Chem. Soc.* **1992**, *114*, 8751. (b) Win, W. W.; Kao, M.; Eiermann, M.; McNamara, J. J.; Wudl, F.; Pole, D. L.; Kassam, K.; Warkentin, J. *J. Org. Chem.* **1994**, *59*, 5871. (c) Colomvakos, J. D.; Egle, I.; Ma, J.; Pole, D. L.; Tidwell, T. T.; Warkentin, J. *J. Org. Chem.* **1996**, *61*, 9522. (d) de Meijere, A.; Kozhushkov, S. I.; Yufit, D. S.; Boese, R.; Haumann, T.; Pole, D. L.; Sharma, P. K.; Warkentin, J. *Liebigs Ann.* **1996**, 601. (e) Couture, P.; Pole, D. L.; Warkentin, J. *J. Chem. Soc., Perkin Trans. 2.* **1997**, 1565.

139. (a) Couture; P.; Warkentin, J. *Can. J. Chem.* **1997**, *75*, 1264. (b) Couture, P.; Warkentin, J. *Can. J. Chem.* **1997**, *75*, 1281. (c) Kassam, K.; Venneri, P.; Warkentin, J. *Can. J. Chem.* **1997**, *75*, 1256. (d) Kassam, K.; Warkentin, J. *Can. J. Chem.* **1997**, *75*, 120. (e) Kassam, K.; Warkentin, J. *J. Org. Chem.* **1994**, *59*, 5071. (f) Couture, P.; Terlouw, J. K.; Warkentin, J. *J. Am. Chem. Soc.* **1996**, *118*, 4214. (g) Er, H.-T.; Pole, D. L.; Warkentin, J. *Can. J. Chem.* **1996**, *74*, 1480. (h) Kassam, K.; Pole, D. L.; El-Saidi, M.; Warkentin, J. *J. Am. Chem. Soc.* **1994**, *116*, 1161. (i) Isaacs, L.; Diederich, F. *Helv. Chim. Acta.* **1993**, *76*, 2454.

140. Hoffmann, R.W.; Lilienblum, W.; Dittrich, B. *Chem. Ber.* **1974**, *107*, 3395.

141. Moss, R. A.; Huselton, J. K. *J. Chem. Soc., Chem. Commun.* **1976**, 950.

142. Enders, D.; Breuer, K.; Runsink, Teles, J. H. *Liebigs Ann.* **1996**, 2019.

143. Lilienblum, W.; Hoffmann, R. W. *Chem. Ber.* **1977**, *110*, 3405.

144. (a) Kümmell, A.; Seitz, G. *Tetrahedron Lett.* **1991**, *32*, 2743. (b) Gerninghaus, C.; Kümmell, A.; Seitz, G. *Chem. Ber.* **1993**, *126*, 733. (c) Frenzen, G.; Kümmell, A.; Meyer-Dulheuer, C.; Seitz, G. *Chem. Ber.* **1994**, *127*, 1803.

145. Ross, J. P.; Couture, P.; Warkentin, J. *Can. J. Chem.* **1997**, *75*, 1331.

146. Dunn, J. A.; Pezacki, J. P.; McGlinchey, M. J.; Warkentin, J. article submitted for publication

147. We could not detect $(MeO)_2CCl_2$ by GC-MS but there was some polymeric material of unknown origin produced in the reaction.

148. Kovacs, D.; Lee, M.-S.; Olson, D.; Jackson, J. E. *J. Am. Chem. Soc.* **1996**, *118*, 8144 and references therein.

149. (a) Matzinger, S.; Bally, T.; Patterson, E. V.; McMahon, R. J. *J. Am. Chem. Soc.* **1996**, *118*, 1535. (b) McMahon, R. J.; Abelt, C. J.; Chapman, O. L.; Johnson, J. W.; Kreil, C. L.; LeRoux, J.-P.; Mooring, A. M.; West, P. R. *J. Am. Chem. Soc.* **1987**, *109*, 2456. (c) Johnson, R. P. *Chem. Rev.* **1989**, *89*, 1111. and references therein. For organometallic trapping of C_7H_6 carbene/allene: (d) Lu, Z.; Jones, W. M.; Winchester, W. R. *Organometallics* **1993**, *12*, 1344.

150. (a) Kirmse, W.; Sluma, H.-D. *J. Org. Chem.* **1988**, *53*, 763. (b) Saito, K.; Ishihara, H. *Bull. Chem. Soc. Jpn.* **1985**, *58*, 2664. (c) Saito, K.; Omura, Y.; Mukai, T. *Bull. Chem. Soc. Jpn.* **1985**, *58*, 1663. (d) Saito, K.; Omura, Y.; Mukai, T. *Chem. Lett.* **1980**, 349.

151. We attempted to trap **100/100**-allene with **DPIBF** in the reaction of n-BuLi with octachlorocycloheptatriene (**82**). Although we were able to detect minor products with the mass of adduct **121**, we were unable to isolate them in pure form despite repeated attempts to do so.

152. (a) Pauson, P. L. *Chem. Rev.* **1955**, *55*, 1. (b) Doering, W. von E.; Knox, L. H. *J. Am. Chem. Soc.* **1952**, *74*, 5683. (c) Doering, W. von E.; Hiskey, C. F. *J. Am. Chem. Soc.* **1952**, *74*, 5688.

153. Scherer, K. V. *J. Am. Chem. Soc.* **1968**, *90*, 7352.

154. Mukai, T.; Nakazawa, T.; Okayama, K. *Tetrahedron Lett.*, **1968**, *14*, 1695.

155. For an example see: Pole, D. L.; Warkentin, J. *J. Org. Chem.* **1997**, *62*, 4065.

156. Dunn, J. A.; Pezacki, J.P.; Warkentin, J. McGlinchey, M. J. manuscript in preparation.

157. Hoffman, R. W.; Lilienblum, W.; Dittrich, B. *Chem. Ber.* **1974**, *107*, 3395.

158. (a) Winstein, S.; Lewin, A. H.; Pande, K. C. (b)Diaz, A.; Brookhart, M.; Winstein, S. *J. Am. Chem. Soc.* **1966**, *88*, 3133. (c) Lhomme, J.; Diaz, A.; Winstein, S. *J. Am. Chem. Soc.* **1969**, *91*, 1548.

159. (a)Winstein, S.; Ordronneau, C. *J. Am. Chem. Soc.* **1960**, *82*, 2084. (b) Winstein, S. *Quart. Rev. Chem. Soc.* **1969**, *91*, 141. and references therein

160. Brown, H. C.; Bell, H. M. *J. Am. Chem. Soc.* **1963**, *85*, 2324.

161. Bremer, M.; Schötz, K.; Schleyer, P. v. R.; Fleischer, U.; Schindler, M.; Kutzelnigg, W.; Koch, W.; Pulay, P. *Angew. Chem., Int. Ed. Engl.* **1989**, *28*, 1042.

162. Laube, T. *J. Am. Chem. Soc.* **1989**, *111*, 9224.

163. Allen, F. H.; Kennard, O.; Watson, D. G.; Brammer, L.; Orpen, A. G.; Taylor, R. *J. Chem. Soc. Perkin Trans.* **1987**, *2*, S1-S19.

164. Evans, W. J.; Forrestal, K. J.; Ziller, J. W. *J. Am. Chem. Soc.* **1995**, *117*, 12635.

165. Perrin, D. D.; Armarego, W. L. F.; Perrin, D. R. In *Purification of Laboratory Chemicals, 2nd Ed.*, Permagon Press, Elmsford, New York, **1980**.

166. Sheldrick, G. M.; SHELTXL PC Release 4.1. Siemens Crystallographic Research Systems, Madison, WI. **1990**.

167. SMART, Release 4.05; Siemens Energy and Automation Inc., Madison, WI 53719, **1996**.

168. SAINT, Release 4.05; Siemens Energy and Automation Inc., Madison, WI 53719, **1996**.

169. Sheldrick, G. M. SADABS (Siemens Area Detector Absorption Corrections), unpublished, **1994**.

170. Sheldrick, G. M. SHELXTL, Release 5.03; Siemens Analytical X-Ray Instruments, Madison, WI, 1994.

171. (a) Hoffmann, R. *J. Chem. Phys.* **1963**, *39*, 1397. (b) Hoffmann, R.; Lipscomb, W. N. *J. Chem. Phys.* **1962**, *36*, 2179. (c) Ammeter, J. H.; Burgi, H-B.; Thibeault, J. C.; Hoffmann, R. *J. Am. Chem. Soc.* **1978**, *100*, 3686.

172. Mealli, C.; Proserpio, D. M. *J. Chem. Educ.* **1990**, *67*, 3399.

X-ray Crystallographic Appendix

Compound	Appendix Tables
9-(Trimethylsilylethynylfluorenyl)$FeCo(CO)_6$, **47**.	A1-A5
{(1-Trimethylsilylethynyl)-2,3-diphenyl-indenyl}$FeCo(CO)_6$, **53**.	B1-B5
(η^5-$Fe(CO)_2${μ-H}[C_5Ph_4-C≡C-TMS]$Co_2(CO)_6$), **64**.	C1-C5
(η^5-$Fe(CO)_2${μ-H}[$C_5Ph_2Et_2$-C≡C-TMS]$Co_2(CO)_6$), **65**.	D1-D5
(Trimethylsilylethynylpentachlorophenylketone)$Co_2(CO)_6$, **79**.	E1-E5
Octachlorocycloheptatriene, **82**.	F1-F5
7-Carbomethoxy-1,2,3,4,5,6-hexachlorocycloheptatriene, **112**.	G1-G5
(*Z*)-2-(2-Benzoylphenyl)- 1-chloro-1-pentachlorophenyl-2-phenylethene, **121**.	H1-H5
Diels-Alder adduct, **142a**.	I1-I5

Table A1. Crystal data and structure refinement for 9-(trimethylsilylethynylfluorenyl)$FeCo(CO)_6$, **47**.

	47
empirical formula	$C_{24}H_{17}CoFeO_6Si$
M_r	544.25
T [K]	293(2)
λ [Å]	0.71073
description	red plate
crystal size [mm]	0.14 x 0.22 x 0.41
crystal system	Triclinic
space group	$P\bar{1}$
a [Å]	9.293(2)
b [Å]	15.865(2)
c [Å]	18.697(3)
α [°]	106.462(10)
β [°]	104.059(14)
γ [°]	102.17(2)
V [Å^3]	2445.7(7)
Z	4
ρ_{calcd} [g cm^{-3}]	1.478
abs. Coeff. [mm^{-1}]	1 1.356
F(000)	1104
θ range for collection [°]	2.14 to 22.50
limiting indices	$0 < h < 9, -15 < k < 15, -20 < l < 19$
reflections collected	6684
independent reflections	6220
R(int)	0.0304
refinement method	Full-matrix least-squares on F^2
weighting scheme	$w=1/[\sigma^2F_o^2 + (0.0336((F_o^2+ 2F_c^2)/3))^2 + 1.6288((F_o^2 +2F_c^2)/3))^2]$
data/restraints/parameters	6220 / 0 / 595
goodness-of-fit on F^2	0.895
final R indices [I>2σ(I)][a]	R1 = 0.0499, wR2 = 0.1023
R indices (all data)[a]	R1 = 0.0960, wR2 = 0.1166
Largest diff. peak [eÅ^{-3}]	0.410
Largest diff hole [eÅ^{-3}]	-0.246

[a] $R1 = \Sigma (|| F_o | - | F_c ||)/ \Sigma | F_o |$; $wR2 = [\Sigma[w(F_o^2 - F_c^2)^2]/\Sigma[w(F_o^2)^2]]^{0.5}$

Table A2. Atomic coordinates [x 10^4] and equivalent isotropic displacement parameters [$Å^2$ x 10^3] for **47**. U(eq) is defined as one third of the trace of the orthogonalized U_{ij} tensor.

	x	y	z	U(eq)
Fe(1)	9487(1)	-2127(1)	1795(1)	64(1)
Co(1)	11550(1)	-2513(1)	2680(1)	71(1)
Si(1)	12272(2)	-2745(1)	897(1)	68(1)
C(1)	11658(9)	-66(5)	3989(4)	86(2)
C(2)	11333(9)	586(6)	4532(4)	93(2)
C(3)	10942(11)	1298(6)	4377(6)	123(3)
C(4)	10810(11)	1375(5)	3640(5)	118(3)
C(4A)	11116(8)	739(5)	3087(4)	73(2)
C(4B)	11218(8)	705(5)	2320(4)	70(2)
C(5)	10967(11)	1292(5)	1908(6)	125(3)
C(6)	11217(12)	1117(6)	1193(6)	130(4)
C(7)	11720(9)	394(6)	889(4)	101(3)
C(8)	11943(8)	-192(5)	1293(4)	88(2)
C(8A)	11655(8)	-44(5)	1995(4)	72(2)
C(9)	11771(10)	-580(5)	2555(4)	102(3)
C(9A)	11521(8)	-2(4)	3252(4)	69(2)
C(10)	11748(7)	-1467(4)	2322(4)	64(2)
C(11)	11566(7)	-2224(4)	1705(4)	60(2)
C(12)	14358(8)	-2134(5)	1170(4)	122(3)
C(13)	11155(9)	-2663(5)	-32(4)	115(3)
C(14)	11999(10)	-3993(5)	728(5)	136(3)
C(16)	8661(7)	-1722(5)	1049(4)	72(2)
O(16)	8102(6)	-1482(4)	553(3)	105(2)
C(15)	8406(7)	-1795(5)	2451(4)	77(2)
O(15)	7745(6)	-1582(4)	2875(3)	120(2)
C(17)	8378(10)	-3287(6)	1217(5)	93(3)
O(17)	7702(8)	-4029(4)	824(4)	139(2)
C(18)	10828(9)	-2311(5)	3504(4)	86(2)
O(18)	10353(7)	-2210(4)	4016(3)	126(2)
C(19)	13554(12)	-2286(6)	3172(5)	107(3)
O(19)	14856(8)	-2139(6)	3478(4)	160(3)
C(20)	10879(11)	-3769(6)	2310(5)	104(3)
O(20)	10442(9)	-4542(4)	2081(4)	155(3)
Fe(1A)	7827(1)	3829(1)	3311(1)	57(1)
Co(1A)	5691(1)	4228(1)	3808(1)	72(1)
Si(1A)	5033(2)	4321(1)	1925(1)	79(1)
C(1A)	5729(9)	1711(5)	1397(5)	95(2)
C(2A)	6154(10)	1092(6)	890(4)	96(3)
C(3A)	6685(11)	439(6)	1109(6)	123(3)
C(4C)	6804(10)	384(6)	1834(6)	111(3)
C(4D)	6343(7)	995(5)	2343(5)	74(2)
C(4E)	6206(8)	1036(5)	3112(4)	73(2)
C(5A)	6438(11)	473(6)	3534(6)	123(3)
C(6A)	6078(13)	648(7)	4225(6)	129(4)
C(7A)	5500(10)	1333(7)	4483(5)	108(3)
C(8B)	5257(9)	1898(6)	4061(5)	102(3)
C(8C)	5644(8)	1763(5)	3375(4)	81(2)
C(9C)	5843(8)	1675(5)	2144(4)	72(2)

C(9B)	5487(11)	2251(6)	2797(5)	119(3)
C(10A)	5589(7)	3151(5)	2959(4)	65(2)
C(11A)	5761(6)	3856(4)	2692(3)	63(2)
C(13A)	5676(12)	3894(6)	1056(5)	152(4)
C(12A)	2887(8)	3933(6)	1602(6)	174(5)
C(14A)	5790(10)	5593(5)	2295(5)	122(3)
C(15A)	8939(8)	3517(5)	4065(4)	82(2)
O(15A)	9642(7)	3301(5)	4533(3)	140(3)
C(17A)	8894(8)	5003(5)	3568(4)	81(2)
O(17A)	9558(7)	5744(4)	3708(3)	122(2)
C(16A)	8687(7)	3434(4)	2579(4)	69(2)
O(16A)	9245(6)	3183(4)	2105(3)	105(2)
C(18A)	3671(9)	3930(5)	3694(4)	90(2)
O(18A)	2372(6)	3708(4)	3607(4)	134(2)
C(19A)	6498(9)	4120(6)	4724(4)	100(3)
O(19A)	7005(7)	4084(5)	5329(3)	146(3)
C(20A)	6176(9)	5468(6)	4119(5)	100(3)
O(20A)	6481(8)	6247(4)	4338(4)	141(2)

Table A3. Bond lengths [Å] and angles [deg] for **47**.

Fe(1)-C(16)	1.773(8)	C(9)-C(10)	1.344(8)
Fe(1)-C(17)	1.775(9)	C(10)-C(11)	1.356(7)
Fe(1)-C(15)	1.801(7)	C(16)-O(16)	1.150(7)
Fe(1)-C(10)	1.991(6)	C(15)-O(15)	1.137(7)
Fe(1)-C(11)	2.014(6)	C(17)-O(17)	1.138(8)
Fe(1)-Co(1)	2.5130(13)	C(18)-O(18)	1.133(7)
Co(1)-C(19)	1.772(10)	C(19)-O(19)	1.147(9)
Co(1)-C(18)	1.800(7)	C(20)-O(20)	1.122(8)
Co(1)-C(20)	1.824(9)	Fe(1A)-C(16A)	1.778(7)
Co(1)-C(10)	1.949(6)	Fe(1A)-C(17A)	1.779(8)
Co(1)-C(11)	2.004(6)	Fe(1A)-C(15A)	1.789(8)
Si(1)-C(11)	1.843(6)	Fe(1A)-C(10A)	1.976(6)
Si(1)-C(12)	1.845(7)	Fe(1A)-C(11A)	2.003(6)
Si(1)-C(13)	1.849(7)	Fe(1A)-Co(1A)	2.5093(12)
Si(1)-C(14)	1.865(7)	Co(1A)-C(19A)	1.766(9)
C(1)-C(2)	1.371(9)	Co(1A)-C(18A)	1.780(8)
C(1)-C(9A)	1.387(8)	Co(1A)-C(20A)	1.806(9)
C(2)-C(3)	1.342(9)	Co(1A)-C(10A)	1.941(7)
C(3)-C(4)	1.395(10)	Co(1A)-C(11A)	2.023(6)
C(4)-C(4A)	1.357(8)	Si(1A)-C(11A)	1.843(7)
C(4A)-C(9A)	1.398(8)	Si(1A)-C(12A)	1.846(7)
C(4A)-C(4B)	1.448(8)	Si(1A)-C(14A)	1.849(7)
C(4B)-C(8A)	1.364(8)	Si(1A)-C(13A)	1.863(8)
C(4B)-C(5)	1.388(9)	C(1A)-C(2A)	1.355(9)
C(5)-C(6)	1.373(10)	C(1A)-C(9C)	1.393(8)
C(6)-C(7)	1.357(10)	C(2A)-C(3A)	1.357(10)
C(7)-C(8)	1.372(9)	C(3A)-C(4C)	1.362(10)
C(8)-C(8A)	1.368(8)	C(4C)-C(4D)	1.371(9)
C(9A)-C(9)	1.466(8)	C(4D)-C(9C)	1.369(8)
C(8A)-C(9)	1.522(8)	C(4D)-C(4E)	1.459(9)

C(4E)-C(5A)	1.364(9)
C(4E)-C(8C)	1.379(8)
C(5A)-C(6A)	1.381(11)
C(6A)-C(7A)	1.333(11)
C(7A)-C(8B)	1.368(9)
C(8B)-C(8C)	1.386(9)
C(8C)-C(9B)	1.495(9)
C(9C)-C(9B)	1.459(9)
C(9B)-C(10A)	1.351(9)
C(10A)-C(11A)	1.344(8)
C(15A)-O(15A)	1.139(7)
C(17A)-O(17A)	1.129(7)
C(16A)-O(16A)	1.150(7)
C(18A)-O(18A)	1.140(7)
C(19A)-O(19A)	1.138(8)
C(20A)-O(20A)	1.135(8)

C(16)-Fe(1)-C(17)	92.3(3)
C(16)-Fe(1)-C(15)	99.2(3)
C(17)-Fe(1)-C(15)	102.5(3)
C(16)-Fe(1)-C(10)	111.6(3)
C(17)-Fe(1)-C(10)	134.6(3)
C(15)-Fe(1)-C(10)	110.6(3)
C(16)-Fe(1)-C(11)	106.9(3)
C(17)-Fe(1)-C(11)	97.7(3)
C(15)-Fe(1)-C(11)	146.2(3)
C(10)-Fe(1)-C(11)	39.6(2)
C(16)-Fe(1)-Co(1)	157.5(2)
C(17)-Fe(1)-Co(1)	95.6(3)
C(15)-Fe(1)-Co(1)	99.7(2)
C(10)-Fe(1)-Co(1)	49.6(2)
C(11)-Fe(1)-Co(1)	51.1(2)
C(19)-Co(1)-C(18)	100.5(4)
C(19)-Co(1)-C(20)	101.5(4)
C(18)-Co(1)-C(20)	98.2(3)
C(19)-Co(1)-C(10)	97.4(3)
C(18)-Co(1)-C(10)	110.8(3)
C(20)-Co(1)-C(10)	141.7(3)
C(19)-Co(1)-C(11)	102.6(3)
C(18)-Co(1)-C(11)	144.8(3)
C(20)-Co(1)-C(11)	102.8(3)
C(10)-Co(1)-C(11)	40.1(2)
C(19)-Co(1)-Fe(1)	148.1(3)
C(18)-Co(1)-Fe(1)	96.6(2)
C(20)-Co(1)-Fe(1)	102.5(3)
C(10)-Co(1)-Fe(1)	51.1(2)
C(11)-Co(1)-Fe(1)	51.5(2)
C(11)-Si(1)-C(12)	108.3(3)
C(11)-Si(1)-C(13)	110.3(3)
C(12)-Si(1)-C(13)	110.7(4)
C(11)-Si(1)-C(14)	110.6(3)
C(12)-Si(1)-C(14)	109.7(4)
C(13)-Si(1)-C(14)	107.2(4)
C(2)-C(1)-C(9A)	118.9(7)
C(3)-C(2)-C(1)	121.5(7)
C(2)-C(3)-C(4)	120.2(8)

C(4A)-C(4)-C(3)	119.7(7)
C(4)-C(4A)-C(9A)	119.8(7)
C(4)-C(4A)-C(4B)	130.8(7)
C(9A)-C(4A)-C(4B)	109.2(6)
C(8A)-C(4B)-C(5)	119.4(7)
C(8A)-C(4B)-C(4A)	109.6(6)
C(5)-C(4B)-C(4A)	130.9(7)
C(6)-C(5)-C(4B)	118.8(8)
C(7)-C(6)-C(5)	121.6(8)
C(6)-C(7)-C(8)	119.4(8)
C(8A)-C(8)-C(7)	119.9(7)
C(1)-C(9A)-C(4A)	119.8(6)
C(1)-C(9A)-C(9)	132.0(7)
C(4A)-C(9A)-C(9)	108.2(6)
C(4B)-C(8A)-C(8)	120.9(7)
C(4B)-C(8A)-C(9)	107.9(6)
C(8)-C(8A)-C(9)	131.2(7)
C(10)-C(9)-C(9A)	131.4(7)
C(10)-C(9)-C(8A)	122.3(6)
C(9A)-C(9)-C(8A)	104.7(6)
C(9)-C(10)-C(11)	146.1(6)
C(9)-C(10)-Co(1)	140.8(5)
C(11)-C(10)-Co(1)	72.1(4)
C(9)-C(10)-Fe(1)	102.3(5)
C(11)-C(10)-Fe(1)	71.1(4)
Co(1)-C(10)-Fe(1)	79.2(2)
C(10)-C(11)-Si(1)	147.1(5)
C(10)-C(11)-Co(1)	67.8(4)
Si(1)-C(11)-Co(1)	130.3(3)
C(10)-C(11)-Fe(1)	69.3(4)
Si(1)-C(11)-Fe(1)	135.3(3)
Co(1)-C(11)-Fe(1)	77.4(2)
O(16)-C(16)-Fe(1)	178.2(7)
O(15)-C(15)-Fe(1)	178.9(6)
O(17)-C(17)-Fe(1)	177.1(8)
O(18)-C(18)-Co(1)	178.0(7)
O(19)-C(19)-Co(1)	178.8(9)
O(20)-C(20)-Co(1)	178.9(9)
C(16A)-Fe(1A)-C(17A)	93.1(3)
C(16A)-Fe(1A)-C(15A)	98.1(3)
C(17A)-Fe(1A)-C(15A)	101.9(3)
C(16A)-Fe(1A)-C(10A)	111.3(3)
C(17A)-Fe(1A)-C(10A)	134.0(3)
C(15A)-Fe(1A)-C(10A)	111.8(3)
C(16A)-Fe(1A)-C(11A)	103.7(3)
C(17A)-Fe(1A)-C(11A)	98.5(3)
C(15A)-Fe(1A)-C(11A)	149.2(3)
C(10A)-Fe(1A)-C(11A)	39.5(2)
C(16A)-Fe(1A)-Co(1A)	155.3(2)
C(17A)-Fe(1A)-Co(1A)	93.4(2)
C(15A)-Fe(1A)-Co(1A)	103.8(2)
C(10A)-Fe(1A)-Co(1A)	49.6(2)
C(11A)-Fe(1A)-Co(1A)	51.8(2)
C(19A)-Co(1A)-C(18A)	101.8(3)
C(19A)-Co(1A)-C(20A)	99.3(4)
C(18A)-Co(1A)-C(20A)	100.6(4)
C(19A)-Co(1A)-C(10A)	109.6(3)

C(18A)-Co(1A)-C(10A)	96.7(3)	C(6A)-C(7A)-C(8B)	120.1(9)
C(20A)-Co(1A)-C(10A)	142.2(3)	C(7A)-C(8B)-C(8C)	119.5(8)
C(19A)-Co(1A)-C(11A)	141.4(3)	C(4E)-C(8C)-C(8B)	119.2(7)
C(18A)-Co(1A)-C(11A)	104.3(3)	C(4E)-C(8C)-C(9B)	109.4(6)
C(20A)-Co(1A)-C(11A)	103.2(3)	C(8B)-C(8C)-C(9B)	131.3(8)
C(10A)-Co(1A)-C(11A)	39.6(2)	C(4D)-C(9C)-C(1A)	119.1(7)
C(19A)-Co(1A)-Fe(1A)	92.8(2)	C(4D)-C(9C)-C(9B)	109.9(6)
C(18A)-Co(1A)-Fe(1A)	147.5(2)	C(1A)-C(9C)-C(9B)	131.0(7)
C(20A)-Co(1A)-Fe(1A)	105.5(2)	C(10A)-C(9B)-C(9C)	125.7(7)
C(10A)-Co(1A)-Fe(1A)	50.8(2)	C(10A)-C(9B)-C(8C)	126.4(7)
C(11A)-Co(1A)-Fe(1A)	51.1(2)	C(9C)-C(9B)-C(8C)	103.7(6)
C(11A)-Si(1A)-C(12A)	108.2(3)	C(11A)-C(10A)-C(9B)	145.5(7)
C(11A)-Si(1A)-C(14A)	111.2(3)	C(11A)-C(10A)-Co(1A)	73.5(4)
C(12A)-Si(1A)-C(14A)	110.9(4)	C(9B)-C(10A)-Co(1A)	140.9(6)
C(11A)-Si(1A)-C(13A)	111.2(3)	C(11A)-C(10A)-Fe(1A)	71.3(4)
C(12A)-Si(1A)-C(13A)	108.6(5)	C(9B)-C(10A)-Fe(1A)	106.5(6)
C(14A)-Si(1A)-C(13A)	106.6(4)	Co(1A)-C(10A)-Fe(1A)	79.7(2)
C(2A)-C(1A)-C(9C)	119.6(7)	C(10A)-C(11A)-Si(1A)	148.0(5)
C(1A)-C(2A)-C(3A)	120.2(8)	C(10A)-C(11A)-Fe(1A)	69.2(4)
C(2A)-C(3A)-C(4C)	121.6(8)	Si(1A)-C(11A)-Fe(1A)	136.9(3)
C(3A)-C(4C)-C(4D)	118.6(8)	C(10A)-C(11A)-Co(1A)	66.9(4)
C(9C)-C(4D)-C(4C)	120.9(7)	Si(1A)-C(11A)-Co(1A)	128.0(3)
C(9C)-C(4D)-C(4E)	109.1(6)	Fe(1A)-C(11A)-Co(1A)	77.1(2)
C(4C)-C(4D)-C(4E)	130.0(8)	O(15A)-C(15A)-Fe(1A)	178.5(7)
C(5A)-C(4E)-C(8C)	120.8(8)	O(17A)-C(17A)-Fe(1A)	178.0(8)
C(5A)-C(4E)-C(4D)	131.5(8)	O(16A)-C(16A)-Fe(1A)	179.6(6)
C(8C)-C(4E)-C(4D)	107.5(7)	O(18A)-C(18A)-Co(1A)	177.7(8)
C(4E)-C(5A)-C(6A)	118.0(9)	O(19A)-C(19A)-Co(1A)	177.1(8)
C(7A)-C(6A)-C(5A)	122.2(9)	O(20A)-C(20A)-Co(1A)	177.9(8)

Table A4. Anisotropic displacement parameters [$Å^2 \times 10^3$] for **47**. The anisotropic displacement factor exponent takes the form: $-2p^2 [(ha^*)^2 U_{11} + ... + 2hka^*b^* U_{12}]$

	U11	U22	U33	U23	U13	U12
Fe(1)	62(1)	66(1)	77(1)	30(1)	36(1)	27(1)
Co(1)	94(1)	67(1)	72(1)	33(1)	43(1)	38(1)
Si(1)	61(1)	78(1)	65(1)	19(1)	27(1)	23(1)
C(1)	126(7)	64(5)	73(5)	26(4)	41(5)	26(5)
C(2)	119(7)	92(6)	67(5)	20(5)	48(5)	16(5)
C(3)	193(10)	86(7)	111(8)	21(6)	88(7)	63(7)
C(4)	196(10)	93(7)	104(7)	40(6)	77(7)	82(6)
C(4A)	87(5)	56(5)	73(5)	12(4)	28(4)	27(4)
C(4B)	95(5)	56(5)	63(5)	27(4)	26(4)	23(4)
C(5)	223(11)	84(6)	111(7)	53(6)	76(7)	84(7)
C(6)	217(11)	90(7)	113(8)	55(6)	59(8)	70(7)
C(7)	129(7)	97(7)	81(6)	49(6)	37(5)	16(6)
C(8)	115(6)	86(6)	84(6)	40(5)	52(5)	35(5)
C(9A)	88(5)	57(5)	67(5)	18(4)	36(4)	21(4)
C(8A)	97(5)	67(5)	67(5)	28(4)	37(4)	34(4)
C(9)	191(9)	80(6)	80(5)	45(5)	73(6)	76(6)
C(10)	82(5)	50(4)	63(4)	24(4)	32(4)	12(4)

C(11)	62(4)	57(4)	65(4)	22(4)	23(3)	25(3)
C(12)	69(5)	158(8)	117(7)	19(6)	41(5)	21(5)
C(13)	123(7)	158(8)	59(5)	27(5)	31(5)	48(6)
C(14)	199(10)	88(6)	159(8)	40(6)	114(8)	64(6)
C(16)	52(4)	80(5)	74(5)	24(4)	17(4)	8(4)
O(16)	100(4)	127(5)	101(4)	57(4)	22(3)	47(4)
C(15)	58(5)	84(5)	96(6)	31(4)	37(4)	23(4)
O(15)	96(4)	155(5)	121(5)	33(4)	68(4)	48(4)
C(17)	100(7)	82(6)	109(7)	33(5)	49(6)	33(5)
O(17)	163(6)	89(5)	149(6)	25(4)	61(5)	16(5)
C(18)	125(7)	76(5)	72(5)	29(4)	48(5)	40(5)
O(18)	198(6)	91(4)	122(5)	38(4)	111(5)	42(4)
C(19)	126(8)	131(8)	109(7)	69(6)	54(7)	73(7)
O(19)	123(6)	256(9)	134(6)	87(6)	44(5)	93(6)
C(20)	171(9)	90(6)	95(6)	42(6)	82(6)	69(7)
O(20)	251(8)	72(4)	185(6)	51(5)	124(6)	69(5)
Fe(1A)	42(1)	66(1)	59(1)	12(1)	19(1)	19(1)
Co(1A)	55(1)	79(1)	75(1)	7(1)	28(1)	22(1)
Si(1A)	68(1)	74(1)	89(2)	30(1)	16(1)	19(1)
C(1A)	139(7)	69(5)	88(6)	31(5)	46(5)	39(5)
C(2A)	129(7)	66(5)	68(5)	1(5)	46(5)	-4(5)
C(3A)	157(9)	77(7)	132(9)	7(6)	64(7)	49(6)
C(4C)	148(8)	90(7)	96(7)	23(6)	39(6)	51(6)
C(4D)	69(5)	49(5)	90(6)	9(4)	29(4)	10(4)
C(4E)	71(5)	67(5)	70(5)	24(4)	11(4)	15(4)
C(5A)	167(9)	105(7)	104(7)	49(6)	28(7)	57(7)
C(6A)	184(11)	108(8)	99(8)	64(7)	25(7)	37(7)
C(7A)	107(7)	135(9)	76(6)	50(7)	25(5)	11(6)
C(8B)	120(7)	133(7)	88(6)	60(6)	55(5)	53(6)
C(8C)	101(6)	101(6)	64(5)	40(5)	41(4)	43(5)
C(9C)	99(6)	55(5)	75(5)	27(4)	42(4)	28(4)
C(9B)	231(11)	108(7)	89(6)	57(5)	95(7)	114(7)
C(10A)	42(4)	72(5)	69(5)	20(4)	16(3)	-1(4)
C(11A)	44(4)	66(5)	63(4)	9(4)	17(3)	6(3)
C(13A)	263(13)	132(8)	106(7)	64(6)	79(8)	97(8)
C(12A)	68(6)	204(11)	257(12)	162(10)	-7(7)	12(6)
C(14A)	154(8)	75(6)	130(7)	47(5)	30(6)	27(6)
C(15A)	67(5)	107(6)	65(5)	13(4)	27(4)	30(5)
O(15A)	126(5)	224(7)	106(5)	74(5)	32(4)	107(5)
C(17A)	60(5)	79(6)	82(5)	10(5)	20(4)	8(4)
O(17A)	109(5)	91(4)	139(5)	19(4)	42(4)	-2(4)
C(16A)	47(4)	75(5)	73(5)	14(4)	12(4)	19(4)
O(16A)	89(4)	135(5)	92(4)	15(3)	55(3)	42(3)
C(18A)	59(5)	117(7)	87(5)	23(5)	22(4)	30(5)
O(18A)	50(3)	182(6)	155(5)	42(4)	41(4)	20(4)
C(19A)	86(6)	146(8)	55(5)	-3(5)	37(5)	47(5)
O(19A)	145(6)	228(7)	67(4)	22(5)	34(4)	99(5)
C(20A)	96(6)	82(6)	101(6)	-7(5)	43(5)	24(5)
O(20A)	152(6)	86(4)	163(6)	-1(4)	73(5)	27(4)

Table A5. Hydrogen coordinates (x 10^4) and isotropic displacement parameters ($Å^2$ x 10^3) for **47**.

	x	y	z	U(eq)
H(1A)	11964(9)	-543(5)	4112(4)	103
H(2A)	11385(9)	534(6)	5020(4)	112
H(3A)	10757(11)	1742(6)	4761(6)	147
H(4A)	10515(11)	1861(5)	3529(5)	142
H(5A)	10635(11)	1795(5)	2112(6)	149
H(6A)	11038(12)	1503(6)	911(6)	156
H(7A)	11912(9)	297(6)	411(4)	121
H(8A)	12289(8)	-689(5)	1091(4)	106
H(12A)	14746(8)	-2396(5)	755(4)	183
H(12B)	14919(8)	-2193(5)	1647(4)	183
H(12C)	14493(8)	-1493(5)	1249(4)	183
H(13A)	11534(9)	-2936(5)	-448(4)	172
H(13B)	11278(9)	-2026(5)	33(4)	172
H(13C)	10075(9)	-2983(5)	-163(4)	172
H(14A)	12372(10)	-4252(5)	306(5)	203
H(14B)	10914(10)	-4307(5)	592(5)	203
H(14C)	12570(10)	-4061(5)	1200(5)	203
H(1AA)	5362(9)	2158(5)	1247(5)	114
H(2AA)	6082(10)	1114(6)	392(4)	115
H(3AA)	6975(11)	19(6)	756(6)	148
H(4CA)	7191(10)	-59(6)	1980(6)	133
H(5AA)	6828(11)	-13(6)	3361(6)	148
H(6AA)	6243(13)	275(7)	4522(6)	155
H(7AA)	5262(10)	1428(7)	4949(5)	130
H(8CA)	4834(9)	2369(6)	4234(5)	122
H(13D)	5282(12)	4146(6)	667(5)	228
H(13E)	5285(12)	3234(6)	836(5)	228
H(13F)	6791(12)	4082(6)	1218(5)	228
H(12D)	2485(8)	4168(6)	1202(6)	261
H(12E)	2540(8)	4156(6)	2044(6)	261
H(12F)	2520(8)	3271(6)	1394(6)	261
H(14D)	5394(10)	5817(5)	1885(5)	182
H(14E)	6905(10)	5779(5)	2455(5)	182
H(14F)	5464(10)	5845(5)	2738(5)	182

Table B1. Crystal data and structure refinement for {(1-trimethylsilylethynyl)-2,3-diphenyl-indenyl}$FeCo(CO)_6$, **53**.

	53
empirical formula	$C_{32}H_{23}CoFeO_6Si{\cdot}CH_2Cl_2$
M_r	717.27
T [K]	300(2)
λ [Å]	0.71073
description	red plate
crystal size [mm]	0.06 x 0.25 x 0.50
crystal system	Triclinic
space group	$P\bar{1}$
a [Å]	11.58980(10)
b [Å]	12.57340(10)
c [Å]	12.63060(10)
α [°]	65.97 (10)
β [°]	73.21 (10)
γ [°]	75.940(10)
V [Å^3]	1592.74(2)
Z	2
ρ_{calcd} [g cm^{-3}]	1.496
abs. Coeff. [mm^{-1}]	1.223
F(000)	728
θ range for collection [°]	1.79 to 26.35
limiting indices	-14 < h < 14, -15 < k < 14, -15 < l < 14
reflections collected	12901
independent reflections	6000
R(int)	0.0243
refinement method	Full-matrix least-squares on F^2
weighting scheme	$w=1/[\sigma^2F_o^2 + (0.0638((F_o^2+ 2F_c^2)/3))^2 + 0.7704((F_o^2 +2F_c^2)/3))^2]$
data/restraints/parameters	6000 / 0 / 425
goodness-of-fit on F^2	1.045
final R indices [I>2σ(I)][a]	R1 = 0.0444, wR2 = 0.1171
R indices (all data)[a]	R1 = 0.0631, wR2 = 0.1308
rel. trans. (max., min.)	0.9010, 0.5152
Largest diff. peak [eÅ^{-3}]	0.856
Largest diff hole [eÅ^{-3}]	-0.302

[a] $R1 = \Sigma (|| F_o | - | F_c ||)/ \Sigma | F_o |$; $wR2 =[\Sigma[w(F_o^2 - F_c^2)^2]/\Sigma[w(F_o^2)^2]]^{0.5}$

Table B2. Atomic coordinates [x 10^4] and equivalent isotropic displacement parameters [$Å^2$ x 10^3] for **53**. U(eq) is defined as one third of the trace of the orthogonalized U_{ij} tensor.

	x	y	z	U(eq)
Fe(1)	7398(1)	5889(1)	3577(1)	50(1)
Co(1)	9085(1)	7163(1)	2700(1)	58(1)
C(1)	6298(3)	7667(3)	3743(3)	49(1)
C(2)	5026(3)	7786(3)	3611(3)	56(1)
C(3)	4597(3)	7802(3)	2694(4)	71(1)
C(4)	3340(4)	7970(4)	2791(5)	86(1)
C(5)	2555(4)	8117(4)	3778(5)	92(2)
C(6)	2970(3)	8120(3)	4699(4)	79(1)
C(7)	4227(3)	7948(3)	4620(3)	57(1)
C(8)	4938(3)	8001(3)	5384(3)	55(1)
C(9)	6150(3)	7885(2)	4856(3)	49(1)
C(10)	4384(3)	8210(3)	6507(3)	63(1)
C(11)	4743(3)	9025(3)	6783(3)	66(1)
C(12)	4210(4)	9206(4)	7839(4)	87(1)
C(13)	3278(6)	8580(6)	8621(5)	121(2)
C(14)	2913(6)	7793(6)	8362(5)	135(2)
C(15)	3453(4)	7590(4)	7315(4)	98(2)
C(16)	7147(3)	8026(3)	5277(3)	50(1)
C(17)	7359(3)	7316(3)	6407(3)	62(1)
C(18)	8256(4)	7492(4)	6817(4)	75(1)
C(19)	8943(4)	8380(4)	6118(4)	86(1)
C(20)	8745(4)	9110(4)	5005(4)	77(1)
C(21)	7843(3)	8928(3)	4588(3)	61(1)
C(22)	7332(3)	7644(3)	2854(3)	51(1)
C(23)	7731(3)	7220(3)	1963(3)	58(1)
C(24)	9556(4)	8589(5)	1959(4)	91(1)
O(24)	9821(5)	9512(4)	1519(4)	162(2)
C(25)	10368(4)	6303(4)	2025(4)	83(1)
O(25)	11170(3)	5773(4)	1606(4)	131(1)
C(26)	9511(3)	6689(3)	4118(3)	58(1)
O(26)	9859(2)	6327(2)	4964(2)	76(1)
C(27)	6085(3)	5337(3)	3627(3)	57(1)
O(27)	5303(2)	4927(2)	3633(3)	76(1)
C(28)	8385(3)	4786(3)	3070(3)	68(1)
O(28)	8982(3)	4071(3)	2731(3)	99(1)
C(29)	7452(3)	5176(3)	5146(3)	54(1)
O(29)	7508(2)	4729(2)	6111(2)	72(1)
Si(1)	7802(1)	7479(1)	388(1)	78(1)
C(30)	7350(86)	9149(34)	-593(115)	124(7)
C(31)	6813(87)	6486(63)	363(95)	124(7)
C(32)	9543(44)	7035(102)	-268(102)	129(8)
Si(1A)	7802(1)	7479(1)	388(1)	78(1)
C(30A)	6876(73)	9064(25)	-97(97)	124(7)
C(31A)	7011(74)	6394(57)	315(93)	124(7)
C(32A)	9395(31)	7599(83)	-670(88)	129(8)
Si(1B)	7802(1)	7479(1)	388(1)	78(1)
C(30B)	6758(70)	8912(33)	-234(79)	124(7)
C(31B)	7167(65)	6147(38)	536(51)	124(7)
C(32B)	9364(42)	7579(78)	-635(84)	129(8)

Si(1C)	7802(1)	7479(1)	388(1)	78(1)
C(30C)	7516(47)	9157(17)	-327(52)	124(7)
C(31C)	6669(41)	6814(36)	98(41)	124(7)
C(32C)	9402(25)	6936(53)	-213(62)	129(8)
Si(1D)	7802(1)	7479(1)	388(1)	78(1)
C(30D)	6339(20)	8211(26)	-136(24)	124(7)
C(31D)	8113(28)	5873(16)	364(21)	124(7)
C(32D)	9089(23)	8246(28)	-549(25)	129(8)
Cl(1)	5777(4)	4682(5)	9046(4)	231(3)
C(41)	5328(21)	4336(18)	10413(23)	134(7)

Table B3. Bond lengths [Å] and angles [deg] for **53**.

Fe(1)-C(1)	2.347(3)	C(23)-Si(1B)	1.860(3)
Fe(1)-C(28)	1.781(4)	C(23)-Si(1)	1.860(3)
Fe(1)-C(27)	1.795(4)	C(23)-Si(1A)	1.860(3)
Fe(1)-C(29)	1.825(3)	C(24)-O(24)	1.140(5)
Fe(1)-C(22)	2.006(3)	C(25)-O(25)	1.136(5)
Fe(1)-C(23)	2.047(3)	C(26)-O(26)	1.128(4)
Fe(1)-Co(1)	2.5381(6)	C(27)-O(27)	1.143(4)
Co(1)-C(24)	1.790(5)	C(28)-O(28)	1.145(4)
Co(1)-C(26)	1.818(4)	C(29)-O(29)	1.130(4)
Co(1)-C(25)	1.829(4)	Si(1)-C(32D)	1.82(2)
Co(1)-C(22)	1.949(3)	Si(1)-C(30D)	1.88(2)
Co(1)-C(23)	2.018(3)	Si(1)-C(31C)	1.90(2)
C(1)-C(22)	1.389(4)	Si(1)-C(31B)	1.91(2)
C(1)-C(9)	1.495(4)	Si(1)-C(31A)	1.86(2)
C(1)-C(2)	1.495(4)	Si(1)-C(32C)	1.86(2)
C(2)-C(3)	1.378(5)	Si(1)-C(31)	1.90(2)
C(2)-C(7)	1.400(5)	Si(1)-C(30C)	1.91(2)
C(3)-C(4)	1.396(5)	Si(1)-C(32)	1.98(4)
C(4)-C(5)	1.366(7)	Si(1)-C(32B)	1.89(2)
C(5)-C(6)	1.383(6)	Si(1)-C(32A)	1.94(3)
C(6)-C(7)	1.400(4)	Si(1A)-C(31A)	1.86(2)
C(7)-C(8)	1.467(5)	Si(1A)-C(32A)	1.94(3)
C(8)-C(9)	1.370(4)	Si(1A)-C(30A)	1.96(2)
C(8)-C(10)	1.480(5)	Si(1B)-C(31B)	1.91(2)
C(9)-C(16)	1.476(4)	Si(1B)-C(32B)	1.89(2)
C(10)-C(11)	1.387(5)	Si(1B)-C(30B)	1.91(2)
C(10)-C(15)	1.392(5)	Si(1C)-C(31C)	1.90(2)
C(11)-C(12)	1.385(5)	Si(1C)-C(32C)	1.86(2)
C(12)-C(13)	1.388(7)	Si(1C)-C(30C)	1.91(2)
C(13)-C(14)	1.345(8)	Si(1D)-C(32D)	1.82(2)
C(14)-C(15)	1.388(7)	Si(1D)-C(30D)	1.88(2)
C(16)-C(21)	1.389(5)	Si(1D)-C(31D)	1.97(2)
C(16)-C(17)	1.397(4)	Cl(1)-C(41)	1.56(3)
C(17)-C(18)	1.384(5)	Cl(1)-C(41)#1	1.75(2)
C(18)-C(19)	1.373(6)	C(41)-C(41)#1	1.70(4)
C(19)-C(20)	1.380(6)	C(41)-Cl(1)#1	1.75(2)
C(20)-C(21)	1.398(5)	C(28)-Fe(1)-C(27)	90.9(2)
C(22)-C(23)	1.354(4)	C(28)-Fe(1)-C(29)	98.2(2)
C(23)-Si(1D)	1.860(3)	C(27)-Fe(1)-C(29)	98.5(2)
C(23)-Si(1C)	1.860(3)	C(28)-Fe(1)-C(22)	129.4(2)

C(27)-Fe(1)-C(22)	115.67(13)	C(12)-C(11)-C(10)	121.3(4)
C(29)-Fe(1)-C(22)	117.47(14)	C(11)-C(12)-C(13)	119.0(4)
C(28)-Fe(1)-C(23)	94.2(2)	C(14)-C(13)-C(12)	120.3(5)
C(27)-Fe(1)-C(23)	106.39(14)	C(13)-C(14)-C(15)	121.1(5)
C(29)-Fe(1)-C(23)	151.95(14)	C(14)-C(15)-C(10)	120.0(5)
C(22)-Fe(1)-C(23)	39.01(13)	C(21)-C(16)-C(17)	118.2(3)
C(28)-Fe(1)-C(1)	165.0(2)	C(21)-C(16)-C(9)	120.5(3)
C(27)-Fe(1)-C(1)	94.44(12)	C(17)-C(16)-C(9)	121.2(3)
C(29)-Fe(1)-C(1)	94.79(12)	C(18)-C(17)-C(16)	120.8(4)
C(22)-Fe(1)-C(1)	36.16(11)	C(19)-C(18)-C(17)	120.1(4)
C(23)-Fe(1)-C(1)	70.85(12)	C(18)-C(19)-C(20)	120.6(4)
C(28)-Fe(1)-Co(1)	90.11(13)	C(19)-C(20)-C(21)	119.3(4)
C(27)-Fe(1)-Co(1)	157.22(11)	C(16)-C(21)-C(20)	121.0(4)
C(29)-Fe(1)-Co(1)	103.91(10)	C(23)-C(22)-C(1)	137.7(3)
C(22)-Fe(1)-Co(1)	49.11(9)	C(23)-C(22)-Co(1)	72.8(2)
C(23)-Fe(1)-Co(1)	50.85(9)	C(1)-C(22)-Co(1)	138.7(2)
C(1)-Fe(1)-Co(1)	79.59(7)	C(23)-C(22)-Fe(1)	72.1(2)
C(24)-Co(1)-C(26)	101.6(2)	C(1)-C(22)-Fe(1)	85.4(2)
C(24)-Co(1)-C(25)	100.1(2)	Co(1)-C(22)-Fe(1)	79.81(11)
C(26)-Co(1)-C(25)	97.4(2)	C(22)-C(23)-Si(1D)	147.3(3)
C(24)-Co(1)-C(22)	98.6(2)	C(22)-C(23)-Si(1C)	147.3(3)
C(26)-Co(1)-C(22)	111.11(13)	C(22)-C(23)-Si(1B)	147.3(3)
C(25)-Co(1)-C(22)	141.8(2)	C(22)-C(23)-Si(1)	147.3(3)
C(24)-Co(1)-C(23)	105.4(2)	C(22)-C(23)-Si(1A)	147.3(3)
C(26)-Co(1)-C(23)	142.65(14)	C(22)-C(23)-Co(1)	67.4(2)
C(25)-Co(1)-C(23)	102.7(2)	Si(1D)-C(23)-Co(1)	128.2(2)
C(22)-Co(1)-C(23)	39.86(13)	Si(1C)-C(23)-Co(1)	128.2(2)
C(24)-Co(1)-Fe(1)	149.6(2)	Si(1B)-C(23)-Co(1)	128.2(2)
C(26)-Co(1)-Fe(1)	92.80(11)	Si(1)-C(23)-Co(1)	128.2(2)
C(25)-Co(1)-Fe(1)	104.5(2)	Si(1A)-C(23)-Co(1)	128.2(2)
C(22)-Co(1)-Fe(1)	51.08(9)	C(22)-C(23)-Fe(1)	68.9(2)
C(23)-Co(1)-Fe(1)	51.88(9)	Si(1D)-C(23)-Fe(1)	137.3(2)
C(22)-C(1)-C(9)	129.1(3)	Si(1C)-C(23)-Fe(1)	137.3(2)
C(22)-C(1)-C(2)	124.5(3)	Si(1B)-C(23)-Fe(1)	137.3(2)
C(9)-C(1)-C(2)	104.7(3)	Si(1)-C(23)-Fe(1)	137.3(2)
C(22)-C(1)-Fe(1)	58.4(2)	Si(1A)-C(23)-Fe(1)	137.3(2)
C(9)-C(1)-Fe(1)	119.4(2)	Co(1)-C(23)-Fe(1)	77.27(11)
C(2)-C(1)-Fe(1)	109.4(2)	O(24)-C(24)-Co(1)	177.3(5)
C(3)-C(2)-C(7)	121.2(3)	O(25)-C(25)-Co(1)	179.6(4)
C(3)-C(2)-C(1)	130.9(3)	O(26)-C(26)-Co(1)	173.7(3)
C(7)-C(2)-C(1)	107.9(3)	O(27)-C(27)-Fe(1)	175.3(3)
C(2)-C(3)-C(4)	118.7(4)	O(28)-C(28)-Fe(1)	177.3(3)
C(5)-C(4)-C(3)	120.4(4)	O(29)-C(29)-Fe(1)	178.8(3)
C(4)-C(5)-C(6)	121.6(4)	C(32D)-Si(1)-C(23)	109.0(10)
C(5)-C(6)-C(7)	118.8(4)	C(32D)-Si(1)-C(30D)	112.9(12)
C(6)-C(7)-C(2)	119.2(3)	C(23)-Si(1)-C(30D)	115.1(9)
C(6)-C(7)-C(8)	131.7(3)	C(23)-Si(1)-C(31C)	116.9(14)
C(2)-C(7)-C(8)	108.9(3)	C(23)-Si(1)-C(31B)	102(2)
C(9)-C(8)-C(7)	109.1(3)	C(23)-Si(1)-C(31A)	110(3)
C(9)-C(8)-C(10)	127.3(3)	C(23)-Si(1)-C(32C)	106(2)
C(7)-C(8)-C(10)	123.5(3)	C(31C)-Si(1)-C(32C)	111(2)
C(8)-C(9)-C(16)	125.6(3)	C(23)-Si(1)-C(31)	108(3)
C(8)-C(9)-C(1)	109.1(3)	C(23)-Si(1)-C(30C)	103(2)
C(16)-C(9)-C(1)	125.2(3)	C(31C)-Si(1)-C(30C)	109.8(13)
C(11)-C(10)-C(15)	118.1(3)	C(32C)-Si(1)-C(30C)	109(2)
C(11)-C(10)-C(8)	122.3(3)	C(23)-Si(1)-C(32)	105(4)
C(15)-C(10)-C(8)	119.5(3)	C(31)-Si(1)-C(32)	111(2)

C(23)-Si(1)-C(32B)	116(3)	C(23)-Si(1C)-C(32C)	106(2)
C(31B)-Si(1)-C(32B)	110.7(14)	C(31C)-Si(1C)-C(32C)	111(2)
C(23)-Si(1)-C(32A)	117(3)	C(23)-Si(1C)-C(30C)	103(2)
C(31A)-Si(1)-C(32A)	112(2)	C(31C)-Si(1C)-C(30C)	109.8(13)
C(23)-Si(1A)-C(31A)	110(3)	C(32C)-Si(1C)-C(30C)	109(2)
C(23)-Si(1A)-C(32A)	117(3)	C(32D)-Si(1D)-C(23)	109.0(10)
C(31A)-Si(1A)-C(32A)	112(2)	C(32D)-Si(1D)-C(30D)	112.9(12)
C(23)-Si(1A)-C(30A)	100(3)	C(23)-Si(1D)-C(30D)	115.1(9)
C(31A)-Si(1A)-C(30A)	111.0(14)	C(32D)-Si(1D)-C(31D)	109.4(12)
C(32A)-Si(1A)-C(30A)	105.9(14)	C(23)-Si(1D)-C(31D)	103.3(7)
C(23)-Si(1B)-C(31B)	102(2)	C(30D)-Si(1D)-C(31D)	106.6(11)
C(23)-Si(1B)-C(32B)	116(3)	C(41)-Cl(1)-C(41)#1	61.5(12)
C(31B)-Si(1B)-C(32B)	110.7(14)	Cl(1)-C(41)-C(41)#1	65(2)
C(23)-Si(1B)-C(30B)	108(3)	Cl(1)-C(41)-Cl(1)#1	118.5(12)
C(31B)-Si(1B)-C(30B)	111(2)	C(41)#1-C(41)-Cl(1)#1	53.7(14)
C(32B)-Si(1B)-C(30B)	108(2)		
C(23)-Si(1C)-C(31C)	116.9(14)		

Symmetry transformations used to generate equivalent atoms
#1 -x+1,-y+1,-z+2

Table B4. Anisotropic displacement parameters [$Å^2$ x 10^3] for **53**. The anisotropic displacement factor exponent takes the form: $-2p^2$ [$(ha^*)^2 U_{11}$ + ... + 2hka*b* U_{12}]

	U11	U22	U33	U23	U13	U12
Fe(1)	45(1)	50(1)	52(1)	-18(1)	-11(1)	-3(1)
Co(1)	46(1)	72(1)	53(1)	-23(1)	-4(1)	-13(1)
C(1)	44(2)	44(2)	55(2)	-13(1)	-12(1)	-5(1)
C(2)	51(2)	44(2)	71(2)	-16(2)	-22(2)	-3(1)
C(3)	67(2)	65(2)	85(3)	-23(2)	-33(2)	-3(2)
C(4)	73(3)	74(3)	126(4)	-35(3)	-57(3)	4(2)
C(5)	53(2)	80(3)	162(5)	-54(3)	-46(3)	4(2)
C(6)	46(2)	65(2)	131(4)	-48(2)	-14(2)	-1(2)
C(7)	43(2)	41(2)	87(2)	-25(2)	-12(2)	-5(1)
C(8)	48(2)	39(2)	71(2)	-20(1)	-4(2)	-6(1)
C(9)	47(2)	39(2)	56(2)	-16(1)	-9(1)	-3(1)
C(10)	53(2)	52(2)	75(2)	-28(2)	2(2)	-4(2)
C(11)	70(2)	50(2)	73(2)	-24(2)	-11(2)	-1(2)
C(12)	100(3)	72(3)	91(3)	-43(2)	-17(3)	6(2)
C(13)	126(5)	127(5)	106(4)	-71(4)	26(3)	-20(4)
C(14)	120(5)	153(5)	123(5)	-74(4)	56(4)	-60(4)
C(15)	87(3)	102(3)	105(3)	-56(3)	29(3)	-40(3)
C(16)	46(2)	47(2)	57(2)	-23(1)	-8(1)	-3(1)
C(17)	61(2)	65(2)	57(2)	-24(2)	-9(2)	-2(2)
C(18)	73(2)	95(3)	65(2)	-37(2)	-25(2)	1(2)
C(19)	80(3)	100(3)	106(3)	-53(3)	-41(3)	-5(2)
C(20)	71(2)	64(2)	106(3)	-37(2)	-23(2)	-15(2)
C(21)	57(2)	53(2)	74(2)	-24(2)	-16(2)	-7(2)
C(22)	49(2)	49(2)	52(2)	-11(1)	-16(1)	-9(1)

C(23)	57(2)	66(2)	48(2)	-16(2)	-10(1)	-12(2)
C(24)	86(3)	103(4)	80(3)	-21(3)	-7(2)	-42(3)
O(24)	172(4)	123(3)	166(4)	-5(3)	-13(3)	-91(3)
C(25)	59(2)	117(4)	75(3)	-45(3)	-3(2)	-11(2)
O(25)	75(2)	189(4)	128(3)	-94(3)	5(2)	14(2)
C(26)	42(2)	64(2)	70(2)	-31(2)	-9(2)	-5(1)
O(26)	63(2)	94(2)	77(2)	-40(2)	-29(1)	9(1)
C(27)	55(2)	50(2)	62(2)	-20(2)	-13(2)	-2(2)
O(27)	64(2)	71(2)	100(2)	-32(2)	-23(1)	-15(1)
C(28)	58(2)	71(2)	79(2)	-33(2)	-19(2)	0(2)
O(28)	82(2)	97(2)	134(3)	-73(2)	-26(2)	18(2)
C(29)	48(2)	50(2)	62(2)	-18(2)	-15(2)	-4(1)
O(29)	78(2)	72(2)	60(2)	-12(1)	-24(1)	-9(1)
Si(1)	80(1)	105(1)	50(1)	-27(1)	-13(1)	-21(1)
C(30)	164(19)	117(7)	82(6)	-5(7)	-71(12)	-5(8)
C(31)	171(14)	174(15)	61(9)	-29(9)	-40(8)	-88(14)
C(32)	91(5)	209(23)	96(13)	-83(16)	10(6)	-27(8)
Si(1A)	80(1)	105(1)	50(1)	-27(1)	-13(1)	-21(1)
C(30A)	164(19)	117(7)	82(6)	-5(7)	-71(12)	-5(8)
C(31A)	171(14)	174(15)	61(9)	-29(9)	-40(8)	-88(14)
C(32A)	91(5)	209(23)	96(13)	-83(16)	10(6)	-27(8)
Si(1B)	80(1)	105(1)	50(1)	-27(1)	-13(1)	-21(1)
C(30B)	164(19)	117(7)	82(6)	-5(7)	-71(12)	-5(8)
C(31B)	171(14)	174(15)	61(9)	-29(9)	-40(8)	-88(14)
C(32B)	91(5)	209(23)	96(13)	-83(16)	10(6)	-27(8)
Si(1C)	80(1)	105(1)	50(1)	-27(1)	-13(1)	-21(1)
C(30C)	164(19)	117(7)	82(6)	-5(7)	-71(12)	-5(8)
C(31C)	171(14)	174(15)	61(9)	-29(9)	-40(8)	-88(14)
C(32C)	91(5)	209(23)	96(13)	-83(16)	10(6)	-27(8)
Si(1D)	80(1)	105(1)	50(1)	-27(1)	-13(1)	-21(1)
C(30D)	164(19)	117(7)	82(6)	-5(7)	-71(12)	-5(8)
C(31D)	171(14)	174(15)	61(9)	-29(9)	-40(8)	-88(14)
C(32D)	91(5)	209(23)	96(13)	-83(16)	10(6)	-27(8)
Cl(1)	165(4)	279(6)	179(4)	-32(4)	28(3)	-77(4)
C(41)	125(15)	117(14)	169(19)	-34(14)	-73(14)	-15(12)

Table B5. Hydrogen coordinates (x 10^4) and isotropic displacement parameters ($Å^2$ x 10^3) for **53**.

	x	y	z	U(eq)
H(3A)	5134(3)	7701(3)	2024(4)	85
H(4A)	3036(4)	7983(4)	2180(5)	103
H(5A)	1721(4)	8216(4)	3832(5)	111
H(6A)	2423(3)	8235(3)	5359(4)	95
H(11A)	5353(3)	9458(3)	6247(3)	79
H(12A)	4474(4)	9740(4)	8023(4)	105
H(13A)	2904(6)	8704(6)	9327(5)	145
H(14A)	2288(6)	7378(6)	8895(5)	162
H(15A)	3193(4)	7039(4)	7153(4)	118
H(17A)	6892(3)	6717(3)	6889(3)	75
H(18A)	8393(4)	7007(4)	7568(4)	90
H(19A)	9547(4)	8492(4)	6397(4)	104
H(20A)	9207(4)	9716(4)	4538(4)	92
H(21A)	7708(3)	9418(3)	3838(3)	73
H(30A)	7381(86)	9210(34)	-1384(115)	186
H(30B)	7910(86)	9614(34)	-619(115)	186
H(30C)	6540(86)	9429(34)	-251(115)	186
H(31A)	6839(87)	6608(63)	-444(95)	186
H(31B)	5989(87)	6670(63)	752(95)	186
H(31C)	7113(87)	5679(63)	769(95)	186
H(32A)	9646(44)	7120(102)	-1079(102)	193
H(32B)	9805(44)	6232(102)	188(102)	193
H(32C)	10023(44)	7537(102)	-230(102)	193

Table C1. Crystal data and structure refinement for (η^5-Fe(CO)$_2${μ-H}[C_5Ph_4-C≡C-TMS]$Co_2(CO)_6$), **64**.

	64
empirical formula	$C_{42}H_{29}Co_2FeO_8Si$
M_r	863.45
T [K]	210(2)
λ [Å]	0.71073
description	red plate
crystal system	Triclinic
space group	$P\bar{1}$
a [Å]	17.1732(4)
b [Å]	24.2279(3)
c [Å]	28.1743(7)
α [°]	104.694(2)
β [°]	102.575(1)
γ [°]	100.52
V [Å^3]	10710.3(4)
Z	10
ρ_{calcd} [g cm^{-3}]	1.339
abs. Coeff. [mm^{-1}]	1.175
F(000)	4390
θ range for collection [°]	0.78 to 22.50
limiting indices	-21 < h < 21, -30 < k < 30, -35 < l < 35
reflections collected	75561
independent reflections	27446
R(int)	0.4588
refinement method	Full-matrix least-squares on F^2
weighting scheme	$w=1/[\sigma^2F_o^2 + (0.0336((F_o^2+ 2F_c^2)/3))^2 + 1.6288((F_o^2 +2F_c^2)/3))^2]$
data/restraints/parameters	26992 / 0 / 1421
goodness-of-fit on F^2	0.976
final R indices [I>2σ(I)][a]	R1 = 0.1981, wR2 = 0.4111
R indices (all data)[a]	R1 = 0.4456, wR2 = 0.5758
rel. trans. (max., min.)	0.9575, 0.5206
Largest diff. peak [eÅ^{-3}]	1.340
Largest diff hole [eÅ^{-3}]	-1.251

[a] $R1 = \Sigma (|| F_o | - | F_c ||)/ \Sigma | F_o |$; $wR2 =[\Sigma[w(F_o^2 - F_c^2)^2]/\Sigma[w(F_o^2)^2]]^{0.5}$

Table C2. Atomic coordinates [x 10^4] and equivalent isotropic displacement parameters [$Å^2$ x 10^3] for **64**. U(eq) is defined as one third of the trace of the orthogonalized U_{ij} tensor.

	x	y	z	U(eq)
Fe(1)	3270(3)	-3559(2)	4367(2)	45(2)
Co(1)	5049(3)	-3748(2)	5613(2)	57(2)
Co(2)	5002(4)	-3431(3)	4813(2)	66(2)
Si(1)	5985(7)	-2268(6)	5971(5)	64(4)
C(1A)	3587(20)	-3233(13)	5170(12)	28(9)
C(2A)	2863(21)	-3726(14)	5003(12)	33(9)
C(3A)	2197(20)	-3560(13)	4651(12)	28(9)
C(4A)	2529(20)	-2977(13)	4622(12)	26(8)
C(5A)	3358(23)	-2791(15)	4964(13)	43(10)
C(6A)	2682(19)	-4222(11)	5174(11)	28(8)
C(7A)	2279(23)	-4796(11)	4869(14)	53(11)
C(8A)	2153(25)	-5294(18)	5018(15)	62(12)
C(9A)	2407(23)	-5194(16)	5537(14)	58(11)
C(10A)	2795(26)	-4607(17)	5873(16)	68(13)
C(11A)	2929(19)	-4166(13)	5663(12)	27(8)
C(12A)	1311(19)	-3908(11)	4428(9)	22(8)
C(13A)	974(22)	-4270(18)	3927(11)	48(10)
C(14A)	146(25)	-4576(16)	3763(15)	62(12)
C(15A)	-369(26)	-4438(16)	4054(14)	52(11)
C(16A)	-50(27)	-4022(17)	4524(15)	77(12)
C(17A)	786(23)	-3805(15)	4742(14)	44(10)
C(18A)	1966(25)	-2671(13)	4350(13)	56(11)
C(19A)	1887(21)	-2154(12)	4667(12)	31(9)
C(20A)	1430(25)	-1823(17)	4494(15)	67(12)
C(21A)	1067(33)	-1946(22)	3943(19)	96(17)
C(22A)	1191(26)	-2491(17)	3630(16)	67(13)
C(23A)	1679(22)	-2826(15)	3818(13)	45(10)
C(24A)	3783(22)	-2151(14)	5085(10)	43(10)
C(25A)	4026(21)	-1816(13)	5597(10)	43(10)
C(26A)	4312(23)	-1214(15)	5739(14)	47(11)
C(27A)	4377(26)	-920(18)	5367(15)	61(13)
C(28A)	4157(21)	-1264(14)	4870(13)	39(10)
C(29A)	3877(24)	-1874(14)	4690(13)	52(10)
C(30A)	4421(23)	-3276(15)	5410(13)	43(10)
C(31A)	5202(23)	-2915(15)	5570(13)	43(10)
C(32A)	5725(24)	-1967(16)	6574(13)	58(11)
C(33A)	6102(28)	-1703(18)	5579(16)	83(15)
C(34A)	6992(26)	-2424(18)	6169(16)	71(14)
C(35A)	5032(25)	-2915(16)	4457(14)	51(11)
O(35A)	5159(17)	-2540(12)	4254(10)	68(8)
C(36A)	5993(37)	-3425(22)	4892(19)	104(17)
O(36A)	6720(25)	-3369(15)	4926(13)	112(12)
C(37A)	4715(32)	-4136(23)	4302(20)	94(16)
O(37A)	4694(24)	-4558(17)	4027(14)	117(13)
C(38A)	5995(32)	-3873(19)	5741(17)	76(14)
O(38A)	6739(20)	-3947(12)	5888(11)	89(10)
C(39A)	4442(24)	-4500(16)	5259(14)	69(11)
O(39A)	4121(18)	-5003(13)	5087(11)	82(9)

C(40A)	5059(37)	-3703(24)	6281(23)	104(19)
O(40A)	4905(21)	-3631(14)	6659(13)	98(10)
C(41A)	3068(23)	-4280(15)	4014(13)	47(10)
O(41A)	2802(17)	-4780(12)	3744(10)	69(8)
C(42A)	3390(19)	-3319(12)	3848(12)	25(8)
O(42A)	3410(16)	-3163(11)	3482(10)	63(8)
Fe(2)	3056(3)	7822(2)	7321(2)	42(1)
Co(3)	2354(3)	8415(2)	6638(2)	54(2)
Co(4)	1732(3)	9088(2)	7198(2)	50(2)
Si(2)	167(7)	8073(5)	6187(4)	52(3)
C(1B)	1909(18)	7898(12)	7402(11)	19(8)
C(2B)	1881(20)	7293(13)	7152(12)	29(8)
C(3B)	2433(18)	7090(12)	7485(11)	21(8)
C(4B)	2852(20)	7552(13)	7962(12)	32(8)
C(5B)	2473(20)	8043(13)	7893(11)	24(8)
C(6B)	1210(18)	6872(15)	6704(13)	46(10)
C(7B)	371(18)	6809(14)	6649(13)	35(9)
C(8B)	-205(24)	6326(15)	6264(13)	47(10)
C(9B)	17(25)	5957(16)	5907(14)	49(11)
C(10B)	864(25)	5972(17)	5944(15)	68(12)
C(11B)	1477(25)	6457(15)	6310(13)	46(11)
C(12B)	2540(16)	6478(11)	7417(10)	18(7)
C(13B)	1866(19)	6047(14)	7398(15)	60(11)
C(14B)	1949(29)	5483(18)	7333(15)	75(13)
C(15B)	2590(23)	5299(15)	7271(12)	46(10)
C(16B)	3282(26)	5726(16)	7299(14)	62(12)
C(17B)	3215(19)	6292(12)	7390(10)	25(8)
C(18B)	3367(20)	7531(13)	8426(11)	30(8)
C(19B)	3011(23)	7300(16)	8754(13)	50(11)
C(20B)	3508(28)	7205(17)	9162(16)	66(13)
C(21B)	4274(31)	7277(18)	9318(17)	86(14)
C(22B)	4718(32)	7518(18)	8987(17)	84(14)
C(23B)	4195(31)	7600(19)	8532(18)	84(15)
C(24B)	2554(23)	8544(15)	8297(14)	41(11)
C(25B)	3296(30)	8876(85)	8651(48)	103(21)
C(26B)	3341(37)	9327(22)	9114(21)	130(18)
C(27B)	2685(34)	9563(22)	9175(20)	109(17)
C(28B)	1961(31)	9263(19)	8817(17)	82(14)
C(29B)	1862(21)	8756(13)	8395(12)	35(9)
C(30B)	1632(21)	8256(13)	7125(12)	33(9)
C(31B)	1140(23)	8270(14)	6687(13)	48(10)
C(32B)	-10(28)	8694(17)	5947(16)	82(15)
C(33B)	-745(26)	7842(17)	6461(15)	77(13)
C(34B)	198(28)	7440(17)	5645(16)	77(14)
C(35B)	3463(30)	8829(18)	6849(16)	70(13)
O(35B)	4114(20)	9100(12)	6961(11)	76(9)
C(36B)	2139(28)	8769(18)	6151(17)	67(13)
O(36B)	1874(19)	8891(12)	5776(11)	80(9)
C(37B)	2332(21)	7713(14)	6173(13)	36(9)
O(37B)	2298(16)	7358(11)	5829(10)	57(7)
C(38B)	1706(29)	9686(20)	6891(18)	78(14)
O(38B)	1603(19)	9984(13)	6647(11)	81(9)
C(39B)	2692(25)	9492(15)	7670(14)	48(11)
O(39B)	3321(19)	9734(12)	7991(11)	76(9)
C(40B)	1005(28)	9254(17)	7520(15)	62(12)
O(40B)	420(24)	9312(15)	7686(13)	112(12)
C(41B)	3981(26)	8342(16)	7629(15)	56(11)

O(41B)	4581(19)	8692(12)	7872(11)	79(9)
C(42B)	3509(21)	7449(14)	6882(13)	36(9)
O(42B)	3833(19)	7183(12)	6583(11)	78(9)
Fe(3)	3796(3)	1605(2)	7023(2)	39(1)
Co(5)	6216(3)	2174(2)	7921(2)	57(2)
Co(6)	4819(4)	2244(2)	8046(2)	59(2)
Si(3)	6141(9)	3628(5)	8219(5)	73(4)
C(1C)	4818(16)	2166(10)	6965(9)	4(6)
C(2C)	4143(19)	2355(12)	6795(11)	22(8)
C(3C)	3492(22)	1880(14)	6368(13)	37(10)
C(4C)	3923(21)	1448(13)	6281(12)	31(9)
C(5C)	4679(20)	1557(13)	6611(12)	24(8)
C(6C)	3992(19)	2979(14)	6936(13)	42(10)
C(7C)	4740(20)	3316(15)	6937(13)	64(11)
C(8C)	4630(23)	3955(15)	6966(13)	47(10)
C(9C)	3976(28)	4157(19)	7072(16)	73(14)
C(10C)	3266(27)	3698(17)	7112(15)	63(12)
C(11C)	3306(23)	3122(15)	7047(12)	41(10)
C(12C)	2702(26)	1959(16)	6048(15)	58(12)
C(13C)	2743(40)	2417(19)	5833(18)	92(16)
C(14C)	2016(28)	2455(18)	5544(16)	75(13)
C(15C)	1277(28)	2100(17)	5522(15)	70(13)
C(16C)	1254(25)	1675(16)	5752(14)	55(11)
C(17C)	1989(28)	1567(18)	6050(16)	72(13)
C(18C)	3568(19)	924(12)	5829(13)	42(10)
C(19C)	2998(19)	402(13)	5758(14)	54(10)
C(20C)	2717(25)	-54(16)	5336(14)	54(11)
C(21C)	3102(31)	-80(22)	4932(19)	85(16)
C(22C)	3638(25)	456(16)	4948(15)	61(12)
C(23C)	3865(20)	897(13)	5375(11)	31(9)
C(24C)	5353(21)	1269(11)	6552(12)	42(9)
C(25C)	5303(26)	680(12)	6514(17)	62(11)
C(26C)	5884(27)	399(18)	6426(15)	64(12)
C(27C)	6618(29)	711(19)	6423(15)	72(14)
C(28C)	6728(27)	1251(18)	6460(15)	72(13)
C(29C)	6107(19)	1596(13)	6562(11)	35(8)
C(30C)	5381(21)	2358(14)	7483(12)	34(9)
C(31C)	5668(21)	2827(14)	7899(12)	41(9)
C(32C)	6758(25)	3876(17)	7770(14)	61(12)
C(33C)	6924(24)	3757(16)	8840(14)	67(12)
C(34C)	5329(24)	4023(16)	8312(14)	64(12)
C(35C)	6811(28)	2278(18)	8523(17)	67(13)
O(35C)	7193(23)	2399(15)	8965(14)	116(12)
C(36C)	5974(35)	1427(25)	7743(20)	99(18)
O(36C)	5811(23)	921(16)	7628(13)	114(12)
C(37C)	7148(39)	2366(24)	7670(21)	106(19)
O(37C)	7649(28)	2492(17)	7520(15)	132(14)
C(38C)	4018(20)	2583(13)	8066(11)	28(8)
O(38C)	3506(16)	2872(10)	8123(9)	53(7)
C(39C)	5214(22)	2498(14)	8679(14)	42(10)
O(39C)	5475(16)	2718(10)	9135(10)	61(8)
C(40C)	4295(23)	1570(16)	8069(13)	47(10)
O(40C)	4096(17)	1112(12)	8179(10)	70(8)
C(41C)	3686(23)	880(16)	7069(13)	41(10)
O(41C)	3552(18)	401(12)	7035(10)	71(8)
C(42C)	2930(27)	1656(16)	7218(15)	62(12)
O(42C)	2299(19)	1716(11)	7311(10)	75(8)

Fe(4)	1560(3)	3478(2)	9127(2)	37(1)
Co(7)	356(3)	2407(2)	8931(2)	51(2)
Co(8)	-37(3)	2071(2)	7958(2)	48(2)
Si(4)	871(7)	1061(4)	8441(5)	58(4)
C(1D)	1816(18)	2843(12)	8573(11)	16(7)
C(2D)	2421(21)	2983(13)	9018(12)	30(9)
C(3D)	2860(20)	3604(13)	9188(12)	24(8)
C(4D)	2451(22)	3821(14)	8832(13)	37(10)
C(5D)	1807(20)	3375(13)	8386(12)	28(9)
C(6D)	2776(18)	2587(11)	9267(10)	21(8)
C(7D)	2991(21)	2109(12)	8985(12)	36(9)
C(8D)	3383(24)	1746(16)	9194(14)	53(11)
C(9D)	3647(23)	1888(15)	9751(13)	47(10)
C(10D)	3369(24)	2325(15)	10049(15)	56(11)
C(11D)	2996(25)	2712(17)	9817(15)	56(12)
C(12D)	3571(16)	3932(12)	9592(11)	29(8)
C(13D)	4283(15)	3731(13)	9625(11)	22(8)
C(14D)	4977(25)	4022(16)	10026(14)	53(11)
C(15D)	5016(27)	4533(17)	10403(15)	59(12)
C(16D)	4327(27)	4725(18)	10358(16)	67(12)
C(17D)	3589(25)	4447(15)	9965(13)	57(11)
C(18D)	2704(22)	4419(14)	8736(12)	41(10)
C(19D)	2528(37)	4921(17)	9013(15)	68(14)
C(20D)	2865(26)	5460(18)	8934(15)	66(13)
C(21D)	3293(27)	5525(19)	8571(16)	71(13)
C(22D)	3527(23)	5033(15)	8346(13)	51(10)
C(23D)	3243(25)	4466(17)	8405(14)	59(12)
C(24D)	1405(17)	3393(11)	7886(10)	16(7)
C(25D)	1037(21)	3844(14)	7822(18)	49(11)
C(26D)	752(22)	3898(15)	7329(13)	39(10)
C(27D)	725(27)	3471(18)	6900(17)	66(13)
C(28D)	1079(21)	3007(15)	6998(13)	40(10)
C(29D)	1391(22)	2965(15)	7458(13)	38(10)
C(30D)	1094(22)	2356(14)	8403(12)	37(9)
C(31D)	759(20)	1822(13)	8461(11)	26(8)
C(32D)	-155(25)	539(17)	8159(15)	71(13)
C(33D)	1520(28)	830(18)	8014(16)	81(14)
C(34D)	1310(22)	1031(14)	9091(12)	45(10)
C(35D)	-331(20)	2719(14)	7883(12)	36(9)
O(35D)	-610(17)	3125(11)	7859(9)	62(8)
C(36D)	159(30)	1743(20)	7370(19)	77(15)
O(36D)	297(20)	1564(13)	6996(12)	82(9)
C(37D)	-1075(31)	1559(19)	7810(17)	76(14)
O(37D)	-1672(25)	1315(15)	7749(13)	108(12)
C(38D)	-453(27)	1838(17)	8932(15)	58(12)
O(38D)	-929(20)	1520(13)	9009(11)	87(9)
C(39D)	891(22)	2438(14)	9507(14)	39(10)
O(39D)	1221(15)	2444(10)	9942(9)	52(7)
C(40D)	-196(32)	2914(21)	9035(18)	83(16)
O(40D)	-598(18)	3259(12)	9171(10)	76(8)
C(41D)	953(19)	3946(13)	9098(11)	25(8)
O(41D)	502(18)	4276(12)	9042(10)	79(9)
C(42D)	1626(25)	3655(16)	9800(16)	54(11)
O(42D)	1786(16)	3793(11)	10236(10)	66(8)
Fe(5)	-1311(3)	7513(2)	8230(2)	49(2)
Co(9)	-943(4)	6428(2)	7804(2)	62(2)
Co(10)	-2053(4)	5709(2)	7968(2)	64(2)

Si(5)	-125(13)	5666(7)	8663(6)	116(7)
C(1E)	-1349(21)	7011(14)	8731(12)	32(9)
C(2E)	-2115(25)	7254(16)	8674(14)	49(11)
C(3E)	-1808(22)	7872(14)	8807(13)	35(9)
C(4E)	-956(21)	8033(13)	9028(12)	34(9)
C(5E)	-666(19)	7518(12)	8936(11)	21(8)
C(6E)	-2946(23)	6912(14)	8548(13)	45(10)
C(7E)	-3077(23)	6557(15)	8855(13)	52(10)
C(8E)	-3897(29)	6238(19)	8782(17)	87(14)
C(9E)	-4572(22)	6254(13)	8369(12)	46(9)
C(10E)	-4458(37)	6634(23)	8071(21)	122(19)
C(11E)	-3612(28)	6929(18)	8141(16)	67(13)
C(12E)	-2335(19)	8301(13)	8917(11)	25(8)
C(13E)	-2979(32)	8361(28)	8554(18)	109(19)
C(14E)	-3433(34)	8787(22)	8606(21)	101(18)
C(15E)	-3309(29)	9040(19)	9145(17)	79(14)
C(16E)	-2803(22)	8968(14)	9515(14)	43(9)
C(17E)	-2248(25)	8618(16)	9438(15)	59(11)
C(18E)	-404(20)	8640(13)	9279(12)	31(9)
C(19E)	-482(29)	9041(21)	9007(21)	73(14)
C(20E)	42(29)	9636(19)	9243(17)	82(14)
C(21E)	561(27)	9741(19)	9697(16)	76(13)
C(22E)	731(35)	9353(22)	9998(21)	119(18)
C(23E)	159(21)	8766(14)	9740(13)	38(9)
C(24E)	172(19)	7474(14)	9172(13)	38(10)
C(25E)	890(19)	7818(14)	9141(14)	51(10)
C(26E)	1612(32)	7898(19)	9405(17)	85(15)
C(27E)	1789(33)	7616(20)	9783(18)	88(16)
C(28E)	1147(29)	7213(19)	9837(17)	79(14)
C(29E)	380(23)	7206(14)	9530(13)	49(10)
C(30E)	-1274(25)	6465(16)	8473(14)	52(11)
C(31E)	-881(22)	6053(14)	8423(13)	39(10)
C(32E)	-272(32)	5592(20)	9327(17)	106(17)
C(33E)	-397(39)	4895(24)	8234(22)	154(24)
C(34E)	1123(40)	6169(26)	8756(23)	137(25)
C(35E)	-1454(26)	6528(16)	7254(15)	56(12)
O(35E)	-1796(20)	6636(13)	6864(12)	86(10)
C(36E)	83(33)	6884(21)	7981(18)	84(15)
O(36E)	754(22)	7155(14)	8006(12)	97(11)
C(37E)	-2048(30)	5034(21)	7529(18)	87(14)
O(37E)	-2015(21)	4597(15)	7261(13)	111(11)
C(38E)	-2575(26)	5397(15)	8366(15)	77(11)
O(38E)	-2715(22)	5230(14)	8728(13)	116(11)
C(39E)	-2839(22)	5855(14)	7586(13)	34(9)
O(39E)	-3327(21)	5939(13)	7272(12)	94(10)
C(40E)	-665(25)	5863(17)	7455(15)	70(11)
O(40E)	-446(21)	5464(14)	7227(12)	102(11)
C(41E)	-2040(29)	7507(18)	7700(17)	67(13)
O(41E)	-2576(27)	7560(16)	7391(15)	132(14)
C(42E)	-613(30)	7913(19)	8030(17)	79(14)
O(42E)	-139(22)	8179(14)	7855(12)	96(11)

Table C3. Selected Bond lengths [Å] and angles [deg] for one of the five rotamers of **64**.

Fe(1)-C(41A)	1.70(4)	C(25A)-C(26A)	1.37(4)
Fe(1)-C(42A)	1.74(3)	C(26A)-C(27A)	1.42(5)
Fe(1)-C(1A)	2.11(3)	C(27A)-C(28A)	1.36(5)
Fe(1)-C(5A)	2.12(4)	C(28A)-C(29A)	1.39(4)
Fe(1)-C(2A)	2.16(3)	C(30A)-C(31A)	1.37(5)
Fe(1)-C(4A)	2.16(3)	C(35A)-O(35A)	1.20(4)
Fe(1)-C(3A)	2.16(3)	C(36A)-O(36A)	1.21(6)
Fe(1)-Co(2)	2.891(8)	C(37A)-O(37A)	1.10(5)
Co(1)-C(38A)	1.69(5)	C(38A)-O(38A)	1.31(5)
Co(1)-C(30A)	1.82(3)	C(39A)-O(39A)	1.17(4)
Co(1)-C(39A)	1.82(4)	C(40A)-O(40A)	1.13(6)
Co(1)-C(40A)	1.85(6)	C(41A)-O(41A)	1.20(4)
Co(1)-C(31A)	2.03(3)	C(42A)-O(42A)	1.19(3)
Co(1)-Co(2)	2.550(8)	C(41A)-Fe(1)-C(42A)	92(2)
Co(2)-C(36A)	1.66(6)	C(41A)-Fe(1)-C(1A)	125.9(14)
Co(2)-C(35A)	1.79(4)	C(42A)-Fe(1)-C(1A)	139.6(13)
Co(2)-C(37A)	1.84(5)	C(41A)-Fe(1)-C(5A)	161(2)
Co(2)-C(31A)	2.10(4)	C(42A)-Fe(1)-C(5A)	106.0(13)
Co(2)-C(30A)	2.12(4)	C(1A)-Fe(1)-C(5A)	39.1(11)
Si(1)-C(31A)	1.79(4)	C(41A)-Fe(1)-C(2A)	96(2)
Si(1)-C(34A)	1.84(4)	C(42A)-Fe(1)-C(2A)	164.3(13)
Si(1)-C(32A)	1.85(4)	C(1A)-Fe(1)-C(2A)	39.8(12)
Si(1)-C(33A)	1.98(4)	C(5A)-Fe(1)-C(2A)	65.1(13)
C(1A)-C(5A)	1.41(4)	C(41A)-Fe(1)-C(4A)	135(2)
C(1A)-C(2A)	1.45(4)	C(42A)-Fe(1)-C(4A)	96.6(13)
C(1A)-C(30A)	1.48(4)	C(1A)-Fe(1)-C(4A)	68.4(12)
C(2A)-C(6A)	1.41(4)	C(5A)-Fe(1)-C(4A)	39.6(12)
C(2A)-C(3A)	1.53(4)	C(2A)-Fe(1)-C(4A)	68.3(12)
C(3A)-C(4A)	1.45(4)	C(41A)-Fe(1)-C(3A)	101(2)
C(3A)-C(12A)	1.51(4)	C(42A)-Fe(1)-C(3A)	123.8(13)
C(4A)-C(5A)	1.45(4)	C(1A)-Fe(1)-C(3A)	67.7(12)
C(4A)-C(18A)	1.51(4)	C(5A)-Fe(1)-C(3A)	64.7(13)
C(5A)-C(24A)	1.51(4)	C(2A)-Fe(1)-C(3A)	41.3(11)
C(6A)-C(7A)	1.39	C(4A)-Fe(1)-C(3A)	39.3(11)
C(6A)-C(11A)	1.31(4)	C(41A)-Fe(1)-Co(2)	95.6(12)
C(7A)-C(8A)	1.37(4)	C(42A)-Fe(1)-Co(2)	96.3(10)
C(8A)-C(9A)	1.38(5)	C(1A)-Fe(1)-Co(2)	68.8(9)
C(9A)-C(10A)	1.44(5)	C(5A)-Fe(1)-Co(2)	87.5(10)
C(10A)-C(11A)	1.36(4)	C(2A)-Fe(1)-Co(2)	96.2(9)
C(12A)-C(13A)	1.39	C(4A)-Fe(1)-Co(2)	127.1(9)
C(12A)-C(17A)	1.40(4)	C(3A)-Fe(1)-Co(2)	135.3(8)
C(13A)-C(14A)	1.39(5)	C(38A)-Co(1)-C(30A)	147(2)
C(14A)-C(15A)	1.36(5)	C(38A)-Co(1)-C(39A)	99(2)
C(15A)-C(16A)	1.37(5)	C(30A)-Co(1)-C(39A)	105(2)
C(16A)-C(17A)	1.38(5)	C(38A)-Co(1)-C(40A)	88(2)
C(18A)-C(19A)	1.39	C(30A)-Co(1)-C(40A)	108(2)
C(18A)-C(23A)	1.40(4)	C(39A)-Co(1)-C(40A)	103(2)
C(19A)-C(20A)	1.33(4)	C(38A)-Co(1)-C(31A)	107(2)
C(20A)-C(21A)	1.47(6)	C(30A)-Co(1)-C(31A)	41.3(14)
C(21A)-C(22A)	1.47(6)	C(39A)-Co(1)-C(31A)	141(2)
C(22A)-C(23A)	1.38(5)	C(40A)-Co(1)-C(31A)	107(2)
C(24A)-C(25A)	1.39	C(38A)-Co(1)-Co(2)	101(2)
C(24A)-C(29A)	1.46(4)	C(30A)-Co(1)-Co(2)	55.1(12)

C(39A)-Co(1)-Co(2)	94.0(12)
C(40A)-Co(1)-Co(2)	159(2)
C(31A)-Co(1)-Co(2)	53.1(10)
C(36A)-Co(2)-C(35A)	94(2)
C(36A)-Co(2)-C(37A)	90(2)
C(35A)-Co(2)-C(37A)	102(2)
C(36A)-Co(2)-C(31A)	93(2)
C(35A)-Co(2)-C(31A)	105(2)
C(37A)-Co(2)-C(31A)	153(2)
C(36A)-Co(2)-C(30A)	125(2)
C(35A)-Co(2)-C(30A)	117(2)
C(37A)-Co(2)-C(30A)	123(2)
C(31A)-Co(2)-C(30A)	37.9(13)
C(36A)-Co(2)-Co(1)	89(2)
C(35A)-Co(2)-Co(1)	155.3(12)
C(37A)-Co(2)-Co(1)	103(2)
C(31A)-Co(2)-Co(1)	50.5(9)
C(30A)-Co(2)-Co(1)	44.7(9)
C(36A)-Co(2)-Fe(1)	163(2)
C(35A)-Co(2)-Fe(1)	77.9(13)
C(37A)-Co(2)-Fe(1)	78(2)
C(31A)-Co(2)-Fe(1)	102.9(11)
C(30A)-Co(2)-Fe(1)	71.4(10)
Co(1)-Co(2)-Fe(1)	104.4(2)
C(31A)-Si(1)-C(34A)	113(2)
C(31A)-Si(1)-C(32A)	110(2)
C(34A)-Si(1)-C(32A)	105(2)
C(31A)-Si(1)-C(33A)	108(2)
C(34A)-Si(1)-C(33A)	108(2)
C(32A)-Si(1)-C(33A)	113(2)
C(5A)-C(1A)-C(2A)	107(3)
C(5A)-C(1A)-C(30A)	129(3)
C(2A)-C(1A)-C(30A)	123(3)
C(5A)-C(1A)-Fe(1)	71(2)
C(2A)-C(1A)-Fe(1)	72(2)
C(30A)-C(1A)-Fe(1)	112(2)
C(1A)-C(2A)-C(6A)	131(3)
C(1A)-C(2A)-C(3A)	106(3)
C(6A)-C(2A)-C(3A)	122(3)
C(1A)-C(2A)-Fe(1)	68(2)
C(6A)-C(2A)-Fe(1)	136(2)
C(3A)-C(2A)-Fe(1)	69(2)
C(4A)-C(3A)-C(12A)	125(3)
C(4A)-C(3A)-C(2A)	109(3)
C(12A)-C(3A)-C(2A)	125(3)
C(4A)-C(3A)-Fe(1)	70(2)
C(12A)-C(3A)-Fe(1)	133(2)
C(2A)-C(3A)-Fe(1)	69(2)
C(3A)-C(4A)-C(5A)	104(3)
C(3A)-C(4A)-C(18A)	120(3)
C(5A)-C(4A)-C(18A)	135(3)
C(3A)-C(4A)-Fe(1)	71(2)
C(5A)-C(4A)-Fe(1)	69(2)
C(18A)-C(4A)-Fe(1)	133(2)
C(1A)-C(5A)-C(4A)	114(3)
C(1A)-C(5A)-C(24A)	131(3)
C(4A)-C(5A)-C(24A)	115(3)
C(1A)-C(5A)-Fe(1)	70(2)
C(4A)-C(5A)-Fe(1)	72(2)
C(24A)-C(5A)-Fe(1)	133(3)
C(7A)-C(6A)-C(11A)	114(3)
C(7A)-C(6A)-C(2A)	126(3)
C(11A)-C(6A)-C(2A)	120(3)
C(8A)-C(7A)-C(6A)	128(4)
C(7A)-C(8A)-C(9A)	115(4)
C(10A)-C(9A)-C(8A)	120(4)
C(11A)-C(10A)-C(9A)	118(4)
C(10A)-C(11A)-C(6A)	125(3)
C(13A)-C(12A)-C(17A)	119(3)
C(13A)-C(12A)-C(3A)	125(3)
C(17A)-C(12A)-C(3A)	116(3)
C(14A)-C(13A)-C(12A)	120(4)
C(15A)-C(14A)-C(13A)	120(4)
C(14A)-C(15A)-C(16A)	119(4)
C(17A)-C(16A)-C(15A)	122(4)
C(16A)-C(17A)-C(12A)	118(4)
C(19A)-C(18A)-C(23A)	122(3)
C(19A)-C(18A)-C(4A)	114(3)
C(23A)-C(18A)-C(4A)	123(3)
C(20A)-C(19A)-C(18A)	122(3)
C(19A)-C(20A)-C(21A)	121(4)
C(22A)-C(21A)-C(20A)	113(4)
C(21A)-C(22A)-C(23A)	124(4)
C(22A)-C(23A)-C(18A)	116(4)
C(25A)-C(24A)-C(29A)	121(3)
C(25A)-C(24A)-C(5A)	116(3)
C(29A)-C(24A)-C(5A)	123(3)
C(26A)-C(25A)-C(24A)	121(3)
C(27A)-C(26A)-C(25A)	121(4)
C(26A)-C(27A)-C(28A)	117(4)
C(27A)-C(28A)-C(29A)	127(4)
C(28A)-C(29A)-C(24A)	114(3)
C(31A)-C(30A)-C(1A)	136(3)
C(31A)-C(30A)-Co(1)	77(2)
C(1A)-C(30A)-Co(1)	147(3)
C(31A)-C(30A)-Co(2)	70(2)
C(1A)-C(30A)-Co(2)	106(2)
Co(1)-C(30A)-Co(2)	80.1(14)
C(30A)-C(31A)-Si(1)	153(3)
C(30A)-C(31A)-Co(1)	61(2)
Si(1)-C(31A)-Co(1)	128(2)
C(30A)-C(31A)-Co(2)	72(2)
Si(1)-C(31A)-Co(2)	132(2)
Co(1)-C(31A)-Co(2)	76.4(12)
O(35A)-C(35A)-Co(2)	172(3)
O(36A)-C(36A)-Co(2)	173(5)
O(37A)-C(37A)-Co(2)	167(5)
O(38A)-C(38A)-Co(1)	174(4)
O(39A)-C(39A)-Co(1)	170(3)
O(40A)-C(40A)-Co(1)	164(5)
O(41A)-C(41A)-Fe(1)	170(3)
O(42A)-C(42A)-Fe(1)	175(3)

Table C4. Anisotropic displacement parameters [$Å^2$ x 10^3] for **64**. The anisotropic displacement factor exponent takes the form: $-2p^2$ [$(ha^*)^2 U_{11}$ + ... + 2hka*b* U_{12}]

	U11	U22	U33	U23	U13	U12
Fe(1)	47(4)	51(3)	49(4)	9(3)	41(3)	13(3)
Co(1)	42(4)	72(4)	67(4)	20(3)	37(3)	15(3)
Co(2)	49(4)	96(5)	66(4)	23(4)	45(3)	15(3)
Si(1)	31(7)	98(10)	73(9)	38(8)	29(7)	3(7)
Fe(2)	36(3)	35(3)	55(3)	4(3)	35(3)	-7(3)
Co(3)	52(4)	51(3)	71(4)	18(3)	50(3)	3(3)
Co(4)	57(4)	27(3)	77(4)	12(3)	53(3)	5(3)
Si(2)	42(8)	58(7)	71(8)	24(6)	33(6)	25(6)
Fe(3)	31(3)	40(3)	51(3)	16(3)	29(3)	-1(3)
Co(5)	51(4)	58(4)	67(4)	12(3)	38(3)	7(3)
Co(6)	66(4)	50(3)	62(4)	10(3)	48(3)	-8(3)
Si(3)	79(10)	40(7)	80(9)	-2(7)	43(8)	-30(7)
Fe(4)	34(3)	38(3)	48(3)	16(3)	35(3)	-1(2)
Co(7)	51(4)	52(3)	59(4)	20(3)	44(3)	-1(3)
Co(8)	43(4)	43(3)	58(4)	20(3)	26(3)	-11(3)
Si(4)	64(9)	25(6)	84(9)	12(6)	48(7)	-20(6)
Fe(5)	48(4)	55(3)	53(4)	20(3)	43(3)	-1(3)
Co(9)	54(4)	71(4)	71(4)	18(3)	49(3)	8(3)
Co(10)	85(5)	43(3)	72(4)	9(3)	61(4)	-4(3)
Si(5)	189(20)	123(13)	88(12)	33(11)	78(12)	118(14)

Table C5. Hydrogen coordinates (x 10^4) and isotropic displacement parameters ($Å^2$ x 10^3) for **64**.

	x	y	z	U(eq)
H(7AA)	2067(181)	-4849(32)	4519(22)	63
H(8AA)	1913(25)	-5673(18)	4784(15)	74
H(9AA)	2325(23)	-5511(16)	5672(14)	69
H(10A)	2952(26)	-4530(17)	6229(16)	81
H(11A)	3223(19)	-3789(13)	5885(12)	32
H(13A)	1303(37)	-4309(92)	3699(34)	58
H(14A)	-58(25)	-4879(16)	3450(15)	74
H(15A)	-936(26)	-4625(16)	3934(14)	62
H(16A)	-412(27)	-3881(17)	4703(15)	92
H(17A)	1001(23)	-3593(15)	5091(14)	53
H(19A)	2168(112)	-2034(65)	5017(32)	37
H(20A)	1337(25)	-1505(17)	4727(15)	80
H(21A)	784(33)	-1700(22)	3805(19)	115
H(22A)	921(26)	-2620(17)	3278(16)	80
H(23A)	1810(22)	-3138(15)	3601(13)	54
H(25A)	3995(184)	-2004(37)	5848(12)	51
H(26A)	4466(23)	-993(15)	6087(14)	57
H(27A)	4563(26)	-508(18)	5460(15)	73

H(28A)	4200(21)	-1068(14)	4625(13)	47
H(29A)	4264(24)	-2034(14)	4520(13)	63
H(29B)	3343(24)	-1980(14)	4433(13)	63
H(32A)	6152(24)	-1618(16)	6789(13)	87
H(32B)	5685(24)	-2261(16)	6751(13)	87
H(32C)	5202(24)	-1865(16)	6497(13)	87
H(33A)	6522(28)	-1347(18)	5789(16)	124
H(33B)	5581(28)	-1605(18)	5477(16)	124
H(33C)	6262(28)	-1879(18)	5277(16)	124
H(34A)	7393(26)	-2062(18)	6387(16)	107
H(34B)	7168(26)	-2582(18)	5870(16)	107
H(34C)	6947(26)	-2709(18)	6356(16)	107
H(7BA)	189(32)	7087(31)	6867(87)	42
H(8BA)	-765(24)	6261(15)	6258(13)	56
H(9BA)	-393(25)	5683(16)	5626(14)	58
H(10B)	1012(25)	5666(17)	5730(15)	81
H(11B)	2032(25)	6519(15)	6307(13)	55
H(13B)	1368(24)	6140(66)	7428(112)	72
H(14B)	1494(29)	5202(18)	7335(15)	90
H(15B)	2592(23)	4900(15)	7209(12)	55
H(16B)	3773(26)	5627(16)	7257(14)	74
H(17B)	3695(19)	6582(12)	7438(10)	30
H(19B)	2436(24)	7210(119)	8698(60)	60
H(20B)	3215(28)	7055(17)	9368(16)	79
H(21B)	4535(31)	7188(18)	9609(17)	104
H(22B)	5296(32)	7612(18)	9063(17)	101
H(23B)	4457(31)	7708(19)	8298(18)	101
H(25B)	3790(52)	8805(84)	8588(94)	123
H(26B)	3833(37)	9462(22)	9381(21)	156
H(27B)	2734(34)	9903(22)	9442(20)	131
H(28B)	1490(31)	9398(19)	8850(17)	99
H(29C)	1331(21)	8558(13)	8177(12)	42
H(32D)	-531(28)	8569(17)	5684(16)	124
H(32E)	433(28)	8820(17)	5805(16)	124
H(32F)	-24(28)	9020(17)	6226(16)	124
H(33D)	-1262(26)	7738(17)	6197(15)	115
H(33E)	-744(26)	8167(17)	6745(15)	115
H(33F)	-685(26)	7504(17)	6578(15)	115
H(34D)	-313(28)	7328(17)	5374(16)	115
H(34E)	263(28)	7107(17)	5768(16)	115
H(34F)	658(28)	7560(17)	5515(16)	115
H(7CA)	5221(24)	3188(113)	6923(90)	77
H(8CA)	5046(23)	4216(15)	6906(13)	57
H(9CA)	3961(28)	4553(19)	7118(16)	88
H(10C)	2798(27)	3812(17)	7181(15)	75
H(11C)	2879(23)	2840(15)	7077(12)	49
H(13C)	3245(43)	2687(107)	5885(138)	110
H(14C)	2020(28)	2726(18)	5357(16)	90
H(15C)	781(28)	2155(17)	5345(15)	83
H(16C)	737(25)	1436(16)	5720(14)	66
H(17C)	1986(28)	1277(18)	6217(16)	86
H(19C)	2792(139)	369(53)	6036(39)	65
H(20C)	2265(25)	-360(16)	5302(14)	65
H(21C)	3008(31)	-433(22)	4669(19)	102
H(22C)	3822(25)	492(16)	4664(15)	74
H(23C)	4260(20)	1231(13)	5392(11)	37
H(25C)	4823(95)	461(17)	6554(80)	74

H(26C)	5782(27)	-11(18)	6367(15)	77
H(27C)	7048(29)	525(19)	6393(15)	86
H(28C)	7224(27)	1449(18)	6422(15)	86
H(29D)	6223(19)	2007(13)	6627(11)	42
H(32G)	7021(25)	4294(17)	7912(14)	92
H(32H)	6385(25)	3798(17)	7435(14)	92
H(32I)	7175(25)	3658(17)	7741(14)	92
H(33G)	7159(24)	4178(16)	9001(14)	101
H(33H)	7357(24)	3566(16)	8777(14)	101
H(33I)	6660(24)	3595(16)	9064(14)	101
H(34G)	5583(24)	4441(16)	8478(14)	96
H(34H)	5029(24)	3868(16)	8523(14)	96
H(34I)	4952(24)	3968(16)	7983(14)	96
H(7DA)	2861(127)	2029(80)	8628(21)	43
H(8DA)	3481(24)	1412(16)	8984(14)	64
H(9DA)	3998(23)	1690(15)	9906(13)	56
H(10D)	3425(24)	2364(15)	10396(15)	67
H(11D)	2895(25)	3048(17)	10022(15)	67
H(13D)	4291(53)	3395(63)	9373(46)	26
H(14D)	5444(25)	3869(16)	10045(14)	63
H(15D)	5496(27)	4732(17)	10672(15)	70
H(16D)	4337(27)	5070(18)	10608(16)	80
H(17D)	3124(25)	4602(15)	9952(13)	69
H(19D)	2203(191)	4904(54)	9240(66)	82
H(20D)	2796(26)	5806(18)	9144(15)	80
H(21D)	3411(27)	5878(19)	8489(16)	85
H(22D)	3889(23)	5069(15)	8143(13)	62
H(23D)	3401(25)	4135(17)	8237(14)	70
H(25D)	978(158)	4116(54)	8108(38)	59
H(26D)	578(22)	4236(15)	7296(13)	46
H(27D)	493(27)	3480(18)	6569(17)	80
H(28D)	1093(21)	2708(15)	6714(13)	48
H(29E)	1601(22)	2640(15)	7490(13)	46
H(32J)	-515(25)	644(17)	8370(15)	106
H(32K)	-103(25)	143(17)	8141(15)	106
H(32L)	-386(25)	555(17)	7818(15)	106
H(33J)	1277(28)	849(18)	7675(16)	122
H(33K)	1552(28)	429(18)	7993(16)	122
H(33L)	2070(28)	1091(18)	8151(16)	122
H(34J)	958(22)	1147(14)	9304(12)	68
H(34K)	1856(22)	1298(14)	9236(12)	68
H(34L)	1348(22)	632(14)	9074(12)	68
H(7EA)	-2636(58)	6529(102)	9104(87)	62
H(8EA)	-4008(29)	6015(19)	8999(17)	104
H(9EA)	-5097(22)	6004(13)	8301(12)	55
H(10E)	-4902(37)	6691(23)	7842(21)	146
H(11E)	-3490(28)	7138(18)	7916(16)	81
H(13E)	-3131(133)	8078(183)	8230(29)	131
H(14E)	-3754(34)	8887(22)	8341(21)	121
H(15E)	-3646(29)	9291(19)	9236(17)	95
H(16E)	-2802(22)	9157(14)	9851(14)	52
H(17E)	-1844(25)	8593(16)	9711(15)	71
H(19E)	-859(211)	8932(28)	8683(31)	87
H(20E)	14(29)	9931(19)	9083(17)	98
H(21E)	872(27)	10134(19)	9850(16)	91
H(22E)	1142(35)	9458(22)	10309(21)	143
H(23E)	183(21)	8469(14)	9899(13)	46

H(25E)	826(73)	8013(103)	8891(33)	62
H(26E)	2045(32)	8152(19)	9352(17)	102
H(27E)	2329(33)	7698(20)	9993(18)	105
H(28E)	1220(29)	6976(19)	10052(17)	94
H(29F)	-73(23)	6972(14)	9584(13)	59
H(32M)	121(32)	5393(20)	9466(17)	159
H(32N)	-828(32)	5366(20)	9275(17)	159
H(32O)	-180(32)	5982(20)	9564(17)	159
H(33M)	-4(39)	4689(24)	8361(22)	230
H(33N)	-383(39)	4898(24)	7892(22)	230
H(33O)	-947(39)	4695(24)	8225(22)	230
H(34M)	1519(40)	5969(26)	8889(23)	206
H(34N)	1225(40)	6560(26)	8993(23)	206
H(34O)	1177(40)	6201(26)	8428(23)	206
H(38A)	-3115(26)	5281(15)	8150(15)	93

Table D1. Crystal data and structure refinement for (η^5-Fe(CO)$_2${μ-H}[$C_5Ph_2Et_2$-C≡C-TMS]$Co_2(CO)_6$), **65**.

	65
empirical formula	$C_{34}H_{30}Co_2FeO_8Si$
M_r	768.38
T [K]	213(2)
λ [Å]	0.71073
description	thin red plate
crystal size [mm]	0.04 x 0.10 x 0.14
crystal system	Triclinic
space group	$P\bar{1}$
a [Å]	12.288(2)
b [Å]	16.247(3)
c [Å]	19.010(3)
α [°]	64.707(4)
β [°]	80.891(4)
γ [°]	89.839(5)
V [Å^3]	3379.2(9)
Z	4
ρ_{calcd} [g cm^{-3}]	1.510
abs. Coeff. [mm^{-1}]	1.478
F(000)	1568
θ range for collection [°]	2.20 to 24.00
limiting indices	-16 < h < 15, -20 < k < 21, -24 < l < 12
reflections collected	18996
independent reflections	10578
R(int)	0.0955
refinement method	Full-matrix least-squares on F^2
weighting scheme	$w=1/[\sigma^2F_o^2 + (0.2347((F_o^2+ 2F_c^2)/3))^2 + 0.000((F_o^2 +2F_c^2)/3))^2]$
data/restraints/parameters	10552 / 0 / 830
goodness-of-fit on F^2	1.076 final
R indices [I>2σ(I)][a]	R1 = 0.1419, wR2 = 0.3648
R indices (all data)[a]	R1 = 0.2242, wR2 = 0.4062
rel. trans. (max., min.)	0.8577, 0.3731
Largest diff. peak [eÅ^{-3}]	4.534
Largest diff hole [eÅ^{-3}]	-1.524

[a] $R1 = \Sigma (|| F_o | - | F_c ||)/ \Sigma | F_o |$; $wR2 = [\Sigma[w(F_o^2 - F_c^2)^2]/\Sigma[w(F_o^2)^2]]^{0.5}$

Table D2. Atomic coordinates [x 10^4] and equivalent isotropic displacement parameters [$Å^2$ x 10^3] for **65**. U(eq) is defined as one third of the trace of the orthogonalized U_{ij} tensor.

	x	y	z	U(eq)
Co(1)	8006(2)	6311(2)	1453(1)	32(1)
Co(2)	6708(2)	6578(2)	2499(1)	38(1)
Fe(1)	4664(2)	5857(2)	2342(1)	31(1)
Si(1)	8707(4)	4888(4)	3290(3)	42(1)
C(1)	5863(11)	4956(10)	2357(8)	23(4)
C(2)	5111(14)	4531(10)	3134(8)	28(4)
C(3)	4030(13)	4428(10)	2963(9)	31(4)
C(4)	4121(14)	4754(11)	2119(9)	31(4)
C(5)	5251(13)	5036(9)	1765(8)	26(4)
C(6)	3017(15)	3997(11)	3553(9)	35(4)
C(7)	2583(17)	4265(13)	4114(10)	48(5)
C(8)	1606(17)	3814(16)	4635(10)	55(6)
C(9)	1147(18)	3106(18)	4609(13)	66(7)
C(10)	1568(18)	2782(14)	4094(11)	61(7)
C(11)	2550(14)	3238(13)	3513(10)	43(5)
C(12)	3198(13)	4672(11)	1731(8)	28(4)
C(13)	3133(15)	3912(13)	1564(9)	41(5)
C(14)	2241(16)	3762(14)	1256(10)	49(5)
C(15)	1379(15)	4322(13)	1126(9)	40(5)
C(16)	1472(16)	5074(14)	1283(10)	46(5)
C(17)	2337(15)	5247(13)	1605(11)	47(5)
C(18)	5650(15)	5342(11)	881(8)	38(4)
C(19)	6124(16)	4510(13)	773(10)	52(6)
C(20)	5412(15)	4186(11)	3954(9)	37(4)
C(21)	5690(18)	3179(11)	4226(10)	54(6)
C(22)	6897(14)	5420(10)	2276(9)	34(4)
C(23)	7687(14)	5506(11)	2651(8)	30(4)
C(24)	8070(19)	4530(18)	4365(11)	74(7)
C(25)	9027(18)	3874(16)	3089(13)	69(7)
C(26)	10007(18)	5639(14)	3060(13)	74(8)
C(27)	8553(14)	5615(11)	963(10)	33(4)
O(27)	8922(11)	5221(9)	634(8)	52(4)
C(28)	9319(17)	6931(14)	1309(11)	46(5)
O(28)	10134(12)	7333(10)	1162(9)	64(4)
C(29)	7338(16)	7173(14)	685(11)	47(5)
O(29)	6958(13)	7731(9)	216(7)	63(4)
C(30)	7790(16)	7208(13)	2593(10)	40(5)
O(30)	8490(12)	7587(10)	2682(8)	61(4)
C(31)	5981(15)	7556(13)	1957(11)	42(5)
O(31)	5599(12)	8213(9)	1640(9)	65(4)
C(32)	5973(18)	6369(14)	3409(13)	58(6)
O(32)	5548(14)	6201(11)	4084(8)	79(5)
C(33)	4399(15)	6743(12)	1463(10)	39(5)
O(33)	4215(12)	7300(8)	865(8)	60(4)
C(34)	3853(17)	6309(12)	2915(11)	47(5)
O(34)	3257(14)	6583(10)	3286(9)	75(5)
Co(1A)	6265(2)	1358(2)	1345(1)	31(1)
Co(2A)	7054(2)	1644(2)	2377(1)	37(1)

Fe(1A)	9156(2)	898(2)	2249(1)	30(1)
Si(1A)	4625(4)	13(4)	3170(3)	40(1)
C(1A)	7944(13)	-26(10)	2317(8)	27(4)
C(2A)	8857(12)	63(10)	1692(9)	25(4)
C(3A)	9816(12)	-230(10)	2061(7)	21(3)
C(4A)	9477(12)	-504(11)	2904(9)	29(4)
C(5A)	8306(14)	-379(10)	3066(8)	28(4)
C(6A)	10907(13)	-322(11)	1687(9)	28(4)
C(7A)	11833(15)	234(11)	1553(8)	34(4)
C(8A)	12851(15)	59(13)	1263(9)	41(5)
C(9A)	13024(15)	-671(14)	1108(10)	44(5)
C(10A)	12098(16)	-1269(12)	1252(9)	43(5)
C(11A)	11069(14)	-1060(13)	1507(10)	41(5)
C(12A)	10196(13)	-915(11)	3496(8)	32(4)
C(13A)	10829(13)	-1636(11)	3506(9)	34(4)
C(14A)	11529(14)	-2017(13)	4029(10)	45(5)
C(15A)	11581(18)	-1707(15)	4629(11)	57(6)
C(16A)	10949(17)	-1032(15)	4645(10)	53(6)
C(17A)	10277(16)	-616(12)	4084(9)	41(5)
C(18A)	7592(15)	-738(11)	3870(8)	38(5)
C(19A)	7122(17)	-1709(11)	4049(10)	55(6)
C(20A)	8839(15)	329(11)	820(9)	36(4)
C(21A)	8422(16)	-509(11)	740(10)	41(5)
C(22A)	6940(13)	489(11)	2177(8)	27(4)
C(23A)	5970(13)	572(11)	2538(9)	30(4)
C(24A)	4397(18)	-1036(13)	3033(12)	60(6)
C(25A)	3496(17)	736(14)	2910(12)	62(6)
C(26A)	4671(19)	-266(20)	4242(12)	87(9)
C(27A)	5088(17)	2055(14)	1136(10)	43(5)
O(27A)	4370(12)	2486(10)	983(8)	60(4)
C(28A)	5922(13)	622(13)	896(9)	36(5)
O(28A)	5678(11)	194(9)	609(7)	48(3)
C(29A)	7311(16)	2156(12)	599(10)	42(5)
O(29A)	7927(11)	2677(9)	97(7)	63(4)
C(30A)	5917(18)	2250(12)	2522(10)	42(5)
O(30A)	5166(12)	2660(10)	2609(8)	58(4)
C(31A)	7350(14)	1423(13)	3322(12)	40(5)
O(31A)	7529(12)	1302(10)	3939(8)	63(4)
C(32A)	8026(18)	2606(15)	1824(12)	56(6)
O(32A)	8587(12)	3285(9)	1501(8)	64(4)
C(33A)	9774(17)	1382(14)	2781(10)	53(6)
O(33A)	10198(13)	1690(10)	3123(9)	69(5)
C(34A)	9854(14)	1757(10)	1340(10)	34(4)
O(34A)	10324(12)	2293(10)	740(8)	70(4)

Table D3. Bond lengths [Å] and angles [deg] for **65**.

Co(1)-C(27)	1.81(2)	C(32)-O(32)	1.22(2)
Co(1)-C(28)	1.82(2)	C(33)-O(33)	1.17(2)
Co(1)-C(29)	1.84(2)	C(34)-O(34)	1.16(2)
Co(1)-C(22)	1.95(2)	Co(1A)-C(29A)	1.79(2)
Co(1)-C(23)	2.057(14)	Co(1A)-C(27A)	1.82(2)
Co(1)-Co(2)	2.532(3)	Co(1A)-C(28A)	1.82(2)
Co(2)-C(32)	1.71(2)	Co(1A)-C(22A)	1.92(2)
Co(2)-C(30)	1.76(2)	Co(1A)-C(23A)	2.04(2)
Co(2)-C(31)	1.81(2)	Co(1A)-Co(2A)	2.528(3)
Co(2)-C(23)	2.06(2)	Co(2A)-C(30A)	1.76(2)
Co(2)-C(22)	2.10(2)	Co(2A)-C(31A)	1.77(2)
Co(2)-Fe(1)	2.885(3)	Co(2A)-C(32A)	1.78(2)
Fe(1)-C(34)	1.75(2)	Co(2A)-C(22A)	2.08(2)
Fe(1)-C(33)	1.76(2)	Co(2A)-C(23A)	2.08(2)
Fe(1)-C(1)	2.07(2)	Co(2A)-Fe(1A)	2.869(3)
Fe(1)-C(5)	2.12(2)	Fe(1A)-C(34A)	1.77(2)
Fe(1)-C(4)	2.14(2)	Fe(1A)-C(33A)	1.77(2)
Fe(1)-C(2)	2.167(14)	Fe(1A)-C(1A)	2.07(2)
Fe(1)-C(3)	2.18(2)	Fe(1A)-C(2A)	2.11(2)
Si(1)-C(23)	1.87(2)	Fe(1A)-C(5A)	2.13(2)
Si(1)-C(25)	1.87(2)	Fe(1A)-C(3A)	2.15(2)
Si(1)-C(26)	1.89(2)	Fe(1A)-C(4A)	2.15(2)
Si(1)-C(24)	1.90(2)	Si(1A)-C(25A)	1.81(2)
C(1)-C(5)	1.41(2)	Si(1A)-C(24A)	1.86(2)
C(1)-C(22)	1.43(2)	Si(1A)-C(23A)	1.86(2)
C(1)-C(2)	1.49(2)	Si(1A)-C(26A)	1.90(2)
C(2)-C(3)	1.44(2)	C(1A)-C(5A)	1.43(2)
C(2)-C(20)	1.52(2)	C(1A)-C(2A)	1.46(2)
C(3)-C(4)	1.44(2)	C(1A)-C(22A)	1.48(2)
C(3)-C(6)	1.48(2)	C(2A)-C(3A)	1.44(2)
C(4)-C(5)	1.43(2)	C(2A)-C(20A)	1.53(2)
C(4)-C(12)	1.48(2)	C(3A)-C(4A)	1.46(2)
C(5)-C(18)	1.53(2)	C(3A)-C(6A)	1.45(2)
C(6)-C(7)	1.35(2)	C(4A)-C(5A)	1.46(2)
C(6)-C(11)	1.40(2)	C(4A)-C(12A)	1.47(2)
C(7)-C(8)	1.40(3)	C(5A)-C(18A)	1.50(2)
C(8)-C(9)	1.31(3)	C(6A)-C(7A)	1.38(2)
C(9)-C(10)	1.33(3)	C(6A)-C(11A)	1.39(2)
C(10)-C(11)	1.45(3)	C(7A)-C(8A)	1.36(2)
C(12)-C(17)	1.39(2)	C(8A)-C(9A)	1.35(3)
C(12)-C(13)	1.40(2)	C(9A)-C(10A)	1.41(3)
C(13)-C(14)	1.39(2)	C(10A)-C(11A)	1.38(2)
C(14)-C(15)	1.38(3)	C(12A)-C(13A)	1.40(2)
C(15)-C(16)	1.38(2)	C(12A)-C(17A)	1.41(2)
C(16)-C(17)	1.39(3)	C(13A)-C(14A)	1.36(2)
C(18)-C(19)	1.55(2)	C(14A)-C(15A)	1.44(3)
C(20)-C(21)	1.55(2)	C(15A)-C(16A)	1.35(3)
C(22)-C(23)	1.33(2)	C(16A)-C(17A)	1.39(2)
C(27)-O(27)	1.12(2)	C(18A)-C(19A)	1.56(2)
C(28)-O(28)	1.13(2)	C(20A)-C(21A)	1.53(2)
C(29)-O(29)	1.13(2)	C(22A)-C(23A)	1.31(2)
C(30)-O(30)	1.13(2)	C(27A)-O(27A)	1.12(2)
C(31)-O(31)	1.12(2)	C(28A)-O(28A)	1.12(2)

C(29A)-O(29A)	1.13(2)
C(30A)-O(30A)	1.17(2)
C(31A)-O(31A)	1.16(2)
C(32A)-O(32A)	1.17(2)
C(33A)-O(33A)	1.15(2)
C(34A)-O(34A)	1.16(2)

C(27)-Co(1)-C(28)	95.9(7)
C(27)-Co(1)-C(29)	101.4(8)
C(28)-Co(1)-C(29)	101.0(9)
C(27)-Co(1)-C(22)	98.9(7)
C(28)-Co(1)-C(22)	141.8(8)
C(29)-Co(1)-C(22)	110.3(8)
C(27)-Co(1)-C(23)	108.5(7)
C(28)-Co(1)-C(23)	103.0(8)
C(29)-Co(1)-C(23)	139.1(8)
C(22)-Co(1)-C(23)	38.7(6)
C(27)-Co(1)-Co(2)	152.9(5)
C(28)-Co(1)-Co(2)	106.3(5)
C(29)-Co(1)-Co(2)	89.5(6)
C(22)-Co(1)-Co(2)	54.1(5)
C(23)-Co(1)-Co(2)	52.0(5)
C(32)-Co(2)-C(30)	93.3(10)
C(32)-Co(2)-C(31)	95.4(9)
C(30)-Co(2)-C(31)	95.6(8)
C(32)-Co(2)-C(23)	107.0(8)
C(30)-Co(2)-C(23)	90.8(8)
C(31)-Co(2)-C(23)	156.3(7)
C(32)-Co(2)-C(22)	114.7(8)
C(30)-Co(2)-C(22)	124.9(8)
C(31)-Co(2)-C(22)	125.2(7)
C(23)-Co(2)-C(22)	37.4(6)
C(32)-Co(2)-Co(1)	158.9(7)
C(30)-Co(2)-Co(1)	89.4(6)
C(31)-Co(2)-Co(1)	105.1(6)
C(23)-Co(2)-Co(1)	52.0(4)
C(22)-Co(2)-Co(1)	48.7(4)
C(32)-Co(2)-Fe(1)	82.0(8)
C(30)-Co(2)-Fe(1)	167.9(6)
C(31)-Co(2)-Fe(1)	73.9(6)
C(23)-Co(2)-Fe(1)	101.2(5)
C(22)-Co(2)-Fe(1)	67.0(5)
Co(1)-Co(2)-Fe(1)	98.99(10)
C(34)-Fe(1)-C(33)	91.7(9)
C(34)-Fe(1)-C(1)	144.1(8)
C(33)-Fe(1)-C(1)	122.6(7)
C(34)-Fe(1)-C(5)	163.6(7)
C(33)-Fe(1)-C(5)	92.7(7)
C(1)-Fe(1)-C(5)	39.3(6)
C(34)-Fe(1)-C(4)	124.6(7)
C(33)-Fe(1)-C(4)	96.7(7)
C(1)-Fe(1)-C(4)	66.5(6)
C(5)-Fe(1)-C(4)	39.1(6)
C(34)-Fe(1)-C(2)	107.8(7)
C(33)-Fe(1)-C(2)	159.0(7)
C(1)-Fe(1)-C(2)	41.1(6)
C(5)-Fe(1)-C(2)	66.4(5)
C(4)-Fe(1)-C(2)	65.9(6)
C(34)-Fe(1)-C(3)	100.1(7)
C(33)-Fe(1)-C(3)	131.3(7)
C(1)-Fe(1)-C(3)	66.7(6)
C(5)-Fe(1)-C(3)	65.4(6)
C(4)-Fe(1)-C(3)	39.0(6)
C(2)-Fe(1)-C(3)	38.8(6)
C(34)-Fe(1)-Co(2)	93.3(6)
C(33)-Fe(1)-Co(2)	100.9(6)
C(1)-Fe(1)-Co(2)	71.5(4)
C(5)-Fe(1)-Co(2)	101.3(4)
C(4)-Fe(1)-Co(2)	137.6(5)
C(2)-Fe(1)-Co(2)	86.4(4)
C(3)-Fe(1)-Co(2)	125.0(4)
C(23)-Si(1)-C(25)	106.4(9)
C(23)-Si(1)-C(26)	111.4(8)
C(25)-Si(1)-C(26)	110.5(11)
C(23)-Si(1)-C(24)	109.1(9)
C(25)-Si(1)-C(24)	111.4(11)
C(26)-Si(1)-C(24)	108.1(10)
C(5)-C(1)-C(22)	128.7(13)
C(5)-C(1)-C(2)	108.2(12)
C(22)-C(1)-C(2)	120.6(14)
C(5)-C(1)-Fe(1)	72.3(9)
C(22)-C(1)-Fe(1)	106.4(11)
C(2)-C(1)-Fe(1)	73.0(8)
C(3)-C(2)-C(1)	106.0(12)
C(3)-C(2)-C(20)	125.8(14)
C(1)-C(2)-C(20)	128.0(14)
C(3)-C(2)-Fe(1)	71.2(8)
C(1)-C(2)-Fe(1)	65.9(8)
C(20)-C(2)-Fe(1)	131.5(11)
C(4)-C(3)-C(2)	108.4(13)
C(4)-C(3)-C(6)	126(2)
C(2)-C(3)-C(6)	125.9(14)
C(4)-C(3)-Fe(1)	68.9(9)
C(2)-C(3)-Fe(1)	70.0(8)
C(6)-C(3)-Fe(1)	130.3(12)
C(5)-C(4)-C(3)	108.4(14)
C(5)-C(4)-C(12)	127.5(14)
C(3)-C(4)-C(12)	123.6(14)
C(5)-C(4)-Fe(1)	69.7(9)
C(3)-C(4)-Fe(1)	72.2(9)
C(12)-C(4)-Fe(1)	130.5(11)
C(1)-C(5)-C(4)	108.9(13)
C(1)-C(5)-C(18)	129.3(14)
C(4)-C(5)-C(18)	121.8(14)
C(1)-C(5)-Fe(1)	68.3(9)
C(4)-C(5)-Fe(1)	71.1(9)
C(18)-C(5)-Fe(1)	127.7(10)
C(7)-C(6)-C(11)	121(2)
C(7)-C(6)-C(3)	125(2)
C(11)-C(6)-C(3)	114(2)
C(6)-C(7)-C(8)	120(2)
C(9)-C(8)-C(7)	120(2)
C(8)-C(9)-C(10)	123(2)

C(9)-C(10)-C(11)	120(2)
C(6)-C(11)-C(10)	116(2)
C(17)-C(12)-C(13)	119(2)
C(17)-C(12)-C(4)	123(2)
C(13)-C(12)-C(4)	118(2)
C(14)-C(13)-C(12)	120(2)
C(15)-C(14)-C(13)	122(2)
C(14)-C(15)-C(16)	116(2)
C(15)-C(16)-C(17)	124(2)
C(12)-C(17)-C(16)	119(2)
C(5)-C(18)-C(19)	107.5(13)
C(2)-C(20)-C(21)	108.5(14)
C(23)-C(22)-C(1)	145.4(14)
C(23)-C(22)-Co(1)	75.0(10)
C(1)-C(22)-Co(1)	139.5(12)
C(23)-C(22)-Co(2)	69.5(11)
C(1)-C(22)-Co(2)	112.8(11)
Co(1)-C(22)-Co(2)	77.3(6)
C(22)-C(23)-Si(1)	144.9(13)
C(22)-C(23)-Co(1)	66.3(9)
Si(1)-C(23)-Co(1)	126.9(8)
C(22)-C(23)-Co(2)	73.2(10)
Si(1)-C(23)-Co(2)	138.1(9)
Co(1)-C(23)-Co(2)	76.0(5)
O(27)-C(27)-Co(1)	176.6(14)
O(28)-C(28)-Co(1)	175(2)
O(29)-C(29)-Co(1)	177(2)
O(30)-C(30)-Co(2)	177(2)
O(31)-C(31)-Co(2)	173(2)
O(32)-C(32)-Co(2)	174(2)
O(33)-C(33)-Fe(1)	177(2)
O(34)-C(34)-Fe(1)	176(2)
C(29A)-Co(1A)-C(27A)	98.7(9)
C(29A)-Co(1A)-C(28A)	102.7(7)
C(27A)-Co(1A)-C(28A)	96.7(7)
C(29A)-Co(1A)-C(22A)	109.4(7)
C(27A)-Co(1A)-C(22A)	143.9(7)
C(28A)-Co(1A)-C(22A)	98.6(7)
C(29A)-Co(1A)-C(23A)	139.3(7)
C(27A)-Co(1A)-C(23A)	105.6(7)
C(28A)-Co(1A)-C(23A)	106.3(7)
C(22A)-Co(1A)-C(23A)	38.6(6)
C(29A)-Co(1A)-Co(2A)	89.3(6)
C(27A)-Co(1A)-Co(2A)	106.3(5)
C(28A)-Co(1A)-Co(2A)	152.2(5)
C(22A)-Co(1A)-Co(2A)	53.6(5)
C(23A)-Co(1A)-Co(2A)	52.9(5)
C(30A)-Co(2A)-C(31A)	90.6(8)
C(30A)-Co(2A)-C(32A)	97.2(9)
C(31A)-Co(2A)-C(32A)	96.8(9)
C(30A)-Co(2A)-C(22A)	124.1(7)
C(31A)-Co(2A)-C(22A)	114.2(7)
C(32A)-Co(2A)-C(22A)	125.8(8)
C(30A)-Co(2A)-C(23A)	89.5(7)
C(31A)-Co(2A)-C(23A)	106.7(7)
C(32A)-Co(2A)-C(23A)	155.5(8)
C(22A)-Co(2A)-C(23A)	36.9(6)
C(30A)-Co(2A)-Co(1A)	91.7(6)
C(31A)-Co(2A)-Co(1A)	158.0(6)
C(32A)-Co(2A)-Co(1A)	104.6(7)
C(22A)-Co(2A)-Co(1A)	48.1(4)
C(23A)-Co(2A)-Co(1A)	51.5(4)
C(30A)-Co(2A)-Fe(1A)	167.7(6)
C(31A)-Co(2A)-Fe(1A)	81.4(6)
C(32A)-Co(2A)-Fe(1A)	74.6(7)
C(22A)-Co(2A)-Fe(1A)	68.0(5)
C(23A)-Co(2A)-Fe(1A)	101.7(4)
Co(1A)-Co(2A)-Fe(1A)	99.22(10)
C(34A)-Fe(1A)-C(33A)	90.7(8)
C(34A)-Fe(1A)-C(1A)	123.0(7)
C(33A)-Fe(1A)-C(1A)	145.3(7)
C(34A)-Fe(1A)-C(2A)	90.9(7)
C(33A)-Fe(1A)-C(2A)	161.6(8)
C(1A)-Fe(1A)-C(2A)	40.8(6)
C(34A)-Fe(1A)-C(5A)	158.9(7)
C(33A)-Fe(1A)-C(5A)	108.7(7)
C(1A)-Fe(1A)-C(5A)	39.9(6)
C(2A)-Fe(1A)-C(5A)	68.0(6)
C(34A)-Fe(1A)-C(3A)	95.7(7)
C(33A)-Fe(1A)-C(3A)	122.0(7)
C(1A)-Fe(1A)-C(3A)	67.0(6)
C(2A)-Fe(1A)-C(3A)	39.6(6)
C(5A)-Fe(1A)-C(3A)	67.4(6)
C(34A)-Fe(1A)-C(4A)	131.2(7)
C(33A)-Fe(1A)-C(4A)	98.9(7)
C(1A)-Fe(1A)-C(4A)	66.3(6)
C(2A)-Fe(1A)-C(4A)	66.7(6)
C(5A)-Fe(1A)-C(4A)	39.7(6)
C(3A)-Fe(1A)-C(4A)	39.7(5)
C(34A)-Fe(1A)-Co(2A)	100.9(5)
C(33A)-Fe(1A)-Co(2A)	96.1(7)
C(1A)-Fe(1A)-Co(2A)	71.7(5)
C(2A)-Fe(1A)-Co(2A)	101.6(4)
C(5A)-Fe(1A)-Co(2A)	85.4(5)
C(3A)-Fe(1A)-Co(2A)	138.1(4)
C(4A)-Fe(1A)-Co(2A)	125.1(4)
C(25A)-Si(1A)-C(24A)	110.4(10)
C(25A)-Si(1A)-C(23A)	112.7(8)
C(24A)-Si(1A)-C(23A)	105.9(9)
C(25A)-Si(1A)-C(26A)	106.1(10)
C(24A)-Si(1A)-C(26A)	111.6(11)
C(23A)-Si(1A)-C(26A)	110.3(9)
C(5A)-C(1A)-C(2A)	110.4(14)
C(5A)-C(1A)-C(22A)	122.0(14)
C(2A)-C(1A)-C(22A)	123.8(13)
C(5A)-C(1A)-Fe(1A)	72.6(9)
C(2A)-C(1A)-Fe(1A)	71.1(9)
C(22A)-C(1A)-Fe(1A)	105.2(10)
C(3A)-C(2A)-C(1A)	106.9(12)
C(3A)-C(2A)-C(20A)	124.1(13)
C(1A)-C(2A)-C(20A)	128.9(14)
C(3A)-C(2A)-Fe(1A)	71.6(8)
C(1A)-C(2A)-Fe(1A)	68.1(8)
C(20A)-C(2A)-Fe(1A)	129.3(11)

C(2A)-C(3A)-C(4A)	107.7(12)	C(14A)-C(13A)-C(12A)	123(2)
C(2A)-C(3A)-C(6A)	127.2(12)	C(13A)-C(14A)-C(15A)	119(2)
C(4A)-C(3A)-C(6A)	124.9(13)	C(16A)-C(15A)-C(14A)	119(2)
C(2A)-C(3A)-Fe(1A)	68.8(8)	C(15A)-C(16A)-C(17A)	122(2)
C(4A)-C(3A)-Fe(1A)	70.3(9)	C(16A)-C(17A)-C(12A)	121(2)
C(6A)-C(3A)-Fe(1A)	130.4(11)	C(5A)-C(18A)-C(19A)	106.1(14)
C(3A)-C(4A)-C(5A)	109.2(12)	C(2A)-C(20A)-C(21A)	108.6(13)
C(3A)-C(4A)-C(12A)	124.5(14)	C(23A)-C(22A)-C(1A)	142.4(14)
C(5A)-C(4A)-C(12A)	126.1(13)	C(23A)-C(22A)-Co(1A)	75.8(10)
C(3A)-C(4A)-Fe(1A)	70.0(9)	C(1A)-C(22A)-Co(1A)	141.7(11)
C(5A)-C(4A)-Fe(1A)	69.6(9)	C(23A)-C(22A)-Co(2A)	71.7(10)
C(12A)-C(4A)-Fe(1A)	130.7(12)	C(1A)-C(22A)-Co(2A)	111.5(10)
C(1A)-C(5A)-C(4A)	105.9(13)	Co(1A)-C(22A)-Co(2A)	78.4(6)
C(1A)-C(5A)-C(18A)	127(2)	C(22A)-C(23A)-Si(1A)	148.1(14)
C(4A)-C(5A)-C(18A)	125.8(14)	C(22A)-C(23A)-Co(1A)	65.6(9)
C(1A)-C(5A)-Fe(1A)	67.5(8)	Si(1A)-C(23A)-Co(1A)	127.2(8)
C(4A)-C(5A)-Fe(1A)	70.7(9)	C(22A)-C(23A)-Co(2A)	71.4(10)
C(18A)-C(5A)-Fe(1A)	135.7(12)	Si(1A)-C(23A)-Co(2A)	136.8(9)
C(7A)-C(6A)-C(11A)	116(2)	Co(1A)-C(23A)-Co(2A)	75.6(6)
C(7A)-C(6A)-C(3A)	125(2)	O(27A)-C(27A)-Co(1A)	178(2)
C(11A)-C(6A)-C(3A)	118.9(14)	O(28A)-C(28A)-Co(1A)	177(2)
C(8A)-C(7A)-C(6A)	121(2)	O(29A)-C(29A)-Co(1A)	176(2)
C(9A)-C(8A)-C(7A)	123(2)	O(30A)-C(30A)-Co(2A)	179(2)
C(8A)-C(9A)-C(10A)	118(2)	O(31A)-C(31A)-Co(2A)	178(2)
C(11A)-C(10A)-C(9A)	119(2)	O(32A)-C(32A)-Co(2A)	173(2)
C(10A)-C(11A)-C(6A)	123(2)	O(33A)-C(33A)-Fe(1A)	179(2)
C(13A)-C(12A)-C(17A)	117(2)	O(34A)-C(34A)-Fe(1A)	178(2)
C(13A)-C(12A)-C(4A)	121(2)		
C(17A)-C(12A)-C(4A)	122(2)		

Table D4. Anisotropic displacement parameters [$Å^2$ x 10^3] for **65**. The anisotropic displacement factor exponent takes the form: $-2p^2$ [$(ha^*)^2 U_{11}$ + ... + 2hka*b* U_{12}]

	U11	U22	U33	U23	U13	U12
Co(1)	32(1)	23(1)	28(1)	-1(1)	4(1)	-10(1)
Co(2)	41(2)	27(1)	35(1)	-6(1)	2(1)	-9(1)
Fe(1)	33(2)	20(1)	27(1)	-2(1)	1(1)	-6(1)
Si(1)	42(3)	39(3)	41(3)	-12(2)	-11(2)	-2(2)
C(1)	9(8)	21(8)	26(8)	1(7)	-2(7)	-6(6)
C(2)	41(11)	12(8)	22(8)	0(7)	0(7)	-3(7)
C(3)	22(10)	22(9)	29(8)	4(7)	5(7)	-8(7)
C(4)	36(11)	22(9)	26(8)	-4(7)	-1(8)	0(8)
C(5)	32(10)	0(7)	25(8)	12(6)	4(7)	-18(7)
C(6)	44(11)	27(10)	21(8)	1(7)	-7(8)	-8(8)
C(7)	67(15)	47(12)	30(9)	-22(9)	6(10)	4(10)
C(8)	48(14)	68(16)	21(9)	2(10)	11(9)	8(12)
C(9)	39(14)	83(19)	54(14)	-15(14)	14(11)	-21(13)
C(10)	74(16)	45(13)	30(10)	17(10)	-10(11)	-47(11)
C(11)	28(11)	54(13)	38(10)	-13(9)	3(8)	-15(9)
C(12)	22(9)	29(10)	25(8)	-7(7)	5(7)	-5(7)
C(13)	41(12)	56(13)	28(9)	-18(9)	-7(8)	-6(9)

C(14)	49(14)	52(13)	37(10)	-13(10)	-5(10)	-5(11)
C(15)	32(11)	49(12)	25(9)	-3(9)	-5(8)	-12(9)
C(16)	47(13)	60(14)	36(10)	-20(10)	-23(9)	20(10)
C(17)	38(12)	42(12)	54(11)	-19(10)	3(10)	-3(9)
C(18)	44(11)	33(10)	15(8)	5(7)	5(7)	-13(8)
C(19)	47(13)	55(13)	51(11)	-37(11)	41(10)	-30(10)
C(20)	39(11)	28(10)	30(9)	-2(8)	-2(8)	-11(8)
C(21)	89(17)	19(10)	33(10)	8(8)	-8(10)	-6(10)
C(22)	39(11)	7(8)	33(9)	12(7)	-4(8)	2(7)
C(23)	31(10)	29(10)	17(7)	-2(7)	10(7)	-16(8)
C(24)	63(16)	113(21)	55(13)	-37(14)	-31(12)	7(14)
C(25)	53(15)	90(18)	84(16)	-55(15)	-19(13)	27(13)
C(26)	64(16)	48(13)	86(16)	7(12)	-58(14)	-13(11)
C(27)	30(11)	25(10)	34(9)	-5(8)	-3(8)	-23(8)
O(27)	49(9)	49(9)	62(9)	-34(8)	14(7)	-12(7)
C(28)	42(13)	66(14)	57(12)	-57(12)	2(10)	-3(11)
O(28)	48(10)	61(10)	90(11)	-41(9)	-4(8)	-20(8)
C(29)	44(13)	42(12)	49(12)	-16(10)	-3(10)	-8(10)
O(29)	90(12)	33(8)	32(7)	16(6)	-4(7)	-6(8)
C(30)	48(13)	38(11)	41(10)	-19(9)	-15(9)	1(10)
O(30)	63(10)	57(10)	70(9)	-38(8)	-3(8)	-13(8)
C(31)	37(12)	31(11)	58(12)	-22(10)	0(9)	-6(9)
O(31)	64(10)	23(8)	98(11)	-16(8)	-18(9)	1(7)
C(32)	55(14)	42(13)	70(14)	-25(11)	14(11)	-2(10)
O(32)	106(13)	76(11)	41(8)	-27(8)	33(8)	-31(10)
C(33)	42(12)	37(11)	29(9)	-7(9)	-4(8)	-19(9)
O(33)	65(10)	31(8)	54(8)	13(7)	-15(7)	-1(7)
C(34)	59(14)	22(10)	42(10)	-4(9)	13(10)	-26(9)
O(34)	92(13)	55(10)	69(10)	-32(9)	24(9)	13(9)
Co(1A)	31(1)	25(1)	26(1)	-3(1)	0(1)	-3(1)
Co(2A)	37(2)	31(1)	35(1)	-8(1)	-4(1)	-3(1)
Fe(1A)	30(2)	23(1)	26(1)	-3(1)	0(1)	-6(1)
Si(1A)	27(3)	47(3)	32(2)	-10(2)	9(2)	-15(2)
C(1A)	35(10)	19(9)	25(8)	-5(7)	-10(7)	-4(7)
C(2A)	17(9)	28(9)	28(8)	-13(7)	6(7)	-10(7)
C(3A)	30(10)	18(8)	7(6)	0(6)	1(6)	-2(7)
C(4A)	13(9)	40(10)	29(8)	-13(8)	0(7)	-6(7)
C(5A)	36(11)	22(9)	17(7)	-2(7)	0(7)	-8(7)
C(6A)	16(9)	30(10)	31(9)	-10(8)	3(7)	0(7)
C(7A)	54(13)	32(10)	19(8)	-12(8)	-10(8)	1(9)
C(8A)	28(11)	38(11)	29(9)	5(9)	16(8)	-22(9)
C(9A)	25(11)	66(14)	31(9)	-14(10)	2(8)	-1(10)
C(10A)	54(13)	25(10)	35(9)	-3(8)	1(9)	3(9)
C(11A)	20(10)	50(12)	44(10)	-17(9)	12(8)	-8(9)
C(12A)	21(9)	29(10)	15(7)	16(7)	4(7)	-21(8)
C(13A)	25(10)	34(10)	26(8)	4(8)	-5(7)	5(8)
C(14A)	23(10)	43(12)	48(11)	-8(10)	18(9)	4(9)
C(15A)	51(14)	47(14)	45(12)	3(10)	6(10)	-18(11)
C(16A)	53(14)	58(14)	29(10)	-2(10)	-9(9)	-20(11)
C(17A)	58(13)	33(11)	23(8)	-2(8)	-12(9)	2(9)
C(18A)	42(11)	35(10)	12(7)	7(7)	11(7)	-26(8)
C(19A)	74(15)	14(9)	33(10)	23(8)	16(10)	-13(9)
C(20A)	37(11)	29(10)	32(9)	-6(8)	-3(8)	-8(8)
C(21A)	52(13)	30(10)	40(10)	-10(8)	-17(9)	5(9)
C(22A)	32(11)	29(9)	21(8)	-11(7)	-4(7)	-2(8)
C(23A)	15(9)	36(10)	37(9)	-16(8)	-1(8)	1(7)
C(24A)	56(15)	46(13)	67(13)	-15(11)	-2(11)	-19(11)

C(25A)	62(15)	51(14)	55(12)	-12(11)	4(11)	-25(11)
C(26A)	51(16)	141(25)	54(13)	-36(16)	15(11)	-4(16)
C(27A)	45(13)	65(14)	46(11)	-47(11)	-15(10)	18(11)
O(27A)	47(9)	75(11)	70(9)	-38(8)	-22(8)	26(8)
C(28A)	19(10)	42(11)	21(8)	7(8)	7(7)	8(8)
O(28A)	58(9)	49(9)	37(7)	-23(7)	6(6)	-11(7)
C(29A)	60(14)	24(10)	26(9)	1(8)	0(9)	1(9)
O(29A)	51(9)	52(9)	35(7)	21(7)	12(7)	-31(7)
C(30A)	58(14)	31(11)	34(10)	-16(9)	4(9)	-19(10)
O(30A)	48(9)	49(9)	65(9)	-21(8)	16(7)	-4(7)
C(31A)	24(10)	47(12)	57(12)	-32(10)	0(9)	-2(8)
O(31A)	82(12)	71(10)	55(9)	-43(8)	-16(8)	1(8)
C(32A)	54(14)	46(14)	54(12)	-12(11)	3(11)	-8(11)
O(32A)	62(10)	30(8)	73(9)	3(7)	-9(8)	-8(7)
C(33A)	54(14)	43(13)	27(9)	15(9)	2(9)	4(11)
O(33A)	89(12)	48(9)	90(11)	-37(9)	-47(10)	0(8)
C(34A)	27(10)	13(9)	45(10)	2(8)	0(8)	-14(7)
O(34A)	60(10)	50(9)	60(9)	5(8)	17(8)	-25(8)

Table D5. Hydrogen coordinates (x 10^4) and isotropic displacement parameters ($Å^2$ x 10^3) for **65**.

	x	y	z	U(eq)
H(7A)	2935(17)	4752(13)	4155(10)	58
H(8A)	1279(17)	4022(16)	5005(10)	67
H(9A)	495(18)	2814(18)	4966(13)	79
H(10A)	1228(18)	2256(14)	4109(11)	74
H(11B)	2851(14)	3036(13)	3133(10)	52
H(11A)	3099(14)	2801(13)	3588(10)	52
H(13A)	3694(15)	3504(13)	1662(9)	50
H(14A)	2225(16)	3262(14)	1131(10)	58
H(15A)	761(15)	4200(13)	942(9)	48
H(16A)	922(16)	5491(14)	1164(10)	55
H(17A)	2339(15)	5744(13)	1735(11)	56
H(18A)	6222(15)	5846(11)	677(8)	45
H(18B)	5033(15)	5551(11)	592(8)	45
H(19A)	6384(16)	4684(13)	216(10)	78
H(19B)	5551(16)	4017(13)	976(10)	78
H(19C)	6734(16)	4310(13)	1060(10)	78
H(20A)	4791(15)	4233(11)	4325(9)	44
H(20B)	6051(15)	4556(11)	3940(9)	44
H(21A)	5884(18)	2949(11)	4748(10)	81
H(21B)	6308(18)	3139(11)	3858(10)	81
H(21C)	5052(18)	2817(11)	4241(10)	81
H(24A)	8597(19)	4208(18)	4700(11)	111
H(24B)	7409(19)	4131(18)	4500(11)	111
H(24C)	7880(19)	5067(18)	4445(11)	111
H(25A)	9557(18)	3529(16)	3410(13)	103
H(25B)	9335(18)	4078(16)	2535(13)	103
H(25C)	8354(18)	3490(16)	3220(13)	103

H(26A)	10520(18)	5300(14)	3400(13)	110
H(26B)	9824(18)	6171(14)	3149(13)	110
H(26C)	10345(18)	5831(14)	2512(13)	110
H(7AA)	11763(15)	744(11)	1664(8)	41
H(8AA)	13458(15)	467(13)	1166(9)	49
H(9AA)	13735(15)	-778(14)	912(10)	53
H(10B)	12183(16)	-1801(12)	1174(9)	51
H(11C)	10449(14)	-1434(13)	1562(10)	50
H(13B)	10768(13)	-1867(11)	3136(9)	41
H(14B)	11972(14)	-2476(13)	3998(10)	54
H(15B)	12047(18)	-1970(15)	5003(11)	69
H(16B)	10963(17)	-839(15)	5044(10)	63
H(17B)	9871(16)	-130(12)	4097(9)	49
H(18C)	6990(15)	-341(11)	3871(8)	45
H(18D)	8029(15)	-768(11)	4268(8)	45
H(19D)	6652(17)	-1973(11)	4565(10)	83
H(19E)	7728(17)	-2092(11)	4045(10)	83
H(19F)	6694(17)	-1668(11)	3650(10)	83
H(20C)	9584(15)	542(11)	511(9)	43
H(20D)	8351(15)	824(11)	619(9)	43
H(21D)	8407(16)	-350(11)	189(10)	62
H(21E)	7683(16)	-714(11)	1044(10)	62
H(21F)	8912(16)	-994(11)	937(10)	62
H(24D)	5009(18)	-1417(13)	3175(12)	91
H(24E)	4349(18)	-869(13)	2485(12)	91
H(24F)	3714(18)	-1370(13)	3368(12)	91
H(25D)	3625(17)	1279(14)	2985(12)	93
H(25E)	2811(17)	407(14)	3244(12)	93
H(25F)	3445(17)	910(14)	2361(12)	93
H(26D)	5267(19)	-656(20)	4413(12)	130
H(26E)	3974(19)	-578(20)	4569(12)	130
H(26F)	4796(19)	295(20)	4292(12)	130

Table E1. Crystal data and structure refinement for (trimethylsilylethynyl-pentachlorophenylketone)$Co_2(CO)_6$, **79**.

	79
empirical formula	$C_{18}H_9Cl_5Co_2O_7Si$
M_r	660.45
T [K]	213(2)
λ [Å]	0.71073
description	red plate
crystal size [mm]	0.05 x 0.10 x 0.15
crystal system	Monoclinic
space group	$P2_1/c$
a [Å]	7.8366(3)
b [Å]	31.568(2)
c [Å]	20.0254(11)
α [°]	90
β [°]	91.535(3)
γ [°]	90
V [Å^3]	4952.2(4)
Z	8
ρ_{calcd} [g cm^{-3}]	1.772
abs. Coeff. [mm^{-1}]	1.964
F(000)	2608
θ range for collection [°]	2.13 to 24.00
limiting indices	-4 < h < 10, -41 < k < 39, -25 < l < 23
reflections collected	27466
independent reflections	7751
R(int)	0.1263
refinement method	Full-matrix least-squares on F^2
weighting scheme	$w=1/[\sigma^2F_o^2 + (0.1432((F_o^2+ 2F_c^2)/3))^2 + 0.0000((F_o^2 +2F_c^2)/3))^2]$
data/restraints/parameters	7669 / 0 / 596
goodness-of-fit on F^2	0.933
final R indices [I>2σ(I)][a]	R1 = 0.0773, wR2 = 0.1855
R indices (all data)[a]	R1 = 0.1549, wR2 = 0.2370
rel. trans. (max., min.)	1.000, 0.7553
Largest diff. peak [eÅ^{-3}]	1.256
Largest diff hole [eÅ^{-3}]	-1.027

[a] $R1 = \Sigma (|| F_o | - | F_c ||)/ \Sigma | F_o |$; $wR2 =[\Sigma[w(F_o^2 - F_c^2)^2]/\Sigma[w(F_o^2)^2]]^{0.5}$

Table E2. Atomic coordinates [x 10^4] and equivalent isotropic displacement parameters [$Å^2$ x 10^3] for **79**. U(eq) is defined as one third of the trace of the orthogonalized U_{ij} tensor.

	x	y	z	U(eq)
Co(1)	2388(2)	3855(1)	4902(1)	28(1)
Co(2)	4523(2)	3413(1)	5514(1)	28(1)
Si(1)	4241(4)	4420(1)	6254(1)	28(1)
Cl(2)	-393(4)	4093(1)	6898(2)	49(1)
Cl(3)	-51(5)	4058(1)	8455(2)	64(1)
Cl(4)	1611(5)	3266(1)	9148(2)	64(1)
Cl(5)	2981(5)	2532(1)	8282(2)	63(1)
Cl(6)	2693(4)	2578(1)	6738(2)	47(1)
C(1)	1242(13)	3331(3)	6906(5)	29(3)
C(2)	593(12)	3669(3)	7281(5)	30(3)
C(3)	717(13)	3646(4)	7984(6)	37(3)
C(4)	1462(14)	3301(4)	8285(5)	35(3)
C(5)	2095(14)	2971(3)	7915(6)	38(3)
C(6)	1965(13)	2993(3)	7209(5)	32(3)
C(7)	995(13)	3373(3)	6139(5)	26(2)
O(7)	-189(10)	3197(3)	5864(4)	47(2)
C(8)	2281(12)	3616(3)	5800(5)	25(2)
C(9)	3398(12)	3936(3)	5818(5)	26(2)
C(10)	2666(13)	4851(4)	6170(6)	42(3)
C(11)	4651(15)	4294(4)	7154(5)	47(3)
C(12)	6237(14)	4579(4)	5839(6)	45(3)
C(13)	5703(14)	3272(3)	6282(6)	34(3)
O(13)	6453(11)	3203(3)	6758(4)	52(2)
C(14)	6324(14)	3568(4)	5036(6)	37(3)
O(14)	7428(10)	3676(3)	4700(4)	59(3)
C(15)	3941(14)	2879(4)	5188(5)	36(3)
O(15)	3516(12)	2561(3)	5001(4)	54(2)
C(16)	3768(14)	4126(4)	4321(5)	33(3)
O(16)	4643(11)	4288(3)	3971(4)	65(3)
C(17)	1338(13)	3453(4)	4388(6)	33(3)
O(17)	616(11)	3222(3)	4065(5)	57(2)
C(18)	737(16)	4238(4)	4928(5)	39(3)
O(18)	-291(11)	4495(3)	4939(4)	58(3)
Co(1A)	7602(2)	3928(1)	12488(1)	32(1)
Co(2A)	9627(2)	3478(1)	11887(1)	29(1)
Si(1A)	9228(4)	4485(1)	11131(2)	36(1)
Cl(2A)	7624(4)	2626(1)	10711(2)	48(1)
Cl(3A)	7838(4)	2555(1)	9171(2)	59(1)
Cl(4A)	6541(4)	3293(1)	8263(1)	56(1)
Cl(5A)	4960(4)	4098(1)	8902(2)	58(1)
Cl(6A)	4602(4)	4142(1)	10449(2)	48(1)
C(1A)	6194(12)	3396(3)	10504(5)	26(2)
C(2A)	6892(13)	3040(3)	10221(5)	30(3)
C(3A)	7043(13)	3006(3)	9523(6)	33(3)
C(4A)	6390(14)	3328(4)	9123(5)	38(3)
C(5A)	5669(13)	3690(3)	9399(5)	29(3)
C(6A)	5558(13)	3713(3)	10087(5)	31(3)

C(7A)	6002(13)	3430(4)	11258(5)	32(3)
O(7A)	4868(10)	3257(3)	11533(4)	55(2)
C(8A)	7343(12)	3683(3)	11599(5)	30(3)
C(9A)	8462(12)	3994(3)	11561(5)	30(3)
C(10A)	9517(16)	4345(4)	10225(6)	53(4)
C(11A)	7632(14)	4917(4)	11203(6)	50(3)
C(12A)	11277(14)	4652(4)	11514(6)	50(3)
C(13A)	9115(15)	4199(5)	13027(6)	46(3)
O(13A)	10110(12)	4380(3)	13343(5)	63(3)
C(14A)	6606(16)	3520(4)	13004(6)	47(3)
O(14A)	5957(11)	3278(3)	13331(4)	61(3)
C(15A)	5894(15)	4313(4)	12465(5)	37(3)
O(15A)	4850(11)	4556(3)	12437(4)	52(2)
C(16A)	11501(16)	3632(4)	12377(6)	41(3)
O(16A)	12648(11)	3714(3)	12709(5)	64(3)
C(17A)	9075(14)	2959(4)	12223(5)	35(3)
O(17A)	8695(12)	2636(3)	12441(5)	62(3)
C(18A)	10713(14)	3333(3)	11138(6)	35(3)
O(18A)	11340(11)	3254(3)	10641(4)	57(2)

Table E3. Bond lengths [Å] and angles [deg] for **79**.

Co(1)-C(18)	1.774(14)	C(13)-O(13)	1.128(13)
Co(1)-C(17)	1.817(13)	C(14)-O(14)	1.160(12)
Co(1)-C(16)	1.824(11)	C(15)-O(15)	1.119(13)
Co(1)-C(8)	1.953(10)	C(16)-O(16)	1.118(12)
Co(1)-C(9)	1.995(10)	C(17)-O(17)	1.117(13)
Co(1)-Co(2)	2.475(2)	C(18)-O(18)	1.143(13)
Co(2)-C(14)	1.795(11)	Co(1A)-C(13A)	1.80(2)
Co(2)-C(13)	1.827(14)	Co(1A)-C(15A)	1.809(13)
Co(2)-C(15)	1.861(14)	Co(1A)-C(14A)	1.836(14)
Co(2)-C(8)	1.968(9)	Co(1A)-C(8A)	1.947(10)
Co(2)-C(9)	1.974(10)	Co(1A)-C(9A)	2.003(10)
Si(1)-C(10)	1.844(11)	Co(1A)-Co(2A)	2.467(2)
Si(1)-C(12)	1.859(10)	Co(2A)-C(18A)	1.803(12)
Si(1)-C(11)	1.866(11)	Co(2A)-C(16A)	1.810(14)
Si(1)-C(9)	1.870(11)	Co(2A)-C(17A)	1.826(12)
Cl(2)-C(2)	1.717(11)	Co(2A)-C(9A)	1.971(11)
Cl(3)-C(3)	1.724(10)	Co(2A)-C(8A)	1.975(10)
Cl(4)-C(4)	1.732(10)	Si(1A)-C(12A)	1.837(12)
Cl(5)-C(5)	1.706(11)	Si(1A)-C(11A)	1.858(11)
Cl(6)-C(6)	1.723(11)	Si(1A)-C(9A)	1.880(11)
C(1)-C(6)	1.344(14)	Si(1A)-C(10A)	1.887(12)
C(1)-C(2)	1.408(14)	Cl(2A)-C(2A)	1.725(11)
C(1)-C(7)	1.549(14)	Cl(3A)-C(3A)	1.713(11)
C(2)-C(3)	1.41(2)	Cl(4A)-C(4A)	1.733(11)
C(3)-C(4)	1.37(2)	Cl(5A)-C(5A)	1.712(10)
C(4)-C(5)	1.38(2)	Cl(6A)-C(6A)	1.718(10)
C(5)-C(6)	1.42(2)	C(1A)-C(2A)	1.376(14)
C(7)-O(7)	1.203(12)	C(1A)-C(6A)	1.388(14)
C(7)-C(8)	1.449(13)	C(1A)-C(7A)	1.526(14)
C(8)-C(9)	1.337(13)	C(2A)-C(3A)	1.409(14)

C(3A)-C(4A)	1.39(2)
C(4A)-C(5A)	1.39(2)
C(5A)-C(6A)	1.383(14)
C(7A)-O(7A)	1.191(12)
C(7A)-C(8A)	1.47(2)
C(8A)-C(9A)	1.320(14)
C(13A)-O(13A)	1.145(14)
C(14A)-O(14A)	1.137(14)
C(15A)-O(15A)	1.122(12)
C(16A)-O(16A)	1.134(14)
C(17A)-O(17A)	1.151(12)
C(18A)-O(18A)	1.149(12)

C(18)-Co(1)-C(17)	100.0(5)
C(18)-Co(1)-C(16)	98.2(5)
C(17)-Co(1)-C(16)	103.5(5)
C(18)-Co(1)-C(8)	100.8(4)
C(17)-Co(1)-C(8)	102.8(5)
C(16)-Co(1)-C(8)	144.0(5)
C(18)-Co(1)-C(9)	99.1(4)
C(17)-Co(1)-C(9)	140.7(5)
C(16)-Co(1)-C(9)	107.4(4)
C(8)-Co(1)-C(9)	39.6(4)
C(18)-Co(1)-Co(2)	148.6(3)
C(17)-Co(1)-Co(2)	100.2(4)
C(16)-Co(1)-Co(2)	100.1(3)
C(8)-Co(1)-Co(2)	51.1(3)
C(9)-Co(1)-Co(2)	51.0(3)
C(14)-Co(2)-C(13)	97.3(5)
C(14)-Co(2)-C(15)	104.4(5)
C(13)-Co(2)-C(15)	100.8(5)
C(14)-Co(2)-C(8)	141.9(5)
C(13)-Co(2)-C(8)	105.7(4)
C(15)-Co(2)-C(8)	100.6(5)
C(14)-Co(2)-C(9)	107.5(4)
C(13)-Co(2)-C(9)	99.5(4)
C(15)-Co(2)-C(9)	139.3(4)
C(8)-Co(2)-C(9)	39.7(4)
C(14)-Co(2)-Co(1)	96.5(4)
C(13)-Co(2)-Co(1)	150.9(3)
C(15)-Co(2)-Co(1)	100.4(3)
C(8)-Co(2)-Co(1)	50.6(3)
C(9)-Co(2)-Co(1)	51.8(3)
C(10)-Si(1)-C(12)	109.2(5)
C(10)-Si(1)-C(11)	110.0(5)
C(12)-Si(1)-C(11)	111.3(6)
C(10)-Si(1)-C(9)	109.5(5)
C(12)-Si(1)-C(9)	107.6(5)
C(11)-Si(1)-C(9)	109.1(5)
C(6)-C(1)-C(2)	120.9(10)
C(6)-C(1)-C(7)	123.8(9)
C(2)-C(1)-C(7)	115.2(9)
C(1)-C(2)-C(3)	118.6(10)
C(1)-C(2)-Cl(2)	121.2(8)
C(3)-C(2)-Cl(2)	120.2(8)
C(4)-C(3)-C(2)	119.8(10)
C(4)-C(3)-Cl(3)	120.7(9)
C(2)-C(3)-Cl(3)	119.5(9)
C(3)-C(4)-C(5)	121.4(10)
C(3)-C(4)-Cl(4)	120.5(9)
C(5)-C(4)-Cl(4)	118.1(9)
C(4)-C(5)-C(6)	118.7(10)
C(4)-C(5)-Cl(5)	122.1(9)
C(6)-C(5)-Cl(5)	119.2(9)
C(1)-C(6)-C(5)	120.6(10)
C(1)-C(6)-Cl(6)	119.9(8)
C(5)-C(6)-Cl(6)	119.5(8)
O(7)-C(7)-C(8)	124.7(10)
O(7)-C(7)-C(1)	119.2(9)
C(8)-C(7)-C(1)	116.1(9)
C(9)-C(8)-C(7)	148.2(9)
C(9)-C(8)-Co(1)	71.9(6)
C(7)-C(8)-Co(1)	133.0(8)
C(9)-C(8)-Co(2)	70.4(6)
C(7)-C(8)-Co(2)	127.0(7)
Co(1)-C(8)-Co(2)	78.3(3)
C(8)-C(9)-Si(1)	148.5(7)
C(8)-C(9)-Co(2)	69.9(6)
Si(1)-C(9)-Co(2)	132.1(5)
C(8)-C(9)-Co(1)	68.5(6)
Si(1)-C(9)-Co(1)	131.3(6)
Co(2)-C(9)-Co(1)	77.2(4)
O(13)-C(13)-Co(2)	177.0(10)
O(14)-C(14)-Co(2)	176.4(10)
O(15)-C(15)-Co(2)	176.8(10)
O(16)-C(16)-Co(1)	178.6(10)
O(17)-C(17)-Co(1)	175.9(11)
O(18)-C(18)-Co(1)	177.9(10)
C(13A)-Co(1A)-C(15A)	99.8(5)
C(13A)-Co(1A)-C(14A)	106.2(5)
C(15A)-Co(1A)-C(14A)	99.2(5)
C(13A)-Co(1A)-C(8A)	142.0(5)
C(15A)-Co(1A)-C(8A)	100.7(5)
C(14A)-Co(1A)-C(8A)	101.6(5)
C(13A)-Co(1A)-C(9A)	105.9(5)
C(15A)-Co(1A)-C(9A)	100.0(4)
C(14A)-Co(1A)-C(9A)	138.8(5)
C(8A)-Co(1A)-C(9A)	39.0(4)
C(13A)-Co(1A)-Co(2A)	98.3(3)
C(15A)-Co(1A)-Co(2A)	149.4(3)
C(14A)-Co(1A)-Co(2A)	99.2(4)
C(8A)-Co(1A)-Co(2A)	51.5(3)
C(9A)-Co(1A)-Co(2A)	51.0(3)
C(18A)-Co(2A)-C(16A)	97.2(5)
C(18A)-Co(2A)-C(17A)	101.6(5)
C(16A)-Co(2A)-C(17A)	103.8(5)
C(18A)-Co(2A)-C(9A)	99.1(4)
C(16A)-Co(2A)-C(9A)	108.6(5)
C(17A)-Co(2A)-C(9A)	138.7(5)
C(18A)-Co(2A)-C(8A)	106.5(5)
C(16A)-Co(2A)-C(8A)	141.8(5)
C(17A)-Co(2A)-C(8A)	100.4(5)
C(9A)-Co(2A)-C(8A)	39.1(4)

C(18A)-Co(2A)-Co(1A)	151.1(3)	C(5A)-C(6A)-C(1A)	122.0(9)
C(16A)-Co(2A)-Co(1A)	96.0(3)	C(5A)-C(6A)-Cl(6A)	120.1(8)
C(17A)-Co(2A)-Co(1A)	100.1(3)	C(1A)-C(6A)-Cl(6A)	117.9(8)
C(9A)-Co(2A)-Co(1A)	52.2(3)	O(7A)-C(7A)-C(8A)	124.5(10)
C(8A)-Co(2A)-Co(1A)	50.5(3)	O(7A)-C(7A)-C(1A)	121.3(10)
C(12A)-Si(1A)-C(11A)	109.9(6)	C(8A)-C(7A)-C(1A)	114.2(9)
C(12A)-Si(1A)-C(9A)	109.3(5)	C(9A)-C(8A)-C(7A)	147.5(10)
C(11A)-Si(1A)-C(9A)	110.2(5)	C(9A)-C(8A)-Co(1A)	72.8(6)
C(12A)-Si(1A)-C(10A)	110.0(6)	C(7A)-C(8A)-Co(1A)	134.0(7)
C(11A)-Si(1A)-C(10A)	110.2(6)	C(9A)-C(8A)-Co(2A)	70.3(6)
C(9A)-Si(1A)-C(10A)	107.2(5)	C(7A)-C(8A)-Co(2A)	126.0(8)
C(2A)-C(1A)-C(6A)	118.7(9)	Co(1A)-C(8A)-Co(2A)	78.0(4)
C(2A)-C(1A)-C(7A)	121.1(9)	C(8A)-C(9A)-Si(1A)	149.4(9)
C(6A)-C(1A)-C(7A)	120.1(9)	C(8A)-C(9A)-Co(2A)	70.6(7)
C(1A)-C(2A)-C(3A)	121.1(10)	Si(1A)-C(9A)-Co(2A)	133.1(5)
C(1A)-C(2A)-Cl(2A)	120.9(8)	C(8A)-C(9A)-Co(1A)	68.2(6)
C(3A)-C(2A)-Cl(2A)	118.0(8)	Si(1A)-C(9A)-Co(1A)	129.1(6)
C(4A)-C(3A)-C(2A)	118.4(10)	Co(2A)-C(9A)-Co(1A)	76.8(4)
C(4A)-C(3A)-Cl(3A)	120.4(9)	O(13A)-C(13A)-Co(1A)	176.7(11)
C(2A)-C(3A)-Cl(3A)	120.9(9)	O(14A)-C(14A)-Co(1A)	177.8(11)
C(3A)-C(4A)-C(5A)	121.3(10)	O(15A)-C(15A)-Co(1A)	178.3(10)
C(3A)-C(4A)-Cl(4A)	119.6(9)	O(16A)-C(16A)-Co(2A)	176.4(11)
C(5A)-C(4A)-Cl(4A)	119.1(9)	O(17A)-C(17A)-Co(2A)	178.4(9)
C(6A)-C(5A)-C(4A)	118.3(9)	O(18A)-C(18A)-Co(2A)	176.3(10)
C(6A)-C(5A)-Cl(5A)	120.8(8)		
C(4A)-C(5A)-Cl(5A)	120.9(8)		

Table E4. Anisotropic displacement parameters [$Å^2$ x 10^3] for **79**. The anisotropic displacement factor exponent takes the form: $-2p^2$ [$(ha^*)^2 U_{11}$ + ... + 2hka*b* U_{12}]

	U11	U22	U33	U23	U13	U12
Co(1)	33(1)	39(1)	14(1)	2(1)	10(1)	1(1)
Co(2)	32(1)	37(1)	17(1)	-2(1)	10(1)	3(1)
Si(1)	37(2)	31(2)	17(2)	1(1)	8(1)	0(1)
Cl(2)	53(2)	47(2)	47(2)	6(2)	18(2)	13(2)
Cl(3)	78(2)	68(2)	47(2)	-25(2)	37(2)	-15(2)
Cl(4)	79(2)	97(3)	15(2)	6(2)	7(2)	-27(2)
Cl(5)	76(2)	62(2)	51(2)	29(2)	1(2)	-3(2)
Cl(6)	64(2)	32(2)	48(2)	0(1)	27(2)	2(1)
C(1)	34(6)	39(7)	15(6)	-1(5)	9(5)	-2(5)
C(2)	22(5)	46(7)	24(6)	-9(5)	15(5)	-7(5)
C(3)	36(6)	38(7)	39(8)	-16(6)	24(6)	-10(6)
C(4)	38(6)	64(9)	5(5)	-1(5)	11(5)	-8(6)
C(5)	41(7)	33(7)	39(8)	7(6)	1(6)	-7(5)
C(6)	40(6)	35(7)	23(7)	3(5)	17(5)	3(5)
C(7)	31(6)	23(6)	25(6)	3(5)	11(5)	1(5)
O(7)	47(5)	75(6)	20(4)	-7(4)	3(4)	-31(5)
C(8)	26(6)	41(7)	8(5)	-5(4)	6(4)	9(5)
C(9)	23(5)	38(7)	17(6)	0(5)	10(5)	1(5)
C(10)	44(7)	39(7)	45(8)	-2(6)	14(6)	4(6)
C(11)	59(8)	49(8)	33(8)	1(6)	9(6)	-6(6)

C(12)	44(7)	46(8)	47(8)	-5(6)	17(6)	-16(6)
C(13)	35(7)	30(7)	38(8)	-6(5)	22(6)	12(5)
O(13)	60(6)	69(6)	28(5)	5(4)	-7(5)	12(5)
C(14)	37(7)	52(8)	23(7)	-7(5)	6(6)	5(6)
O(14)	36(5)	88(7)	53(6)	-4(5)	15(5)	-8(5)
C(15)	39(7)	59(9)	9(6)	3(6)	6(5)	7(6)
O(15)	79(7)	42(6)	42(6)	-18(4)	0(5)	-9(5)
C(16)	44(7)	41(7)	15(6)	3(5)	3(5)	5(6)
O(16)	65(6)	77(7)	54(6)	20(5)	41(5)	-11(5)
C(17)	20(6)	50(8)	31(7)	9(6)	5(5)	-1(6)
O(17)	58(6)	65(7)	48(6)	-10(5)	7(5)	-10(5)
C(18)	54(8)	50(8)	13(6)	9(5)	11(6)	-9(7)
O(18)	56(6)	63(6)	56(6)	7(5)	12(5)	17(5)
Co(1A)	38(1)	43(1)	15(1)	-1(1)	10(1)	5(1)
Co(2A)	34(1)	38(1)	17(1)	2(1)	9(1)	4(1)
Si(1A)	41(2)	38(2)	30(2)	4(2)	9(2)	-8(2)
Cl(2A)	66(2)	31(2)	47(2)	5(1)	-11(2)	0(2)
Cl(3A)	72(2)	53(2)	53(2)	-25(2)	18(2)	5(2)
Cl(4A)	72(2)	80(2)	16(2)	-8(2)	16(2)	-18(2)
Cl(5A)	75(2)	64(2)	35(2)	22(2)	-4(2)	6(2)
Cl(6A)	50(2)	50(2)	44(2)	-6(2)	3(2)	17(2)
C(1A)	22(5)	41(7)	14(6)	1(5)	6(4)	-10(5)
C(2A)	32(6)	28(6)	29(7)	-2(5)	-3(5)	6(5)
C(3A)	30(6)	38(7)	32(7)	-14(5)	-1(5)	0(5)
C(4A)	42(7)	55(8)	17(6)	-2(6)	6(5)	-10(6)
C(5A)	32(6)	39(7)	17(6)	8(5)	-2(5)	4(5)
C(6A)	34(6)	33(6)	26(7)	1(5)	12(5)	5(5)
C(7A)	29(6)	47(7)	19(6)	3(5)	9(5)	15(6)
O(7A)	51(5)	76(6)	39(5)	0(4)	23(4)	-24(5)
C(8A)	29(6)	50(7)	10(6)	-1(5)	11(5)	0(5)
C(9A)	26(6)	39(7)	25(6)	-4(5)	11(5)	-2(5)
C(10A)	63(8)	62(9)	35(8)	11(6)	24(7)	5(7)
C(11A)	57(8)	37(8)	58(9)	5(6)	25(7)	-4(6)
C(12A)	50(7)	44(8)	56(9)	-10(6)	12(7)	-8(6)
C(13A)	37(7)	81(10)	20(7)	-5(7)	8(6)	27(7)
O(13A)	65(6)	76(7)	46(6)	-29(5)	-11(5)	21(5)
C(14A)	49(8)	72(10)	20(7)	-1(6)	3(6)	13(7)
O(14A)	73(6)	69(7)	42(6)	20(5)	22(5)	-3(5)
C(15A)	50(7)	46(8)	15(6)	-3(5)	10(5)	-4(6)
O(15A)	51(5)	50(6)	57(6)	-6(4)	4(5)	21(5)
C(16A)	47(8)	44(8)	32(8)	0(6)	17(6)	1(6)
O(16A)	35(5)	105(8)	54(6)	-26(6)	-4(5)	3(5)
C(17A)	56(8)	31(7)	18(6)	-7(5)	8(6)	11(6)
O(17A)	85(7)	39(6)	63(7)	15(5)	25(5)	5(5)
C(18A)	49(7)	25(6)	30(7)	5(5)	3(6)	2(5)
O(18A)	66(6)	79(7)	26(5)	-3(4)	26(5)	1(5)

Table E5. Hydrogen coordinates (x 10^4) and isotropic displacement parameters ($Å^2$ x 10^3) for **79**.

	x	y	z	U(eq)
H(10A)	1624(13)	4770(4)	6387(6)	64
H(10B)	2421(13)	4906(4)	5701(6)	64
H(10C)	3125(13)	5106(4)	6379(6)	64
H(11A)	5478(15)	4067(4)	7194(5)	71
H(11B)	3594(15)	4208(4)	7355(5)	71
H(11C)	5095(15)	4544(4)	7382(5)	71
H(12A)	7068(14)	4352(4)	5880(6)	68
H(12B)	6694(14)	4832(4)	6050(6)	68
H(12C)	5990(14)	4634(4)	5370(6)	68
H(10D)	8430(16)	4257(4)	10027(6)	79
H(10E)	10333(16)	4115(4)	10194(6)	79
H(10F)	9935(16)	4590(4)	9988(6)	79
H(11D)	6553(14)	4826(4)	11001(6)	76
H(11E)	8034(14)	5167(4)	10975(6)	76
H(11F)	7475(14)	4982(4)	11671(6)	76
H(12D)	12104(14)	4425(4)	11475(6)	75
H(12E)	11122(14)	4716(4)	11982(6)	75
H(12F)	11685(14)	4902(4)	11287(6)	75

Table F1. Crystal data and structure refinement for octachlorocycloheptatriene, **82**

	82
empirical formula	C_7Cl_8
formula wt.	367.67
dimensions, mm	0.36 x 0.31 x 0.20
Cryst. syst.	orthorhombic
Space group.	*Pnma*
a, [Å]	7.140(1)
b, [Å]	13.329(3)
c, [Å]	12.595(3)
V, [Å^3]	1198.7(4)
F(000)	712
Z	4
D_{calc}, g.cm^{-3}	2.037
radiation	Ag Kα (0.56086)
monochromator	graphite
temp, K	293
(Ag Kα), mm^{-1}	0.928
Absorption correction	psi scan
Transmission max	0.794
Transmission min	0.600
scan method	θ-2θ
2θ range, deg	3.52-40.1
index ranges	$-1 < h < 8$, $-16 < k < 1$, $-1 < l < 15$
no of measd rflcns	1928
no of unique rflcns	1202
no of obsd rflcns	1202 ($I \geq -3\sigma(I)$)
no of variables	73
R1 [$I>2\sigma(I)$]	0.0335
R_w	0.0767
GOF	0.848
weighting scheme	*a*
largest diff peak eÅ^{-3}	0.279
largest diff hole eÅ^{-3}	-0.302

a. $w = [F^2F_o^2 + (0.0410p)^2 + (0.00p)]^{-1}$, where $p = [\max(F_o^2,0) + 2F_c^2]/3$

Table F2. Atomic coordinates [x 10^4] and equivalent isotropic displacement parameters [$Å^2$ x 10^3] for **82**. U(eq) is defined as one third of the trace of the orthogonalized U_{ij} tensor.

	x	y	z	U(eq)
Cl(7A)	1709(2)	2500	4120(1)	61(1)
Cl(7B)	3322(2)	2500	6166(1)	86(1)
Cl(1)	652(1)	4115(1)	6850(1)	72(1)
Cl(2)	-2870(2)	4683(1)	5600(1)	65(1)
Cl(3)	-3427(1)	3642(1)	3406(1)	65(1)
C(7)	-1140(6)	2500	5516(3)	51(1)
C(1)	-33(4)	3406(2)	5792(2)	45(1)
C(2)	-1627(4)	3618(2)	5287(2)	43(1)
C(3)	-2424(4)	3003(2)	4452(2)	42(1)

Table F3. Bond lengths [Å] and angles [deg] for **82**.

Cl(7A)-C(7)	1.804(4)	C(2)-C(7)-Cl(7A)	110.4(2)
Cl(7B)-C(7)	1.760(5)	Cl(7A)-C(7)-C(7B)	104.7(2)
Cl(1)-C(1)	1.705(3)	C(2)-C(1)-C(7)	122.2(3)
Cl(2)-C(2)	1.720(3)	C(2)-C(1)-Cl(1)	120.0(2)
Cl(3)-C(3)	1.725(3)	C(7)-C(1)-Cl(1)	117.6(3)
C(7)-C(1)	1.511(4)	C(1)-C(2)-C(3)	124.1(3)
C(1)-C(2)	1.334(4)	C(1)-C(2)-Cl(2)	120.4(2)
C(2)-C(3)	1.450(4)	C(3)-C(2)-Cl(2)	115.5(2)
C(3)-C(4)	1.340(5)	C(4)-C(3)-C(2)	124.4(2)
		C(4)-C(3)-Cl(3)	119.6(1)
C(2)-C(7)-C(6)	106.2(3)	C(2)-C(3)-Cl(3)	116.0(2)
C(2)-C(7)-Cl(7B)	112.6(2)		

Table F4. Anisotropic displacement parameters [$Å^2$ x 10^3] for **82**. The anisotropic displacement factor exponent takes the form: $-2p^2$ [$(ha^*)^2 U_{11}$ + ... + 2hka*b* U_{12}]

	U11	U22	U33	U23	U13	U12
Cl(7A)	59(1)	78(1)	45(1)	0	18(1)	0
Cl(7B)	50(1)	133(1)	76(1)	0	15(1)	0
Cl(1)	82(1)	85(1)	50(1)	22(1)	-4(1)	-23(1)
Cl(2)	94(1)	46(1)	56(1)	-3(1)	9(1)	14(1)
Cl(3)	86(1)	60(1)	48(1)	9(1)	16(1)	10(1)
C(7)	48(3)	70(3)	34(2)	0	1(2)	0
C(1)	55(2)	49(2)	32(1)	-6(1)	4(2)	-12(2)
C(2)	55(2)	37(1)	37(2)	0(1)	7(2)	-1(2)
C(3)	45(2)	45(1)	35(1)	1(1)	-1(1)	3(1)

Table G1. Crystal data and structure refinement for 7-Carbomethoxy-1,2,3,4,5,6-hexachlorocycloheptatriene, **112**.

	112
empirical formula	$C_9H_4Cl_6O_2$
M_r	356.82
T [K]	300(2)
λ [Å]	0.71073
description	colorless plate
crystal size [mm]	0.06 x 0.18 x 0.37
crystal system	Orthorhombic
space group	$P2_12_12_1$
a [Å]	7.7583(1)
b [Å]	9.2561(1)
c [Å]	18.3732(2)
α [°]	90.0
β [°]	90.0
γ [°]	90.0
V [Å^3]	1319.41(3)
Z	4
ρ_{calcd} [g cm^{-3}]	1.796
abs. Coeff. [mm^{-1}]	1.285
F(000)	704
θ range for collection [°]	2.22 to 27.66
limiting indices	$-10 < h < 10$ $-12 < k < 10$ $-23 < l < 24$
reflections collected	11778
independent reflections	3059
R(int)	0.0310
refinement method	Full-matrix least-squares on F^2
weighting scheme	$w=1/[\sigma^2F_o^2 + (0.0316((F_o^2+ 2F_c^2)/3))^2 + 0.3915((F_o^2 +2F_c^2)/3))^2]$
data/restraints/parameters	3059 / 0 / 171
goodness-of-fit on F^2	1.065
final R indices [I>2σ(I)][a]	$R1 = 0.0340$, $wR2 = 0.0714$
R indices (all data)[a]	$R1 = 0.0452$, $wR2 = 0.0770$
rel. trans. (max., min.)	0.8372, 0.6210
Extinction coeff.	0.0045(10)
Largest diff. peak [eÅ^{-3}]	0.241
Largest diff hole [eÅ^{-3}]	-0.257

[a] $R1 = \Sigma (|| F_o | - | F_c ||)/ \Sigma | F_o |$; $wR2 =[\Sigma[w(F_o^2 - F_c^2)^2]/\Sigma[w(F_o^2)^2]]^{0.5}$

Table G2. Atomic coordinates [x 10^4] and equivalent isotropic displacement parameters [Å x 10^3] for **112**. U(eq) is defined as one third of the trace of the orthogonalized U_{ij} tensor.

	x	y	z	U(eq)
O(1)	6595(3)	11027(3)	1981(1)	70(1)
O(2)	6926(3)	9103(2)	1276(1)	59(1)
C(1)	3060(3)	10547(3)	2105(1)	41(1)
C(2)	2730(3)	11693(3)	1694(1)	42(1)
C(3)	3529(4)	11878(3)	985(1)	43(1)
C(4)	3678(4)	10848(3)	483(1)	41(1)
C(5)	3126(3)	9367(3)	586(1)	39(1)
C(6)	3396(3)	8663(3)	1201(1)	41(1)
C(7)	4228(4)	9365(3)	1850(1)	41(1)
C(8)	6062(3)	9963(3)	1709(2)	48(1)
C(9)	8713(5)	9547(7)	1135(3)	85(1)
Cl(1)	2132(1)	10323(1)	2941(1)	68(1)
Cl(2)	1401(1)	13050(1)	1985(1)	73(1)
Cl(3)	4342(1)	13570(1)	821(1)	74(1)
Cl(4)	4633(1)	11206(1)	-338(1)	73(1)
Cl(5)	2162(1)	8537(1)	-147(1)	60(1)
Cl(6)	2716(1)	6928(1)	1318(1)	76(1)

Table G3. Bond lengths [Å] and angles [deg] for **112**.

O(1)-C(8)	1.179(4)	C(6)-C(5)-C(4)	122.1(2)
O(2)-C(8)	1.310(3)	C(6)-C(5)-Cl(5)	121.1(2)
O(2)-C(9)	1.469(4)	C(4)-C(5)-Cl(5)	116.7(2)
C(1)-Cl(1)	1.708(2)	C(3)-C(4)-C(5)	124.2(2)
C(1)-C(2)	1.327(4)	C(3)-C(4)-Cl(4)	120.6(2)
C(1)-C(7)	1.496(4)	C(5)-C(4)-Cl(4)	115.2(2)
C(2)-Cl(2)	1.711(3)	C(4)-C(3)-C(2)	125.0(2)
C(2)-C(3)	1.452(4)	C(4)-C(3)-Cl(3)	120.0(2)
C(3)-Cl(3)	1.715(3)	C(2)-C(3)-Cl(3)	115.0(2)
C(3)-C(4)	1.332(4)	C(1)-C(2)-C(3)	121.5(2)
C(4)-Cl(4)	1.713(3)	C(1)-C(2)-Cl(2)	121.7(2)
C(4)-C(5)	1.448(4)	C(3)-C(2)-Cl(2)	116.8(2)
C(5)-Cl(5)	1.720(2)	C(2)-C(1)-C(7)	121.5(2)
C(5)-C(6)	1.322(4)	C(2)-C(1)-Cl(1)	121.9(2)
C(6)-Cl(6)	1.704(3)	C(7)-C(1)-Cl(1)	116.6(2)
C(6)-C(7)	1.504(4)	C(1)-C(7)-C(6)	107.8(2)
C(7)-C(8)	1.548(4)	C(1)-C(7)-C(8)	110.3(2)
		C(6)-C(7)-C(8)	114.6(2)
C(8)-O(2)-C(9)	114.8(3)	O(1)-C(8)-O(2)	125.8(3)
C(5)-C(6)-C(7)	122.2(2)	O(1)-C(8)-C(7)	123.4(3)
C(5)-C(6)-Cl(6)	121.6(2)	O(2)-C(8)-C(7)	110.8(2)
C(7)-C(6)-Cl(6)	116.1(2)		

Table G4. Anisotropic displacement parameters [Å x 10^3] for **112**. The anisotropic displacement factor exponent takes the form: $-2p^2[(ha^*)^2 U_{11} + ... + 2hka^*b^* U_{12}]$

	U11	U22	U33	U23	U13	U12
O(1)	52(1)	82(2)	76(2)	-27(1)	-8(1)	-8(1)
O(2)	43(1)	72(1)	63(1)	-16(1)	6(1)	7(1)
C(1)	39(1)	55(2)	30(1)	-7(1)	-1(1)	1(1)
C(2)	44(1)	45(1)	38(1)	-12(1)	-5(1)	6(1)
C(3)	49(1)	36(1)	44(1)	2(1)	-5(1)	-1(1)
C(4)	44(1)	49(2)	31(1)	3(1)	2(1)	-1(1)
C(5)	40(1)	40(1)	36(1)	-9(1)	0(1)	2(1)
C(6)	45(1)	36(1)	43(1)	-3(1)	1(1)	2(1)
C(7)	46(1)	44(1)	34(1)	6(1)	-1(1)	4(1)
C(8)	42(1)	62(2)	38(1)	4(1)	-6(1)	8(1)
C(9)	44(2)	107(4)	103(4)	-11(3)	19(2)	-5(2)
Cl(1)	72(1)	94(1)	37(1)	-1(1)	15(1)	1(1)
Cl(2)	90(1)	73(1)	56(1)	-21(1)	-6(1)	39(1)
Cl(3)	97(1)	44(1)	83(1)	6(1)	-5(1)	-17(1)
Cl(4)	93(1)	84(1)	43(1)	6(1)	21(1)	-15(1)
Cl(5)	72(1)	63(1)	46(1)	-19(1)	-11(1)	-2(1)
Cl(6)	107(1)	40(1)	81(1)	7(1)	-10(1)	-13(1)

Table G5. Hydrogen coordinates (x 10^4) and isotropic displacement parameters (A^2 x 10^3) for **112**.

	x	y	z	U(eq)
H(7)	4363(36)	8660(31)	2215(15)	48(8)
H(9A)	8752(90)	10181(65)	736(33)	156(27)
H(9B)	9188(73)	8792(57)	1005(30)	122(21)
H(9C)	9128(98)	10274(73)	1685(39)	205(29)

Table H1. Crystal data and structure refinement for (*Z*)-2-(2-Benzoylphenyl)-1-chloro-1-pentachlorophenyl-2-phenylethene, **121**.

	121
empirical formula	$C_{27}H_{14}Cl_6O$
M_r	567.08
T [K]	300(2)
λ [Å]	0.71073
description	light yellow plate
crystal size [mm]	0.02 x 0.12 x 0.22
crystal system	Monoclinic
space group	$P2_1/c$
a [Å]	17.7762(1)
b [Å]	11.2519(3)
c [Å]	12.7982(3)
α [°]	90.0
β [°]	102.965(1)
γ [°]	90.0
V [Å^3]	2494.59(9)
Z	4
ρ_{calcd} [g cm^{-3}]	1.510
abs. Coeff. [mm^{-1}]	0.709
F(000)	1144
θ range for collection [°]	1.18 to 22.50
limiting indices	$-19 < h < 19$ $-12 < k < 12$ $-14 < l < 13$
reflections collected	13848
independent reflections	3241
R(int)	0.0986
refinement method	Full-matrix least-squares on F^2
weighting scheme	$w=1/[\sigma^2F_o^2 + (0.0336((F_o^2+ 2F_c^2)/3))^2 + 1.6288((F_o^2 +2F_c^2)/3))^2]$
data/restraints/parameters	3220 / 0 / 308
goodness-of-fit on F^2	1.033
final R indices [I>2σ(I)][a]	$R1 = 0.0547$, $wR2 = 0.0922$
R indices (all data)[a]	$R1 = 0.1068$, $wR2 = 0.1116$
rel. trans. (max., min.)	0.9423, 0.6368
Extinction coeff.	0.0044(5)
Largest diff. peak [eÅ^{-3}]	0.227
Largest diff hole [eÅ^{-3}]	-0.268

[a] $R1 = \Sigma (|| F_o | - | F_c ||)/ \Sigma | F_o |$; $wR2 = [\Sigma[w(F_o^2 - F_c^2)^2]/\Sigma[w(F_o^2)^2]]^{0.5}$

Table H2. Atomic coordinates [x 10^4] and equivalent isotropic displacement parameters [$Å^2$ x 10^3] for **121**. U(eq) is defined as one third of the trace of the orthogonalized U_{ij} tensor.

	x	y	z	U(eq)
Cl(1)	3295(1)	2251(1)	6611(1)	54(1)
Cl(4)	4138(1)	-390(1)	7645(1)	62(1)
Cl(5)	5192(1)	-1870(1)	6503(1)	65(1)
Cl(6)	4853(1)	-1940(1)	4017(1)	69(1)
Cl(7)	3406(1)	-682(2)	2679(1)	76(1)
Cl(8)	2337(1)	743(1)	3823(1)	65(1)
O(1)	876(3)	44(4)	8571(4)	94(2)
C(1)	2823(3)	908(4)	6226(4)	39(1)
C(2)	2120(3)	718(4)	6373(4)	38(1)
C(3)	3293(3)	110(4)	5697(4)	38(1)
C(4)	3932(3)	-482(4)	6266(4)	39(1)
C(5)	4410(3)	-1132(4)	5759(4)	41(1)
C(6)	4250(3)	-1187(4)	4647(4)	42(1)
C(7)	3608(3)	-607(5)	4061(4)	45(1)
C(8)	3128(3)	20(4)	4577(4)	39(1)
C(9)	1727(3)	-442(5)	6087(4)	43(1)
C(10)	1040(3)	-501(6)	5337(5)	66(2)
C(11)	648(4)	-1555(7)	5071(6)	84(2)
C(12)	941(4)	-2564(6)	5608(6)	81(2)
C(13)	1618(4)	-2539(5)	6371(5)	71(2)
C(14)	2013(3)	-1486(5)	6599(4)	51(2)
C(15)	1643(3)	1669(5)	6715(4)	44(1)
C(16)	1301(3)	1556(5)	7602(4)	49(2)
C(17)	799(3)	2439(6)	7787(5)	70(2)
C(18)	647(4)	3411(7)	7146(6)	79(2)
C(19)	986(4)	3541(6)	6281(5)	71(2)
C(20)	1470(3)	2681(5)	6068(5)	55(2)
C(21)	1427(4)	528(5)	8347(5)	58(2)
C(22)	2226(3)	176(5)	8907(4)	49(2)
C(23)	2350(4)	-945(6)	9370(5)	66(2)
C(24)	3066(5)	-1262(7)	9967(5)	81(2)
C(25)	3664(4)	-479(8)	10125(5)	76(2)
C(26)	3545(3)	629(6)	9677(4)	62(2)
C(27)	2835(3)	952(5)	9073(4)	50(2)

Table H3. Bond lengths [Å] and angles [deg] for **121**.

Cl(8)-C(8)	1.721(5)	C(8)-C(7)	1.384(7)
Cl(7)-C(7)	1.726(5)	C(8)-C(3)	1.401(6)
Cl(6)-C(6)	1.704(5)	C(7)-C(6)	1.381(7)
Cl(5)-C(5)	1.713(5)	C(6)-C(5)	1.388(6)
Cl(4)-C(4)	1.724(5)	C(5)-C(4)	1.388(6)
Cl(1)-C(1)	1.745(5)	C(4)-C(3)	1.375(6)
O(1)-C(21)	1.209(6)	C(3)-C(1)	1.490(6)

C(1)-C(2)	1.322(6)	C(4)-C(3)-C(8)	117.8(4)
C(2)-C(9)	1.488(7)	C(4)-C(3)-C(1)	122.1(4)
C(2)-C(15)	1.490(7)	C(8)-C(3)-C(1)	119.9(4)
C(9)-C(10)	1.375(7)	C(2)-C(1)-C(3)	127.8(5)
C(9)-C(14)	1.385(7)	C(2)-C(1)-Cl(1)	120.7(4)
C(10)-C(11)	1.378(8)	C(3)-C(1)-Cl(1)	111.5(4)
C(11)-C(12)	1.368(8)	C(1)-C(2)-C(9)	120.9(5)
C(12)-C(13)	1.369(8)	C(1)-C(2)-C(15)	123.0(5)
C(13)-C(14)	1.375(7)	C(9)-C(2)-C(15)	115.8(4)
C(15)-C(20)	1.401(7)	C(10)-C(9)-C(14)	117.6(5)
C(15)-C(16)	1.408(7)	C(10)-C(9)-C(2)	120.6(5)
C(16)-C(17)	1.390(7)	C(14)-C(9)-C(2)	121.7(5)
C(16)-C(21)	1.485(8)	C(9)-C(10)-C(11)	122.3(6)
C(17)-C(18)	1.358(8)	C(12)-C(11)-C(10)	118.4(6)
C(18)-C(19)	1.383(8)	C(11)-C(12)-C(13)	121.0(6)
C(19)-C(20)	1.362(7)	C(12)-C(13)-C(14)	119.7(6)
C(21)-C(22)	1.493(8)	C(13)-C(14)-C(9)	120.9(5)
C(22)-C(27)	1.369(7)	C(20)-C(15)-C(16)	118.2(5)
C(22)-C(23)	1.390(7)	C(20)-C(15)-C(2)	118.3(5)
C(23)-C(24)	1.377(8)	C(16)-C(15)-C(2)	123.3(5)
C(24)-C(25)	1.360(9)	C(17)-C(16)-C(15)	118.8(6)
C(25)-C(26)	1.368(8)	C(17)-C(16)-C(21)	117.2(6)
C(26)-C(27)	1.374(7)	C(15)-C(16)-C(21)	123.9(5)
		C(18)-C(17)-C(16)	121.5(6)
C(7)-C(8)-C(3)	120.9(5)	C(17)-C(18)-C(19)	120.3(6)
C(7)-C(8)-Cl(8)	119.2(4)	C(20)-C(19)-C(18)	119.5(6)
C(3)-C(8)-Cl(8)	119.9(4)	C(19)-C(20)-C(15)	121.7(6)
C(6)-C(7)-C(8)	120.4(4)	O(1)-C(21)-C(16)	119.3(6)
C(6)-C(7)-Cl(7)	119.3(4)	O(1)-C(21)-C(22)	120.0(6)
C(8)-C(7)-Cl(7)	120.3(4)	C(16)-C(21)-C(22)	120.3(5)
C(7)-C(6)-C(5)	119.3(5)	C(27)-C(22)-C(23)	117.9(6)
C(7)-C(6)-Cl(6)	120.6(4)	C(27)-C(22)-C(21)	122.6(5)
C(5)-C(6)-Cl(6)	120.1(4)	C(23)-C(22)-C(21)	119.2(6)
C(4)-C(5)-C(6)	119.8(5)	C(24)-C(23)-C(22)	120.7(6)
C(4)-C(5)-Cl(5)	120.1(4)	C(25)-C(24)-C(23)	120.6(7)
C(6)-C(5)-Cl(5)	120.2(4)	C(24)-C(25)-C(26)	119.1(7)
C(3)-C(4)-C(5)	121.8(4)	C(25)-C(26)-C(27)	120.9(6)
C(3)-C(4)-Cl(4)	118.3(4)	C(22)-C(27)-C(26)	120.9(6)
C(5)-C(4)-Cl(4)	119.9(4)		

Table H4. Anisotropic displacement parameters [$Å^2 \times 10^3$] for **121**. The anisotropic displacement factor exponent takes the form: $-2p^2 [(ha^*)^2 U_{11} + ... + 2hka^*b^* U_{12}]$

	U11	U22	U33	U23	U13	U12
Cl(1)	46(1)	49(1)	64(1)	-7(1)	10(1)	-6(1)
Cl(4)	63(1)	85(1)	33(1)	2(1)	5(1)	22(1)
Cl(5)	50(1)	78(1)	65(1)	6(1)	9(1)	23(1)
Cl(6)	72(1)	76(1)	70(1)	-19(1)	36(1)	5(1)
Cl(7)	88(1)	106(1)	34(1)	-13(1)	12(1)	-4(1)
Cl(8)	60(1)	82(1)	45(1)	9(1)	-7(1)	15(1)
O(1)	58(3)	116(4)	114(4)	11(3)	31(3)	-32(3)

C(1)	38(3)	43(3)	33(3)	-1(2)	3(3)	6(3)
C(2)	35(3)	46(3)	32(3)	-1(2)	2(3)	3(3)
C(3)	39(3)	45(3)	30(3)	2(2)	5(3)	-2(3)
C(4)	39(3)	49(3)	25(3)	-1(3)	3(3)	-3(3)
C(5)	35(3)	46(3)	41(3)	5(3)	8(3)	3(3)
C(6)	45(4)	45(3)	40(3)	-7(3)	16(3)	-7(3)
C(7)	58(4)	48(3)	28(3)	-4(3)	10(3)	-10(3)
C(8)	34(3)	42(3)	38(3)	4(2)	2(3)	-1(3)
C(9)	35(3)	52(4)	41(3)	-8(3)	9(3)	2(3)
C(10)	43(4)	65(4)	85(5)	-11(4)	0(4)	8(3)
C(11)	42(4)	74(5)	122(6)	-29(5)	-8(4)	-3(4)
C(12)	54(5)	57(5)	136(7)	-38(5)	30(5)	-13(4)
C(13)	69(5)	48(4)	95(5)	-13(4)	14(4)	0(4)
C(14)	46(4)	49(4)	55(4)	-10(3)	8(3)	2(3)
C(15)	31(3)	45(4)	49(3)	-11(3)	-4(3)	6(3)
C(16)	30(3)	60(4)	56(4)	-18(3)	7(3)	-3(3)
C(17)	43(4)	91(5)	73(5)	-30(4)	8(3)	9(4)
C(18)	54(4)	86(6)	82(5)	-39(5)	-13(4)	26(4)
C(19)	61(4)	60(4)	77(5)	-7(4)	-16(4)	17(4)
C(20)	50(4)	49(4)	60(4)	-5(3)	-3(3)	9(3)
C(21)	60(5)	61(4)	59(4)	-14(3)	27(4)	-11(4)
C(22)	54(4)	51(4)	45(3)	-4(3)	20(3)	-1(3)
C(23)	90(6)	60(5)	58(4)	3(3)	35(4)	-8(4)
C(24)	111(7)	79(5)	57(5)	19(4)	30(5)	33(5)
C(25)	78(6)	114(6)	39(4)	8(4)	17(4)	30(5)
C(26)	50(4)	86(5)	47(4)	-9(4)	6(3)	5(4)
C(27)	50(4)	56(4)	43(3)	-10(3)	9(3)	3(3)

Table H5. Hydrogen coordinates (x 10^4) and isotropic displacement parameters ($Å^2$ x 10^3) for **121**.

	x	y	z	U(eq)
H(10A)	832(3)	194(6)	4998(5)	80
H(11A)	196(4)	-1579(7)	4539(6)	100
H(12A)	677(4)	-3278(6)	5452(6)	97
H(13A)	1809(4)	-3230(5)	6733(5)	85
H(14A)	2479(3)	-1475(5)	7104(4)	61
H(17A)	563(3)	2361(6)	8362(5)	84
H(18A)	312(4)	3992(7)	7290(6)	94
H(19A)	885(4)	4212(6)	5847(5)	85
H(20A)	1691(3)	2767(5)	5479(5)	66
H(23A)	1945(4)	-1486(6)	9275(5)	80
H(24A)	3141(5)	-2018(7)	10266(5)	97
H(25A)	4147(4)	-694(8)	10530(5)	92
H(26A)	3951(3)	1170(6)	9784(4)	74
H(27A)	2766(3)	1708(5)	8773(4)	60

Table 11. Crystal data and structure refinement for (TCNE + 5-Trimethylsilylethynyl-1,4-diethyl-2,3-diphenylcyclopentadien-5-ol) Adduct, **142a**.

	142a
empirical formula	$C_{32}H_{30}N_4OSi$
M_r	514.69
T [K]	210(2)
λ [Å]	0.71073
description	colorless plate
crystal size [mm]	0.14 x 0.24 x 0.50
crystal system	Monoclinic
space group	$P2_1/n$
a [Å]	9.90710(10)
b [Å]	16.9188(2)
c [Å]	17.58580(10)
α [°]	90
β [°]	93.0010(10)
γ [°]	90
V [Å^3]	2943.62(5)
Z	4
ρ_{calcd} [g cm^{-3}]	1.161
abs. Coeff. [mm^{-1}]	0.110
F(000)	1088
θ range for collection [°]	1.67 to 26.37
limiting indices	$12 < h < 12$, $-20 < k < 20$, $-21 < l < 21$
reflections collected	23778
independent reflections	5854
R(int)	0.0453
refinement method	Full-matrix least-squares on F^2
weighting scheme	$w=1/[\sigma^2F_o^2 + (0.0846((F_o^2+ 2F_c^2)/3))^2 + 2.223((F_o^2 +2F_c^2)/3))^2]$
data/restraints/parameters	5854 / 0 / 463
goodness-of-fit on F^2	1.076
final R indices [$I>2\sigma(I)$][a]	R1 = 0.0641, wR2 = 0.1641
R indices (all data)[a]	R1 = 0.0937, wR2 = 0.1874
rel. trans. (max., min.)	0.9811, 0.8040
Largest diff. peak [eÅ^{-3}]	0.432
Largest diff hole [eÅ^{-3}]	-0.232

[a] $R1 = \Sigma (|| F_o | - | F_c ||)/ \Sigma | F_o |$; $wR2 =[\Sigma[w(F_o^2 - F_c^2)^2]/\Sigma[w(F_o^2)^2]]^{0.5}$

Table I2. Atomic coordinates [x 10^4] and equivalent isotropic displacement parameters [$Å^2$ x 10^3] for **142a**. U(eq) is defined as one third of the trace of the orthogonalized U_{ij} tensor.

	x	y	z	U(eq)
Si(1)	1209(1)	5261(1)	2368(1)	39(1)
O(1)	-2165(2)	5626(1)	4482(1)	42(1)
C(1)	-964(3)	6818(2)	4811(2)	33(1)
C(2)	-677(3)	7586(2)	4395(2)	34(1)
C(3)	-1421(3)	7603(2)	3737(2)	33(1)
C(4)	-2398(3)	6897(2)	3730(2)	33(1)
C(5)	-3371(3)	7076(2)	4419(2)	37(1)
C(6)	-2435(3)	6793(2)	5132(2)	38(1)
C(7)	-1436(3)	6276(2)	4140(2)	35(1)
C(8)	280(3)	8209(2)	4685(2)	41(1)
C(9)	32(4)	8605(2)	5363(2)	66(1)
C(10)	892(5)	9217(3)	5623(3)	84(1)
C(11)	2009(4)	9411(3)	5216(3)	75(1)
C(12)	2258(5)	9013(3)	4564(3)	79(1)
C(13)	1392(4)	8419(3)	4292(2)	66(1)
C(14)	-1357(3)	8199(2)	3116(2)	34(1)
C(15)	-1894(4)	8943(2)	3180(2)	53(1)
C(16)	-1834(4)	9480(2)	2580(2)	66(1)
C(17)	-1205(4)	9289(2)	1939(2)	56(1)
C(18)	-658(4)	8556(2)	1873(2)	66(1)
C(19)	-740(4)	8003(2)	2455(2)	58(1)
C(20)	105(3)	6522(2)	5417(2)	51(1)
C(21)	1487(4)	6420(3)	5138(2)	62(1)
C(22)	-3149(3)	6642(2)	2990(2)	42(1)
C(23)	-4196(4)	7217(2)	2649(2)	56(1)
C(24)	-2657(3)	5896(2)	5156(2)	40(1)
N(24)	-3195(3)	5521(2)	5666(2)	54(1)
C(25)	-2636(3)	7199(2)	5851(2)	45(1)
N(25)	-2761(3)	7527(2)	6407(2)	62(1)
C(26)	-3731(3)	7920(2)	4479(2)	42(1)
N(26)	-4037(3)	8567(2)	4551(2)	60(1)
C(27)	-4648(3)	6620(2)	4367(2)	46(1)
N(27)	-5619(3)	6254(2)	4329(2)	65(1)
C(28)	-460(3)	5945(2)	3634(2)	39(1)
C(29)	266(3)	5677(2)	3163(2)	43(1)
C(30)	1126(8)	4172(3)	2469(3)	76(1)
C(31)	286(5)	5596(3)	1486(2)	62(1)
C(32)	2967(4)	5617(4)	2432(3)	72(1)

Table I3. Bond lengths [Å] and angles [deg] for **142a**.

Si(1)-C(32)	1.841(4)	O(1)-C(7)	1.462(3)
Si(1)-C(31)	1.848(4)	C(1)-C(2)	1.526(4)
Si(1)-C(30)	1.854(5)	C(1)-C(20)	1.546(4)
Si(1)-C(29)	1.862(3)	C(1)-C(7)	1.548(4)
O(1)-C(24)	1.384(3)	C(1)-C(6)	1.591(4)

C(2)-C(3)	1.339(4)
C(2)-C(8)	1.490(4)
C(3)-C(14)	1.491(4)
C(3)-C(4)	1.538(4)
C(4)-C(22)	1.527(4)
C(4)-C(7)	1.568(4)
C(4)-C(5)	1.616(4)
C(5)-C(26)	1.477(4)
C(5)-C(27)	1.480(4)
C(5)-C(6)	1.594(4)
C(6)-C(25)	1.461(4)
C(6)-C(24)	1.534(4)
C(7)-C(28)	1.459(4)
C(8)-C(13)	1.377(5)
C(8)-C(9)	1.400(5)
C(9)-C(10)	1.402(5)
C(10)-C(11)	1.389(6)
C(11)-C(12)	1.364(6)
C(12)-C(13)	1.390(5)
C(14)-C(15)	1.373(4)
C(14)-C(19)	1.381(4)
C(15)-C(16)	1.396(5)
C(16)-C(17)	1.355(5)
C(17)-C(18)	1.360(5)
C(18)-C(19)	1.393(5)
C(20)-C(21)	1.488(5)
C(22)-C(23)	1.522(5)
C(24)-N(24)	1.241(4)
C(25)-N(25)	1.137(4)
C(26)-N(26)	1.144(4)
C(27)-N(27)	1.143(4)
C(28)-C(29)	1.212(4)

C(32)-Si(1)-C(31)	112.1(2)
C(32)-Si(1)-C(30)	111.5(3)
C(31)-Si(1)-C(30)	111.3(3)
C(32)-Si(1)-C(29)	109.9(2)
C(31)-Si(1)-C(29)	105.6(2)
C(30)-Si(1)-C(29)	106.1(2)
C(24)-O(1)-C(7)	107.9(2)
C(2)-C(1)-C(20)	117.9(2)
C(2)-C(1)-C(7)	101.3(2)
C(20)-C(1)-C(7)	120.1(2)
C(2)-C(1)-C(6)	113.0(2)
C(20)-C(1)-C(6)	110.7(2)
C(7)-C(1)-C(6)	90.5(2)
C(3)-C(2)-C(8)	126.4(2)
C(3)-C(2)-C(1)	108.9(2)
C(8)-C(2)-C(1)	124.7(2)
C(2)-C(3)-C(14)	127.2(2)
C(2)-C(3)-C(4)	108.0(2)
C(14)-C(3)-C(4)	124.8(2)
C(22)-C(4)-C(3)	120.3(2)
C(22)-C(4)-C(7)	117.3(2)
C(3)-C(4)-C(7)	98.6(2)
C(22)-C(4)-C(5)	114.1(2)
C(3)-C(4)-C(5)	104.4(2)
C(7)-C(4)-C(5)	98.8(2)
C(26)-C(5)-C(27)	107.4(2)
C(26)-C(5)-C(6)	111.5(2)
C(27)-C(5)-C(6)	110.7(2)
C(26)-C(5)-C(4)	113.0(2)
C(27)-C(5)-C(4)	113.4(2)
C(6)-C(5)-C(4)	100.9(2)
C(25)-C(6)-C(24)	114.6(2)
C(25)-C(6)-C(1)	117.6(2)
C(24)-C(6)-C(1)	99.9(2)
C(25)-C(6)-C(5)	116.0(2)
C(24)-C(6)-C(5)	103.9(2)
C(1)-C(6)-C(5)	102.6(2)
C(28)-C(7)-O(1)	108.7(2)
C(28)-C(7)-C(1)	120.5(2)
O(1)-C(7)-C(1)	105.6(2)
C(28)-C(7)-C(4)	112.5(2)
O(1)-C(7)-C(4)	113.1(2)
C(1)-C(7)-C(4)	96.0(2)
C(13)-C(8)-C(9)	119.0(3)
C(13)-C(8)-C(2)	121.5(3)
C(9)-C(8)-C(2)	119.5(3)
C(8)-C(9)-C(10)	120.0(4)
C(11)-C(10)-C(9)	119.6(4)
C(12)-C(11)-C(10)	120.0(4)
C(11)-C(12)-C(13)	120.7(4)
C(8)-C(13)-C(12)	120.6(4)
C(15)-C(14)-C(19)	118.7(3)
C(15)-C(14)-C(3)	121.8(2)
C(19)-C(14)-C(3)	119.5(2)
C(14)-C(15)-C(16)	120.2(3)
C(17)-C(16)-C(15)	120.8(3)
C(16)-C(17)-C(18)	119.5(3)
C(17)-C(18)-C(19)	120.7(3)
C(14)-C(19)-C(18)	120.1(3)
C(21)-C(20)-C(1)	114.8(3)
C(23)-C(22)-C(4)	116.6(3)
N(24)-C(24)-O(1)	129.4(3)
N(24)-C(24)-C(6)	126.4(3)
O(1)-C(24)-C(6)	104.2(2)
N(25)-C(25)-C(6)	178.1(3)
N(26)-C(26)-C(5)	177.3(3)
N(27)-C(27)-C(5)	178.5(3)
C(29)-C(28)-C(7)	174.3(3)
C(28)-C(29)-Si(1)	173.6(3)

Table I4. Anisotropic displacement parameters [$Å^2$ x 10^3] for **142a**. The anisotropic displacement factor exponent takes the form: $-2p^2$ [$(ha^*)^2$ U11 + ... + 2hka*b* U12]

	U11	U22	U33	U23	U13	U12
Si(1)	45(1)	36(1)	36(1)	-3(1)	8(1)	6(1)
O(1)	57(1)	25(1)	47(1)	2(1)	15(1)	-2(1)
C(1)	33(1)	30(1)	37(1)	3(1)	4(1)	2(1)
C(2)	32(1)	28(1)	42(2)	-1(1)	5(1)	-2(1)
C(3)	36(1)	26(1)	38(1)	-4(1)	8(1)	1(1)
C(4)	37(1)	26(1)	38(1)	-2(1)	6(1)	-2(1)
C(5)	36(1)	28(1)	46(2)	-3(1)	9(1)	-6(1)
C(6)	42(2)	29(1)	43(2)	-1(1)	12(1)	-3(1)
C(7)	39(2)	27(1)	41(2)	1(1)	8(1)	0(1)
C(8)	39(2)	38(2)	45(2)	4(1)	-4(1)	-8(1)
C(9)	63(2)	66(2)	71(2)	-24(2)	10(2)	-18(2)
C(10)	82(3)	84(3)	88(3)	-33(2)	10(2)	-37(2)
C(11)	73(3)	71(3)	80(3)	-7(2)	-15(2)	-30(2)
C(12)	63(3)	88(3)	88(3)	-2(2)	17(2)	-36(2)
C(13)	60(2)	77(3)	63(2)	-10(2)	13(2)	-28(2)
C(14)	35(1)	30(1)	38(1)	4(1)	2(1)	-2(1)
C(15)	77(2)	31(2)	54(2)	4(1)	23(2)	4(2)
C(16)	95(3)	34(2)	72(2)	17(2)	22(2)	8(2)
C(17)	70(2)	47(2)	51(2)	21(2)	3(2)	-5(2)
C(18)	79(3)	74(3)	49(2)	20(2)	27(2)	16(2)
C(19)	72(2)	52(2)	52(2)	14(2)	24(2)	23(2)
C(20)	53(2)	43(2)	58(2)	11(2)	-1(2)	-2(2)
C(21)	51(2)	72(3)	62(2)	14(2)	0(2)	18(2)
C(22)	45(2)	36(2)	44(2)	-5(1)	-1(1)	-8(1)
C(23)	56(2)	46(2)	64(2)	1(2)	-13(2)	-5(2)
C(24)	48(2)	32(2)	41(2)	-1(1)	11(1)	-1(1)
N(24)	71(2)	38(2)	56(2)	3(1)	20(1)	-9(1)
C(25)	57(2)	31(2)	47(2)	1(1)	13(1)	-4(1)
N(25)	84(2)	53(2)	49(2)	-10(1)	23(2)	-10(2)
C(26)	40(2)	37(2)	51(2)	0(1)	12(1)	2(1)
N(26)	67(2)	39(2)	75(2)	-2(1)	23(2)	11(1)
C(27)	43(2)	38(2)	60(2)	-2(1)	12(1)	-3(1)
N(27)	47(2)	63(2)	88(2)	2(2)	10(2)	-17(2)
C(28)	45(2)	28(1)	45(2)	-1(1)	6(1)	4(1)
C(29)	52(2)	34(2)	45(2)	1(1)	7(1)	5(1)
C(30)	124(5)	44(2)	62(3)	-3(2)	17(3)	13(3)
C(31)	74(3)	69(3)	43(2)	4(2)	-2(2)	3(2)
C(32)	48(2)	92(4)	77(3)	13(3)	7(2)	-2(2)

Table 15. Hydrogen coordinates (x 10^4) and isotropic displacement parameters ($Å^2$ x 10^3) for **142a**.

	x	y	z	U(eq)
H(9)	-1032(47)	8646(26)	5424(24)	93(14)
H(10)	604(62)	9444(36)	6290(35)	155(22)
H(11)	2577(53)	9844(31)	5358(27)	112(16)
H(12)	3057(58)	8979(32)	4332(30)	119(18)
H(13)	1742(35)	8023(21)	3991(20)	58(10)
H(15)	-2317(38)	9086(23)	3631(21)	69(11)
H(16)	-2026(60)	10006(40)	2699(32)	143(22)
H(17)	-1234(39)	9604(23)	1596(22)	67(12)
H(18)	-323(41)	8384(24)	1456(23)	74(12)
H(19)	-326(37)	7463(23)	2395(20)	68(11)
H(20A)	-217(39)	6010(25)	5577(21)	76(12)
H(20B)	447(28)	6849(17)	5913(16)	37(7)
H(21A)	1164(97)	6296(59)	4543(54)	251(41)
H(21B)	1875(58)	7015(39)	4996(33)	140(21)
H(21C)	2124(48)	6241(28)	5589(27)	101(15)
H(22A)	-3636(30)	6149(19)	3086(16)	42(8)
H(22B)	-2459(33)	6570(19)	2589(18)	49(8)
H(23A)	-4699(40)	6973(24)	2194(23)	78(12)
H(23B)	-3835(35)	7696(23)	2494(19)	58(10)
H(23C)	-5056(44)	7281(24)	3038(24)	84(12)
H(24)	-3138(44)	4986(29)	5513(24)	90(14)
H(30A)	328(72)	4013(41)	2450(36)	143(31)
H(30B)	1481(59)	3880(36)	2103(34)	125(20)
H(30C)	1550(62)	4049(36)	2837(35)	123(24)
H(31A)	224(54)	6072(36)	1460(30)	111(20)
H(31B)	827(49)	5497(29)	1052(28)	99(15)
H(31C)	-660(58)	5424(30)	1453(29)	113(18)
H(32A)	3479(76)	5424(43)	2748(41)	168(32)
H(32B)	2922(42)	6158(29)	2445(24)	77(14)
H(32C)	3380(41)	5418(23)	1977(24)	70(12)